Evaluation of the long-term effects of anaerobic digestion on bovine manure resistomes and mobilomes and the molecular and microbial mechanisms involved

By

Daniel Flores Orozco

A Thesis submitted to the Faculty of Graduate Studies of

The University of Manitoba

In partial fulfillment of the requirements of the degree of

DOCTOR OF PHILOSOPHY

Department of Biosystems Engineering

University of Manitoba

Winnipeg, Manitoba

Supervisory Committee

Dr. Nazim Cicek (Supervisor) - Department of Biosystems Engineering, University of Manitoba.

Dr. David B. Levin - Department of Biosystems Engineering, University of Manitoba.

Dr. Richard Sparling - Department of Microbiology, University of Manitoba.

Dr. Ayush Kumar - Department of Microbiology, University of Manitoba.

Dr. Anthony Lau (External Reviewer) - Chemical and Biological Engineering, University of British Columbia

Thesis Abstract

Anaerobic digestion (AD) has shown the potential to reduce the abundance of antimicrobial resistance genes (ARGs) and mobile genetic elements (MGEs) in animal manures. It stands as a promising option to reduce the risk of the spread of antimicrobial resistance (AMR) due to livestock production and manure applications. However, the underlying mechanisms driving these changes still need to be fully understood. This multidisciplinary study aimed to utilize metagenomics to investigate the molecular and microbial mechanisms associated with the evolution of ARGs and MGEs during the anaerobic digestion (AD) of bovine dairy manure. The research focused on three main aspects: 1) examining the long-term effects of mesophilic (MAD) and thermophilic (TAD) anaerobic digestion on the entire set of ARGs (resistome) and MGEs (mobilome) in manure; 2) comparing the impact of alternative manure treatments, such as storage and solid-liquid separation, on resistomes and mobilomes; 3) identifying microbial groups potentially associated with ARGs and MGEs and microbial shifts potentially driving changes in resistomes and mobilomes. A meta-analysis conducted early in this research informed the primary focus of this research.

Two anaerobic digesters operating at mesophilic (36 °C) and the other at thermophilic (55 °C) temperatures were set up, operated, monitored, and studied for 4 and 2 years, respectively. Metagenomics analyses were used to evaluate resistomes, mobilomes, and microbiomes in the mesophilic and thermophilic digesters operating under steady state and in the bovine manure used as substrate. The results indicated that MAD and TAD lowered ARG levels in fresh cattle manure by over 50% and MGEs by over 65%. Surprisingly, TAD did not outperform MAD at reducing ARGs and MGEs. Co-occurrence analysis indicated a strong association between microbial groups from the phyla Bacillota (e.g., *Jeotgalicoccus*, *Streptococcus*, *Enterococcus*), Actinomycetota

(e.g., *Brevibacterium*, *Rhodococcus*), and Pseudomonadota (e.g., *Acinetobacter*, *Comamonas*) with these AMR elements. The decline in the abundance of aerobic and facultative anaerobes likely linked to hydrolytic functions was suggested as one of the main drivers of the changes in resistomes and mobilomes. The proximity of toxin-antitoxin systems and transposon structures to specific ARGs (e.g., *Erm*, *tet*, *Ant(6)-Ia*) was discovered, which could explain the persistence of such ARGs in digestates. The study of the effects of other manure treatments, such as aerobic storage in an open tank and solid-liquid separation, revealed that they are less efficient in reducing ARGs and MGEs from manures than AD. In this study, the high levels of ARGs and genes conferring resistance to heavy metals in a farm operating in an antibiotic-free environment suggested that other antimicrobials, such as foot bathing solutions, may be causing the indirect selection of ARGs.

Overall, this research made several contributions to understanding AMR in the context of anaerobic digestion of animal manure that could be extrapolated to other manure treatments. These contributions not only bridge existing gaps in the literature but also pave the way for future research, providing valuable insights that can be used to inform the development of more effective strategies to mitigate the dissemination of AMR associated with manure management, application, and disposal.

Acknowledgments

My journey through graduate studies has undoubtedly been the greatest challenge I have had in my professional career. Undertaking this multidisciplinary project, especially in areas unfamiliar to me, meant endless hours of reading, coding, writing and rewriting what was already written. The added uncertainties and impacts of the pandemic only intensified this experience. However, it was also fun and gave me the opportunity to connect with wonderful individuals from around the world. This journey expanded my horizons and deepened my understanding of how much more I have to learn. I can confidently say this was an enriching experience, made possible by the immense support of many.

I would like to express my deepest gratitude to my advisor Dr. Nazim Cicek for believing in my abilities and giving me this opportunity. Your expertise, patience, and support were instrumental in this research. Thanks to the members of my committee: Dr. David Levin, Dr. Richar Sparling, Dr. Ayush Kumar. Your extensive guidance and constructive feedback were critical in this research. You helped me to articulate ideas and discussions from different perspectives. I am confident that all I learned from you will help me become a better scientist and a better person.

Thanks to my advisors, the University of Manitoba, and the Natural Sciences and Engineering Research Council of Canada (NSERC) for the financial support in the form of fellowships and awards. These included NSERC Discovery Grants, the University of Manitoba, the Graduate Fellowship (UMGF), the International Graduate Student Entrance Scholarship (IGSES), the Faculty of Graduate Studies Program Completion Scholarship, the Roma Zenovea Hawirko Scholarship, and the Edward R. Toporeck Graduate Fellowship in Engineering.

Thanks to my fellow graduate students and teammates in the Levin, Cicek, Sparling, and Kumar's lab. The list has grown too extensive to include everyone since those early days in 2017. Thanks for all your help, support, feedback, tips, and friendship. Working with all of you made this journey more enjoyable. Special mention to Kenton, Joe, Maciej, Alessandro, and Tanner for the shared moments outside the lab.

Thanks to our administrative team members, Heather Innis, Mandy Tanner, Caitlin Jacques, Matt McDonald, Matthew McDonald, Minami Maeda, Daniel Benedet, and Dale Bourns, for the prompt and consistent assistance. I am also so grateful to the staff members of the Recreational Services, especially Montana Quiring, for providing the means and encouraging me to stay active during all this time. This has been essential to keep me sane and complete this program.

I would like to extend my gratitude to Henry Holtmann, Jason Bourcier and the entire staff of the farms for kindly giving access to their facilities to take samples. You all also played an important role in this journey.

I must acknowledge my family: My parents, Donato and Olivia; my sisters Valeria, Mariana and Emma; my grandparents, Nino and Nina, Esperanza and Socorro; my uncle Ramon and the rest of the family whose names would fill many pages. Nobody has been more important to me in pursuing this project than you. Your unconditional love and support were invaluable. Muchas gracias por todo su apoyo, no hubiese sido posible sin ustedes. Los quiero mucho.

Mayra, thanks for being by my side since day one. There are no words to thank you enough for your support. Your encouragement, patience, the food you prepared, the love you shared, and all our adventures along the way were also invaluable. I will be forever thankful for having you in my life. I also appreciate your help in coloring my figures, which, otherwise, would be inconsistent, to say the least.

Lastly, to my cherished friends: the times we spent together, whether laughing, relaxing, or adventuring, were the essential breaks that recharged my spirit and kept me grounded throughout this journey.

Dedication

I dedicate this to my family for your constant love and support that helped me completed this journey.

Table of Contents

List of Tables

List of Figures

List of Copyrighted Material with Permission

The appropriate permission was obtained from Elsevier through the available online form for the use of the following material in different parts of the thesis:

1. Flores-Orozco, D., R. Patidar, D.B. Levin, R. Sparling, A. Kumar and N. Çiçek. 2020. Effect of mesophilic anaerobic digestion on the resistome profile of dairy manure. *Bioresource Technology* 315: 123889. https://doi.org/10.1016/j.biortech.2020.123889.
2. Flores-Orozco, D., D. Levin, A. Kumar, R. Sparling and N. Cicek. 2022. A meta-analysis reveals that operational parameters influence levels of antibiotic resistance genes during anaerobic digestion of animal manures. *Science of The Total Environment* 814: 152711. https://doi.org/10.1016/j.scitotenv.2021.152711.
3. Flores-Orozco, D., R. Patidar, D. Levin, A. Kumar, R. Sparling and N. Cicek. 2023. Metagenomic analyses reveal that mesophilic anaerobic digestion substantially reduces the abundance of antibiotic resistance genes and mobile genetic elements in dairy manures. *Environmental Technology & Innovation* 30: 103128. https://doi.org/10.1016/j.eti.2023.103128.
4. Flores-Orozco, D., D. Levin, A. Kumar, R. Sparling and N. Cicek. 2023. Influence of three different manure treatments on antimicrobial resistance genes and mobile genetic elements. *Frontiers in Synthetic Biology* 1. https://doi.org/10.3389/fsybi.2023.1301879.
5. Flores-Orozco, D., D. Levin, A. Kumar, R. Sparling, H. Derakhshani and N. Cicek. 2024. Metagenomic comparison of effects of mesophilic and thermophilic manure anaerobic digestion on antimicrobial resistance genes and mobile genetic elements. *Environmental Advances* 15: 100472. https://doi.org/10.1016/j.envadv.2023.100472.

Contribution of Authors

The list of authors and their contributions to the manuscripts included in this thesis are as follows:

Chapters 4 to 8:

- Daniel Flores-Orozco (*Thesis author*): Data curation, Writing-Original draft preparation, Investigation, Formal analysis, Visualization.
- David B. Levin: Writing - Review & Editing, Conceptualization.
- Ayush Kumar: Writing - Review & Editing, Conceptualization.
- Richard Sparling: Writing - Review & Editing, Conceptualization.
- Nazim Çiçek: Resources, Writing - Review & Editing, Supervision, Funding acquisition, Conceptualization.

Chapter 5:

- Rakesh Patidar: Writing - Review & Editing, Investigation.

Chapter 8:

- Hooman Derakhshani: Writing - Review & Editing, Conceptualization

The Preface sections of these Chapters also describe each author's contributions.

Abbreviations

AA	auxiliary activities
AD	anaerobic digestion
AMR	antimicrobial resistance
ARB	antibiotic resistant bacteria
ARG	antimicrobial resistance genes
ARO	antibiotic resistance ontology
BRU	bedding recovery unit
CARD	comprehensive antibiotic resistance database
CBM	carbohydrate binding modules
CE	carbohydrate esterases
CH_4	methane
CO_2	carbon dioxide
COD	chemical oxygen demand
GH	glycoside hydrolases
GT	glycosyl transferases
HGT	horizontal gene transfer
HRT	hydraulic retention time
ICEs	integrative conjugative elements
MAD	mesophilic anaerobic digestion
MGE	mobile genetic elements
MIC	minimum inhibitory concentration

mls	macrolide-lincosamide-streptogramin
NGS	next generation sequencing
OLR	organic loading rate
ORF	open reading frame
PL	polysaccharide lyases
SRT	solids retention time
TAD	thermophilic anaerobic digestion
TS	total solids
VFAs	volatile fatty acids
VS	volatile solids

Chapter 1: Overview of the thesis

1.1. Research objectives

The primary objective of this research was to expand the understanding of the molecular and microbial mechanisms that drive the changes in antimicrobial resistance genes (ARGs) and mobile genetic elements (MGEs) in the microbiome of bovine dairy manure during different treatments. More specifically, this work aimed to use anaerobic digestion (AD) to model the changes in ARGs and MGEs as a function of the microbial dynamics involved in the process, using a set of cutting-edge tools such as next-generation sequencing, metagenomics, and biostatistics. Also, this study aimed to explore the co-occurrence of ARGs and MGEs in manure microbiomes and provide insights into the molecular mechanisms underlying the persistence and dissemination of ARGs in these types of environments.

1.2. Motivation and background

The driving force behind this study was the quest for alternatives to reduce antimicrobial resistance (AMR) markers in animal manures before they spread to the environment. This is crucial as the dissemination of resistance to antimicrobials, used in both human and veterinary medicine, poses significant public health risks. Previous research had assessed the impact of various manure treatments on ARG levels and identified potential ARG-carrying microbial groups. However, these studies primarily relied on quantitative polymerase chain reaction (qPCR), which limits the analysis to a few pre-identified genes. The broader application of metagenomics to study entire resistomes and mobilomes in this field remained underexplored. Furthermore, limited research has examined the progression of ARGs and MGEs in continuously operated anaerobic digesters over

extended operation periods. This project aimed to bridge these knowledge gaps and offer solutions to curb the rise and spread of AMR from manure applications.

1.3. Structure of thesis

The thesis follows a sandwich-format, wherein some chapters (or section of the chapters) are standalone manuscripts that have been published in internationally recognized, peer-reviewed journals. The prefaces of each chapter indicate if the chapter or sections of the chapters have been previously published. The literature review relevant to this research is presented in Chapter 2. Chapter 4 describes a systematic literature review in the form of a series of meta-analyses (published as original research) focused on the effect of AD and variations its operational parameters on the levels of ARGs in animal manures. Chapter 3 outlines the methodology that is common to the subsequent experimental chapters (Chapters 5 to 8) to avoid redundancy throughout the document. Specific methods are elaborated upon within their respective chapters. The concluding chapter (Chapter 9) synthesizes the research findings, offering concise conclusions with an emphasis on their engineering implications. It also underscores impending challenges and potential research avenues. All references are consolidated at the end of the document. Supplementary content, such as figures and tables, is presented in the Appendices. These appendices are organized and labeled by chapter (e.g., Figure A3.1 in appendix A).

Chapter 2: Literature review

2.1. Preface

This chapter serves as an introduction to the problems associated with antimicrobial resistance and the role animal husbandry plays in its dissemination. It delves into the molecular foundations of antimicrobial resistance, detailing various transmission mechanisms and the prevalence of resistance markers in animal manures. The chapter also provides a brief review of how different manure treatments impact the levels of various antimicrobial resistance markers. The last sections explore AD fundamentals and how AD can be used to model changes in ARGs and MGEs as function of microbial dynamics.

2.2. Introduction: Antibiotics, antibiotic resistance, and animal husbandry

The discovery and clinical application of antibiotics in the first half of the last century played a pivotal role in enhancing quality of life and increasing life expectancy (Aminov 2010). Nowadays, antibiotics are indispensable not only for human health but for animal welfare and livestock production (Kumar et al. 2012). However, the extensive use and misuse of antibiotics has caused the accumulation of residual antibiotics in the environment, contributing to the emergence and dissemination of antibiotic-resistant bacteria (ARB). This phenomenon is a growing public health threat as ARB make it increasingly difficult to treat infectious diseases, which leads to longer hospital stays, higher healthcare costs, and increased risk of mortality (Murray et al. 2022). This issue is a global concern, affecting people in all countries and regions, regardless of their level of development or wealth (WHO 2018a). Therefore, it is urgent to take measures and find alternatives to prevent and control the spread of antibiotic resistance.

Animal husbandry is one of the main sources of emissions of antibiotics into the environment due to the large amounts of veterinary pharmaceuticals used not only to treat infectious diseases

but as prophylactic therapies and growth promotors (Kraemer et al. 2019). It is estimated that the amounts of antibiotics used in veterinary applications are much higher than those used by hospitals. For instance, Canada has reported that veterinary antibiotics account for approximately 95% of the total annual antibiotic market (Public Health Agency Canada 2018), while in the USA, veterinary antibiotics represent around 80% of the market (Data M Intelligence 2021). Antibiotics used in veterinary applications include aminoglycosides, cephalosporins, fluoroquinolones, lincosamides, macrolides, cephalosporins, penicillin, sulfonamides, and tetracyclines, many of which are critically important antimicrobials, as they are essential to treat human diseases (FDA 2018; WHO 2018b). Thus, the development of resistance to these antibiotics could have severe consequences to human health.

Antibiotics are generally poorly absorbed in the body, and the largest fraction (> 50%) of the dose is secreted in the urine and feces in the original form or secondary metabolites with antimicrobial activity (Jjemba 2002; Wohde et al. 2016). Consequently, animal manure produced in husbandry operations often contains substantial amounts of residual antibiotics. In fact, numerous studies have documented the presence of considerably high concentrations of residual antibiotics in various types of animal manure (Wohde et al. 2016). While these residual antibiotics can cause the development of ARB within farms, there is also a considerable risk of AMR dissemination into the environment through the application of manure. The use of manure and its derivatives as soil fertilizer is a common practice around the world as they provide essential nutrients such as Nitrogen (N), Phosphorous (P), and Potassium (K) and increase soil carbon content (Madison et al. 1995). Thus, there are growing concerns about the potential enrichment of ARB and antimicrobial resistance genes (ARGs) in agricultural soils and the ultimate

consequences on human and animal health (Hu et al. 2016a; Wang et al. 2020; Xu et al. 2019; Zhang et al. 2021b).

One of the first alternatives to reduce the risk of dissemination of antimicrobial resistance is limiting the use of antibiotics in animal husbandry. However, while more poultry, swine, and dairy farms are opting to limit the use of antibiotics, there are still concerns about animal health and welfare (Singer et al. 2019). Moreover, there is growing evidence of the presence of various ARGs in manure from organic farms where antibiotics are not used (Pitta et al. 2020; Smith et al. 2013). All this implies that limiting the usage of antibiotics alone may not be enough to reduce the risk of the spread of AMR in animal husbandry and manure applications. Therefore, the implementation of a combination of strategies is necessary. The following section describe the fundamentals of antimicrobial resistance and explores the potential of different manure treatments in minimizing the risk of AMR dissemination.

2.3. Fundamentals of antimicrobial resistance

2.3.1. Origins of resistance

Antibiotic resistance is a natural consequence of the microbial evolutionary response to the selective pressure exerted by antibiotics (Franco et al., 2009). Throughout millions of years of evolution, bacteria have developed diverse mechanisms to withstand the toxic effects of naturally occurring antibiotics and other antimicrobial substances (Franco et al., 2009). These mechanisms include the production of enzymes that degrade antibiotics, efflux pumps that expel antibiotics from the cell, subtle modifications or complete replacement of the antibiotic target, mechanisms to impede antibiotic access to their targets, and alterations in membrane permeability (Allen et al., 2010; Reygaert, 2018). The resistance mechanisms are encoded in genes known as ARGs which can be encoded in genomic chromosomes or plasmids. The level of resistance to antimicrobials is

given by the minimum inhibitory concentration (MIC), which is the lowest concentration that inhibits bacterial growth (Reygaert 2018). Bacteria with MIC higher than predefined breakpoint (a concentration achievable under clinical conditions) are considered resistant.

2.3.2. Natural resistance versus acquired resistance

Antimicrobial resistance derived from the natural occurrence of ARGs in bacterial genomes is known as natural resistance. Natural resistance can be further categorized as intrinsic or induced. Intrinsic resistance is an inherent trait of certain species expressed regardless of previous antibiotic exposure (Davies and Davies 2010). A good example of this kind of resistance is the reduced permeability of the membrane in Gram-negative bacteria. On the other hand, induced resistance occurs when bacteria possess genes that can confer resistance, but their expression is triggered only after exposure to an antimicrobial. An example of induced resistance is the activation of efflux pumps following antibiotic exposure (Reygaert 2018).

Bacteria can become resistant due to the acquisition of ARGs, either through random mutation or via horizontal gene transfer (HGT) facilitated by various routes (Frost et al. 2005; Reygaert 2018) (the different mechanisms of gene transfer are described in subsequent sections). The acquired resistance can be temporary or permanent, depending on factors such as the presence of antimicrobials exerting selective pressures and the metabolic burden they impose (Reygaert 2018). Sub-inhibitory concentrations of antimicrobials can cause the selection of highly resistant bacteria in successive generations, increase the mutation rates and lead to the generation of new ARGs, increase the ability to acquire more ARGs and promote the transfer of ARGs via HGT (Reygaert 2018). For all this, acquired resistance represents a much greater threat to public health as pathogenic species can become resistant to multiple antibiotics.

2.3.3. Mechanisms of antimicrobial resistance

Antimicrobial resistance mechanisms can be classified into four main categories (Reygaert, 2018): active drug efflux, antibiotic inactivation, modification of antibiotic targets, and reduced permeability. All four mechanisms are commonly observed in Gram-negative bacteria, while reduced permeability and efflux pumps are less prevalent in Gram-positive bacteria (Reygaert, 2018).

2.3.3.1. Drug efflux

Drug efflux is an important mechanism employed by bacteria to prevent the toxic effects of different antimicrobials. Specialized membrane proteins, known as efflux pumps, actively transport antibiotics and other toxic substances out of the bacterial cell, reducing the intracellular concentration of the drug and preventing its action. Efflux pumps can often recognize and transport a wide variety of compounds, making them highly efficient in conferring multidrug resistance (Li and Nikaido 2009; Reygaert 2018). Efflux pumps are usually encoded in bacterial chromosomes although they can also be plasmid-encoded, and their expression can be either constitutive or induced (Li and Nikaido 2004; Reygaert 2018). Efflux pumps play a significant role in intrinsic resistance of Gram-negative bacteria and their overexpression can produce elevated levels of antimicrobial resistance (Li and Nikaido 2004). Efflux pumps are classified into five families: the adenosine triphosphate (ATP)-binding cassette (ABC) superfamily, the major facilitator superfamily (MFS), the multidrug and toxic compound extrusion (MATE) family, the small multidrug resistance (SMR) family, and the resistance-nodulation-cell division (RND) family (Li and Nikaido 2004; Reygaert 2018).

2.3.3.2. Antibiotic inactivation

The inactivation of antibiotics via enzymes is another important mechanism employed by bacteria to evade their antimicrobial effects. Bacterial enzymes can inactivate antibiotics via degradation or modification of the antibiotic structure either intracellularly or extracellularly. The degradation of antibiotics typically involves the hydrolysis of specific chemical structure, neutralizing the antimicrobial activity of the antibiotic. Examples of enzymes that degrade antibiotics are β-lactamases, which hydrolyze the β-lactam ring present in penicillin, cephalosporins, and related antibiotics, and the monooxygenase encoded in the ARG *tetX* involved in the hydrolyzation of tetracyclines (Reygaert 2018; Yang et al. 2004). On the other hand, inactivation by modifying the antibiotic structure usually involves acetyltransferases, phosphotransferases, or adenyl transferases that transfer acetyl, phosphoryl, and adenyl groups to the antibiotic (Egorov et al. 2018; Reygaert 2018). Examples of enzymatic modification that inactivate antibiotics include acetylation of aminoglycosides, chloramphenicol, streptogramins, and fluoroquinolones (Egorov et al. 2018; Reygaert 2018).

2.3.3.3. Antibiotic target modifications

Bacteria can undergo genetic mutations or acquire new genes that alter the structure or expression of the target sites that antibiotics would normally interact with. These new traits can involve subtle changes (antibiotic target modification) or the replacement (antibiotic target replacement) of the complete target molecules, or the production of proteins that physically bind to the antibiotic target (antibiotic target protection) (Reygaert 2018; Wilson et al. 2020). These modifications reduce the affinity of the antibiotic to its target, preventing effective binding and subsequent antimicrobial effects. For example, bacteria can alter the structure of penicillin-binding proteins (PBP) located at the bacterial cell wall to reduce the binding sites for β-lactam antibiotics,

making them less susceptible to inhibition (Reygaert 2018). Similarly, mutations in genes encoding bacterial ribosomal proteins can lead to changes in the ribosomal structure, decreasing the binding affinity of antibiotics like tetracyclines or macrolides (Egorov et al. 2018; Reygaert 2018).

2.3.3.4. Reduced permeability

This mechanism involves changes in the structure or composition of the cell membrane that limit the pass of antimicrobial through the cell membrane, thereby reducing their intracellular concentration. For example, a reduction of the expression of porins, which are membrane proteins in Gram-negative bacteria that facilitate the entry of certain antibiotics, can restrict antibiotic uptake, leading to reduced susceptibility (Reygaert 2018). Similarly, mutations that cause changes in the selectivity of the porin channel can also lead to reduced permeability. Moreover, changes in the lipid composition of the cell membrane can also affect its permeability, making it more resistant to certain classes of antibiotics (Reygaert 2018). By limiting drug uptake, bacteria can evade the toxic effects of antibiotics and continue to proliferate in the presence of these drugs.

2.3.4. Horizontal gene transfer

Horizontal gene transfer (HGT) is the movement of genetic material between organisms. It is one of the main evolutionary forces as it facilitates a rapid adaptation to changing environmental conditions through the acquisition of new traits, including catabolic genes, virulence factors and ARGs (Shen et al. 2022). HGT is mediated by different groups of elements known as mobile genetic elements (MGEs), which promote intracellular (within the cell) and intercellular (between cells) DNA mobility (Partridge et al. 2018). There are three main types of HGT processes in bacterial cells: transformation, transduction, and conjugation.

2.3.4.1. Transformation

Transformation is the process by which a bacterial cell takes up free extracellular DNA, in the form of plasmids or chromosomal DNA fragment, from the surrounding environment. This DNA usually comes from other bacteria that have released it through cell lysis. The process involves different chromosomally encoded proteins that facilitate the uptake, integration and functional expression of the extracellular DNA (Frost et al. 2005; Thomas and Nielsen 2005). During the first step, competent bacterial cells express specialized proteins that assemble into complexes that allow the take up of foreign DNA (Solomon and Grossman 1996). This competence status often results as a response to specific environmental conditions, including changes in nutrient availability, cell density, starvation, and/or presence of toxic compounds (e.g., antibiotics) (Thomas and Nielsen 2005). In the following steps, the DNA binds to specific sites on the cell surface and then it is converted into single-stranded DNA and translocated across the membrane. Once in the cytoplasm, the DNA is integrated into the bacterial genome via homologous recombination. For this, the incoming DNA must include sequences (25-200 bp) highly similar to the recipient genome (Thomas and Nielsen 2005). Recombination can lead to the replacement of a corresponding segment of the host genome or the introduction of new genetic material, such as genes or virulence factors. In the case of plasmids, the introduced genetic material can reconstitute the plasmid into a functional form or undergo additive integration with existing plasmids (Thomas and Nielsen 2005).

2.3.4.2. Conjugation

Conjugation is the process of transferring genetic material, usually plasmids, from a donor bacterial cell to a recipient bacterial cell in direct contact, facilitated by a structure known as a conjugation pilus or sex pilus (Thomas and Nielsen 2005). The donor cell harbors the machinery

required to form the pilus (e.g., Fertility-factor = F-factor) and carries a conjugative plasmid. Following the pilus-mediated contact, a specialized protein structure called relaxosome is formed. The relaxosome cleaves the plasmid at specific sequences called the origin of transfer (oriT) and initiates the transfer process (Wong et al. 2012). The plasmid is then mobilized and transferred from the donor to the recipient cell through a structure known as the transferosome (Wong et al. 2012). Once inside the recipient cell, the transferred plasmid can be stabilized and expressed. If the plasmid confers a genetic advantage to the recipient cell, it will be maintained. However, if the plasmid imposes a fitness cost without providing a significant benefit, it may be eliminated (Dionisio et al. 2005). Conjugative plasmids can interact with other genetic elements, such as transposons and insertion sequences (IS), enabling the transfer of chromosomally encoded genes to the plasmid and potentially integrating these genes into the recipient bacterial chromosome (Thomas and Nielsen 2005). Subsequent sections describe the role of different MGEs in the conjugation process.

2.3.4.3. Transduction

Transduction is a mechanism of HGT in bacteria that involves the transfer of genetic material via viruses that only infect bacteria, known as bacteriophages (Frost et al. 2005). Bacteriophages consist of small nucleic acid genome enclosed in a protein shell called capsid. Their genomes typically encode a few essential genes, including replicases, capsid proteins, and components necessary to hijack the host's replicative machinery (Frost et al. 2005). The replication of bacteriophages can be lytic or lysogenic. During lytic replication, the bacteriophage genome remains in the cytoplasm of the host cell and utilizes the host's machinery to produce viral proteins, which are then assembled into multiple copies of the phage, ultimately leading to the lysis and death of the host cell (Kasman and Porter 2022). In contrast, during lysogenic replication, the viral

DNA integrates into the bacterial chromosome, where it is replicated and passed to daughter bacterial cells without killing them. However, environmental stimuli can trigger the viral DNA to enter the lytic cycle, resulting in cell lysis and release of new viral particles (Kasman and Porter 2022). In some cases, during the assembly of new viral particles, fragments of bacterial DNA can be mistakenly packaged into the phage capsids. When these phages subsequently infect another cell, the transferred DNA can then be integrated into the recipient's genome through recombination events (Frost et al. 2005; Kasman and Porter 2022). Transduction can facilitate the transfer of various genetic elements, including ARGs, virulence factors, and metabolic pathways, between bacteria. This process contributes to the rapid spread of these traits among bacterial populations, influencing their adaptability and evolution.

2.3.5. Mobile genetic elements

Mobile genetic elements (MGEs) are segments of DNA involved in the machinery responsible for the movement of DNA between locations withing the genome or between bacterial cells (Frost et al. 2005). These elements play a crucial role in the transfer and dissemination of genetic information and are considered one of the main drivers of the spread of AMR as they tend to capture and accumulate ARGs (Partridge et al. 2018). MGEs can be of different nature and are often classified as plasmids, transposable elements (e.g., transposons, insertion sequences), integrons, and bacteriophages (Frost et al. 2005; Partridge et al. 2018).

2.3.5.1. Plasmids

Plasmids are stable and self-replicating circular DNA molecules that exist independently of the bacterial chromosome. They encode a collection of functional genetic modules, including genes that control the plasmid replication and copy number (Frost et al. 2005). Plasmids associated with AMR also tend to encode a variety of transposable elements, virulent factors, ARGs, and

other advantageous genes (Partridge et al. 2018). Plasmids involved in conjugation processes (conjugative plasmids) include a set of genes known as the transfer or *tra* genes, which encode the necessary machinery for the transfer process (Frost et al. 2005; Partridge et al. 2018). Conjugative plasmids play a significant role in the development and spread of antibiotic resistance. They enable the rapid dissemination of resistance genes among bacterial populations, contributing to the emergence of multidrug-resistant strains. However, various factors, such as copy number and maintenance, as well as the metabolic burden, influence whether these types of plasmids are preserved and inherited by daughter cells (Partridge et al. 2018).

2.3.5.2. Transposable elements

Transposable elements are genetic sequences that can change theirs position within a genome and even jump into another genome or plasmid in a process known as transposition, which often results on mutations or genetic rearrangements. The simplest transposable elements are insertion sequences (IS) elements, which usually includes only one gene encoding an enzyme that catalyze the movement of the DNA segment (transposase) flanked by inverted repeat sequences (Partridge et al. 2018; Thomas and Nielsen 2005). Transposons (Tn) are more complex structures that usually include a variety of genes (e.g., ARGs) in addition to the transposase gene and inverted sequences. Both, IS and Tn are capable of moving almost randomly to other locations in the genome or other DNA molecules (Partridge et al. 2018).

2.3.5.3. Integrons

Integrons are genetic structures found in both plasmids and chromosomes, that facilitate the assembly of functional gene cassettes by incorporating exogenous open reading frames (ORFs) through site-specific recombination (Partridge et al. 2018). Typically, integrons consist of a gene encoding an integrase enzyme (*int*) from the tyrosine-recombinase family, a recombination site

(*attl*), and a promoter (Mazel 2006). Although not all integrons are intrinsically mobile, some are linked to IS, Tn, and conjugative plasmids that serve as vehicles for the intraspecies and interspecies (Mazel 2006). Currently, five different classes of integrons have been associated with AMR. Class 1, 2, and 3 are often found in multiple-antibiotic resistant bacteria as can efficiently capture and incorporate ARGs into the *attl* site, making them available for expression (Mazel 2006).

2.3.5.4. Integrative conjugative elements

Integrative conjugative elements (ICEs) form a diverse group of self-transmissible elements capable of integrating into the host chromosome and replicating. They possess features of both integrative and conjugative elements, making them unique in their functionality. Typically, ICEs are composed of a backbone that encode integration and excision functions, plasmid-like conjugation and maintenance components, an integrase (*Int*), and specific sites where accessory genes are inserted (Partridge et al. 2018). The transfer of ICEs involves the conjugation process, the excision from the chromosome, and the movement and integration into the host chromosome. Due to their ability to carry multiple ARGs, ICEs serve as potent vehicles for the spread of antimicrobial resistance in bacteria (Partridge et al. 2018).

2.3.5.5. Bacteriophages

Bacteriophages are viruses that specifically infect and replicate in bacterial cells. They play a significant role in shaping bacterial genetic diversity as they often mobilize genes between cells via transduction (see section 2.3.4.3). In some cases, ARGs are packed into the viral genetic material and transferred to other cells upon infection, which could potentially lead to the development of new ARB (Kasman and Porter 2022).

2.3.5.6. Additional MGE accessory elements

The transmission of genetic material from one bacterial cell to another can impose a metabolic burden on the recipient cell, often leading to the removal of the newly acquired genetic material. However, MGEs have evolved to accumulate a variety of genes that confer advantageous traits, ensuring their survival within the host cell. These traits encompass AMR, resistance to heavy metals, nitrogen fixation for symbiotic interactions, and the ability to degrade recalcitrant compounds (Frost et al., 2005). The presence of these advantageous genes, along with environmental stimuli, often leads to the transmission and preservation of the new genetic material. It is noteworthy that the co-occurrence of antimicrobial resistance genes (ARGs) and genes encoding other advantageous traits suggests that selective pressures other than antibiotics could also drive the dissemination of AMR in bacteria.

2.4. Methods to determine AMR, ARGs, and MGEs

There are several methods available to assess AMR and determine the presence and abundance of ARGs and MGEs in bacteria. These methods can be classified into three main categories: cultured-based tests, polymerase chain reaction (PCR)-based tests, and next-generation sequencing (NGS)-based tests. The following sections briefly describe some of the main methods, their advantages, and disadvantages.

2.4.1. Culture-based methods

Antibiotic resistance is typically determined using a series of culture-based test known as antibiotic susceptibility testing where bacteria are grown under the presence of different antibiotics (Khan et al. 2019). Bacteria that grow in antibiotic concentrations greater than a previously defined minimum inhibitory concentrations (MICs) are considered resistant to the given antibiotic. The

MICs cut-offs are usually defined by different agencies such as the Clinical and Laboratory Standards Institute and European Committee on Antimicrobial Susceptibility Testing.

While antibiotic susceptibility tests are the ultimate method to determine AMR in clinical pathogenic bacteria, they may not offer reliable results when used for complex environmental samples (Milligan et al. 2023). This is because most bacteria found in complex samples do not grow well in laboratory conditions as they often exist in communities with complex synergistic relationships (Czaplicki and Gunsch 2016). Moreover, the presence of microbial groups intrinsically resistant to antibiotics could influence the results. Nowadays, although there are some culture-based methods to monitor AMR in the environment, they are limited to a handful of microbial genera (e.g., *Acinetobacter, Aeromonas*, *Pseudomonas*) only. Therefore, these methods often do not capture the full picture of the potential for AMR (Milligan et al. 2023).

2.4.2. Polymerase chain reaction (PCR)-based methods

An alternative approach to indirectly assess AMR phenotypes in complex samples with high microbial density is by detecting the presence of antimicrobial resistance genes (ARGs) within the microbial community. PCR is a rapid and cost-effective technique used to amplify targeted DNA fragments. The process consists of a series of cycles that include a denaturation step to split the double strain DNA into two single strain DNA (ssDNA) molecules, and the amplification of a specific DNA fragment limited by two oligonucleotides (primers) thanks to a polymerase capable of surviving temperatures of 94 °C (Zhu et al., 2020). PCR enabled the massive productions of very specific DNA regions that were previously inaccessible, providing the opportunity for more detail and specific studies. PCR is a widely used technique in modern biosciences (Zhu et al. 2020) and stands as a powerful tool to determine the presence of known ARGs and MGEs. Quantitative PCR (qPCR) and reverse transcription qPCR (qRT-PCR) are employed to quantify the number of

gene copies and their expression levels (Boulter et al. 2016), aiding in assessing the abundance of ARGs and their potential impact on AMR. Additionally, PCR arrays that target multiple genes can simultaneously screen for various ARGs, saving time and resources. PCR-based methods have been effectively employed to identify the presence of ARGs and MGEs in both untreated and treated manures (Chapter 4).

However, although PCR-based methods have been invaluable in the study of AMR and other genetic aspects of microbial communities, they also have limitations and disadvantages. For instance, these methods rely on primers designed to target sequences of known ARGs and MGEs, potentially leading to bias towards familiar genes and overlooking novel or uncharacterized resistance markers that do not match the primer sequences. Furthermore, the extensive DNA diversity in complex environmental samples can result in overestimation and false-positives (de Abreu et al. 2021). These methods are often constrained by the number of recognized ARGs or MGEs, and the analysis of multiple genes can be time and resource-intensive, limiting the comprehensive understanding of the evolution of entire resistomes.

2.4.3. Metagenomics

Innovations in DNA sequencing technologies have led to the development of next-generation sequencing (NGS) platforms capable of rapidly sequencing millions of nucleotides within short timeframes. NGS technologies typically involve the random fragmentation of genomic DNA coming from any type of sample, the amplification of the fragments by either cloning (first generation) or PCR (second generation), followed by the sequencing of all the fragments using different high throughput sequencing technologies such as pyrosequencing (Fanning et al., 2017). The random sequences obtained are then assembled by complex computer algorithms to reassemble the original genomes (Czaplicki and Gunsch, 2016; Fanning et al., 2017).

Third-generation sequencing, in contrast, does not include the amplification of the DNA fragments, hence, prevents some of the limitations and bias associated with it (Fanning et al. 2017). The most commonly platforms used for NGS include the Illumina MiSeq, Ion Torrent, PacBio, and Oxford Nanopore (Czaplicki and Gunsch 2016). NGS technologies have allowed the acquisition of highly detailed molecular information never seen before and, consequently, are used in a broad range of applications, including medical diagnosis, gene expression analyses, identification of new microorganisms, and studies of human, animal, and environmental microbiomes (Fanning et al., 2017).

The use of NGS technologies to study the genomes of entire microbial communities derived from complex environmental samples is known as metagenomics. Metagenomics allows for the comprehensive analysis of the functional and taxonomic diversity of microbial communities, as well as their interactions with each other and their environment. Metagenomics is a powerful tool that has revolutionized the study of AMR because it provides valuable insights into the genetic diversity, abundance, and dynamics of ARGs and MGEs. It provides a view of complete metagenomes (all genomes in a microbial community) and the genomic context of ARGs, allows for the quantification of the abundance of known and unknown genes within a microbiome, and facilities the study of the dynamics and evolution mechanisms of ARGs and MGEs (de Abreu et al. 2021). Also, NGS-based metagenomics enables environmental surveillance to monitor the presence of ARGs in natural environments, and agricultural, municipal, and clinical settings (Chen et al. 2017; Ma et al. 2020; Zhang et al. 2011). This has facilitated the identification of community-based antimicrobial resistance, sources of resistance, co-resistance, and potential pathways for transmission (de Abreu et al. 2021). However, while this technology stands as a valuable alternative to study not only the levels of ARGs and MGEs but also their potential relationships

with microbial groups, only a few studies have employed metagenomics to assess AMR in animal husbandry and manure-related environments (Chen et al. 2019). This is further discussed in Chapter 4.

Metagenomic analysis for studying resistomes and mobilomes typically involves several key steps. It starts with the collection of a sample from the target environment, followed by DNA extraction. Next, advanced NGS platforms like Illumina generate millions of DNA sequences, often referred to as "reads." These reads are then subjected to initial processing, which includes the removal of artifacts like sequencing adaptors and low-quality reads. Once quality-controlled, the metagenomics reads are aligned against a relevant database to identify sequences that correspond to known genes. This alignment can be accomplished using two main approaches: read-based methods, where reads are directly compared to the database, or assembly-based methods. In assembly-based approaches, reads are combined into longer contigs, and genes are identified through gene prediction algorithms, followed by alignment with the database. This process helps ensure accurate ARG identification (Arango-Argoty et al. 2016; Bragg and Tyson 2014). Additionally, metagenomic reads can also provide insights into the composition of the microbial community within the analyzed sample. By examining the taxonomic distribution at various levels, this approach allows the study of the relationships between different microbial groups, as well as their connection to ARGs and MGEs (Arango-Argoty et al. 2016; Bragg and Tyson 2014). This holistic perspective contributes to a deeper understanding of the complex interactions shaping antimicrobial resistance in diverse environments.

While metagenomics represents a powerful tool to study AMR, it does come with certain limitations. One primary challenge arises from the incompleteness of databases and the natural variations within sequences, leading to potential underrepresentation or overestimation of ARGs

within a sample (de Abreu et al. 2021). Because metagenomics primarily captures DNA sequences, it falls short of providing insights into gene expression dynamics, functional roles, and the actual phenotypic manifestations of resistance. This limitation can hinder a comprehensive understanding of how ARGs contribute to resistance mechanisms. Furthermore, the intricate relationships between ARGs and MGEs, a pivotal aspect of AMR, can sometimes be inadequately captured in metagenomic analyses. This deficiency can limit our understanding of the mechanisms underlying horizontal gene transfer and its implications for resistance dissemination. Accurately quantifying the abundance of ARGs also poses its own set of challenges. Factors such as DNA extraction methodologies, variations in gene copy numbers, and variations in amplification efficiencies all contribute to the complexity of this task (Bragg and Tyson 2014). Additionally, even the bioinformatic workflows and analytical decisions adopted during the analysis process can wield a significant influence on the final outcomes (Thomas et al. 2012). This underscores the importance of meticulous data handling and interpretation to derive accurate insights. Lastly, the absence of standardized guidelines for metagenomic analysis introduces further complexity (Thomas et al. 2012). Establishing such guidelines is essential to ensure the validity and reproducibility of findings, promoting rigour in this innovative alternative.

2.5. ARGs and MGEs databases

As previously described, the effectiveness of metagenomic analyses rely on the databases employed as references. These databases typically encompass a wide array of DNA and/or protein sequences from various genes, which serve as the basis for annotating metagenomic reads. Therefore, these databases must adhere to coherent and standardized nomenclature and grouping criteria to ensure clarity and consistency. Moreover, to remain accurate and comprehensive, these databases must be continuously updated and expanded to incorporate newly discovered genes. In

the field of AMR, comprehensive and updated databases listing ARGs and MGEs are essential. There are several databases related to AMR, many of which focus on specific environments, mutations conferring resistance in distinct microbial species, or collections of ARGs associated with transposable elements (Alcock et al. 2023). A handful of databases are created by curating available literature and incorporate not only sequences but also the scientific knowledge associated with them. The following sections describe some of the most common databases used in metagenomic analyses for the study of resistomes and mobilomes, mainly those used in this research.

2.5.1. Comprehensive antibiotic resistance database (CARD)

The CARD is a centralized repository of bacterial AMR knowledge that provides a highly curated collection of ARG sequences and associated mutations, their metadata, and analytical tools to facilitate the identification and characterization of ARGs in genomic and metagenomic data (Alcock et al. 2023). The database is organized and structured based on the Antibiotic Resistance Ontology (ARO). ARO provides a structured vocabulary to systematically categorize and describe various aspects of antibiotic resistance, including ARGs, mutations, mechanisms of resistance, the antibiotic they exert resistance to, and associated pathogens (Alcock et al. 2023). The database is regularly updated with new information and is actively maintained by a dedicated team of researchers and bioinformaticians. Currently, the CARD includes information of thousands of ARGs and is considered one of the most comprehensive and reliable resources for the study of AMR.

The CARD can be accessed and downloaded on its official webpage (https://card.mcmaster.ca). All the information and detection models can also be accessed and downloaded on the webpage. Additionally, CARD provides other tools, such as the Resistance

Gene identifier (RGI), which can be used online or as stand-alone tools. The RGI is typically used to determine resistomes in long metagenomics reads such as contigs based on homology and SNP models. Overall, CARD is an important resource for understanding and combating AMR. Its curated collection of resistance determinants and associated antibiotics, along with its analytical tools and resistome predictions, make it a valuable tool for studying AMR in different fields.

2.5.2. BacMet

BacMet is a comprehensive repository of information about bactericide and metal (BacMet) resistance genes. It is a manually curated database containing the sequence of various resistance genes, their metadata, and functional context derived from in-depth reviews of the scientific literature. The database also provides the microbial taxa where the resistance has been described. The second version of the BacMet database includes the sequences of 753 experimentally verified resistance genes and over 155,000 potential resistance genes collected from various public repositories conferring resistance to over 80 different compounds, including metals (e.g., Copper, Mercury, Zinc, Iron, etc.) and aromatics (e.g., toluene, n-hexane, benzene) (Pal et al. 2014). BacMet is a valuable and unique resource for studying AMR, focusing on the intersection and relationships between metal and antibiotic resistance. The information provided in this database is often used to address crucial aspects of resistance mechanisms, co-selection of ARGs, and AMR dissemination. BacMet can be accessed through its webpage (http://bacmet.biomedicine.gu.se/), where users can use a variety of tools to explore and analyze the different resistance genes.

2.5.3. MobileOG

The mobileOG database is a comprehensive manually curated and well-structured database of MGEs and protein families that mediate their lifecycle (i.e., integration, excision, replication/recombination/repair, transfer, and stability/defense). It was created through a process

involving the analysis of more than 10 million protein sequences derived from seven different MGE databases (Brown et al. 2021). The sequences contained in this database are classified into five major categories based on the MGE-associated molecular machinery they are involved. These categories are replication/recombination/repair (RRR), integration/excision (IE), stability/transfer/defense (STD), inter-organism transfer (T), and phage related biological processes (P). Each entry includes distinctive labels associated with their class and a list of keywords that describe the MGE functional modules. Overall, the mobileOG stands from other databases because it includes accessory MGE functional modules which provide more context of the potentially mobility of core MGEs.

The mobileOG database can be accessed and downloaded through its webpage (https://mobileogdb.flsi.cloud.vt.edu/). The home webpage provides several options to allow users explore, analyze, and design custom subsets of MGEs. Overall, the mobileOG database is an important resource for understanding and combating the mechanisms underlying the spread of antibiotic resistance and virulence bacterial populations.

2.6. Resistomes and mobilomes in animal manure

As previously discussed, the extensive use of veterinary antibiotics results in significant quantities of antimicrobials in animal manure. These residual antibiotics can potentially drive the generation and maintenance of ARGs and MGEs within animal manure. Over the last decade, numerous studies have reported the presence of ARGs encoding resistance to various antibiotics in animal manure. These findings have raised concerns about the risk of ARG dissemination into the environment, particularly when manure is used as a soil amendment (Chen et al., 2019; Duan et al., 2019; Heuer et al., 2011; Ruuskanen et al., 2016; Yuan et al., 2020).

ARGs that provide resistance to common veterinary antibiotics, such as tetracyclines, beta-lactams, sulfonamides, and glycopeptides, are typically found in all types of animal manure. However, some studies have also identified resistance to more complex antibiotics like fluoroquinolones (Gurmessa et al. 2020). In general, pig manure tends to contain higher levels of ARGs compared to chicken, cattle, and dairy manure. This difference is often attributed to the greater use of antimicrobials in pig farming operations and the nutrient-rich nature of pig manure (Duan et al. 2019; Yuan et al. 2020).

Animal manures have also been shown as significant MGE reservoirs. The MGEs detected in animal manures include several plasmids (e.g., *pBS228*), different families of transposons and transposases (e.g., *tnpA*, *IS6*, *tn916/1545*), and integrons and integrases (e.g., *intl1*, *intl2*) (Guo et al., 2020; Lu et al., 2020; Ma et al., 2019). These MGEs have been associated with a variety of ARGs in manure microbiomes, confirming that HGT of ARG is likely to happen in manure and even soils amended with it (Guo et al., 2020; Lu et al., 2020). All this underscores the urgent need to find methods to reduce the abundance of ARGs and MGEs in animal manures before they reach the environment.

2.7. Effects of manure management on resistomes and mobilomes

The growing evidence of the presence of high levels of ARGs in and MGEs in manures from farms with limited use of antibiotics demonstrates the need to look for alternatives to reduce the levels of antimicrobial resistance markers. Over the past decade, numerous studies have evaluated how different manure treatment, including aerobic and anaerobic storage, composting, and AD, affect the abundance of ARGs (Chen et al. 2019; Duan et al. 2019; Heuer et al. 2011; Ruuskanen et al. 2016; Wallace et al. 2018; Xu et al. 2019; Yuan et al. 2020). The consensus is that the levels and abundances of ARGs in fresh (untreated) manures are different from those in manure that

underwent some treatment. These differences are likely the results of the distinct microbial successions derived from the specific physicochemical and environmental conditions, such as oxygen levels, and nutrient and carbon availability.

Conversely, the fate of mobile genetic elements (MGEs) during these manure treatments remains an understudied area, lacking sufficient data for conclusive findings. The following subsections delve into emerging patterns regarding the fate of ARGs and some insights into MGEs during common manure treatments, as reported in recent studies.

2.7.1. Aerobic/Anaerobic Storage

One of the most common manure management strategies (treatments) is its storage in either lagoons or open tanks. The process is inexpensive and straightforward as it does not require complex equipment. Manure is usually stored between crop seasons (i.e., fall to spring, spring to fall) before being applied to agricultural land as a soil fertilizer. Since open stored manures are not mixed for long periods, the oxygen availability varies in the different zones. Thus, while the top fraction is primarily aerobic, some hypoxic and even anoxic zones exist at lower levels (Duriez and Topp 2007). These conditions cause substantial changes in the microbial communities as different aerobic and anaerobic carbon degradation pathways are active. For instance, an enrichment of hydrolytic and fermentative communities is observed in stored manures (Jang et al. 2021). However, the microbial dynamics are still unclear.

The ARG fate during manure storage has been poorly assessed, and only a handful of studies have been performed. The available data suggests that this practice could enrich ARB and some ARGs. For example, Wallace et al. (2018) observed higher levels of *tetO* and *sul2* in manures stored in lagoons naturally aerated compared to those in raw organic pig manure, although *tetW* and *sul1* levels remained unchanged. On the other hand, Duriez and Topp (2007) did not observe

any changes in resistance levels of *E. coli* populations in stored pig manures. Nevertheless, no metagenomic analyses have been carried out, so the true resistome evolution in this type of system is unknown.

2.7.2. Composting

The solid fraction of animal manures is commonly composted before being used as a soil fertilizer. Composting is a natural aerobic process where different groups of microorganisms convert the biodegradable organic matter present in biowastes into a stable humus-like product. The process can be separated into three stages: mesophilic, thermophilic, and cooling or maturation (Villar et al. 2016). The mesophilic stage is the initial decomposition where readily biodegradable compounds are rapidly consumed by the mesophilic consortia, generating heat. This heat increases the temperature and leads to the thermophilic stage, where the degradation of complex molecules, including proteins, fats, cellulose, and hemicellulose, is accelerated. The high temperatures also cause a decline in the abundance of non-thermotolerant microorganisms, including animal, human, and plant pathogens (Haug 1993). In the final stage, the temperature decreases again, allowing the establishment of mesophilic microorganisms and humification.

Some studies have suggested that manure composting could reduce levels of some ARGs, although the results are often conflicting. For example, Cui et al. (2016) reported a reduction of levels of ARGs for sulfonamides (i.e., *sul1* and *sul2*), tetracyclines (i.e., *tetA, tetB, tetL, tetM, tetW, tetQ, tetO*, and *tetX*) and chloramphenicol (i.e., *fexA*, *cfr*, and *cmlA*) in chicken manure, and the removal rate improved in composting amended with rice biochar but worsened under the presence of mushroom biochar. Cheng et al. (2019) observed a reduction of ARGs for fluoroquinolones (i.e., *qepA* and *qnrB*) and tetracyclines encoding ribosomal protection proteins (i.e., *tetM*, *tetO*, *tetQ* and *tetW*) and efflux (*tetG* and *tetK*) pumps, although an enrichment of ARGs for tetracyclines

encoding enzymatic inactivation mechanisms (i.e., *tetX*) and sulfonamides (i.e., *sul1*, and *sul2*) was also observed during composting of swine manure. Xu et al. (2019) observed an overall increase of levels in ARGs in pig manure after 120 days composting while Riaz et al. (2020) also observed an increased in the *sul1* ARG during chicken manure composting. There is evidence of the increase of ARG levels on soils amended with composted manure, although these levels are usually lower than those observed in soils amended with untreated manure (Chen et al. 2019; Xu et al. 2019).

The changes in ARG levels during composting have been generally attributed to the microbial successions that take place during the process as a result of the different conditions and operational parameters, including temperature, C/N ratios, moisture, and presence of extraneous substances (e.g., antibiotics, heavy metals, biochar). For example, the reduction of some mesophilic species during the thermophilic stage is considered the main reason for the decline in ARG levels (Cheng et al. 2019; Zhang et al. 2020b). However, this is not always the case since there is also evidence of the enrichment of some ARG, especially efflux pumps, during the thermophilic stage (Cheng et al., 2019). Moreover, higher C/N ratios in manures during composting have also been correlated with the enrichment of some ARGs (Cheng et al., 2019).

The great majority of the studies evaluating ARG changes in manure composting had been based on qPCR to measure specific ARG levels, and only a handful of have made use of metagenomic technologies to analyze the whole resistome (Ma et al. 2020; Yue et al. 2022). The studies using a metagenomic approach provided more insights into the evolution of several ARG and the potential microbial groups carrying them. For instance, different microbial species from the phyla Bacillota (previously known as Firmicute), Actinomycetota (previously kwon as Actinobacteria), Pseudomonadota (previously kwon as Proteobacteria), and Bacteroidota

(previously kwon as Bacteroidetes) were identified as potential ARG carriers, and changes in their levels have been suggested as the ultimately drivers of changes in ARGs (Gou et al. 2018; Wang et al. 2022; Xu et al. 2019).

2.7.3. Manure AD

The AD of livestock manure is a common practice applied in farms around the world due to its numerous benefits. For example, AD can significantly reduce organic matter pollution, odors, and pathogens, concentrate nutrients such as P and N, and the treated sludges (digestate) can be used as a crop fertilizer (Kelleher Environmental 2013; Möller and Müller 2012; Parkin and Owen 1986). Moreover, AD yields biogas, an energy-rich gas primary composed of methane (CH_4) and carbon dioxide (CO_2), which can be used to generate heat and electricity (Cheng 2010). In recent years, AD has also shown potential to reduce the levels of a variety of ARGs in all types of animal manures (Gurmessa et al. 2020), making it an excellent alternative not only to reduce the environmental impact related to greenhouse gas emissions but also to reduce the risk of dissemination of AMR.

Over the past decade, several studies have been conducted to study the fate of common ARGs in livestock manure during AD. As part of this research, the available data in the literature about the effects of AD and its different operational parameters on the levels of ARGs in animal manures was collected and used to conduct a series of meta-analysis. The methodology and results of this study is presented in Chapter 4 of this document and were published in Flores-Orozco et al. (2022). In general, the number and levels of ARGs and MGEs in manure microbiomes are significantly reduced after AD, which is often attributed to the distinctive microbial successions involved in the process. For instance, the decline in microbial diversity and the removal of certain aerobic groups, such as Xanthomonadales, Burkholderiales, and Flavobacteriales, have been

linked to the decrease in ARGs and MGEs (Crossman et al. 2008; Liu et al. 2020; Sun et al. 2016). Additionally, studies have suggested that the elimination of mesophilic communities during thermophilic AD (TAD) may contribute to the reduction of ARGs and MGEs (Wen et al. 2021). However, it is important to note that complete removal of ARGs is rarely achieved in AD, indicating that certain microbial groups intrinsically resistant to specific antibiotics may persist within the anaerobic digester microbiomes or that HGT of ARGs take place in these types of environments.

2.8. Molecular and microbiological mechanisms driving resistome dynamics in manure

2.8.1. Molecular mechanisms

At the molecular level, it is well known that ARGs can be transferred vertically and horizontally (via HGT). Vertical transfer refers to the development of an antibiotic-resistant population from a single microorganism with the mechanisms of resistance mainly encoded in its genome (Franco et al. 2009). Hence, the presence of residual antibiotics can impose a selective pressure in favour of microbial species carrying ARGs for a given antibiotic. Moreover, the presence of other antimicrobials, such as heavy metals, can also exert a selective pressure for ARGs encoded near heavy metal resistance genes (Vats et al. 2022). In these scenarios, the offspring of microbial groups carrying these types of resistance survive and proliferate.

On the other hand, the diverse selective pressures caused by toxic compounds (e.g., lignin, detergents, heavy metals, antibiotics), combined with high microbial densities, make animal manure a hotspot for HGT of ARGs linked to MGEs (Lima et al. 2020). For instance, there is evidence of strong correlations between the changes in MGEs (e.g., *intl1*, *intl2*) and ARG levels in manure treatments such as anaerobic digestion and composting (Qiu et al. 2021; Sun et al. 2019; Yang et al. 2020b; Zou et al. 2020). This suggests that HGT of ARGs occurs frequently and

significantly affects the resistome profiles in manure treatment process. However, how the conditions of the different manure treatments influence HGT remains unclear.

2.8.2. Microbial mechanisms

One of the main factors driving the resistome evolution in different manure treatments appears to be the succession of various microbial communities harboring ARGs that take advantage of the ecological niche during the process (Fan et al. 2020; Liu et al. 2020; Sun et al. 2016; Wu et al. 2020; Yang et al. 2020b). For instance, Liu et al. (2020) observed a reduction in ARG levels during the thermophilic stage of pig manure composting which was strongly correlated with the enrichment of thermophilic microorganisms and a decline in mesophilic communities. Similarly, other studies have reported greater ARG removal rates in TAD compared to MAD due to the reduction of mesophilic bacteria, mainly Bacteroidota and Pseudomonadota, and the enrichment of thermophilic microorganisms (Sun et al. 2016; Yang et al. 2020b). Moreover, the results of the meta-analyses discussed in Chapter 4 suggested that increased levels of hydrolytic communities derived from higher levels of organic matter in AD substrates could be linked to increased levels of ARGs.

The microbial succession involved in different manure treatments, especially during AD, are often significantly influenced by different operational and environmental conditions, such as temperature and addition of other co-substrates (Yang et al. 2020b; Zhang et al. 2017). Therefore, it seems plausible to influence resistomes and mobilomes by shaping microbial communities by changing operational parameters.

2.8.3. Putative ARG hosts in animal manures

Previous studies have suggested several microbial taxa as potential ARG carriers in different manures. Pseudomonadales, Xanthomonadales, Burkholderiales, and Flavobacteriales have been

associated with ARGs for tetracyclines, fluoroquinolones, sulfonamides, and several multidrug (Crossman et al. 2008; Liu et al. 2020; Sun et al. 2016); Actinomycetales with ARGs for fluoroquinolones (Liu et al. 2020); Pseudomonadales and Bacilliales with sulfonamides (Byrne-Bailey et al. 2009) and; Clostridiales and Bacteriodales with ARG for tetracyclines and mls (Jia et al. 2017). ARGs encoding resistance to beta-lactams have been associated with several Bacteriodales, including *Prevotella* (Jia et al. 2017). In the preliminary study carried out in this research project (Chapter 5 and Flores-Orozco et al. (2020a)), microbial groups from phyla such as Pseudomonadota, Bacteroidota, and Actinomycetota were identified as potential ARG carriers in bovine manure. Moreover, strong correlations between typical anaerobes found in mesophilic anaerobic digesters and numerous ARGs, including those conferring resistance to tetracycline, aminoglycosides, glycopeptides, peptides, and fluoroquinolones were also observed. Interestingly, some studies have revealed the existence of a potential selective pressure favouring tetracycline resistance genes in microbiomes in ruminant guts (Sabino et al. 2019). Consequently, it is plausible that microbial groups harboring these ARGs could enter anaerobic digesters, proliferate, and potentially facilitate the transmission of ARGs, given the similarities in conditions between these digesters and animal guts. However, further research is warranted to confirm these findings.

The identification of microbial groups harboring ARGs and MGEs, as well as understanding their biological function in different manure treatments, including AD, is essential to develop targeted strategies to minimize the number and levels of ARGs and MGEs in the final effluent of manure treatment processes and ultimately decrease the risk of the dissemination of AMR in farms and agricultural soils.

2.9. Resistomes and mobilomes in municipal wastewater

Like animal manures, municipal wastewaters are important ARG and MGE reservoirs due to high levels of antibiotics and other selection pressures in an environment with high microbial population density (Nguyen et al. 2021). Different studies have documented the presence of different MGEs and ARGs encoding resistance to several antibiotics, including tetracyclines, sulfonamides, fluoroquinolones, beta-lactams, and glycopeptides in municipal wastewaters (Burch et al. 2016; Lee et al. 2017; Quintela-Baluja et al. 2019; Zhao et al. 2021). The ARGs evolution in wastewaters and wastewater treatments is also attributed to the establishment of microbial communities with distinct resistome profiles combined with HGT via MGEs (Ma et al. 2011; Quintela-Baluja et al. 2019). Recent studies have demonstrated that the resistome profile in the sludge and liquid effluents of wastewater treatments plants are substantially different from each other (Quintela-Baluja et al. 2019), providing more evidence of the importance of the environmental conditions and the microbial populations on the changes in ARG levels in complex matrices.

Despite the distinct conditions and microbial communities in livestock wastewater and municipal wastewater, it is not uncommon to find ARGs encoding resistance to similar antibiotics. This phenomenon may be attributed to the shared usage of certain antibiotics in both human healthcare and veterinary practices. Consequently, investigating the dynamics and evolution of resistomes in both animal and municipal wastewater is vital, as it could provide useful insights to help alleviate the pervasive issue of AMR dissemination across both sectors.

2.10. Challenges and limitations in the study of AMR in manure

The comprehensive study of the evolution of resistomes and mobilomes in microbiomes related to livestock production and manure is crucial to address the global challenge AMR

represents. However, while our understanding of the fate and evolution of some ARGs has increased in the last few years, there are different limitations hindering the development of effective strategies to minimize the dissemination of AMR in this important sector.

One of the first challenges is the study of the complete set of ARGs (resistomes) and MGEs (mobilomes) in the complex and diverse microbial communities in animal manures. Many studies have traditionally relied on qPCR techniques, known for their sensitivity but limited to quantifying a relatively small number of previously characterized genes. This often fails to represent the entirety of resistomes and mobilomes. Furthermore, such techniques may inadvertently introduce biases towards specific ARG families and elevate false positive rates, as detailed in section 2.4.2. While the limitations of qPCR techniques can be circumvented through metagenomics, the associated costs and computational resources have limited its application in studying resistomes and mobilomes within animal manures. Also, the absence of standardized methodologies for analyzing, interpreting, and reporting data further complicates efforts to compare findings across studies. Furthermore, an ongoing debate surrounds whether the presence of ARGs in metagenomic samples genuinely leads to antimicrobial resistance phenotypes.

Another important challenge when studying AMR in complex microbiomes involves attributing specific ARGs to particular microbial species and discerning whether these species indeed express an AMR phenotype. A commonly employed approach for assessing the co-occurrence of ARGs and microbial groups relies on conducting Pearson's or Spearman's Correlation analyses. While this method has provided valuable insights into potential ARG carriers, it often yields high false-positive correlations, thereby impacting the reliability of the results. Moreover, the environment profoundly influences the microbial communities within animal manures. Consequently, this exerts a substantial impact on resistomes and mobilomes,

introducing significant variability and posing challenges for reproducibility. These factors collectively hinder efforts to ascertain the origins and transmission mechanisms of ARGs.

Finally, the study of the diversity and abundance of MGEs in animal manures and how they are affected by manure management strategies has been limited. For instance, the analysis has thus far been restricted to only a handful of genes linked to HGT, such as *int1* and *int2*, along with select transposons and a limited number of plasmids. As of the time of writing, comprehensive metagenomic analyses encompassing the entire spectrum of MGEs within these environments remains absent. Consequently, the precise molecular and microbial mechanisms driving the HGT of ARGs continue to elude our understanding. Overcoming all these challenges is crucial for developing effective strategies to mitigate the spread of AMR in livestock production and manure management, ultimately contributing to global efforts to mitigate this issue.

2.11. Manure AD as a model to study the evolution of resistomes and mobilomes

An interesting approach to overcome all the limitations associated with the study of AMR in animal manures is the use of metagenomics to evaluate the evolution of resistomes and mobilomes as a function of the distinct microbial successions of controlled manure treatment processes. In this context, AD offers a unique microcosm for studying the evolution of resistomes in relation to microbial dynamics. The AD process is characterized by a series of well-defined stages, each dominated by specific microbial communities that perform distinct metabolic functions. As these microbial communities evolve and interact, they influence and are influenced by the surrounding environment and operational conditions. Therefore, specific microbial shifts can be induced by manipulating operational parameters (e.g., temperature, pH, retention times), providing a temporal framework to study the emergence, dominance, and decline of specific ARGs and MGEs.

Moreover, metagenomics could also allow the study of genetic cassettes associated with ARGs and provide insights into the survival and maintenance of AMR markers in complex microbiomes.

The following subsections describe the different stages of the AD process, some of the most important AD operational parameters, the general effects of the different operational parameters on ARGs, and a brief discussion about the limitations revealed by the series of meta-analyses (Chapter 4).

2.11.1. Microbiological fundamentals of AD

Anaerobic digestion (AD) is a complex biological process where several interacting microorganisms transform biodegradable organic matter into biogas in an oxygen-free environment. The process is generally divided into four main stages: hydrolysis, acidogenesis, acetogenesis, and methanogenesis (Figure 2.1). However, it is well known that these different AD stages happen in parallel as the different microorganisms involved in the process depend on each other (Parkin and Owen 1986). Therefore, the balance of the sensitive relationships of the different microorganisms is critical for the stability of the process.

2.11.1.1. Hydrolysis

The first step of the AD process is hydrolysis. Here, complex organic molecules, such as cellulose, hemicellulose, lignin, proteins, and fats are broken down into simpler compounds (e.g., mono- and disaccharides, amino acids, long-chain fatty acids) thanks to the action of extracellular enzymes produced by different group of microorganisms (e.g., *Bacillus*, *Bacteroides*, *Clostridium*, *Desulfovibrio*, *Geobacter*, *Mycobacterium*, *Peptococcus*, *Proteiniphilum*, *Staphylococcus*, *Vibrio*) (Amani et al. 2010). The initial substrate composition determines the hydrolysis rate and the total biogas yield (Demirel 2014). Therefore, the more easily degradable material in the feedstock, the more biogas production can be expected.

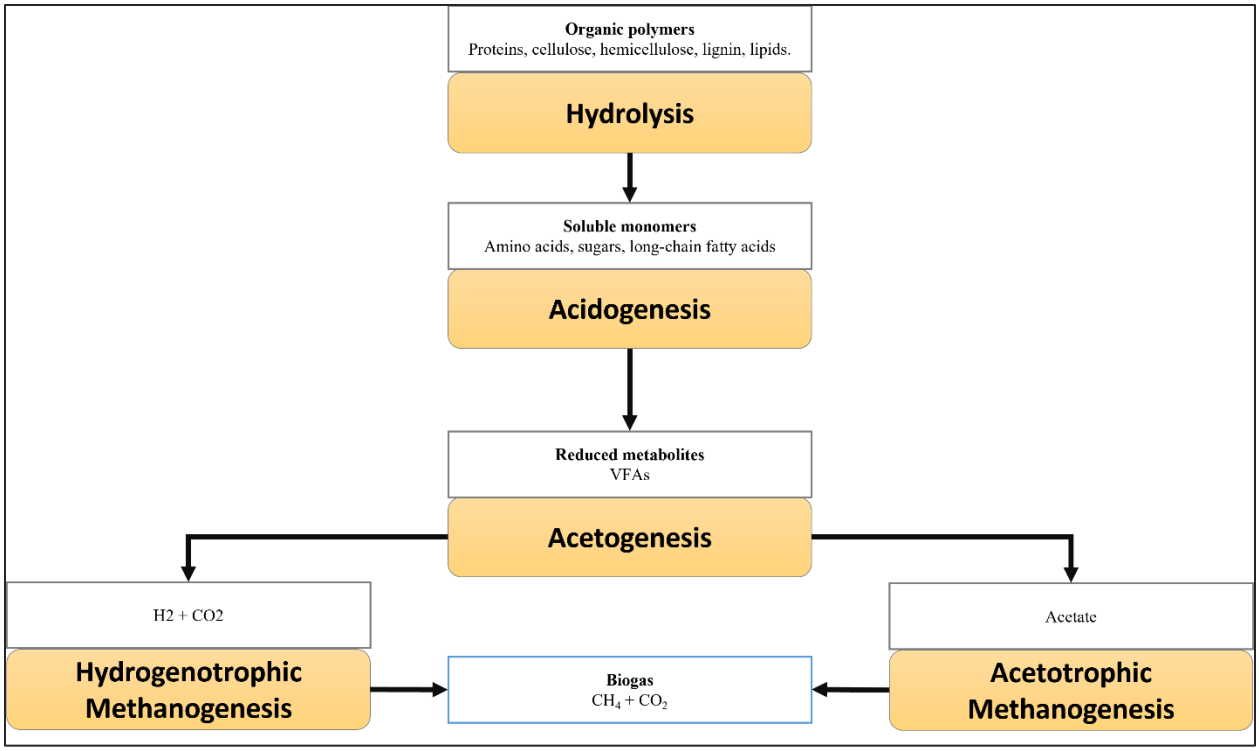

Figure 2.1 Simplified AD process diagram. This diagram illustrates the sequential stages of the anaerobic digestion process, outlining the the conversion of organic polymers to biogas via hydrolysis, acidogenesis, acetogenesis, and methanogenesis.

2.11.1.2. Acidogenesis

The second step is acidogenesis, where molecules produced during the previous stage are transformed into reduce metabolites. The principal products of this stage are lactate, volatile fatty acids (VFAs), some alcohols, H_2, and CO_2 (Cheng 2010). The group of microorganisms involved in this stage are known as acidogens, many of which are also involved in the hydrolysis stage. Examples of typical acidogenic bacteria are *Acetobacterium*, *Bacillus*, *Bifidobacteria*, *Clostridium*, *Lactobacillus*, *Propionibacterium*, *Butyribacterium*, and *Zymomonas* (Amani et al. 2010; Harirchi et al. 2022).

2.11.1.3. Acetogenesis

In acetogenesis, the reduced metabolites produced in the previous stage are transformed into acetate, CO_2, and H_2. The process is mediated by various microorganisms, including *Clostridium*,

Pelotomaculum, *Smithella*, *Syntrophobacter*, *Syntrophus*, *Syntrophomonas*, *Syntrophothermus*, many of which are often associated with hydrogenotrophic methanogens in syntrophic relationships (Amani et al. 2010). Acetogens grow slowly, with a maximum specific growth rate (μ_{max}) of 1 h^{-1} and are sensitive to disturbances (Amani et al. 2010).

2.11.1.4. Methanogenesis

Methanogenesis is the final stage of the AD process, and it is here where the CH_4 is produced. There are two main methanogenic pathways in anaerobic digesters: hydrogenotrophic methanogenesis and acetotrophic methanogenesis. In hydrogenotrophic methanogenesis, H_2 is used to reduced CO_2 to CH_4 in an energetically favorable reaction:

$$4H_2 + CO_2 \rightarrow CH_4 + 2H_2O \quad \text{(Eq. 2.1)}$$

On the other hand, acetate is used to produce CH_4 in the acetotrophic methanogenic pathway:

$$CH_3COOH \rightarrow CH_4 + CO_2 \quad \text{(Eq. 2.2)}$$

About 67% of the CH4 produce during AD comes from the acetotrophic methanogenic pathway, while only about 33% comes from the hydrogenotrophic pathway (Amani et al. 2010; Conrad 1999). The microorganisms responsible for methanogenesis belong to the domain Archaea, mainly from the genera *Methanosaeta* (acetotrophic methanogenesis) and *Methanosarcina* (can use both pathways) (Amani et al. 2010). Methanogens are strict anaerobes and even low oxygen concentrations can severely affect their growth (Sirohi et al. 2010). Typical grow rates of mesophilic methanogens are in the range of 0.05 to 4.07 d^{-1} (Leng et al. 2018).

2.11.2. AD operational parameter

2.11.2.1. Hydraulic retention time (HRT)

The HRT is defined as the time that the substrate spends inside the digester, which is usually the time during which the substrate is consumed in the AD process. In digesters with good mixing

and homogeneous digestates, the HRT is similar to the solids retention time (SRT), which is the time that the solid biomass spends in the digester (Lindmark et al. 2014). Both, the HRT and SRT should be long enough to allow the different microbial groups to grow and avoid microbial populations from wash out. Theoretically, they should be around double the time the lowest microbial groups need to growth. Typical HRT in manure anaerobic digesters range between 10 to 30 days (Komilis et al. 2017).

2.11.2.2. Organic loading rate (OLR)

The organic loading rate (OLR) is defined as the amount of organic matter fed to the digester per volume per unit of time. The OLR is used for digester design and depends on the biowaste characteristics, microbial activity, temperature, pH, toxicity, type of digester, and mass transfer rate between the biowaste and the biomass (Amani et al. 2010; Khanal et al. 2016). The use of co-substrate to increase OLR is a common practice as this boost biogas production. However, acetogens and methanogens are especially sensitive to rapid changes in OLR, therefore, major failures can occur after a rapid OLR change.

2.11.2.3. pH

The optimal pH for the majority of the microbial groups involved in AD process ranges between 6.5 to 8.0 (Amani et al. 2010). Drastic changes in pH may cause methane inhibition and major failures in anaerobic digesters. pH lower than 6 leads to hydrogen production (Cheng, 2010). While the pH can be controlled using acids and alkali, biowastes like livestock manures can provide natural buffering capacity that can help to avoid extreme pH changes and reduce the cost of operation (Amani et al. 2010).

2.11.2.4. Temperature

Temperature is one of the most important parameters of the AD process as many of the biochemical reactions can occur only under specific temperature ranges. Moreover, the operating temperature influences the microbial communities and ultimately the productivity of the process (Tian et al. 2018; Zinder et al. 1984). It has been stablished that temperature fluctuations greater than 3 °C can cause process instability, thus, they should be avoided to ensure productivity (Amani et al. 2010). According to the temperature at which the process is performed, According to the temperature at which the process is perfomed, AD is classified as psychrophilic (10-25°C), mesophilic (30-40°C), and thermophilic (50-65°C).

2.11.2.4.1. Psychrophilic AD

Psychrophilic anaerobic digesters typically operate at ambient temperatures in regions with tropical or subtropical climates, where average temperatures range between 10-25°C. These systems are often straightforward in design, leading to reduced operational costs, especially since there is no need for heat exchangers. However, the cooler temperatures require more robust syntrophic interactions, given that the thermodynamics of AD reactions become less favorable (McKeown et al. 2011). The efficiency of psychrophilic AD is somewhat compromised due to slower biochemical reaction rates. As a result, these systems demand larger digester volumes and extended hydraulic retention times (HRT) of over 50 days (McKeown et al., 2011). Initiating these digesters can be challenging, as the inoculum needs time to adjust to these suboptimal conditions (McKeown et al., 2011).

2.11.2.4.2. Mesophilic AD

Mesophilic AD (MAD) stands as the predominant system for treating various biowastes, including livestock manures (Cheng, 2010). These systems typically function within the 30-40°C

range, which is near the optimal for microbial activity (Amani et al. 2010). Compared to their psychrophilic and thermophilic counterparts, mesophilic digesters offer greater stability and a more straightforward start-up process (Cheng 2010). Their resilience is attributed to a rich microbial diversity, a crucial element in maintaining system stability (Wang et al. 2018). The HRTs and SRTs for these digesters can range from a few days to 30 days, though most operate within a 15–30-day window (Amani et al. 2010). Furthermore, mesophilic digesters can accommodate higher organic loading rates (OLR) of 4,000-12,800 mg/L-d (Bayr et al. 2012).

2.11.2.4.3. Thermophilic AD

Thermophilic AD (TAD) operates within a temperature range of 50-65°C, where peak metabolic rates are typically observed. As a result, these systems often have shorter hydraulic retention times (HRT) of 10-15 days and require smaller digester volumes compared to mesophilic counterparts (Cheng 2010). Enhanced biogas yields and superior organic matter reduction are other notable benefits of TAD (De la Rubia et al., 2012; Wang et al., 2018). A significant advantage of thermophilic digesters is their efficacy in neutralizing most pathogens in sludges, facilitating the safe application of the resulting digestate as a fertilizer on croplands (Cheng, 2010). However, TAD is not without challenges. Initiating these digesters can be a prolonged and intricate process, requiring a mature and robust inoculum. This inoculum should include key microbial populations, which might not be prevalent in mesophilic systems (De la Rubia et al. 2012). Additionally, thermophilic digesters tend to exhibit elevated VFA concentrations. At higher temperatures, acetogenesis becomes more thermodynamically viable, while hydrogenotrophic methanogenesis becomes less so. This dynamic can lead to an accumulation of certain VFAs, like propionate and butyrate, which, at elevated levels, can be detrimental to some anaerobes and induce system instability (Amani et al. 2010).

2.11.2.5. Anaerobic digester configurations

There are many different types of digester configurations that can be used to perform AD. In general, they can be classified as suspended growth and attached- growth depending on the way microorganisms grow.

2.11.2.5.1. Suspended growth digesters

In this type of bioreactor, microorganisms grow freely in the digestate. If there is good mixing, both substrate and microbial biomass are homogeneously suspended, and the HRT and SRT are equivalent. Since the influent (substrate) is diluted as soon as it enters, these types of digesters provide some extra buffering capacity to handle changes in ORL (Cheng 2010). The continuously stirred tank reactor (CSTR) is perhaps the most commonly used reactor of this class. Mixing in suspended-growth digesters can be done by mechanical stirring, gas injection, and hydraulic systems. Mechanical stirring is recommended while using high solid content bio-wastes; gas injection works better in high digesters, whereas hydraulic systems are used when recirculation is needed (Cheng 2010). A representative configuration of a CSTR is shown in Figure 2.2.

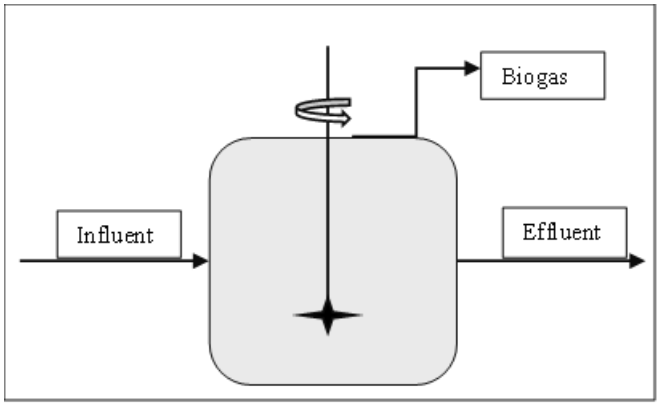

Figure 2.2 Typical CSTR with mechanical mixing.

2.11.2.5.2. Attached growth digesters

In attached-growth digesters, microorganisms proliferate by forming biofilms on the surfaces of support materials. With the biomass being immobilized, these digesters boast higher microbial concentrations and extended solid retention times (SRTs), leading to enhanced performance. They are particularly suited for treating bio-wastes with low organic content, given their reduced hydraulic retention time (HRT) and volume requirements (Cheng 2010). The packed-bed anaerobic digester serves as a prime example of this digester type (see Figure 2.3). This reactor features a bed packed with inert support material, characterized by its expansive surface area and significant porosity. One of the main challenges that these digesters face is the deficiency in mass transfer due to biomass accumulation. However, this issue has been addressed through the development of expanded beds, which, driven by the influent's up-flow, permit the media's movement within the digester (Cheng 2010).

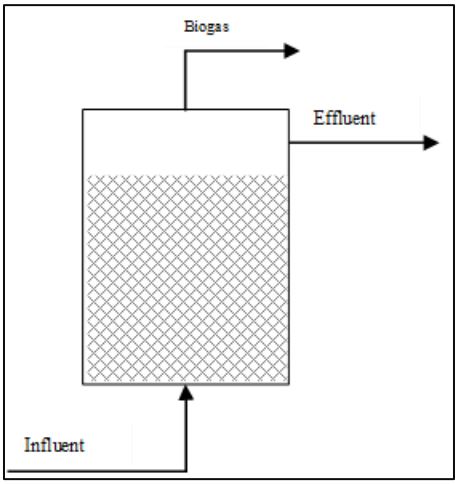

Figure 2.3 Typical up-flow packed anaerobic digester scheme. The influent flows upward through a packed bed. The effluent and biogas are recovered on the top of the reactor.

2.11.2.5.3. Up-Flow Anaerobic Sludge Blanket Digesters (UASB)

The main feature of the UASB is its granule formation, which consists of dense aggregates of diverse microorganisms essential for AD, coexisting symbiotically (Abbasi and Abbasi 2011).

These microorganisms cluster and thrive on the inorganic solids found in the substrate. After several months of incubation, functional granules emerge. In a standard UASB setup (see Figure 2.4), there's a distinct separation of gas, liquid, and solid phases. This configuration facilitates high SRTs, abbreviated HRTs, elevated digestion efficiency, and resilience to both high OLR and toxic substances (Cheng 2010). UASB digesters have proven effective in processing bio-wastes rich in carbohydrates, even with OLRs reaching 20 kg COD/m3-day (Hamza et al. 2016). They offer the advantage of lower capital and operational expenses compared to other digesters and produce minimal sludge.

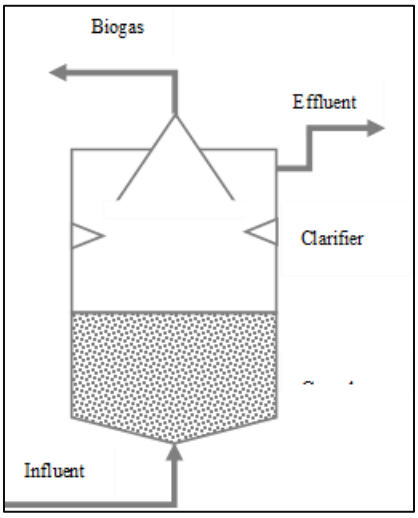

Figure 2.4 Typical UASB digester scheme. The influent enters from the bottom of the UASB digester and moves upward through the biomass granules, facilitating the digestion process. Clarifiers are included for efficient solid-liquid separation, and biogas is collected from the top.

However, UASB digesters are not without challenges. They necessitate extended start-up durations to cultivate a sufficient volume of functional granular inoculum. Bio-wastes abundant in proteins and solids can notably impede the performance of these digesters (Cheng 2010) (Cheng, 2010). Additionally, the effluent produced by UASB is characterized by elevated solid concentrations and specific chemical forms of nitrogen and phosphorus, necessitating subsequent refinement processes (Hamza et al. 2016).

2.11.2.5.4. Anaerobic digesters operation: batch, continuous, and semi-continuous

Depending on the feeding strategies, anaerobic digesters can be classified as batch, continuous, or semi-continuous. Batch anaerobic digesters are characterized by their one-time loading of organic material, which is then sealed for the entire digestion duration, spanning days to weeks. The microbial communities in these systems undergo several changes as there is high nutrients and carbon availability at the beginning, which gradually depletes over time (Peces et al. 2018). Once the digestion concludes, the biogas is harvested, the digester is emptied, and it's prepped for the next batch. This system's primary advantage is its simplicity, making it ideal for smaller operations or when feedstock is sporadically available. However, it has the drawback of inconsistent biogas production. Moreover, batch systems are more susceptible to variations in microbial communities that could impact the process performance as a mature population is not often maintained throughout the process (Peces et al. 2018).

On the other hand, continuous anaerobic digesters receive a steady or near-continuous influx of organic material. As new material is introduced, an equivalent amount of digested material is simultaneously removed, ensuring a consistent volume within the digester and steady biogas production (Cheng 2010). This system is suitable for larger operations with a constant feedstock supply but requires close monitoring to maintain microbial community health and system efficiency. The consistent feed allows microbial communities to stabilize and thrive, as they are continually exposed to nutrients. This often ensures that mature microbial populations are maintained in the digester (Peces et al. 2018).

Semi-continuous anaerobic digesters offer a middle ground, being fed at regular intervals. After each feed, the digester is sealed for digestion, allowing microbial communities to adapt to periodic nutrient availability. This design offers a balance between the batch system's simplicity

and the continuous system's efficiency, making it apt for medium-scale operations with regular but not constant feedstock availability.

2.11.3. Fate of different types of ARGs during manure AD

Another important aspect that should be taken into account when analyzing resistomes in animal manures is the type of resistance encoded in ARGs, since they could provide valuable insights into the potential microbial and molecular mechanisms driving their evolution. It is also possible that the different ARG mechanisms could be associated with other biological functions (e.g., nitrification, denitrification) as previous studies have suggested (Zhang et al. 2019b). The analysis of the raw data used for the meta-analyses in Chapter 4 and published in Flores-Orozco et al. (2022) suggested that the changes in ARG levels encoding distinct resistance mechanisms could be different (Figure 2.5). For example, around 50% of the ARG encoding resistance mechanisms classified as antibiotic target alterations were reduced in cattle manures at mesophilic temperatures, whereas about 75% of efflux pumps were reduced under these conditions. Most mechanisms were reduced to a greater extent at thermophilic temperatures in cattle manures except antibiotic target protection. Antibiotic target protection mechanisms are common in Gram-positive bacteria (Reygaert 2018), so it is possible that the abundance of these types of microorganisms at mesophilic and thermophilic conditions was not very different in cattle manures.

The analyses also showed that all mechanisms were reduced to a much lower extent in pig manures at mesophilic temperatures than thermophilic temperature (Figure 2.5). These differences were more prominent in target protection, target alteration, and antibiotic inactivation mechanisms. Interestingly, the proportion of efflux pump ARGs reduced in pig manures was smaller than in cattle manures. This could suggest that the efflux pump may play an important role in other

biological functions in the microbial populations of pig manure anaerobic digesters. However, more studies are required to test this.

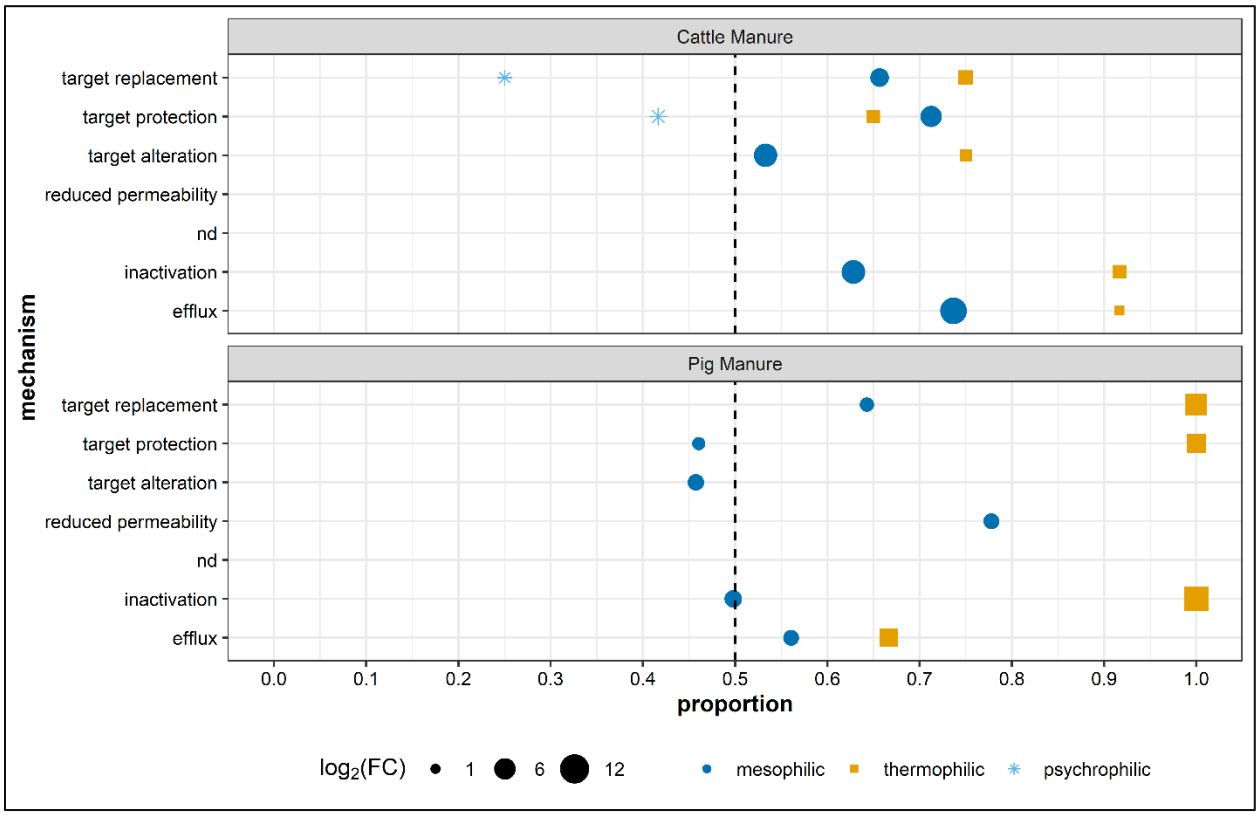

Figure 2.5 Proportion of ARG reduced by ARG mechanisms of data collected for meta-analysis. The size of the figures indicates the $\log_2$ of the fold-changes as described in Chapter 4. Color indicates the temperature at which AD was performed.

2.11.4. Limitations on the study of the fate resistomes during AD

An important aspect that the meta-analysis of the available literature (Chapter 4) revealed was the scarcity of long-term studies investigating the impact of AD on resistomes. For instance, a significant majority of studies have been conducted in small batch digesters, typically with volumes less than 1 L, and for relatively short durations, often less than 20 days. It's well-established that the microbial communities within anaerobic digesters can exhibit substantial variation depending on whether they operate under batch, continuous, or semi-continuous feeding systems (Peces et al. 2018). Given the profound influence of microbial communities on resistomes,

it's reasonable to question whether changes in ARG profiles observed during batch AD accurately represent the dynamics within longer-operating, mature microbial communities associated with continuous or semi-continuous AD systems.

Additionally, the meta-analysis (Chapter 4) revealed a predominant reliance on qPCR techniques in studies investigating the effects of AD on ARGs, with only a limited number of studies employing metagenomics to comprehensively assess entire resistomes. This distinction is vital because the fate of a select few genes may not accurately depict the behavior of entire resistomes during AD. Additionally, there is a notable gap in our understanding regarding how mobilomes and genes conferring resistance to other compounds, such as heavy metals, evolve during manure AD. Since MGEs, such as plasmids, often accumulate various ARGs and other advantageous genes, the absence of detailed insights into their behavior during AD limits our grasp of the mechanisms responsible for the maintenance and dissemination of ARGs. Addressing these limitations is critical for advancing our comprehension of ARG dynamics during AD and, by extension, mitigating antimicrobial resistance.

2.12. Summary and outlooks

In light of the current gaps in the literature, the following chapters of this thesis explore some of these limitations, aiming to provide valuable insights into the molecular and microbial mechanisms driving the evolution of resistomes in animal manures that could ultimately be used to develop strategies for mitigating AMR in this sector. Some of the challenges addressed in this thesis include:

- Using the available data to determine significant effects of different AD parameters on ARGs and determine current limitations. This is explored with a series of meta-analyses in Chapter 4. Here, the main hypothesis was that AD could significantly

reduce the ARG levels in animal manure. The secondary hypothesis was that variation on operational parameters (e.g., temperature, HRT, pH, type of manure) could have significant effects on ARGs.

- The use of metagenomics to evaluate the effect of different manure treatments on full resistomes and mobilomes, as well as on genes conferring resistance to other compounds (e.g., heavy metals, disinfectants) used in animal husbandry. This is described in Chapter 6. The main hypothesis in this chapter was that different manure treatments could have distinctive effects on resistomes and mobilomes.
- The evaluation of the long term-effects of MAD on resistomes and mobilomes in animal manure using metagenomics. This is described in Chapters 5 and 7. The main hypotheses was that the AD process could significantly reduce the levels of ARGs and MGEs, and that this effect would be maintained over time.
- The comparison of the long-terms effects of MAD and TAD on resistomes and mobilomes in bovine manure. This is explored in Chapter 8. Based on the results of the meta-analyses (Chapter 4), the main hypothesis in this chapter was that TAD would not outperform MAD in reducing ARGs and MGEs.
- The evaluation of the co-occurrence of ARGs, MGEs, and microbial communities with the objective of determining potential molecular and microbial mechanisms driving the changes of resistomes and mobilomes. This is explored on Chapters 5-8. The main hypothesis was that distinct shifts in microbial populations (e.g., decline in aerobic communities) would be associated with the reduction of ARGs and MGEs.

Chapter 3: Material and Methods

3.1. Preface

To avoid redundancy throughout the different chapters, this section describes the methods that are common to more than one of the subsequent chapters. It describes the operation and maintenance of the main anaerobic digester used in this research, physicochemical analyses, DNA isolation, and some of the metagenomic analyses. Specific methods applied to a particular chapter are described in that chapter.

3.2. Anaerobic digesters setup and operation

A Continuously Stirred Tank Reactor (CSTR) was set up under mesophilic conditions using a 15-L New Brunswick Scientific vessel with a BioFlo 110 controller. The operational temperature was maintained at 35°C, with a mixing speed of 120 rpm. Both the HRT and SRT were set at 30 days. The digester featured a feeding port and a gas sampling port. The latter connected to a Wet Tip Meter via 4.8 mm ID silicone tubing, with an added liquid trap line for condensation capture. A 1.55 mm ID tube was integrated into the gas line, connecting to a Micro GC (Agilent, US) for in-line biogas composition analysis. The digester's design is illustrated in Figure 3.1, and its operational state is depicted in Figure 3.2.

This CSTR was inoculated on August 21st, 2017, with 2 L of digestate from the anaerobic digester of the Winnipeg North End Sewage Treatment Plant and 2 L of bovine dairy manure. Over the next month, approximately 1 L of manure was added weekly until the volume reached 8 L. Thereafter, the digester was fed with manure generally three times a week (e.g., Mondays, Wednesdays, Fridays). The feeding procedure consisted of increasing the mixing rate to 450 rpm to resuspend particulate and floating material, sampling the biogas contained in the head space, and removing digestate and adding manure through the feeding port. The volume of the digestate

removed and manure fed manure was approximately 0.622 L, maintaining 8 L working volume and 30 days HRT. This digester was used for the studies described in Chapters 5, 6, 7, and 8. In Chapter 7, the digester is referred as the mesophilic digester (MD).

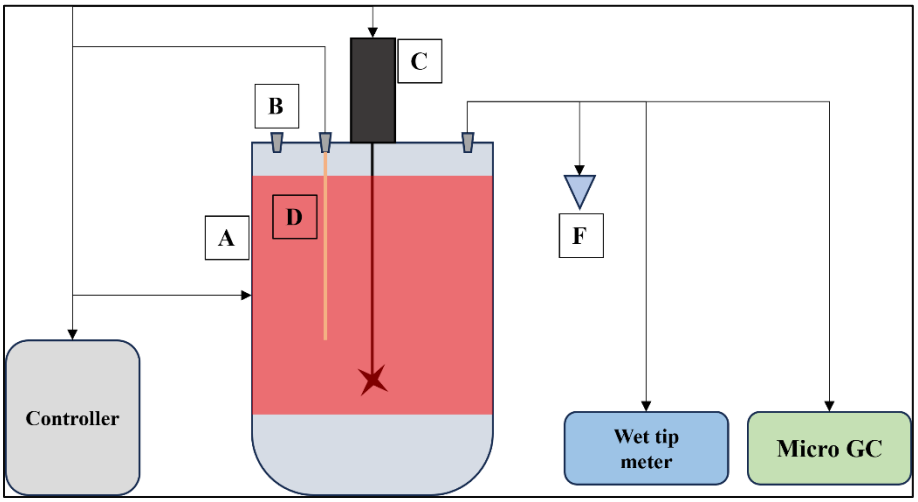

Figure 3.1 Anaerobic digester scheme. A: heating jacket. B: feeding port. C: mixer. D: Temperature probe. F: water trap.

Figure 3.2 Operating mesophilic anaerobic digester.

3.3. Bovine manure

The bovine manure used to feed the digester was sourced from two local dairy farms. Approximately every 3 months, a manure batch was collected from the farm and strained through a 6.35 mm mesh to remove large particles and rocks. The manure used during the first 18 months was collected from the main manure pit of a medium-size dairy farm (200 milking cows) located in Winkler, Manitoba. Thereafter, the manure batches were collected from a larger farm (600 milking cows) located in Rosser, Manitoba. Each batch was divided into feeding portions (~0.63 L) and stored in 800 mL plastic containers at -20°C. Prior to digester feeding, these portions were thawed to room temperature. Comprehensive analyses of the manure batches were conducted, assessing COD, dCOD, TS, VS, alkalinity, and VFAs. Additionally, samples designated for DNA isolation and metagenomic sequencing were preserved at -20°C until further processing.

3.4. Biogas analysis

Biogas production was quantified using a Wet Tip meter, which was calibrated to register every 100 mL of biogas generated. This instrument features an internal magnetic counter that logs each tip, triggered by a specific volume of gas flowing through one of its two chambers. The cumulative biogas produced was calculated by multiplying the total tip counts by the pre-calibrated volume per tip. Then, the volume of the biogas produced was normalized to standard volume at the average room temperature (22 °C).

Methane (CH_4), Carbon dioxide (CO_2), Hydrogen (H_2), Oxygen (O_2), and Nitrogen (N_2) in the biogas contained in the headspace of the digesters were measured using a chromatograph Micro GC 490 (Agilent, USA) equipped with two thermal conductivity detectors (TCD) and two different columns. Methane, H_2, O_2 and N_2 were separated using a Molsieve/5A Plot column with Argon (Ar) as carrier gas. An HP-PLOT U column was used to separate the CO_2 content using Helium

(He) as carrier gas. The chromatograph was calibrated on sampling days using a 50% CH_4 - 50% CO_2 gas mixture (Praxair, Canada) and air (78% N_2, 22% O_2) and occasionally with natural gas (98% CH_4) and different N_2, CO_2, and H_2 gas standards (Praxair, Canada)

3.5. Physicochemical analyses

Total alkalinity, total solids (TS), and volatile solids (VS), were determined following the Standard Methods 2320B, 2540B, and 2540C, respectively (APHA 1995). Total and dissolved chemical oxygen demand were measured with a closed reflux colorimetric method using HACH TNT 822 vials (Method 8000). The dissolved COD (dCOD) samples were filtered through 0.45 µm syringe filters (Wyvern Scientific, Canada) before the analysis. The pH was measured with a pH 5 Acorn potentiometer (Oaklon, Canada) which was calibrated daily with a pH 7 buffer (Thermo Scientific, USA).

3.6. Volatile fatty acids (VFAs)

The VFA samples were centrifuged at 3,000 g and the supernatant filtered through 0.2 µm nylon membrane syringe filters (Wyvern Scientific, Canada). The VFA profile entailing formate, acetate, propionate, iso-butyrate, butyrate, iso-valerate and valerate, was determined by high-performance liquid chromatography 1515 (Waters, USA) with a refractive index detector 2414 (Waters, USA). A resin-based column (AMINEX®, HPX-87H) was used for separation using 0.005 M H_2SO_4 as mobile phase with a flow of 0.80 mL/min at 60 °C. A 10mM VFAs standard solution (Sigma-Aldrich, Canada) was used to generate a 5 point-standard curve for each VFA and then it was used to estimate VFA concentrations.

3.7. DNA isolation

DNA was isolated from untreated, treated, and digested manure samples as follows. First, samples were added to 1.5 mL DNase-free micro tubes and centrifuged at 13,000 g for 10 min.

Then, the PowerSoil DNA extraction kit (Omega Bio-tek, USA) was used to isolate DNA following the method recommended by the manufacturer. The DNA concentration was determined using a NanoDrop 1000 (Thermo Fisher Scientific, Canada). DNA samples were stored at -20 °C in 1.5 mL DNase-free and RNase-free microcentrifuge tubes.

3.8. Whole genome sequencing

DNA samples were sent to Genome Quebec Innovation Centre (Montreal, Canada) for sequencing following the instructions provided by the institute. There, the DNA library was prepared with a NEB Ultra II system and shotgun metagenomic sequencing was performed in an Illumina MiSeq PE250 platform. During the length of this research, three different sample batches were analyzed. In each batch, individual samples accounted for around 1/20 to 1/25 of the total sequencing reads.

3.9. Metagenomics

All metagenomics analyses were conducted in the online platform Galaxy. Galaxy is an open-source platform designed to make computational biology accessible to researchers who might not have deep expertise in computational methods (Afgan et al. 2018). It provides a web-based interface where users can perform and reproduce complete bioinformatics analyses. Galaxy can be accessed through the following link: https://usegalaxy.eu/. A diagram describing the general workflow of the metagenomic analyses is shown in Figure 3.3.

3.9.1. Quality control

Trimmomatic v0.38 (Bolger et al. 2014) was used to trim Illumina adaptors and remove low-quality sequences. The process involved trimming four bases from both the start (leading) and end (trailing) of a read if they fell below the set quality threshold. Additionally, sliding window trimming, a prevalent method for excising low-quality segments of reads, was utilized with a

window size of four and a minimum quality score of 20. Any reads with a length less than 20 bases were discarded. The quality of the reads after trimming was checked using FastQC, a popular tool that provides a set of analyses, including per base sequence quality, per base sequence content, per sequence GC content, sequence length distribution, duplication levels, overrepresented sequences, and adapter content. Quality-controlled reads of individual samples ranged from 400,000 to 850,000.

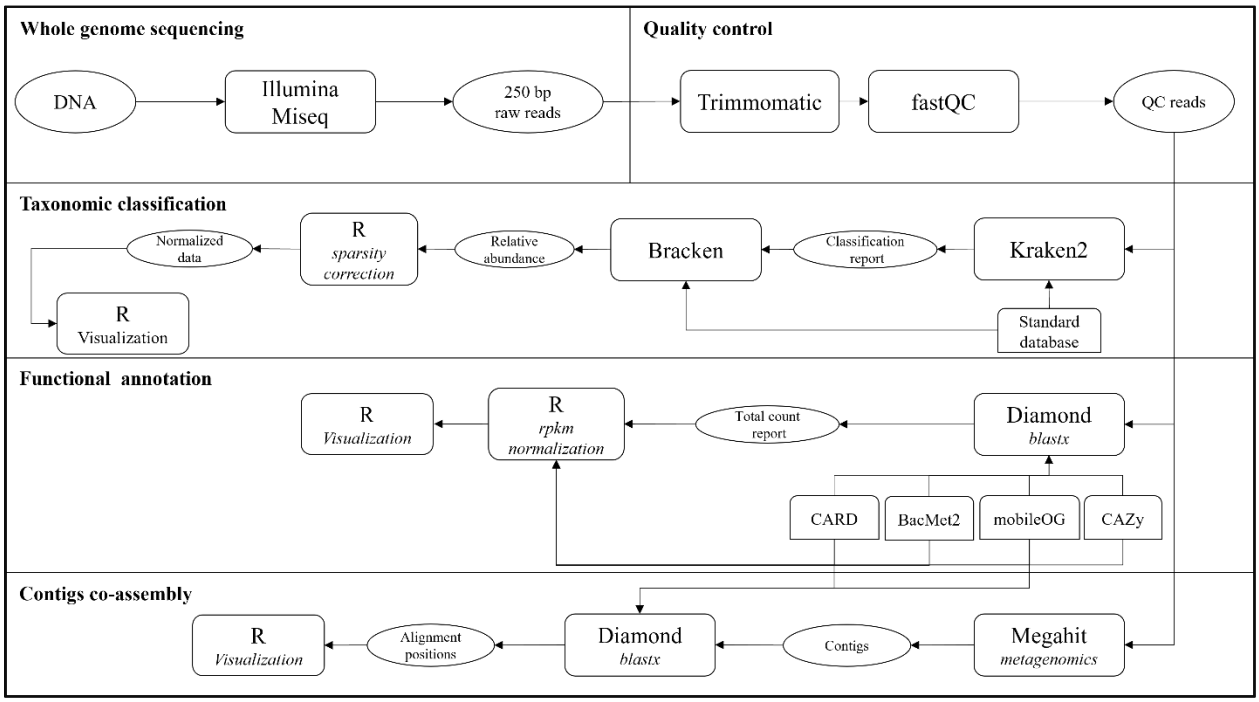

Figure 3.3 Workflow scheme of metagenomic analyses.

3.9.2. Taxonomic annotation

Kraken2 v2.1.1 was used to perform the taxonomic classification of the quality-controlled metagenomic reads. Kraken 2 operates by breaking input sequences into short subsequences called k-mers. It then checks each k-mer against its pre-built database to determine possible taxonomic labels. After checking all k-mers in a sequence, Kraken 2 uses the Lowest Common Ancestor (LCA) algorithm to assign a single taxonomic label to the sequence (Wood et al. 2019). For this

study, the fast operation mode was used with a confidence threshold set at 70%. A sequence required a minimum of 5 k-mer groups to be deemed a match for a specific taxon. The reference database used was the Kraken2 standard database, dated May 17, 2021, which comprises k-mers extracted from the accessible genomes.

The Bayesian Reestimation of Abundance with Kraken (Bracken) was used to estimate the relative abundance of the different microbial groups detected in the metagenomic reads. Bracken uses the k-mer distribution information from the Kraken database to reassign sequences that were classified at higher taxonomic levels. Through a Bayesian approach, it redistributes these sequences to provide more accurate species-level abundance estimates in metagenomic data (Lu et al. 2017). The taxon identifiers were used to update the taxonomic nomenclature to match those in the NCBI as of April 05, 2023.

3.9.3. Functional annotation

The presence and abundance of ARGs, bactericide and metal resistance genes (BacMet), and MGEs in quality-controlled reads were determined using DIAMOND blastx v2.015 (Buchfink et al. 2014). DIAMOND is a high-throughput sequence aligner for protein and translated DNA searches, designed for analyzing large-scale metagenomic data. It is often used as an alternative to BLASTX due to its speed, achieving BLAST-like sensitivity at much faster speeds (Buchfink et al. 2014). DIAMOND was operated in sensitive mode with the following parameters and thresholds: e-values < $1e^{-10}$; identity percentage > 90%, query (read) coverage > 90%; maximum number of query hits < 2; and a minimum of 25 amino acids. The reads were aligned to the CARD, BacMet2, and mobileOG databases. In some chapters, the abundance of carbohydrate-active enzymes in manure and digestate microbiomes was analyzed. For this, quality-controlled reads were aligned to the carbohydrate-active enzyme (CAZy) database following the same procedure.

3.9.3.1. CARD

The CARD database version 3.1 (Alcock et al. 2023) was employed to identify ARGs within the metagenomic reads. The FASTA files, along with the functional details of the ARGs from this version, were sourced directly from the official website (https://card.mcmaster.ca/download). From this database, functional attributes such as the antibiotic resistance ontology (ARO) number and name, gene length, antibiotic class, and resistance mechanisms were extracted. Adjustments were made to ensure a consistent nomenclature for the ARGs, and any duplicate entries were eliminated. ARGs that encoded resistance to multiple antibiotic family classes were categorized under 'multidrug' ARGs. Those that encoded resistance to macrolide, lincoside, and streptogramin were labeled as 'mls'. For ease in subsequent analyses, entries in the FASTA files were renamed based on the ARO names. All these processes were executed using R.

Following the initial curation, the database encompassed 2,767 distinct ARGs, with lengths varying between 159 bp and 4356 bp, with a median of 858 bp. A detailed distribution of these gene lengths is available in Figures A3.1 and A3.2 in the appendices. The predominant resistance mechanism among these ARGs was antibiotic inactivation, accounting for 2,098 entries. This was followed by antibiotic efflux (255), antibiotic target alteration (204), antibiotic target protection (147), and antibiotic target replacement (57), as shown in Figure 3.4. Only six ARGs were identified to encode the reduced permeability resistance mechanism in this CARD version. When categorized by antibiotic class, beta-lactams had the highest representation with 1,686 ARGs. This was succeeded by multidrug (292), aminoglycoside (189), fluoroquinolones (118), mls (104), and tetracyclines (77), as illustrated in Figure 3.5.

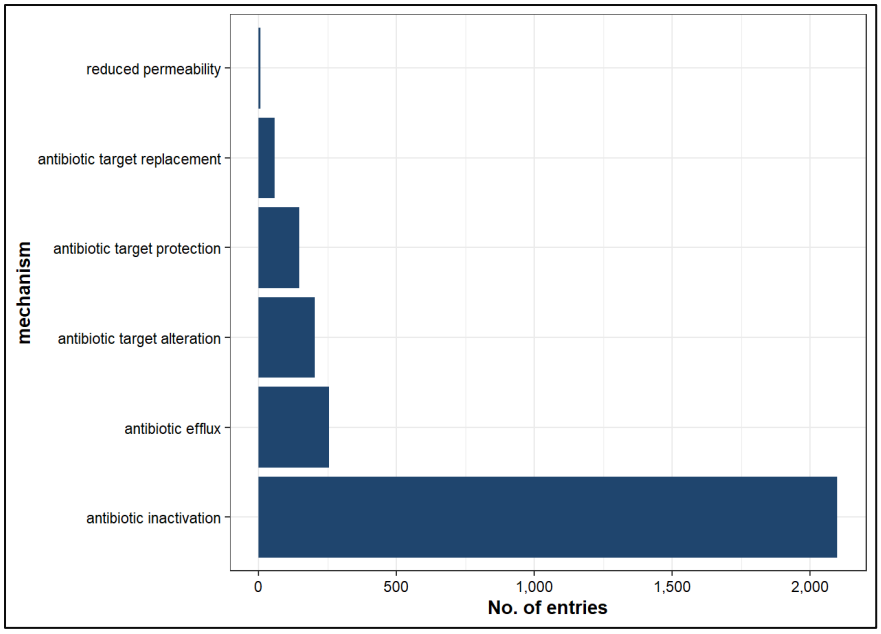

Figure 3.4 Distribution of ARG mechanisms in CARD.

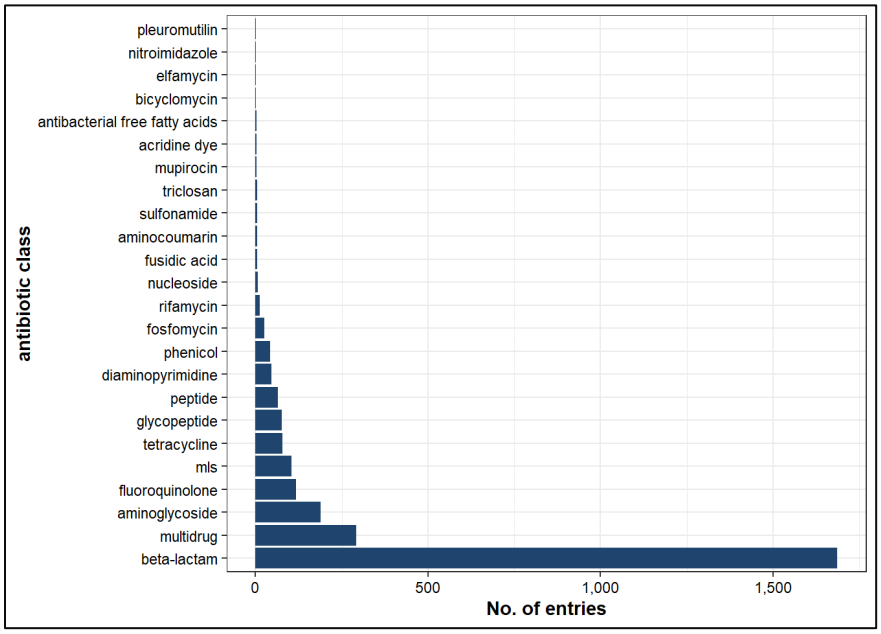

Figure 3.5 Distribution of ARG antibiotic classes in CARD.

3.9.3.2. BacMet2

The second version of the experimentally confirmed BacMet database (Pal et al. 2014) was used to identify genes conferring resistance to bactericides and metals (BacMet) resistance genes.

The FASTA files and functional information were downloaded from the official webpage (http://bacmet.biomedicine.gu.se/download_temporary.html). This functional annotation encompassed a range of details, including gene names, accession numbers, the originating organism of the gene, its location (e.g., Chromosome, plasmid), and the specific compounds to which the genes provide resistance. Text mining was applied to extract the broader compound class associated with each gene. Genes conferring resistance to more than 1 class were groups as multi-resistance. A comprehensive list of these compounds and their respective classes is presented in Table A3.1 in appendix A. It's worth noting that certain gene nomenclatures required adjustments for alignment with the database.

In total, BacMet2 consisted of a total of 753 entries, representing 607 distinct genes, with some genes appearing in multiple instances. The length of these genes spans a range from 159 bp to 4644 bp, with a median of 942 bp, as shown in Figures A3.3 and A3.4. The majority of genes listed in the database encoded resistance to heavy metals (419), followed by multi-resistance (254), acids (24), phenolic compounds (13), and quaternary ammonium compounds (QUACs; 11). The distribution across different compound classes is illustrated in Figure 3.6. When considering the genomic location of these genes, a majority (74%) are encoded on chromosomes, while the remaining 26% are plasmid encoded.

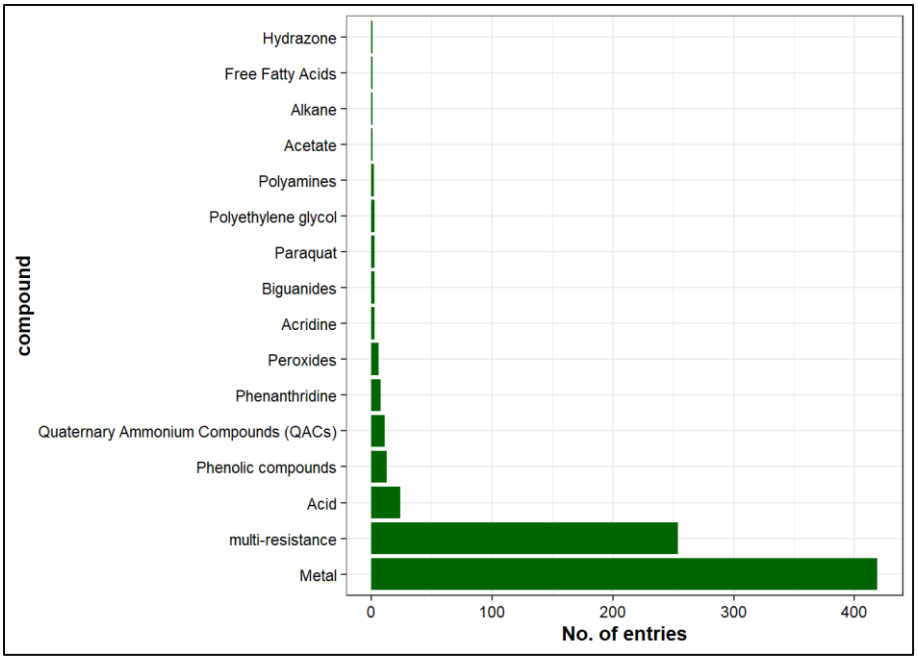

Figure 3.6 Distribution of compound classes in BacMet2 database.

3.9.3.3. MobileOG

The mobileOG version 1.5 (Brown et al. 2021) was used to identify MGE and other genes associated with the transfer of genetic material. The FASTA and functional data were downloaded from the official webpage: https://mobileogdb.flsi.cloud.vt.edu/entries/database_download. The information extracted from the functional annotation file included the mobile ids, MGE names, the gene category based on the MGE-associated molecular machinery, mode of action description. The database boasts a total of 394,701 entries, representing 10,551 distinct genes. Notably, some genes have multiple entries due to their characterization across different species. The gene lengths within this database span from 45 bp to 15,585 bp, with a median of 789 bp as detailed in Figures A3.5 and A3.6.

In terms of gene categories, those associated with phages dominate with 113,522 entries. This is followed by genes related to replication, recombination, and repair (90,544 entries),

integration and excision (71,881 entries), transfer (64,879 entries), and stability, transfer, and defense (53,875 entries). The distribution across these categories is presented in Figure 3.7.

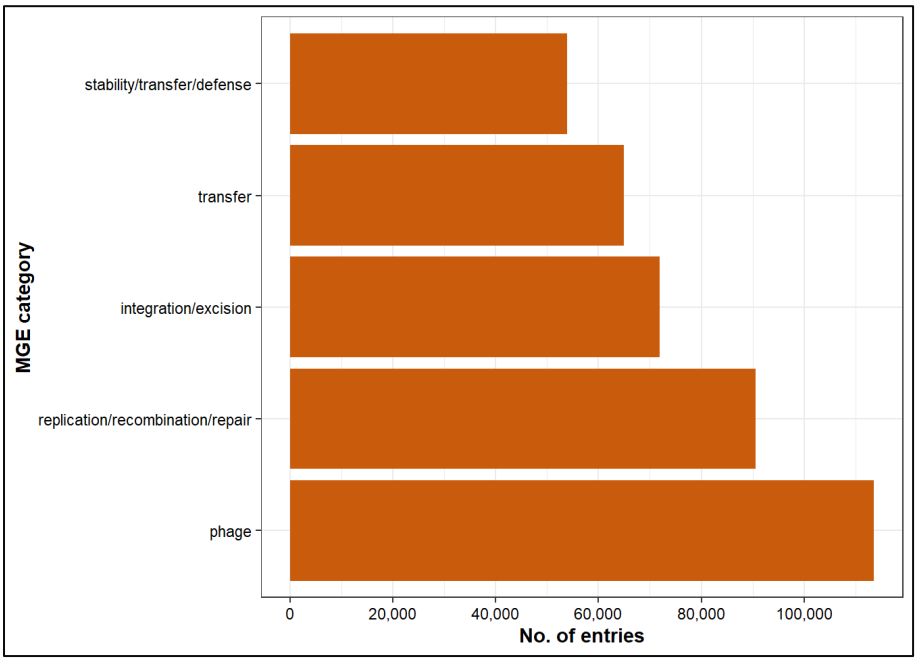

Figure 3.7 Distribution of gene categories in mobileOG database.

3.9.3.4. CAZy

The CAZy FASTA file was downloaded from the official webpage (http://www.cazy.org/) in July 2021. The functional information contained in the headers of the FASTA file, including gene names and enzyme families were extracted using text mining techniques as shown in the R code in this repository: Linkto_GitHub. The CAZy enzymes (CAZymes) families defined in this database are glycoside hydrolases (GH), glycosyl transferases (GT), polysaccharide lyases (PL), carbohydrate esterases (CE), carbohydrate binding modules (CBM), and auxiliary activities (AA), as described in (Drula et al. 2022).

There were 2,161,786 entries representing the same number of different genes. The gene lengths of range from as little as 18 bp to 119,031 bp, with a median of 1,257 bp. A detailed distribution of these gene lengths is illustrated in Figures A3. 7 and A3.8, located in the appendices.

The most abundant enzyme family was GH which accounted for 42.7% of all entries, followed by GT (40.3), CBM (9.8%), CE (4.6%), PL (1.6%), and AA (0.9%) as shown in Figure 3.8.

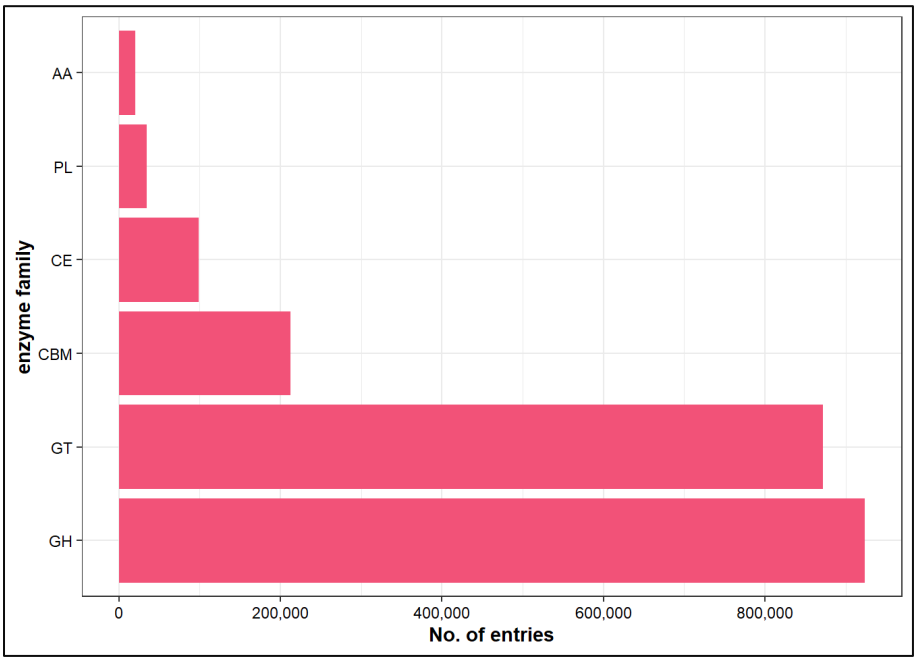

Figure 3.8 Distribution of CAZymes families in CAZy database.

3.9.4. Contigs co-assembly and analysis

Since the number of metagenomic reads in individual samples was not suitable for individual assembly, a co-assembly approach was followed. It consisted of generating contigs with all the sequences of each group of samples (e.g., manures from the same farm, same conditions digestates, etc.) using MEGAHIT, a widely used and efficient de novo assembler designed for large and complex metagenomics sequencing datasets (Li et al. 2015). The default parameters, including a list of k-mers ranging from 21 to 141, and a minimum contig length of 1,000 bp were used for this task. The co-assembled contigs were aligned to the CARD, BacMet, and mobileOG databases using DIAMOND blastx with a stricter criterion to find a match and allowing a maximum of 2 hits per contig (e-value < 1e-10, identity percentage > 90%, subject coverage > 60%, maximum number

of query hits = 2). The position of MGEs, ARGs, and MGEs was also determined in contigs where these elements co-occurred.

3.9.5. Data normalization

3.9.5.1. Sparsity of microbiome data

One of the main challenges of the analysis of microbiome data is sparsity. Sparsity refers to datasets where a large portion of the data consists of zeros or missing values. These zeros can represent either true absences of microbial species in a given sample or a lack of detection due to various reasons, such as sequencing depth or methodological limitations. Statistical analyses are often inefficient in sparse data as there is loss of statistical power, introduction of bias, increase variability, and violation of assumptions (Kumar et al. 2018). To address this problem, a Bayesian-multiplicative replacement was applied to reduce the sparsity of the microbiome data using the R package *zCompositions* (Palarea-Albaladejo and Martín-Fernández 2015).

3.9.5.2. Genes abundances

The total number of times (C) a specific gene was found in each DIAMOND output was calculated. Then, this number, which represented the absolute abundance of each gene in each sample, was normalized to the number of quality-controlled sequences and length of the genes and reported as reads per kilobase million (rpkm):

$$rpkm = \frac{C \; x \; 1{,}000{,}000}{R \; x \; L} \qquad \text{(Eq. 4.1)}$$

Where R is the total number of reads after quality control, L is the gene length in kilo bp, and 1,000,000 is the scaling factor.

3.9.6. Co-occurrence analyses

Co-occurrence analyses were performed to identify microbial groups potentially harboring ARGs and MGEs in untreated and treated manure samples in Chapters 6, 7, and 8. These analyses

consisted of two main parts. Firstly, the Spearman correlation coefficients of ARGs, MGEs, and microbial groups (at genus level) were calculated. Spearman correlations were chosen as non-linear relationships between ARGs and microbial genera were assumed. Secondly, the R package *cooccur* was used to apply the probabilistic model of species co-occurrence described in Veech (2013). Then, microorganisms that co-occurred at a significantly higher frequency (p-value < 0.025) with ARGs and MGEs and had positive and significant correlation coefficients ($r > 0.50$, p-value < 0.05) were defined as potential ARG and/or MGEs carriers. This approach reduced spurious correlations and helped to reduce false positives, a common problem in correlation analyses (Zou et al. 2020).

3.9.7. Metagenomic data analysis and visualization

The R software was used to generate the multiple plots used in this research. Several packages, including *ggplot2*, *metacoder*, *pheatmap*, and *igraph*, were employed for these tasks. Details about how the different plots were created are described in each Chapter. R was also used to perform all statistical tests. The code for the data analysis and visualization of Chapters 6, 7, and 8, as well as the code for the database adaptation can be found can the following GitHub repository: https://github.com/floresod/Metagenomics.git.

3.10. Data availability

A total of 40 samples were sequenced in this research. The metagenomic reads of all these samples were submitted to the NCBI and stored in two repositories. The BioProject accession number of these repositories are PRJNA1020798 and PRJNA1031688. The former contains the samples used in Chapter 6, while the former contains the samples used in Chapters 5, 7, and 8. The distribution of samples in each repository is shown in Table A3.2 in the appendices. These data will become publicly available on April 01, 2024.

Chapter 4: Influence of AD operational parameters on ARGs in animal manures

4.1. Preface

This Chapter is a systematic review of the literature in the form of a series of meta-analyses on the effects of AD on ARG levels. This work was peer-reviewed and published as original research in the journal *Science of the Total Environment* in 2022 in a manuscript entitled "*A meta-analysis reveals that operational parameters influence levels of antibiotic resistance genes during anaerobic digestion of animal manures"* (http://dx.doi.org/10.1016/j.scitotenv.2021.152711). The chapter explores the effect of different AD operational parameters, such as temperature, substrates, HRTs, and feeding configurations on ARG levels. It also discusses the differences between the use of PCR techniques and metagenomics to evaluate resistomes. I alone was responsible for the data collection and analysis, interpretation of the results, and the preparation of the manuscript. The other co-authors provided thoughtful and challenging discussions on the results and reviewed the manuscript prior to publication. Minor modifications were made to the original manuscript to adjust the style to this document.

4.2. Abstract

Anaerobic digestion (AD) has shown the potential to reduce the numbers and types of antibiotic-resistance genes (ARG) present in animal manures. However, the variability of the results has limited the ability to draw solid conclusions. To address this issue, a series of meta-analyses were conducted to assess the impact of AD on ARG levels in pig, cattle, and dairy manures. The analyses also considered various factors, including temperature, pH, digestion durations, and the introduction of other elements like solids and antibiotics. Twenty studies with enough details on changes in ARG levels during the AD process were identified and used for the meta-analyses. The results suggested that AD could significantly reduce ARG levels regardless of

the conditions of the process. Also, thermophilic AD was more effective than mesophilic AD at reducing ARGs, although this difference was only significant for pig manures. The results also suggested that long digestion times (> 50 days) yielded better ARG reduction rates, and that the addition of solids from an external source (co-digestion) negatively affected the efficiency of ARG reduction. In general, the results suggested that ARG changes during AD may be linked to the abundance and activity of hydrolytic communities.

4.3. Introduction

During the last decade, several studies have assessed how ARGs change during traditional manure treatments, including aerobic and anaerobic storage (Wallace et al. 2018), composting (Cheng et al. 2019; Cui et al. 2016), and AD (Gurmessa et al. 2020; Sun et al. 2016; Zou et al. 2020). Most of these studies indicated that ARG could only be partially reduced during manure treatments and that, in some cases, they could even be enriched.

Among all manure treatments, AD is of particular interest not only because of biogas recovery and the ability to degrade veterinary antibiotics (Gurmessa et al. 2020), but because the engineered environment and the understanding of the essential microbial dynamics that drive the process. This makes AD an excellent option to model how resistomes evolve as a function of microbial successions, and how operational parameters affect the ARG fate. Several studies have evaluated how ARG changed during AD of animal manures under different operating conditions, including different temperatures (i.e., psychrophilic, mesophilic, thermophilic) (Sun et al. 2016; Wen et al. 2021), digestion times, the addition of co-substrates (co-digestion and high-solids AD) (Song et al. 2017; Sun et al. 2019), and the presence of toxic components (e.g., antibiotics, heavy metals) (Lu et al. 2020; Zhang et al. 2018b; Zou et al. 2020). These studies have enabled the identification of putative ARG hosts and potential microbial mechanisms associated with changes

in ARG levels. For example, the decline in the abundance of aerobic communities during AD of animal manures was associated with a reduction in ARG levels in the work described in Chapter 5 and Flores-Orozco et al. (2020a). Similarly, the removal of mesophilic species is suggested as the main driver of ARG reduction in thermophilic digesters (Wen et al. 2021).

The results from studies examining the impact of AD on ARG levels have been notably varied and at times contradictory, making it challenging to ascertain how specific AD parameters might affect ARG levels. Consequently, the design of optimized process to maximize ARG removal rates has not been possible. For example, while thermophilic AD typically outperforms mesophilic AD in reducing ARG levels (Sun et al. 2016; Zou et al. 2020), some studies have reported that this is not always the case (Huang et al. 2019). Also, although several studies have quantified ARG levels at different time points of the AD process, it is still unclear if shorter or longer digestion times would benefit ARG removal efficiency. This between-study variability could be attributed to many factors, such as unique biochemical characteristics of manures (as a function of farms operations) and subtle differences in environmental conditions (e.g., temperatures, pH, presence of toxic substances) that lead to the establishment of microbial populations with distinctive ARG profiles (resistomes). Additionally, since ARGs often reside within MGEs, spontaneous HGT might influence resistome development. The absence of standardized methods to assess and quantify ARGs in intricate environments, coupled with the diversity in experimental designs, further amplifies result discrepancies.

Given the extensive data available, a meta-analysis serves as a valuable statistical approach to compare outcomes from different studies, shedding light on trends regarding how various parameters might influence ARG shifts during animal manure AD. In this study, we gathered observations from several studies that evaluated changes in ARG levels in anaerobic digesters fed

with pig, cattle, or dairy manure and performed a series of meta-analyses (and subgroup meta-analyses) to determine: i) if manure AD significantly reduces ARG levels; ii) how AD operational parameters influence ARG changes, and iii) if the ARG changes quantified with metagenomic tools were comparable to qPCR observations. In this context, the respective hypotheses were that: i) AD significantly reduces the levels of ARGs; ii) variations in common operational parameters influence ARG levels, and iii) qPCR and metagenomic analyses yield comparable results for detecting ARGs. This work represented the first systematic review in the form of a meta-analysis in this subject at the time of the submission.

4.4. Methodology

4.4.1. Search strategy, study selection, and data extraction

A search was conducted in English-language literature for studies assessing changes in ARG levels in animal manures (specifically pig and cattle/dairy manures) after mesophilic, thermophilic, or psychrophilic AD. The Scopus platform was utilized for this search with the keywords: "*anaerobic digestion*," "*antibiotic resistance genes*," and "*manure*." The search was limited to studies published up to June 30, 2021.

Studies were selected if they met the following criteria: i) pig and cattle or dairy manure were used in the study in batch, fed-batch, or continuous digesters; ii) individual ARG fold-change (digestate levels/manure levels) or ARG levels in raw and digestate manure that allowed the calculation of the ARG fold-change were reported; iii) ARG levels were normalized to the microbial biomass (e.g., 16S rRNA, total or volatile solids), studies reporting absolute levels were not included; iv) results were presented in a readable format (e.g., bar or scatter plots, tables). Studies presenting results in heatmaps-like plots were not included as inferring an accurate value was not possible.

The primary dependent variable for this study was the fold-change of ARG levels after the AD process for each unique ARG. In the cases where studies reported ARG levels in raw and digestate manure in readable plots, the on-line platform "WebPlotDigitizer" (Rohatgi 2021) was used to extract the values. Then, the fold-change (FC) for each ARG was calculated as follow:

$$FC = \frac{final}{initial} \quad \text{(Eq. 3.1)}$$

where, final represents the ARG levels in digested manure, and initial represents the ARG levels in the raw manure.

Table 4.1 Explanatory variables definitions.

Variable	Level	Definition
Quant. Method	metagenomics	Use of next-generation sequencing followed by ARG annotation
	qPCR	Use of traditional qPCR technologies for quantification
Manure	cattle/dairy	Dairy or cattle manures
	pig	Pig manures
Temperature	mesophilic	Temperatures 30-40°C
	psychrophilic	Temperatures < 30°
	thermophilic	Temperatures > 50°C
Setting	batch	Batch culture
	continuous	Fed-batch or continuous feeding digesters
HRT	hrt_g1	Digestion times < 10 days
	hrt_g2	Digestion times 10-35 days
	hrt_g3	Digestion times 35-50 days
	hrt_g4	Digestion times > 50 days
pH	5	pH 5.0-5.9
	6	pH 6.0-6.9
	7	pH 7.0-7.9
	8	pH 8.0-8.9
	nd	pH no specified
Volume	full-scale	Reaction volumes > 50L
	lab-scale	Reaction volumes 1-50L
	small-scale	Reaction volumes < 1L
Treatment	antibiotics[1]	Digestion supplemented with antibiotics
	metal	Digestion supplemented with heavy metals
	NT	Digestion with no supplements (usually control experiment)
	other	Digestion supplemented with other material such as zeolite, graphene oxide, Dnase, and lignite
	solids	Digestion supplemented with lignocellulose from an external source (i.e., wheat or corn straw)

1: Antibiotic studied included tetracyclines, beta-lactams, sulfonamides, fluoroquinolone.

When multiple time points were reported (e.g., day 3, 5, 15), the same strategy was followed to calculate the FC using the ARG concentration at each time-point. Explanatory variables, including the type of manure, temperature, technology for quantifications (qPCR or

metagenomics), digestion times (HRT), pH, volume (small, lab, or full-scale), settings (batch or continuous), and additional treatment, were also extracted from each study. More details about the definition of these variables are presented in Table 4.1.

4.4.2. Data transformation and response variables

The ARG fold-changes (FC) were $\log_2$ transformed to center the data and generate a symmetric distribution to ease further analyses. The $\log_2$(FC) of the ARG with undetermined values due to concentrations below detection levels in either raw or digested manures were manually set to -12 and +12 for very large reduction and very large increase, respectively involving results where one component may either be below the detection threshold or above saturation.

The second response variable considered in our study was the proportion of the number of ARG reduced after the AD process (P_{red}), which was defined as follows:

$$P_{red} = \frac{\#ARG_{red}}{obs_{total}} \quad \text{(Eq. 3.2)}$$

where, P_{red} is the proportion of ARG reduced after the AD process in each group (e.g., study, condition, variable), $\#ARG_{red}$ is the number of ARG reduced (final < initial) in the given group, and obs_{total} is the total number of observations in the given group.

4.4.3. ARG classification

The CARD database version 3.1.1 (Alcock et al. 2023) was used to classify ARG according to the type of antibiotic they produce resistance to (antibiotic class) and the mechanism by which they exert the effect. ARG whose mechanisms were not specified were defined as not determined (nd).

4.4.4. Data analysis

4.4.4.1. Preliminary analyses of explanatory variables

To start off, the differences in the ARG changes, $\log_2$(FC), within the levels of each explanatory variable were assessed to determine if the variability they introduced could potentially affect the results of the meta-analyses. For this purpose, the observations were grouped by variable and their respective levels, and their central tendencies (e.g., average and median) were compared. Three main assumptions were considered: i) no difference between the changes of the different types of ARG (resistome level analysis); ii) observations of all studies were equally valid, thus comparable; iii) no variable other than the one being analyzed had a substantial effect on the response variable.

Since a preliminary data exploration indicated that the observations in the different levels of the explanatory variables were not normally distributed (not shown), non-parametric statistical tests were performed. Briefly, the Mann-Whitney test was used to compare the medians of the variables with two levels, whereas the Kruskal-Wallis tests followed by the *post-hoc* multigroup comparison Dunn tests were used in variables with three or more levels. An alpha value of 0.05 was considered in all statistical tests. Bonferroni adjustments in Dunn tests were also implemented to reduce the risk of type I errors (false positives). All statistical tests were performed in the software R.

4.4.4.2. Meta-analyses

Two different approaches were followed when performing meta-analyses. The first approach consisted in using the $\log_2$ transformation of the magnitude of the ARG changes (Eq. 3.1) as the response variable. In the second approach, the proportions of number of ARG reduced (P_{red}, Eq. 3.2) were used. Given the high heterogeneity and variability in experimental designs and results,

even within studies, the estimation of a single effect per study was not optimal. Therefore, in order to decrease the within-studies variability, unique AD conditions (combinations of explanatory variables) within the same study were considered independent observations (K) as they could reflect a distinctive effect. This approach also helped to increase the statistical power of the meta-analyses as the number of observations increased. The effects were estimated considering that the changes in ARG levels and proportions did not depend on the type of ARG or their mechanisms and assuming that the ARG quantified in each study represented the whole resistome.

The random-effects model was used to pool effect sizes since substantial between-study heterogeneity was expected. The DerSimonian-Laird estimator (DerSimonian and Laird 1986) was used to calculate the heterogeneity variance ($\tau 2$), and Knapp-Hartung adjustments (Knapp and Hartung 2003) were used to calculate the confidence intervals around the pooled effects. The inverse-variance pooling method with a continuity correction of 0.005 was used for the P_{red} meta-analyses. The packages *dmetar* (Harrer and Cuijpers 2019) and *metafor* (Viechtbauer 2010) were used to perform the meta-analyses in the software R.

Subgroup meta-analyses were performed on all explanatory variables to determine if these AD parameters could influence the changes on ARG levels. All explanatory variables were considered because the analysis of the raw data suggested they could account for some of the variability of the results. Independent estimates of the between-study heterogeneity were calculated for each sub-group. The risk of bias in general and subgroup meta-analyses was evaluated using funnel plots combined with Egger's test, which assesses the correlation between standardized effect estimates and the standard errors. Egger's tests and funnel plots were performed in R using the *metafor* package.

Results were considered statistically significant when the 95%-confidence intervals did not include the non-effect limits (0.5 and 0.0 for $\log_2$(FC) and P_{red}, respectively). Significant differences between groups were considered when the 95%-confidence intervals did not overlap.

4.5. Results

4.5.1. Search results and general aspects of the data

The search in Scopus detected 89 entries, of which 19 passed the criteria (Figure 4.1). Additionally, one unpublished data set on resistome evolution during mesophilic AD of dairy manure from our group was also included for a total of 20 studies (N). This non-published data was the one used in Chapter 7. The list of studies is shown in Appendix B. The total number of unique conditions (K) was 68, while the total number of observations was 2,322. A list with the unique conditions and references are presented in Table B4.1 in Appendix B. The observations included 392 unique ARGs, encoding resistance to 20 different antibiotics (Figure 4.2). ARGs for tetracyclines represented 25.4% of the observations, followed by multidrug (17.4%), macrolide-lincosamide-streptomycin (*mls*, 16.9%), sulfonamide (9.4%), beta-lactams (5.5%), and aminoglycosides (5.6%). All ARG were classified into six types of mechanisms, including efflux pump (28.1%), antibiotic inactivation (21.7%), target alteration (16.6%), target protection (15.7%), target replacement (10.7%), and reduced permeability (0.40%) (Figure 4.3). The cases where no mechanism was defined were included in the 'nd' category (6.7%).

The main features of the collected data are shown in Table 4.2. From the 20 studies, 17 (85%) used qPCR to quantify ARG, and only three studies (15%) used metagenomic techniques (i.e., next-generation sequencing). However, the observations from metagenomic studies accounted for around 60% of the total number of individual observations. Half of the studies used cattle or dairy manures, and the other half used pig manure. The majority of the studies evaluated

mesophilic AD (95%), 20% thermophilic AD, and only 5% psychrophilic AD. Fifteen studies (75%) carried out the experiments in batch reactors with less than 1 L volume, whereas the rest used semi-continuous and/or continuous reactors with larger volumes. Most observations were made at digestion times between 10-35 days (hrt_g2, Table 4.2), although digestion times greater than 50 days were also observed. The pH of the AD processes ranged from 5-8, with pH 7 being the most common (~ 50% of all observations). Finally, although 75% of the observations were made in AD processes with only manure as substrate (NT treatments), a significant number of observations were made in digesters amended with other substances, including antibiotics, heavy metals, foreign solids (e.g., corn and wheat straw), and other materials (Table 4.2).

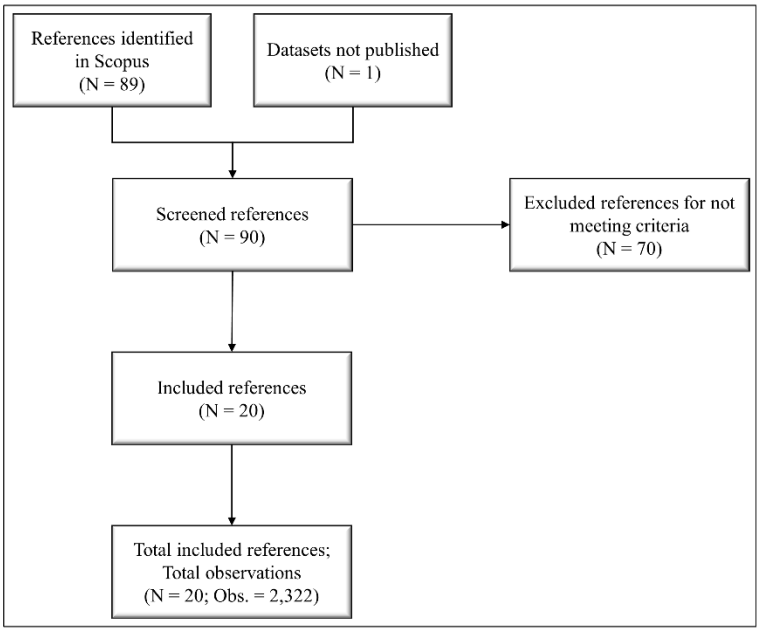

Figure 4.1 Data collection and criteria application flow diagram.

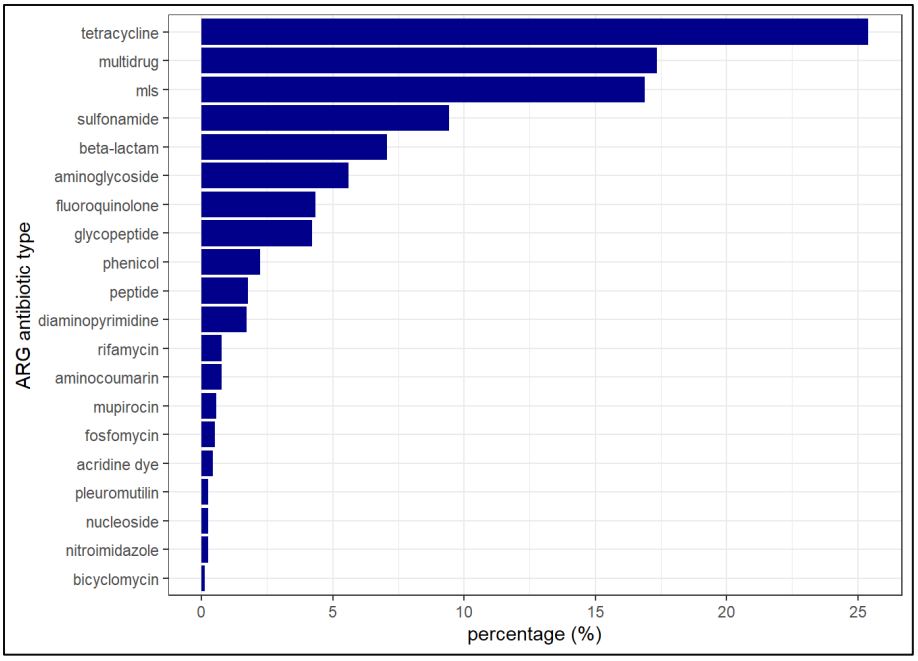

Figure 4.2 Distribution of ARG antibiotic classes in raw data.

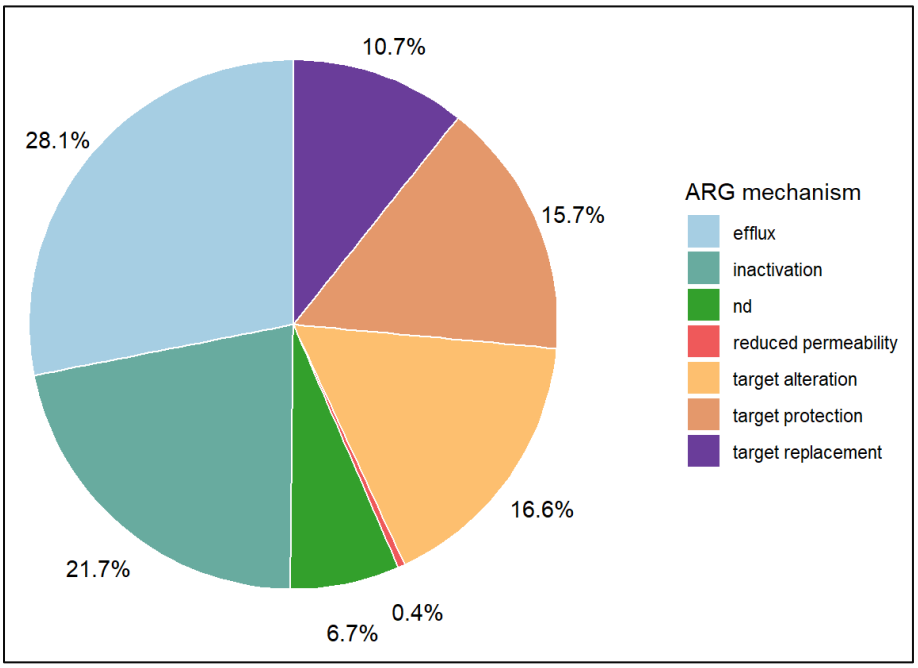

Figure 4.3 Distribution of ARG mechanisms in raw data.

Table 4.2 Prevalence and effects of explanatory variables on resistomes in raw data.

Variable	Level	N	%(N)	obs	%(obs)	avg_{FC}	SD_{FC}	med_{FC}	sig	$\#ARG_{red}$	P_{red}	avg_{red}	med_{red}	$\#ARG_{inc}$	P_{inc}	avg_{inc}	med_{inc}
Quant. Method	metagenomics	3	15.0%	1379	59.4%	-2.45	7.4	-0.87	*[1]	814	0.59	-7.02	-8.12	488	0.35	4.80	1.90
	qPCR	17	85.0%	943	40.6%	-0.79	3.08	-0.28		558	0.59	-2.27	-1.21	378	0.40	1.39	0.96
Manure	cattle/dairy	10	50.0%	1062	45.7%	-2.96	7.95	-1.27	*	700	0.66	-5.22	-2.44	361	0.34	3.36	1.38
	pig	10	50.0%	1260	54.3%	-0.77	3.57	-0.11		672	0.53	-1.38	-1.06	505	0.40	3.29	2.01
Temperature	mesophilic	19	95.0%	2183	94.0%	-1.77	6.18	-0.43	a	1272	0.58	-3.76	-2.27	827	0.38	1.08	0.71
	psychrophilic	1	5.0%	32	1.4%	1.68	3.85	0.76	b	11	0.34	-7.20	-12.00	21	0.66	5.26	1.76
	thermophilic	4	20.0%	107	4.6%	-2.95	3.62	-1.94	c	89	0.83	-2.89	-1.52	18	0.17	1.92	1.17
Setting	batch	15	75.0%	936	40.3%	-0.78	3.08	-0.28	*	552	0.59	-2.28	-1.21	377	0.40	1.40	0.97
	continuous	5	25.0%	1386	59.7%	-2.44	7.38	-0.86		820	0.59	-6.98	-7.95	489	0.35	4.79	1.89
HRT	hrt_g1	7	35.0%	190	8.2%	0.03	1.69	0.00	a	93	0.49	-1.13	-0.66	95	0.50	1.17	0.78
	hrt_g2	15	75.0%	1832	78.9%	-2.01	6.65	-0.59	b	1086	0.59	-5.81	-3.50	666	0.36	3.94	1.59
	hrt_g3	5	25.0%	135	5.8%	-0.43	1.44	-0.36	a,b	85	0.63	-1.22	-0.92	50	0.37	0.93	0.54
	hrt_g4	6	30.0%	165	7.1%	-2.30	4.29	-1.06	b	108	0.66	-4.31	-2.70	55	0.33	1.56	1.50
pH	5	3	15.0%	39	1.7%	-1.89	3.96	-0.32	a, b	25	0.64	-3.42	-1.34	14	0.36	0.83	0.71
	6	3	15.0%	182	7.8%	-0.64	2.16	-0.26	a, b	110	0.60	-1.64	-1.04	71	0.39	0.91	0.65
	7	12	60.0%	1126	48.5%	-2.53	7.73	-0.87	a	698	0.62	-6.97	-12.00	422	0.38	4.78	1.75
	8	3	15.0%	90	3.9%	-3.07	4.22	-1.49	a	62	0.69	-4.81	-2.96	28	0.31	0.80	0.49
	nd	5	25.0%	885	38.1%	-0.90	3.95	-0.17	b	477	0.54	-3.26	-1.69	331	0.37	2.28	1.29
Volume	full-scale	3	15.0%	646	27.8%	-0.99	4.2	-0.17	a	342	0.53	-3.66	-2.30	227	0.35	2.70	1.48
	lab-scale	2	10.0%	740	31.9%	-3.71	9.12	-2.83	b	478	0.65	-9.36	-12.00	262	0.35	6.60	12.00
	small-scale	15	75.0%	936	40.3%	-0.78	3.08	-0.28	a	552	0.59	-2.28	-1.21	377	0.40	1.40	0.97
Treatment	antibiotic	6	30.0%	55	2.4%	-2.41	4.15	-0.31	a,b	33	0.60	-4.43	-2.58	22	0.40	0.62	0.36
	metal	5	25.0%	230	9.9%	-0.41	2.03	-0.20	a,b	130	0.57	-1.50	-0.80	99	0.43	1.01	0.72
	NT	15	75.0%	1770	76.2%	-2.13	6.74	-0.71	a	1063	0.60	-5.95	-3.74	629	0.36	4.07	1.50
	other	3	15.0%	166	7.1%	-0.37	2.36	-0.20	a	101	0.61	-1.58	-1.00	64	0.39	1.53	1.45
	solids	2	10.0%	101	4.3%	-0.55	3.82	0.20	b	45	0.45	-3.43	-1.30	52	0.52	1.90	1.66

N: number of studies. %(N): percentage of studies; obs: number of observations; %(obs): percentage of observations; avgFC: group average log2(FC); SD: standard deviation of group log2(FC); med: group median log2(FC); sig: results of the statistical tests, significant differences in variables with two levels are shown with an *, whereas in those with 3 or more levels are shown with different letters (same letters indicate no significant difference); red: reduced; inc: increased; 1: When considering only ARG quantified with both methods, the difference is not significant.

4.5.2. Analysis of the raw data

4.5.2.1. Metagenomics vs qPCR observations

The first question that needed to be answered before further analyses was whether the observations produced with metagenomic techniques (e.g., Illumina sequencing) and qPCR could be directly compared. The assessment of the distribution and central tendencies of all observations (all ARG) suggested a significant difference (p-value < 0.05), as seen in Table 4.2 and Figure 4.4. In fact, the average and median of the magnitude of the ARG reductions of the metagenomic observations (avg = -2.45, med = -0.87) were substantially greater than qPCR observations (avg = -0.79, med = -0.28). However, the P_{red} observed was similar in the two methods (P_{red} = 0.59).

Since metagenomic technologies allow the detection of substantially more ARGs, there is a higher chance of finding ARG below detection levels after the AD process, resulting in much greater ARG FC. For instance, the number of unique ARGs quantified with metagenomics (383 unique ARGs) was much greater than those quantified with qPCR (25 unique ARGs), and the number of ARG with very large reductions (log2FC = -12) was also much higher in metagenomic observations (26.7%) than in qPCR observations (2.1%). Hence, it is likely that this simple comparison was not valid as the results were biased towards the effects detected with metagenomic technologies. To avoid this problem, another comparison was conducted, including only the observations of the 16 ARG quantified with both technologies (Figure 4.5, Table B4.2). This later analysis suggested no significant difference in the results of these two groups. A handful of previous studies have also suggested that qPCR and metagenomic analyses could lead to similar conclusions about the changes in ARG levels (Tian et al. 2016). Based on this, it was concluded that observations produced with metagenomics technologies and qPCR could be considered

comparable. The list of all ARGs and how they were quantified is shown on Table B4.2 in Appendix B.

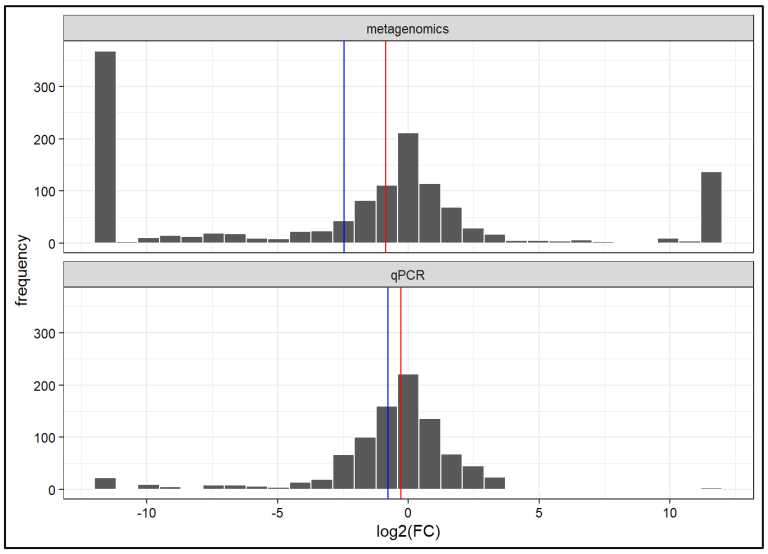

Figure 4.4 Distribution of all ARG changes by quantification method. Red and blue lines represent the mean and median of the observations, respectively.

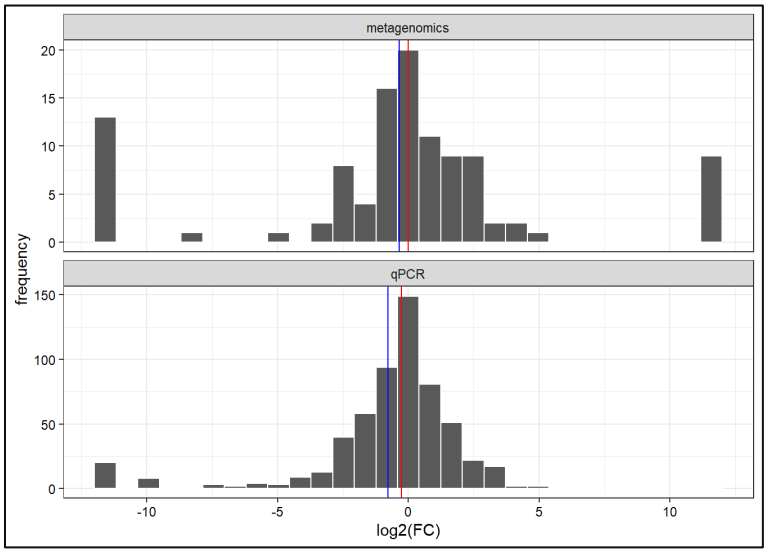

Figure 4.5 Distribution of ARG changes quantified with both metagenomics and qPCR. Red and blue lines represent the mean and median of the observations, respectively.

4.5.2.2. Distribution of the raw data

The distribution and central tendencies of $\log_2$(FC) in the raw data were evaluated to determine if part of the variability of the ARG changes could be attributed to AD parameters and use this information to perform the subgroup meta-analyses. The statistical tests on the raw data (Table 4.2) suggested that there could be significant differences in some levels of all explanatory variables (p-values < 0.05). For instance, the central tendencies of the ARG FC were significantly different in all types of manures, temperatures, and settings. Moreover, these preliminary analyses also suggested that digestion times (HRT), pH, volumes, and the addition of other materials (treatments) could affect the magnitude of the ARG FC. Therefore, sub-group meta-analyses for all explanatory variables were performed.

The analyzes of the raw data allowed the identification of interesting patterns and trends linked to certain AD parameters. For example, greater proportions of ARG reductions were reported in cattle or dairy manures (P_{red} = 0.66) compared to pig manures (P_{red} = 0.53). Greater ARG reductions (FC) and P_{red} were observed in thermophilic conditions ($\log_2$(FC)med = -1.94, P_{red} = 0.83) compared to mesophilic ($\log_2(FC)_{med}$ = -0.43, P_{red} = 0.58) and psychrophilic conditions ($\log_2(FC)_{med}$ = 0.76, P_{red} = 0.34). Regarding digestion times (here defined as HRT), better reductions were observed at long HRT. Interestingly, the addition of antibiotics to the digesters did not seem to affect the AD process capability of reducing ARG (Table 4.2 and Figure 4.6). However, the addition of solids from an external source caused a decrease in ARG reduction.

A deeper analysis of the raw data also revealed substantial differences in ARG reductions between AD of different types of manures at different temperatures. Figure 4.6 shows the P_{red} in cattle/dairy and pig manures at mesophilic and thermophilic temperatures grouped by the different AD parameters considered in this study. This analysis suggested that more ARG were reduced

from cattle and dairy manures than from pig manures at mesophilic conditions regardless of the AD parameters. However, it also showed that thermophilic conditions produced greater P_{red} in pig manures, while this effect was not observed on cattle and dairy manures. The raw data analyses also showed that a significant fraction of the resistomes increased during the AD process (Table 4.2). In fact, under all conditions (excepted thermophilic AD), more than 30% of the ARG were enriched, suggesting that AD not only failed to remove all ARG but also promoted the increase of some ARGs.

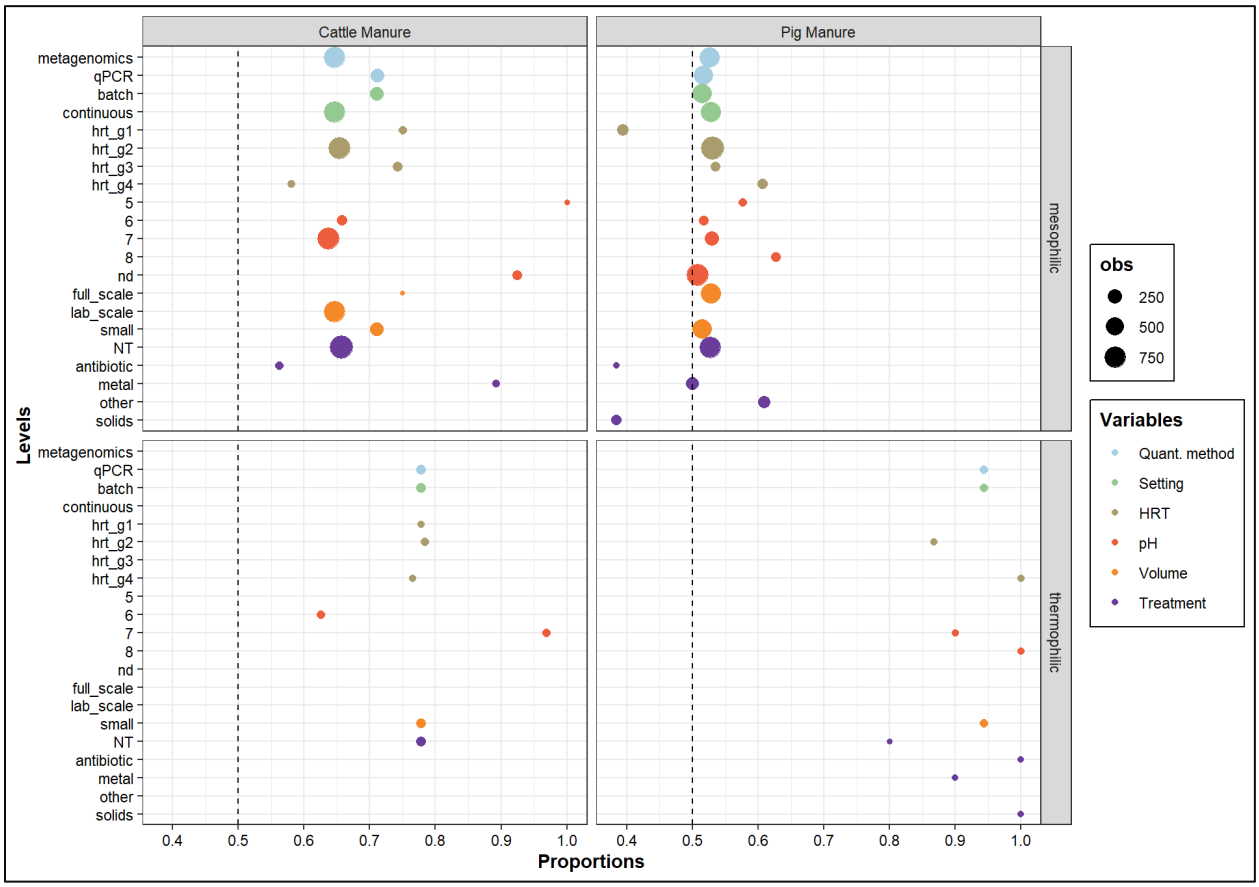

Figure 4.6 Proportion of ARG reduced (P_{red}) in pig and cattle manures at mesophilic and thermophilic temperatures. The size of the figures represents the number of observations in each variable levels.

4.5.3. Meta-analyses results

4.5.3.1. General meta-analysis results

The random-effects model, which assumes that there is not only a true effect but rather a random distribution of true effects, was chosen to pool the effect sizes. We considered that the random-effects model was more appropriate because, given the nature and complexity of the AD process, the variability of the results is presumably caused by several factors rather than by sampling errors only. Since the changes in ARG levels are ultimately the result of the microbial successions during the AD process, which in turn depend on the unique microbial and physicochemical characteristics of the fed manure and other environmental conditions not evaluated here, it is likely that each study started with unique initial conditions and observed substantially different effects.

The meta-analyses were performed on the $\log_2$(FC) and the proportion of ARG reduced (P_{red}) as they could provide different insights. For instance, whereas the P_{red} meta-analyses described how much of the resistome profile (total ARG) was affected during AD, the $\log_2$(FC) meta-analyses described the magnitude of the ARG changes. This distinction is particularly useful when evaluating the evolution of different types of ARG (type of antibiotic or mechanism) since some ARG could represent higher risk or be in higher abundance than others. The forest plots showing the individual effects of the different studies used in the meta-analysis are shown in Figures B4.1 and B4.2 in Appendix B. The results of the general meta-analyses indicated that AD had a significant effect on resistomes regardless of the condition of the process (Figures 4.7 and 4.8). In fact, the results indicated that total ARG levels decreased around 50% ($\log_2$(FC) = -1.05) after AD (Figure 4.8). However, the results also showed that only a proportion (56%) of the total number of ARG were subject to reductions (Figure 4.7).

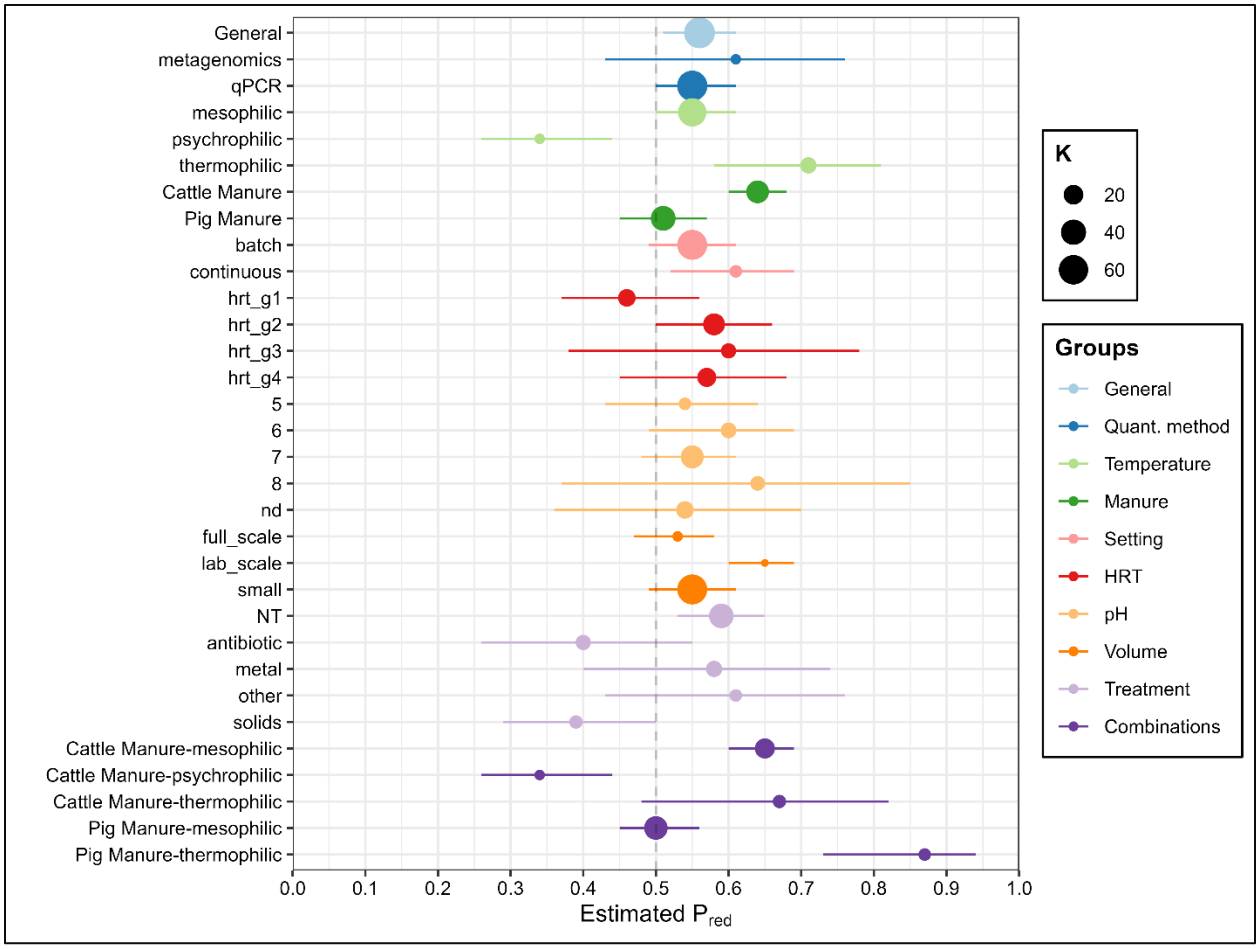

Figure 4.7 Effect of AD parameters on proportion of ARG reduced (P_{red}). Lines around estimated effects cover the 95%-confidence intervals. Estimates of each parameter are code by color. The size of the figure indicates the number of independent observations (K) in each sub-group. The dashed line represents the non-effect limit.

The between-study heterogeneity was substantially greater in the meta-analysis of the magnitudes of the changes (I^2 = 96.5%) than the meta-analysis on the P_{red} (I^2 = 50%). A similar trend in the I^2 values was observed in all subgroups meta-analyses (Section 3.5.3.2), suggesting that, in general, the different studies observed the reduction of similar proportions of the resistomes, although the magnitude of the changes was very distinctive. However, given the high I^2 values, the results of the meta-analyses could be imprecise and should be interpreted with caution.

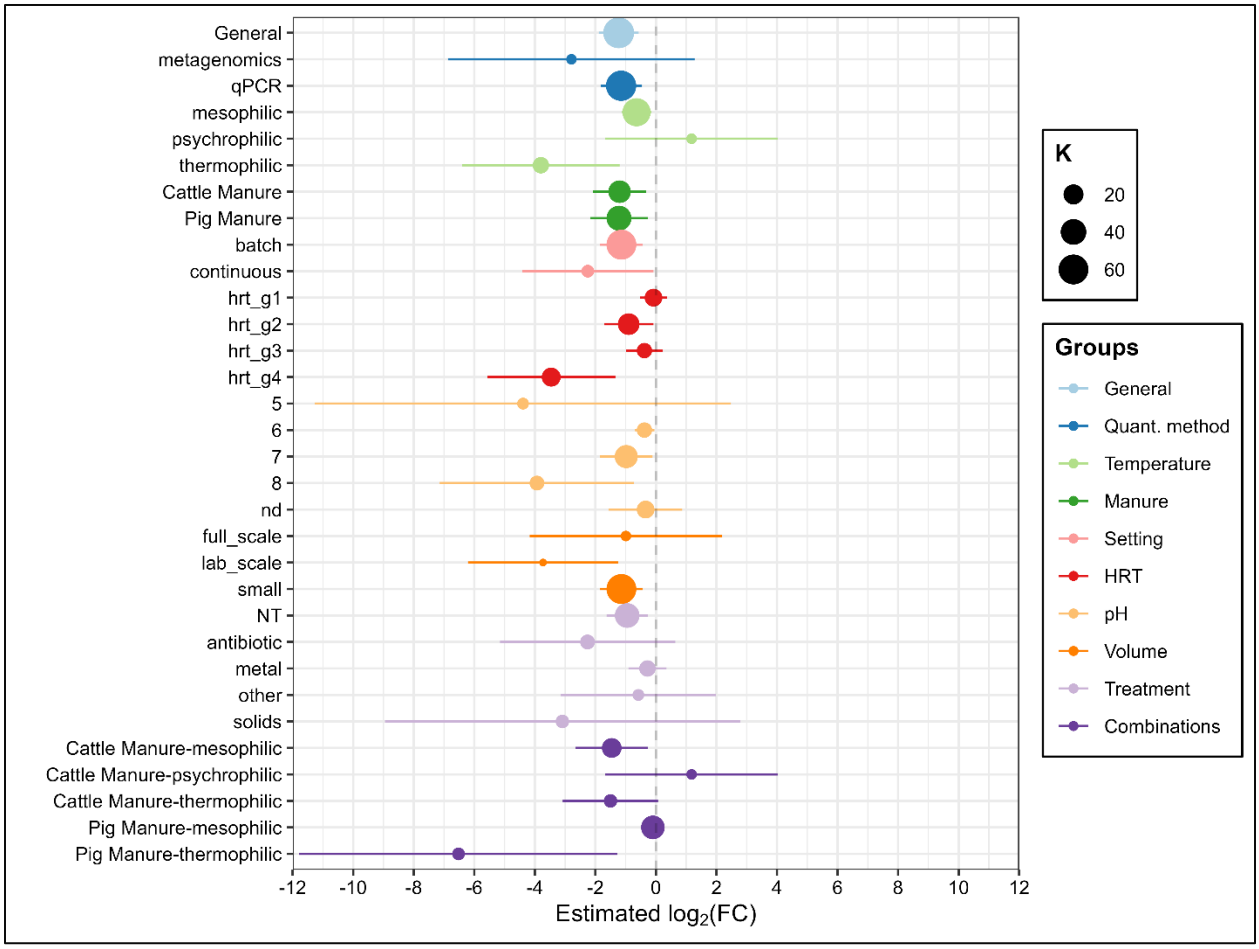

Figure 4.8 Effect of AD parameters on ARG concentration changes (log2(FC)). Lines around estimated effects cover the 95%-confidence intervals. Estimates of each parameter are code by color. The size of the figure indicates the number of independent observations (K) in each sub-group. The dashed line represents the non-effect limit.

4.5.3.2. Sub-group meta-analyses results

Subgroup meta-analyses were performed to determine if the different AD parameters could significantly influence ARG changes and account for some of the between-study variability detected in the general meta-analyses. The sub-group meta-analyses results for proportions and magnitudes are shown in Table 4.3 and Table 4.4, respectively. The pooled effects and their 95%-confidence intervals for each explanatory variable, in terms of the P_{red} and the $log_2(FC)$, are displayed in Figures 4.7 and 4.8, respectively.

Table 4.3 Meta-analysis results in terms of proportion of ARG reduced (P_{red}).

Variable	Level	K	P_{red}	95%-CI	sig	I^2	95%-CI-I^2	p-value group	Egger's test
General	General	68	0.56	0.51; 0.60	*	0.50	0.34; 0.62		0.68
Quant. method	metagenomics	3	0.61	0.43; 0.76		0.90	0.74; 0.96	0.266	0.42
	qPCR	65	0.55	0.49; 0.61		0.42	0.21; 0.57		0.05
Temperature	mesophilic	54	0.55	0.50; 0.60	*	0.54	0.38; 0.66	< 0.001	0.93
	psychrophilic	3	0.34	0.26; 0.44		0.00	0.00; 0.90		< 0.001
	thermophilic	11	0.71	0.58; 0.81	*	0.00	0.00; 0.60		0.05
Manure	Cattle Manure	30	0.63	0.55; 0.70	*	0.39	0.05; 0.61	0.017	0.50
	Pig Manure	38	0.51	0.46; 0.57		0.36	0.05; 0.57		0.76
Setting	batch	63	0.55	0.49; 0.61		0.43	0.23; 0.58	0.16	0.07
	continuous	5	0.61	0.52; 0.69	*	0.81	0.55; 0.92		0.57
HRT	hrt_g1	14	0.46	0.37; 0.55		0.13	0.00; 0.52	0.163	0.55
	hrt_g2	27	0.58	0.51; 0.65	*	0.63	0.44; 0.76		0.56
	hrt_g3	9	0.60	0.39; 0.78		0.61	0.18; 0.81		0.48
	hrt_g4	18	0.56	0.44; 0.66		0.10	0.00; 0.47		0.11
pH	5	5	0.54	0.43; 0.64		0.00	0.00; 0.79	0.793	< 0.001
	6	10	0.60	0.49; 0.69		0.24	0.00; 0.63		0.54
	7	31	0.55	0.48; 0.61		0.44	0.14; 0.63		0.36
	8	8	0.63	0.36; 0.84		0.53	0.00; 0.79		0.40
	nd	14	0.53	0.37; 0.68		0.67	0.42; 0.81		0.88
Volume	full-scale	3	0.53	0.47; 0.58		0.00	0.00; 0.90	< 0.001	0.22
	lab-scale	2	0.65	0.60; 0.69	*	0.00			-
	small-scale	63	0.55	0.49; 0.61		0.43	0.23; 0.58		0.07
Treatment	antibiotic	9	0.40	0.26; 0.55		0.00	0.00; 0.65	0.001	0.10
	metal	11	0.57	0.39; 0.73		0.69	0.41; 0.83		0.08
	NT	37	0.59	0.53; 0.65	*	0.48	0.24; 0.65		0.52
	other	5	0.60	0.43; 0.75		0.41	0.00; 0.78		0.61
	solids	6	0.39	0.29; 0.50		0.00	0.00; 0.75		0.52
Combinations	Cattle Manure-mesophilic	21	0.65	0.57; 0.73	*	0.36	0.00; 0.62	< 0.001	0.27
	Cattle Manure-psychrophilic	3	0.34	0.26; 0.44		0.00	0.00; 0.90		< 0.001
	Cattle Manure-thermophilic	6	0.67	0.48; 0.82		0.00	0.00; 0.75		0.28
	Pig Manure-mesophilic	33	0.50	0.45; 0.56		0.38	0.06; 0.59		0.67
	Pig Manure-thermophilic	5	0.87	0.73; 0.94	*	0.00	0.00; 0.79		0.14

4.5.3.2.1. Quantification method

The pooled effects of the sub-group meta-analyses on the quantification methods were P_{red} = 0.61 for metagenomics and P_{red} = 0.55 for qPCR, whereas the magnitudes of the changes were $\log_2(FC)$ = -2.81 and $\log_2(FC)$ = -0.96, respectively. However, these differences were not significant as their 95% confidence intervals overlapped (Figures 4.7 and 4.8). Moreover, the heterogeneity of the results was not significantly reduced with these subgroups (Tables 4.3 and 4.4), indicating that they were not responsible for the variability of the data. These results suggested that metagenomics observations could be directly compared with those produced with

qPCR techniques, as observed in the preliminary raw data analysis (Figure 4.5). However, to enhance statistical robustness, there's a need for more standalone studies, especially given the limited number of independent observations for the metagenomic group (K = 3).

Table 4.4 Meta-analysis results in terms of the ARG log_2(FC),

Variable	Level	K	log_2(FC)	95%-CI	sig	I^2	95%-CI-I^2	p-value (group)	Egger's test
General	General	65	-1.05	-1.66; -0.44	*	0.97	0.96; 0.97		0.14
Quant. method	metagenomics	3	-2.81	-6.87; 1.26		0.96	0.92; 0.98	0.063	0.08
	qPCR	62	-0.96	-1.58; -0.33	*	0.97	0.96; 0.97		0.08
Temperature	mesophilic	51	-0.51	-0.91; -0.1	*	0.95	0.94; 0.96	0.001	< 0.001
	psychrophilic	3	1.14	-1.70; 3.99		0.35	0; 0.79		0.41
	thermophilic	11	-3.8	-6.40; -1.20	*	0.98	0.98; 0.99		0.24
Manure	Cattle Manure	28	-1.05	-1.72; -0.37	*	0.96	0.95; 0.97	0.837	0.26
	Pig Manure	37	-1.16	-2.12; -0.21	*	0.97	0.96; 0.97		0.06
Setting	batch	60	-0.97	-1.61; -0.32	*	0.96	0.96; 0.97	0.15	0.11
	continuous	5	-2.19	-4.38; -0.01	*	0.969	0.95; 0.98		0.04
HRT	hrt_g1	14	-0.08	-0.52; 0.37		0.87	0.79; 0.91	0.004	0.04
	hrt_g2	25	-0.80	-1.52; -0.09	*	0.95	0.94; 0.96		0.07
	hrt_g3	9	-0.38	-0.98; 0.23		0.79	0.61; 0.89		0.11
	hrt_g4	17	-3.48	-5.60; -1.37	*	0.98	0.97; 0.98		0.77
pH	5	4	-4.15	-10.96; 2.66		0.86	0.65; 0.94	0.019	0.004
	6	9	-0.38	-0.71; -0.05	*	0.42	0.00; 0.73		0.35
	7	30	-0.99	-1.83; -0.16	*	0.97	0.96; 0.97		0.20
	8	8	-3.94	-7.13; -0.75	*	0.98	0.98; 0.99		0.43
	nd	14	-0.25	-1.33; 0.84		0.91	0.87; 0.94		0.92
Volume	full-scale	3	-0.81	-3.52; 1.90		0.93	0.82; 0.97	< 0.001	0.41
	lab-scale	2	-3.73	-6.21; -1.24	*	0.00			-
	small-scale	60	-0.97	-1.61; -0.32	*	0.96	0.96; 0.97		0.11
Treatment	antibiotic	8	-1.82	-4.45; 0.82		0.98	0.96; 0.98	0.31	0.14
	metal	11	-0.27	-0.89; 0.35		0.81	0.67; 0.89		0.06
	NT	36	-0.84	-1.38; -0.29	*	0.90	0.88; 0.92		0.12
	other	4	-0.30	-2.38; 1.77		0.82	0.53; 0.93		0.22
	solids	6	-3.09	-8.95; 2.78		0.99	0.99; 0.99		0.26
Combinations	Cattle Manure-mesophilic	19	-1.11	-1.96; -0.25	*	0.97	0.96; 0.98	< 0.001	0.34
	Cattle Manure-psychrophilic	3	1.14	-1.70; 3.99		0.351	0.00; 0.79		0.41
	Cattle Manure-thermophilic	6	-1.49	-3.05; 0.08		0.89	0.78; 0.94		0.12
	Pig Manure-mesophilic	32	-0.1	-0.44; 0.24		0.75	0.65; 0.82		0.41
	Pig Manure-thermophilic	5	-6.55	-11.8; -1.30	*	0.97	0.95; 0.98		0.15

4.5.3.2.2. Temperature

The subgroup meta-analyses suggested that different temperature conditions could significantly influence the AD capacity of reducing ARG levels (p-values < 0.001). For instance, the results indicated that more than 50% of the total number of different ARGs were reduced at both mesophilic and thermophilic AD (Figures 4.7 and 4.8). The pooled magnitude of the ARG changes were statistically significant (p-value < 0.05) for both mesophilic (log_2(FC) = -0.51) and

thermophilic (log_2(FC) = -3.8) temperatures, although the effect was significantly greater in thermophilic (p-value < 0.05) (Table 4.4). In contrast, the pooled effect of psychrophilic conditions showed that only 34% of the total ARG could be reduced during the AD process (Figure 4.7). Moreover, although the pooled magnitude of the ARG changes in psychrophilic AD was not statistically significant, it could suggest ARG levels might actually increase (log_2(FC) = 1.14). More studies are required to raise the precision of this estimate and reduce the wide 95%-confidence interval.

The I^2 values of these subgroup meta-analyses remained high for the mesophilic group (Tables 4.3 and 4.4). In the thermophilic group, the I^2 also were high in the log_2(FC) meta-analysis, although it dropped to zero in the P_{red} meta-analysis. It suggested that the different studies observed a reduction of a similar proportion of the resistome, but the magnitudes of these changes were substantially heterogeneous. On the other hand, the I^2 estimators for the psychrophilic group were zero in both cases (Tables 4.3 and 4.4), although there were a low number of independent observations (K=3).

4.5.3.2.3. Manure

The subgroup meta-analyses revealed no significant disparities in the estimated effects on pig versus cattle/dairy manures, given the overlapping 95%-confidence intervals observed in Figures 4.7 and 4.8. However, the P_{red} tended to be higher in cattle and dairy manures (P_{red} = 0.63) than in pig manures (P_{red} = 0.51). In fact, the P_{red} was significantly higher than 50% in cattle/dairy manures but not in pig manure (Table 4.3). Moreover, the between-group variability test in the P_{red} meta-analysis suggested significant differences between the two manures (p-value = 0.017). This meta-analysis also indicated that part of the variability of the P_{red} could be attributed to the different types of manures used in the study since the I^2 indicators dropped below 40%.

On the other hand, the outcome of the subgroup meta-analysis on the magnitude of the changes indicated there was no difference between the two groups of manures (p-value = 0.837). For instance, the pooled effects were $\log_2$(FC) = -1.05 and $\log_2$(FC) = -1.16 for cattle/dairy and pig manure, respectively (Figure 4.8). Nevertheless, the between-study heterogeneity variance in this subgroup meta-analysis remained high (I^2 > 96%), as detailed in Table 4.4.

4.5.3.2.4. Digester feeding configuration (Setting)

The subgroup meta-analyses on the type of experiment setting showed no significant influence on ARG reduction (p-values > 0.05). For instance, the estimated P_{red} and $\log_2$(FC) for batch and continuous digesters were 0.55 and -0.97, and 0.61 and -2.19, respectively, although the differences were not statistically significant as seen on the overlapping of their 95%-confidence intervals (Figures 4.7 and 4.8). Moreover, the between-study heterogeneity was not affected, and the I^2 values were comparable to those on the general meta-analyses (Table 4.3 and Table 4.4). However, the number of independent observations was small for continuous digesters (K=5), so the results must be interpreted with caution as the estimates may not be precise.

4.5.3.2.5. Digestion times (HRT)

The digestion times were classified into four groups, as described in Table 4.1, to determine if they could affect the ARG reduction rates. The subgroup meta-analyses did not detect a significant difference between the P_{red} of the different digestion times (p-value = 0.163), although hrt_g2 (10-35d) was the only group with a significant effect (P_{red} = 0.58). In contrast, the estimated magnitudes of the ARG changes between groups were significantly different (p-value = 0.004). For instance, the effect estimates for the hrt_g2 ($\log_2$(FC) = -0.80) and hrt_g4 ($\log_2$(FC) = -3.48) were statistically significant since their 95%-confidence interval did not include the non-effect mark (Figure 4.8). Interestingly, even though all the P_{red} were comparable between all HRT

groups, the magnitude of the changes was significantly larger in hrt_g4 compared to those estimated for the other groups. The between-study variability on the P_{red} meta-analysis tended to be smaller than the general meta-analysis, especially in the hrt_g1 and hrt_g2 groups (Table 4.3). A slight reduction in the I^2 values was also observed in the meta-analysis on the magnitude of the ARG changes, although they remained above 75% (Table 4.4). These results suggested that digestion times could have an effect on ARG reduction or at least account for some of the variation of the results.

4.5.3.2.6. pH

Similar to what was observed for digestion times, the meta-analysis showed no significant difference between the estimated P_{red} at the different pH (p-value = 0.163) but a significant difference in the magnitude of the ARG changes (p-value = 0.019). In this case, the estimated effects were not significantly greater than 50% on all groups, as shown in Figure 4.7. However, the magnitudes of the ARG changes on pH 6, 7, and 8 were significant (Figure 4.8). In fact, ARG seemed to be reduced to a greater extent as pH increased. However, the estimates were highly variable (wide 95%-confidence intervals) as the number of independent observations (K) was small in most cases since many studies did not report the pH during the digestion process. The I^2 values were slightly reduced in this set of subgroup meta-analyses, suggesting that the pH could account for some of the variability of the results (Tables 4.3 and 4.4).

4.5.3.2.7. Volume

The subgroup meta-analyses on the volume showed significant between-group variability (p-values < 0.001), as detailed in Tables 4.3 and 4.4. This suggested that the volume of the digester could affect the ARG reduction rates. For instance, the lab-scale (P_{red} = 0.65) experiments yielded the greatest P_{red}, followed by small-scale (P_{red} = 0.55) and full-scale (P_{red} = 0.53), although the

only significant effects were those of lab-scale (Figure 4.7). In contrast, the estimated $\log_2$(FC) for lab-scale ($\log_2$(FC) = -3.73) and small-scale ($\log_2$(FC) = -0.97) were significant, although the 95%-confidence intervals of all subgroups overlapped (Figure 4.8). The I^2 values were poorly estimated in these subgroup meta-analyses because the number of independent observations was low; only the small-scale group had a large enough K to generate proper estimations, which were comparable to those detected in the general meta-analyses (Tables 4.3 and 4.4). In general, the results of these sub-group meta-analyses should be analyzed with caution since the results could be confounded by the type of quantification method employed. For instance, while small-scale experiments exclusively utilized qPCR for ARG quantification, both lab-scale and full-scale studies relied solely on metagenomic techniques. Therefore, the observed disparities in effects across different volume categories might stem from the inherent sensitivities of the respective quantification methods, as previously discussed.

4.5.3.2.8. Additional treatments

Since most of the studies included in these meta-analyses evaluated the effects of different substances on the resistome evolution during AD, the observations were grouped according to the type of treatment (Table 4.1). The results of the meta-analyses (Figures 4.7 and 4.8) showed that the NT group, which included observations from control experiments (no additional treatments), could significantly reduce around 59% of the total number of ARG (P_{red} = 0.59), with an average reduction of approximately 45% ($\log_2$(FC) = -0.84). The meta-analyses also showed that estimated effects of the antibiotics, heavy metals, and other substances groups were not statistically different than the control group (NT), as seen by the overlapping of their 95%-confidence intervals (Figures 4.7 and 4.8). Moreover, the raw data analyses showed the proportion of ARG enriched during the process was not affected by any of these components (Table 4.2). On the other hand, the results

showed that the solids group, which corresponded to the observations from digesters amended with an external source of solids (e.g., straw), achieved the reduction of a significantly smaller (p-value < 0.05) proportion of the resistome (P_{red} = 0.39) compared to the NT group (P_{red} = 0.59) (Figure 4.7). Although the estimated magnitude of the ARG changes in this group (log_2(FC) = -3.09) was substantially greater than the other groups, it was not statistically different from the NT due to the high variability of the estimate (Figures 4.8).

The between-groups variability of the P_{red} and log_2(FC) meta-analyses were different. Whereas in the former, the statistical test suggested a significant difference between the results of the subgroups (p-value < 0.001) (Table 4.3), the latter showed no significant between-groups variability (p-value = 0.31) (Table 4.4). The heterogeneity indicators (I^2) were also lower in the P_{red} meta-analysis compared to the magnitude of ARG changes meta-analysis. The results suggested that the different treatments could account for some of the variability of the results in terms of the proportion of ARG reduced after the AD process, although they failed to do so in the magnitude of the ARG changes.

4.5.4. Risk of bias

The risk of bias was evaluated through funnel plots of the effects (P_{red} and log_2(FC)) and Egger's tests. Funnel plots of the general meta-analyses are shown in Figure B4.3 and B4.4 in the Appendix B. Despite the high heterogeneity of the data and variability of the results, Egger's tests suggested no significant bias (p-values > 0.05) in the general meta-analyses, and in the majority of the subgroup meta-analyses (Tables 4.3 and 4.4). The only P_{red} subgroup meta-analyses with significant bias were the psychrophilic, pH 5, and cattle manure-psychrophilic groups (Table 4.3). In the log_2(FC) subgroup meta-analyses, continuous, hrt_g1, and pH 5 groups showed significant bias (Table 4.4). In general, these groups had a low number of independent observations (K), which

is the potential reason for the significant bias. However, the subgroup meta-analysis in terms of $\log_2$(FC) at mesophilic conditions also showed significant bias (p-value < 0.001), which suggested that a group of studies could have shifted the estimated magnitude of the ARG changes towards a higher reduction value.

4.6. Discussion

4.6.1. Metagenomic vs qPCR observations

As the use of metagenomics tools to evaluate the evolution of resistomes in animal manures and related processes increases, the need to validate that their outputs are comparable to those from traditional qPCR becomes more evident. Metagenomic tools are preferred over traditional qPCR as they have more discovery power and sensitivity, higher scalability, and are not targeted (Czaplicki and Gunsch 2016). Moreover, metagenomic tools can provide valuable insights into the mechanisms that drive changes in ARG levels. In this study, we compared the changes in ARG levels and number of ARGs determined with metagenomic tools and qPCR in different studies. The results indicated that the two approaches generated comparable results, as suggested by previous studies (Tian et al. 2016), and corroborated that the number of ARG that can be analyzed with metagenomic tools is substantially larger.

4.6.2. Overall effect of AD on manure resistomes

The effects of AD on ARG levels in animal manures have been widely studied during the last decade (Gurmessa et al. 2020). Yet, the results are often inconsistent, limiting our ability to detect relationships between AD parameters and the changes in ARG levels that could lead to the design of more effective AD processes. To address this limitation, we gathered observations from different studies to perform meta-analyses on the proportion of ARGs reduced (P_{red}) and the magnitude of the ARG changes ($\log_2$(FC)) during manure AD, aiming to reveal general trends that

single studies usually are not able to detect. In order to simplify the analyses, we evaluated the changes in ARG levels without making any distinction between the different types of ARGs and their mechanisms since the main objective was to determine how the whole resistome evolves under different conditions. We were aware that the study would account for less variability by ignoring these important factors since different types of ARGs could evolve in different ways, as previous studies have suggested (Goulas et al. 2020; Syafiuddin and Boopathy 2021).

Overall, the results of this study indicated that AD could significantly reduce the levels of ARGs in pig, cattle, and dairy manures, regardless of the conditions of the process (Figures 4.7 and 3.8). However, the results also showed that only a portion (51-60%) of the resistome is actually subject to reduction (Figure 4.7). The data used in this study suggested that the enrichment of some ARGs may also occur during the AD process (Table 4.2). The changes in ARG levels during AD is generally attributed to the microbial successions that take place during the process, which, in turn, lead to the establishment of a steady state microbial community with a different resistome profile. For instance, the enrichment of methanogenic anaerobic communities required for the AD process (e.g., *Methanosarcinales*) at the expense of aerobic microorganisms usually results in the reduction in ARG concentrations (Sun et al. 2016; Zhang et al. 2021a). Nonetheless, some members of anaerobic communities commonly found in anaerobic digesters (e.g., Clostridiales, Synergistales, Anaerolineales) have been reported as potential carriers of different ARGs, which might be the reason of the increase in the levels of some ARG (Tian et al. 2016; Zhang et al. 2021b). Besides, since MGEs seem to be persistent in anaerobic digesters (Ma et al. 2019; Xiang et al. 2019), part of the anaerobic consortium could likely acquire and then reproduce several ARGs due to random HGT. This phenomenon might also be the reason for the different changes

(reductions and enrichments) of the different ARGs, as some ARGs might be more easily transferred and preserved than others.

4.6.3. Effect of specific AD parameters on resistomes

The results of the meta-analyses confirmed that, in general, TAD is better at reducing ARG levels than MAD, and that psychrophilic AD is less efficient and more likely to enrich ARGs (Figure 4.7 and 4.8). The larger reduction in ARG levels in thermophilic AD has been associated with the decline of the microbial diversity, which results from the decrease of mesophilic communities linked to ARGs and MGE (Tian et al. 2016; Wen et al. 2021; Zhang et al. 2021a). A similar effect has been observed in dairy and pig manure composting, where the loss of mesophilic microorganisms (e.g., Pseudomonadales, Xanthomonadales, Bacillales), during the thermophilic stages of composting leads to a reduction of ARG levels (Li et al. 2020; Liu et al. 2020).

A closer look at the effects of temperature on the resistome profiles revealed that thermophilic AD was significantly more efficient than mesophilic AD at reducing ARGs in pig manures, but it was not significantly better in cattle or dairy manures (Figures 4.6, 4.7 and 4.8). In fact, the proportion of ARGs reduced during the process, and the magnitudes of the changes were not significantly different between mesophilic and thermophilic cattle/dairy manure AD. Although the reason for these differences could not be determined in this study, they could be the consequence of the distinct changes in microbial abundance and microbial diversity. Since cattle/dairy manures generally have higher solids content (e.g., cellulose, hemicellulose) and hydrolytic and fermentative communities are usually associated with different ARGs (Zhang et al. 2021a), a reasonable hypothesis is that the smaller differences in removal rates between thermophilic and mesophilic digesters fed with cattle/dairy manures were the result of a smaller decline in the overall microbial abundance of these ARG carriers. A recent study reported lower

ARG removal rates in thermophilic pig manure digesters with a higher abundance of hydrolytic bacteria (i.e., Clostridiales) compared to mesophilic digesters (Huang et al. 2019), which seems to support this hypothesis.

Additionally, the results of our meta-analyses indicated that digesters amended with solids from an external source yielded lower ARG reductions (Figures 4.7 and 4.8), which also might be attributed to an increase in hydrolytic activity. An alternative explanation is that the aromatic compounds derived from lignin degradation exert some selective pressure on the microbial communities present in the digesters. As ARGs are often associated with other resistance elements (e.g., metal and biocide resistance) (Pal et al. 2015), they are likely co-selected in microbial communities resistant to these compounds. For instance, previous studies have observed that the addition of lignin to manure composting could have a negative effect on ARG reduction rates (Qiu et al. 2021). Besides, other studies have observed an increase in ARG levels in wastewater treatment plans and soils contaminated with different aromatic compounds (Chen et al. 2017; Xia et al. 2019). Nonetheless, future studies should investigate this phenomenon further to corroborate the causes of this trend.

The results of the meta-analyses also indicated that some AD parameters, such as digestion times (HRT) and pH, might influence the magnitude of the ARG changes, although the proportion of the resistome (total number of ARGs) reduced during the process seem to be unaffected. For example, the different digestion times reduced a similar proportion of ARGs, but the magnitudes of the ARG changes were greater in long digestion times (> 50 days). This effect could be simply the result of the dilution factor as manure is added at a slower rate. Another possibility is that as the degradable matter is consumed and the hydrolytic activity decreases, the abundance of hydrolytic communities (presumably responsible for carrying ARG) declines to allow other

microbial populations to take the ecological niche. However, it is also likely that the exposure to low oxygen levels and even anoxic conditions for extended periods drives the removal of residual aerobes and some facultative anaerobes, ultimately reducing ARG levels.

In the case of pH, although the results suggested digesters with pH 8 could achieve better efficiencies than those operating at a pH of 6 (Figures 4.7 and 4.8), it is likely that this is caused by a confounding effect of the digestions times, since most of the observations with pH 8 occurred after 50 days (hrt_g4), while pH of 6 was mainly observed at digestion times < 35 days (hrt_g1 and hrt_g2; Table B4.1 in Appendix B). An alternative explanation is that higher pH could have affected the permeability of some toxic compounds (e.g., lignin-derived compounds and antibiotics), reducing the selective pressure they generally exert and the need to maintain resistance elements. However, further analyses are required to demonstrate this effect. On the other hand, the type of digesters (batch or continuous/semi-continuous) and the volume had no significant effect on ARG reduction. However, more studies in continuous and batch digesters at larger scales are required to confirm the systems are equivalent.

Another interesting observation is that the addition of antibiotics to anaerobic digesters did not significantly affect ARG reduction rates (Figures 4.7 and 4.8). Moreover, the analysis of raw data also suggested that, in general, the addition of antibiotics did not increase ARG levels either (Table 4.2). These results seem controversial as several studies have demonstrated that antibiotics could affect some microbial populations involved in the AD process (Mai et al. 2018; Mazzurco Miritana et al. 2020; Wen et al. 2021), and enrichment of antibiotic-resistant populations in digesters spiked with antibiotics is expected. For instance, the addition of antibiotics such as fluoroquinolones (e.g., ciprofloxacin, norfloxacin), tetracyclines (oxytetracycline), and sulfonamides (e.g., sulfamethoxazole, sulfadimethoxine) resulted in an increase in the abundance

of hydrolytic communities (e.g., Clostridiales, Burkholderiales) (Mai et al. 2018; Mazzurco Miritana et al. 2020; Wen et al. 2021), which are presumably the primary ARG hosts in anaerobic digesters. A reasonable explanation for this inconsistency is that the ARGs evaluated in the studies of antibiotic-spiked digesters gathered for these meta-analyses did not represent the fate of the whole resistome. In fact, all the observations of the antibiotic-treatment group were made with qPCR and only included a handful of ARGs (11 different ARGs), mainly for sulfonamides and tetracyclines (Table B4.1 in Appendix B). Hence, it is likely that the antibiotics studied (i.e., tetracyclines, beta-lactams, sulfonamides, fluoroquinolones) selected microbial species with ARGs other than those targeted. Future studies should evaluate the impact of antibiotics on ARGs during AD using metagenomic technologies to evaluate whether or not there is an actual selection.

4.6.4. Limitations of the study and recommendations

There were several limitations in the meta-analyses performed in this study. First, as with most meta-analyses, this study might be affected by the publication bias, which occurs when studies with positive results have a higher probability of being published. A dataset of non-published data from our group to try to address this problem (This is the data used in Chapter 7, which, at the time, was not published). Second, the number of studies (N) and independent observations (K) available are still low, limiting the statistical power of the analyses, especially of the subgroup meta-analyses. Although many studies on this topic have been published recently, most of them displayed the results in a way that did not allow the extraction of accurate data (e.g., heatmaps) and did not provide the data in other ways (e.g., tables in supplementary materials). Hence, we recommend future studies include data on ARG levels observed during the process to facilitate data accessibility. Besides, the number of ARGs quantified was relatively low as most of the studies used qPCR; thus, as metagenomic approaches become increasingly accessible and

relatively inexpensive, we encourage the use of metagenomic tools to increase this number and have a deeper overview of resistomes. Third, the high heterogeneity of experimental designs and reported results led to increased variability on the meta-analyses outcomes, especially in terms of ARG fold-changes, producing noisy estimates and limiting the ability to determine parameters with significant effects. However, the meta-analysis on the proportion of ARG reduced (P_{red}) yielded substantially better results in data heterogeneity (lower I^2 values) which was helpful in finding trends. Fourth, in this work, we did not evaluate or discuss how HGT of ARGs could affect the resistome evolution in complex environments like AD, which could play an essential role. Finally, in this series of meta-analyses, in order to simplify the analyses and get a general picture of how the resistomes evolve, no distinction was made between the different types of ARGs (antibiotic class and mechanisms), assuming that this factor does not influence how they change.

Despite these limitations, this study was able to identify some trends and potential mechanisms by which ARG changes during AD. For instance, the evidence suggested AD could significantly reduce ARG levels in pig and cattle/dairy manures regardless of the conditions of the process. Evidence pointed to hydrolytic communities as one of the main ARG carriers, which could suggest that by reducing microbiological hydrolysis, anaerobic digesters might achieve better ARG removal rates. However, future studies should evaluate this phenomenon in greater depth to confirm this effect and corroborate that the ecological niche is not taken by other groups of ARG carriers.

4.7. Conclusion

The meta-analyses suggested that AD of animal manures (pig and cattle/dairy) could significantly reduce ARG levels regardless of the condition of the process. The results also indicated that thermophilic AD is more efficient than mesophilic AD, although this effect was

statistically significant in pig manures only. Subgroup meta-analyses suggested that long digestion times (> 50 days) could yield better ARG removal rates and that the addition of solids from an external source (anaerobic co-digestion) could affect the ARG reduction efficiency of the process. The results suggested hydrolytic bacteria as one of the main ARG carriers in the AD process. Finally, this study indicated that qPCR and metagenomic analyses yield comparable results regarding changes in ARG levels, validating the use of metagenomics to evaluate resistomes. Overall, this work provided valuable insights into interesting aspects and knowledge gaps that could be addressed in the thesis research.

4.8. Acknowledgments

This research work was financially supported by the National Sciences and Engineering Research Council of Canada (NSERC) through the Discovery Grants program [RGPIN-2016-05929].

Chapter 5: Preliminary study of the effects of mesophilic AD on resistomes of dairy bovine manure

5.1. Preface

This chapter represents the first study conducted to evaluate the effects of mesophilic AD on ARGs present in bovine manure. The metagenomic analyses in this study were performed in MetaStorm, an online user-friendly platform that allows quick taxonomical classification and functional annotation of metagenomic reads. The study was the first experience using metagenomics and bioinformatic tools and provided valuable results that ultimately shaped the research. The work described in this chapter was peer-reviewed and published in the Journal *Bioresource and Technology* in 2020 as original research in a manuscript titled "*Effect of mesophilic anaerobic digestion on the resistome profile of dairy manure*" (https://doi.org/10.1016/j.biortech.2020.123889). I alone was responsible for the data collection and analysis, interpretation of the results, and the preparation of the manuscript. Rakesh Patidar helped with the DNA sample preparation and submission for metagenomic sequencing and the initial quality control of the metagenomic reads. The other co-authors provided thoughtful and challenging discussions on the results and reviewed the manuscript prior to publication. Minor modifications were made to the original manuscript to adjust the style to this document and reduce redundancy.

5.2. Abstract

The effect of mesophilic anaerobic digestion (AD) on the resistome profile of manures from two different dairy farms was evaluated using a metagenomic approach. A total of 187 unique Antibiotic resistance genes (ARGs) for 17 different classes of antibiotics were detected in raw (undigested) manures. The results indicate that regardless of the origin of the dairy manure,

mesophilic AD was capable of reducing or enriching the relative abundance of some ARGs. The main driver of these changes was strongly correlated with the evolution of the microbial community during the AD process. Putative ARG hosts were suggested by analyses of the co-occurrence of microbial groups and ARGs. Finally, network analyses revealed that mesophilic AD could also reduce the co-occurrence of different groups of ARGs potentially located in the same genetic elements. Our results provide valuable insights into the microbial mechanisms driving the diversity and abundance of ARGs during mesophilic AD.

5.3. Introduction

As previously described, numerous studies have assessed the fate of various antibiotic ARGs during manure AD. Yet, the majority of studies have employed qPCR techniques, limiting the analysis to a select set of previously identified genes. The research focus had predominantly been on ARGs encoding resistance to frequently used antibiotics, such as tetracyclines, beta-lactams, and sulfonamides (Gurmessa et al. 2020; Sun et al. 2016, 2019; Zou et al. 2020). However, it is very likely that a small number of genes do not represent the entire ARG profile (resistome). For instance, some studies have documented diverging evolution of ARGs from the same family of antibiotics (e.g., *tetO*, *tetW*, *tetX*) in the same process (Ma et al. 2011; Wu et al. 2020). Moreover, the fate and evolution of entire resistomes in continuously operated anaerobic digesters remains understudied, as most of the previous studies have used batch systems.

In this study, a metagenomic approach was employed to assess the impact of mesophilic anaerobic digestion (MAD) on the resistome profiles of bovine manure from two dairy farms in Manitoba, Canada. The methodology involved establishing and operating a mesophilic anaerobic digester, fed with manure from these farms. Following DNA extraction from both untreated and digested manures, various bioinformatic tools were utilized to analyze their microbial communities

and resistomes. The hypotheses were that the microbiomes and resistomes in the anaerobic digester would changes as a result of the change of the source of manure; that AD would significantly reduce the levels of ARGs; and that shifts in microbial communities would be associated with changes in resistomes. While the findings offer insights into the dynamics and evolution of resistomes during AD and potential underlying mechanisms, this study also served as a foundational learning experience for subsequent metagenomic investigations in the research.

5.4. Material and Methods

5.4.1. Mesophilic anaerobic digester operation

This research utilized the lab-scale mesophilic anaerobic digester detailed in Chapter 3 (Section 3.2). Both the operation procedures and performance evaluations can be found in Chapter 4. This study corresponded to the first 28 months of operation of the CSTR.

5.4.2. Sample collection

For this resistome study, two dairy manure batches from Farm 1 (DMF1_1 and DMF1_2) and two from Farm 2 (DMF2_1 and DMF2_2) were analyzed. A layout of the manure management strategies in the farms is shown in the Figure C5.1 in Appendix C. Digestate (AD processed manure; here referred as Dig) from the CSTR was sampled after 45 days (1.5 HRT) of being fed with each manure batch. The digestate samples for DMF1 were designated as DigF1_1 and DigF1_2, whereas digestate samples for DMF2 were designated as DigF2_1 and DigF2_2. All samples (manures and digestates) were analyzed for COD, dCOD, TS, VS, alkalinity, and volatile fatty acids composition. They were also sampled for DNA isolation and metagenomic sequencing.

5.4.3. Physicochemical analyses and DNA isolation

The methodology of the physicochemical characterization, including COD, dCOD, TS, VS, alkalinity, pH, and VFAs concentrations is described in Chapter 3.

5.4.4. DNA isolation and metagenomic sequencing

DNA was isolated from manure and digestate samples and then sequenced following the methodology described in Chapter 3, sections 3.7 and 3.8.

5.4.5. Resistome, microbial community determination

The metagenomic data sets were uploaded to Metastorm, an online server that facilitates the annotation of several taxonomic and functional gene markers, including ARGs. The Comprehensive Antibiotic Resistance Database (CARD v3.0.2) was used for the ARG annotation with the read matching pipeline (identity > 90%) following the methodology described by the creators (Arango-Argoty et al. 2016). The relative ARG abundance was determined by normalizing the number of ARG reads to the 16S rRNA gene reads. The microbial community was determined similarly, using the Greengenes database (DeSantis et al. 2006) for microbial taxonomy annotation at the order level. Note that the taxonomic annotation of this study was conducted before the change in the names of some phyla.

5.4.6. Bioinformatics analysis

ARGs were classified and grouped according to the antibiotic class to which they confer resistance to. ARGs conferring resistance to two or more different antibiotic classes were grouped as “multidrug” resistance genes. ARGs for macrolide, lincosamide, and streptogramin were grouped together (MLS), as these antibiotics have similar mode of action and the ARGs encode a similar mechanism of resistance. The mode of action of the different antibiotics to which the ARGs found in this study exert resistance is shown in Table C5.1 in Appendix C. The squared root of the relative abundance of the microbial composition was displayed in heatmaps using the *ggplot2* package of the software R (Wickham 2016). The Shannon and Simpson diversity indices were calculated with the R-package *vegan* (Oksanen et al. 2019). The similarities between samples,

based on the combination of the bacterial communities and the resistome profiles, were evaluated performing a Principal Coordinate analysis (PCoA) using the Bray-Curtis distances with the R-packages *vegan* and *stats*. The co-occurrence of microbial taxa, ARGs for antibiotic class, and their combinations were evaluated calculating the Pearson's correlation coefficients using the *Hmisc* package in R and were plotted with the package *corrplot*. Network analyses of the Pearsons's correlations of the co-occurrence of all individual ARGs in manures and digestates were performed with the *qgraph* package using the least absolute shrinkage and selection operator (LASSO) method in R.

5.4.7. Statistical analyses

All the mathematical analyses were conducted in R. The average (n = 6) and standard deviations of the physicochemical analyses of the samples were reported and the differences were evaluated with t-tests with a significance level of 0.05. Diversity indices (Shannon and Simpson) were evaluated with an ANOVA and a Tukey's honest significance test (HSD) with a significance level of 0.05 using the software R. Only differences whose statistical tests p-values were lower than 0.05 were deemed significant. The microbial community and resistome profiles were reported for each individual sample as they were independent of time.

5.5. Results and Discussion

5.5.1. Manure properties and anaerobic CSTR performance

Table 5.1 shows the physicochemical properties of the manures from DMF1 and DMF2, before and after the MAD process. Manures had similar pH, COD, TS, VS, and total VFAs concentrations. They only differed in acetate and isovalerate levels, soluble COD (dCOD) and alkalinity. Higher acetate and dCOD levels were associated with higher levels of easily degradable carbon in dairy manure from Farm 2 (DMF2) since higher methane production rates (*p-value* <

0.05) were observed in the CSTR when this manure was fed (Table 5.1). Besides, the residual dCOD in the digestate was also significatively higher (*p-value* < 0.05), although the dCOD removal rates in the CSTR with DMF1 (58%) and DMF2 (57%) were similar (*p-value* > 0.05). The difference in alkalinity might be associated with farm operations such as the feed, disinfection protocols, and manure collection systems. The digestates produced in the AD process with both manures were similar in pH, COD, TS, VS, and VFAs. The CH_4/CO_2 ratios of the biogas were also similar (1.9 and 2.0 for DMF1 and DMF2, respectively). All these results indicated that the anaerobic CSTR operated in steady conditions regardless of the change in manure source.

Table 5.1 Physicochemical properties of manures and their respective digestates.

Parameter	Units	DMF1	DMF2	DigF1	DigF2
COD	g/L	59.0 ± 17	67.8 ± 3.7	32.7 ± 8.6	39.3 ± 5.2
dCOD	g/L	16.2 ± 1.9	20.1 ± 0.7*	6.7 ± 0.7	8.6 ± 0.8*
TS	g/L	57.9 ± 20.8	59.5 ± 5.9	38.2 ± 9.1	40.9 ± 3.0
VS	g/L	47.1 ± 7.3	48.9 ± 4.6	28 ± 8.9	30.4 ± 2.2
Alkalinity	g/L	7.3 ± 1.3	13.2 ± 0.6*	15.9 ± 5	21.5 ± 0.2*
Total VFA	mg/L	6,644 ± 899	5,407 ± 1990	144 ± 13	148 ± 99
Formate	mg/L	72 ± 50	33 ± 24	31 ± 20	34 ± 24
Acetate	mg/L	4741 ± 611	2885 ± 845*	94 ± 33	108 ± 70
Propionate	mg/L	1133 ± 239	1236 ± 583	6 ± 5	1 ± 1
Isobutyrate	mg/L	26 ± 25	1 ± 0.1*	10 ± 10	0 ± 1
Butyrate	mg/L	522 ± 137	468 ± 164	3 ± 4	1 ± 2
Isovalerate	mg/L	78 ± 12	44 ± 7*	0 ± 1	0 ± 1
Valerate	mg/L	71 ± 46	473 ± 400	1 ± 1	4 ± 5
pH		6.9 ± 0.2	7.3 ± 0.5	7.5 ± 0.1	7.4 ± 0.1
Daily CH_4 yield	mL/day-gVS	215 ± 77 (n=111)	275 ± 90* (n=70)	-	-
CH_4/CO_2 ratio		1.9 ± 0.2	2.0 ± 0.3	-	-

* Indicates statistical significative difference between samples from Farm 1 (DMF1 and DigF1) and Farm 2 (DMF2 and DigF2) with p-values < 0.05. n=6 in case otherwise indicated.

5.5.2. Resistome profile of dairy manures

A total of 80 and 105 different ARGs were detected in manures from Farm 1 (DMF1) and (DMF2), respectively, encoding resistance to 17 different antibiotic classes (Figure 5.1). DMF1_2 had slightly higher ARG levels than the first batch (DMF1_1), mainly multidrug, beta-lactams, and sulfonamides. ARGs for nucleosides and phenicol were not detected in DMF1_1 but were

found in DMF1_2. However, the relative ARG abundance (%) for all other antibiotic classes was similar for both (Figure 5.2).

The two DMF2 batches (DMF2_1 and DMF2_2) also differed in ARG levels. DMF2_1 had more than double ARGs encoding multidrug resistance, 33% more tetracyclines, and 5-fold ARG levels for beta-lactams than DMF2_2, although ARGs for aminoglycosides were around 80% richer in DMF2_2 (Figure 5.1). The difference in the relative ARG composition between the two DMF2 batches was greater than that observed in DMF1 (Figure 5.2). The difference between manures from the same farm was expected because they were collected at different times of the year. Hence, variations in the operations of the farms such as the seasonal use of different feed and antibiotics, surface disinfection, and ambient temperature during the collection day could have affected the results. Unfortunately, this study did not have access to detailed farm operation information that could have helped correlate ARGs to these factors. Futures studies should consider evaluating how farm operation and manure characteristics affect the ARGs evolution.

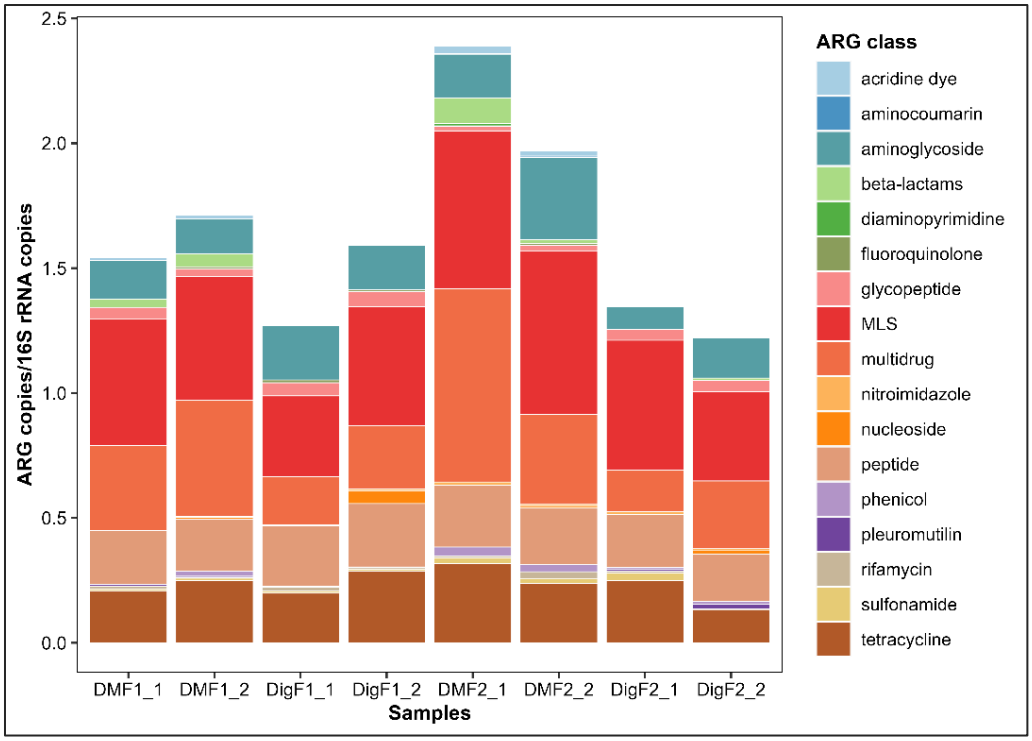

Figure 5.1 Total abundance of ARG resistance class.

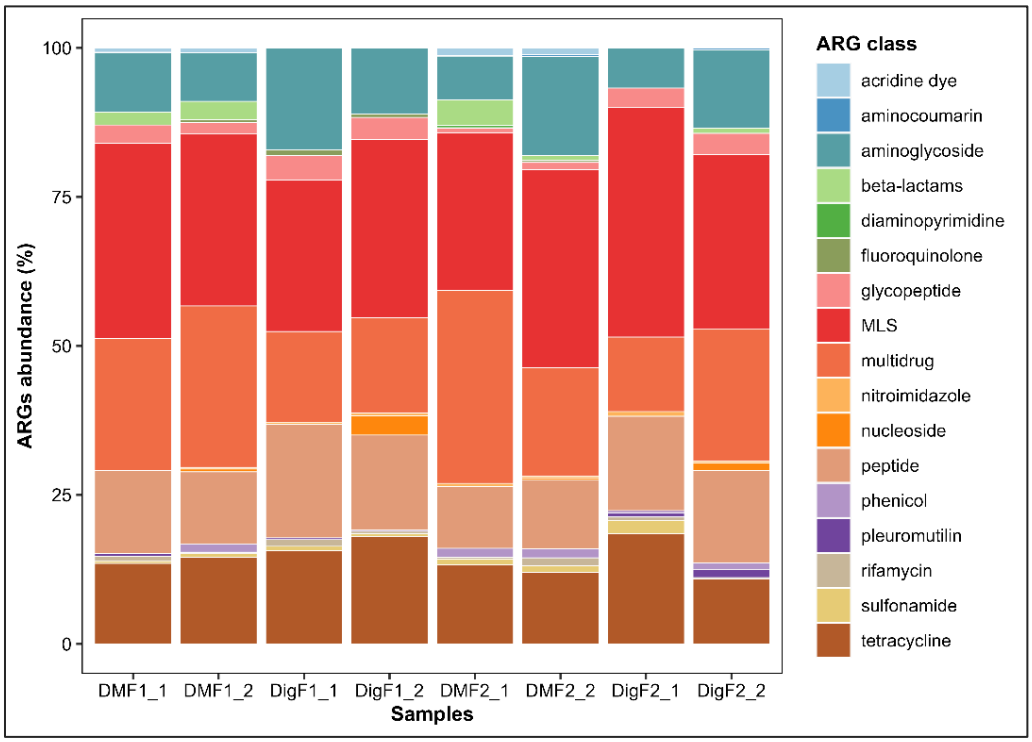

Figure 5.2 Relative abundance of ARG resistance class.

ARGs for MLS, multidrug, tetracyclines, aminoglycosides, and peptides were the most abundant in all manure batches (Figure 5.2). Also, ARGs for beta-lactams and sulfonamides were observed in all manures. ARGs associated with these antibiotics have been detected in swine, dairy, cattle, and chicken manures (Flores-Orozco et al. 2020b; Gou et al. 2018; Jia et al. 2017; Ruuskanen et al. 2016) and their occurrence, in most cases, can be linked to the historical use of these types of antibiotics. Besides, the presence of ARGs for these antibiotics seems to be consistent in manure from farms all over the world. These study's results confirm that there is an accumulation of ARGs for commonly used veterinary antibiotics, which could potentially threaten the health of animal husbandries since the treatment of infectious diseases might require more advanced antibiotics.

The presence of ARGs for highly specific antibiotics (e.g., pleuromutilin and fluoroquinolones) were also detected in manures from both farms. For instance, pleuromutilin, an antibiotic class generally used as a treatment of Gram-negative pathogens, mycoplasmas, and intracellular organisms, and whose resistance is rarely observed (Paukner and Riedl 2017), not only was found in raw manure (DMF1), but it was also persistent in digestate samples (Figures 5.1 and 5.2), which suggests that a group of microorganisms carrying these ARGs may be present in both of these environments. Future studies should consider analyzing these types of ARGs in animal manures and find alternatives to reduce, remove, and prevent their emission into the environment as they represent a higher risk for human health.

5.5.3. Effect of AD on ARG levels

A total of 65 different ARGs were found in the digestates, which represented a reduction of 19% in DMF1 and 38% in DMF2. The richness (Figure 5.1) and abundance (Figure 5.2) of ARGs in the different digestate samples were comparable. However, the fate of ARGs was different for

the different antibiotic classes, with some decreasing and others increasing after the mesophilic AD process. Figure 5.3 displays the average of the relative changes (%) in ARG levels in DMF1, while Figure 5.4 displays the changes observed in DMF2. The absolute change of ARG levels (Δ ARG copies/16S rRNA) can be consulted in Table C5.2 in in Appendix C.

Significant reductions in ARG levels in the two manures were observed after the mesophilic AD process. In DMF1 (Figure 5.3), ARGs encoding resistance to seven different classes of antibiotics were reduced (i.e., pleuromutilin, phenicol, multidrug, MLS, beta-lactams, aminocumarin, and acridine dye), although only the complete removal of ARGs for beta-lactams and acridine-type antibiotics, and the partial reduction of ARGs encoding multidrug resistance were statistically significant (p-value < 0.05). Nevertheless, ARG levels for nine different types of antibiotics increased after AD. For DMF2, reduction in ARG levels encoding resistance to fourteen classes of antibiotics was observed (Figure 5.4). The results were statistically significant for peptide, fluoroquinolone, aminoglycoside, and acridine dye-type antibiotics (p-value < 0.05). Pleuromutilin, nucleoside, and glycopeptide resistances increased in DMF2 after the AD process. In both manures (DMF1 and DMF2), the reduction of multidrug ARGs was the greatest, accounting for more than 0.18 and 0.35 ARG copies/16s RNA copies, respectively (Table C5.2 in Appendix C).

The effect of AD on the fate of ARGs during the AD process is often contradictory as Gurmessa et al. (2020) reported. For instance, regardless of the temperature at which AD is performed and the type of manure used, ARGs encoding resistance to tetracyclines, sulfonamides, and MLS, were reduced in some studies and enriched in others. Our results showed that some ARGs in dairy manures from two farms with different manure management strategies had a different fate. Whereas ARGs for tetracyclines, sulfonamides, rifamycin, peptide, nitroimidazole,

fluoroquinolones, and aminoglycosides were reduced in DMF2 (Figure 5.4), they were enriched in DMF1 after the AD process (Figure 5.3). Since the changes in levels of ARGs for these types of resistances seemed to be grouped, some of the ARGs were likely encoded in the same elements (e.g., *intl1* and *intl2*) as some studies have suggested (Cui et al. 2016; Resende et al. 2014; Sun et al. 2016). Cui et al. (2016) observed a positive correlation between several ARGs for tetracyclines and sulfonamides and the integrase gene of class 1 (*intl1*) in chicken manure. Hence, the reduction of ARGs for different antibiotic classes might be linked to a reduction of MGEs during the process. The co-occurrence of ARGs and microbes, which provides more insight into this area is discussed subsequent sections.

Many studies have demonstrated that AD is capable of reducing levels of ARGs encoding resistance to different beta-lactams (e.g., *cmy-2, blaCTX-M, bla-TEM, blaVIM*) in swine, cattle, and dairy manures(Flores-Orozco et al. 2020b; Gurmessa et al. 2020). In this study, beta-lactam ARGs were reduced in the two manures (DMF1 and DMF2), providing more evidence of the potential of AD to reduce levels of this type of ARGs. On the other hand, levels of ARGs for nucleosides (e.g., streptothricin) and glycopeptides (e.g., vancomycin) consistently increased after the mesophilic AD, suggesting that some of the anaerobes involved in the AD process could be carrying them. Further studies should consider evaluating the presence of these types of ARGs and alternatives to reduce them.

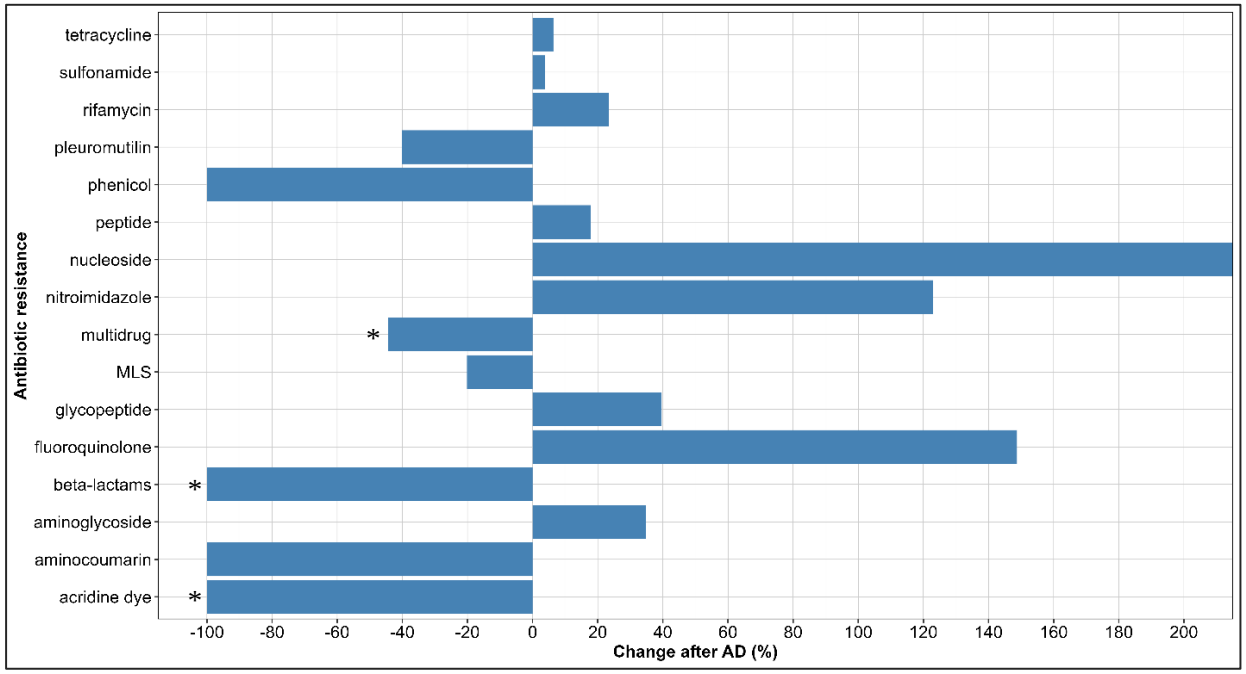

Figure 5.3 Relative changes (%) in ARG levels in manure from Farm 2 (DMF2). * Indicates statistical significance with a p-value < 0.05.

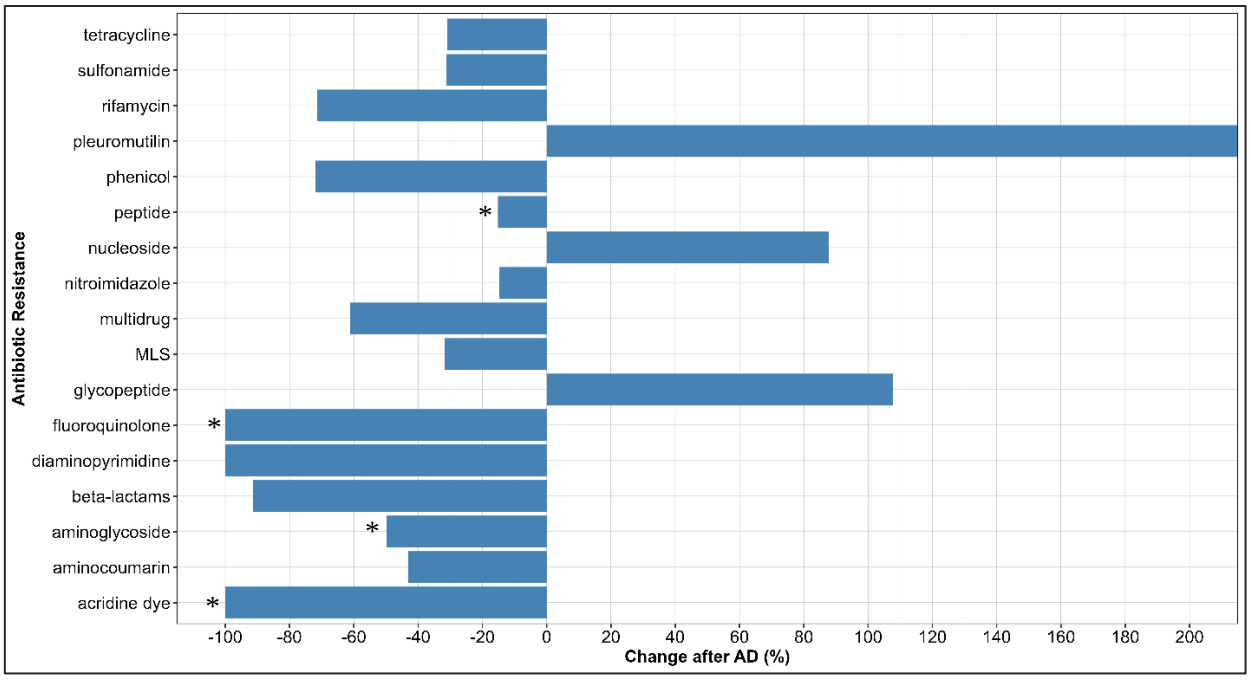

Figure 5.4 Relative changes (%) in ARG levels in manure from Farm 2 (DMF2). * Indicates statistical significance with a p-value < 0.05.

5.5.4. Microbial community structure in manure and digestate samples

Figure 5.5 displays the microbial community structures of the different manure and digestate samples, highlighting the 20 most abundant microbial orders. The phylogenetic classification revealed that the microbial communities of manure batches from the same farm were similar to each other (DMF1_1 to DMF1_2 and DMF2_1 to DMF2_2), but different from batches from different farms (DMF1 to DMF2). The most abundant phyla in manures were Firmicutes (Clostridiales, Lactobacilliales, Turicibacteriales, and Erysipelotrichales), Actinobacteria (Actinomycetales and Bifidobacteriales), and Bacteroidetes (Bacteroidales), which are commonly found in dairy and cattle manures (Gou et al. 2018; Zhang et al. 2019a).

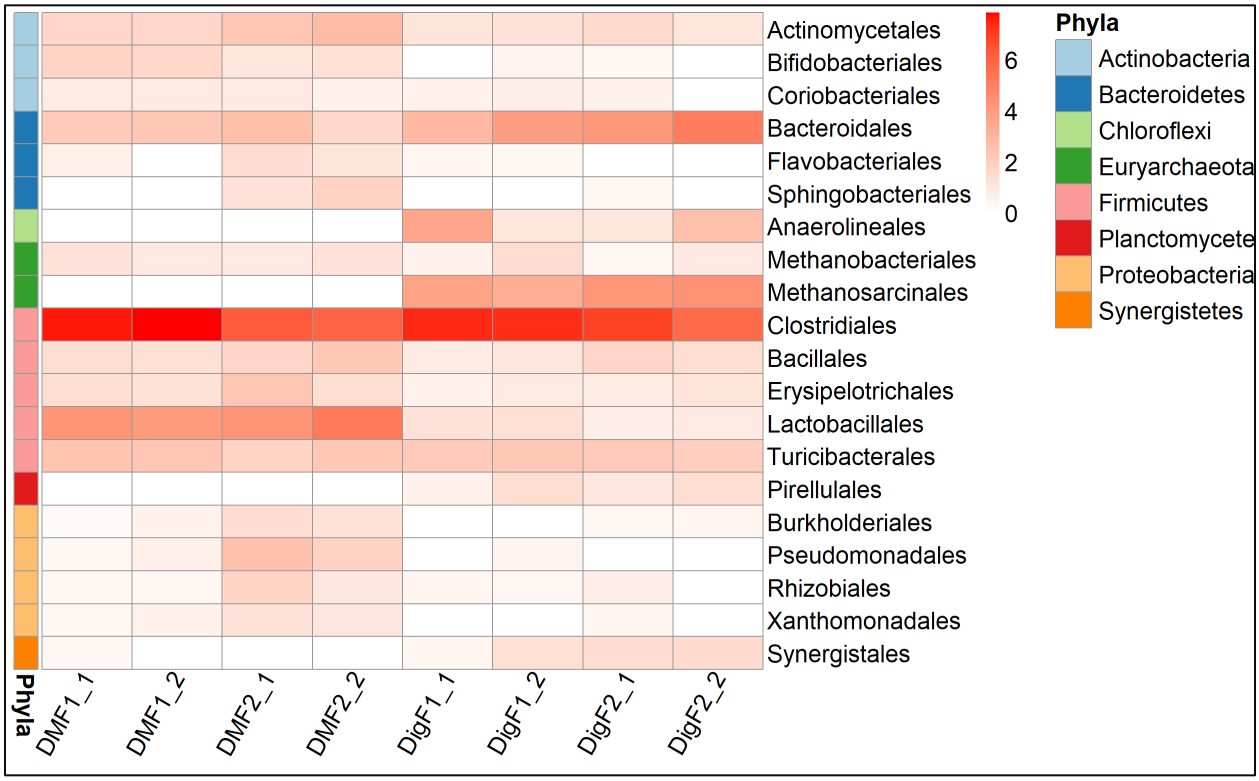

Figure 5.5 Relative abundance of the microbial groups at order level of manure and digestates. The squared root of the relative abundance (normalized to 16S rRNA) is shown to ease visualization.

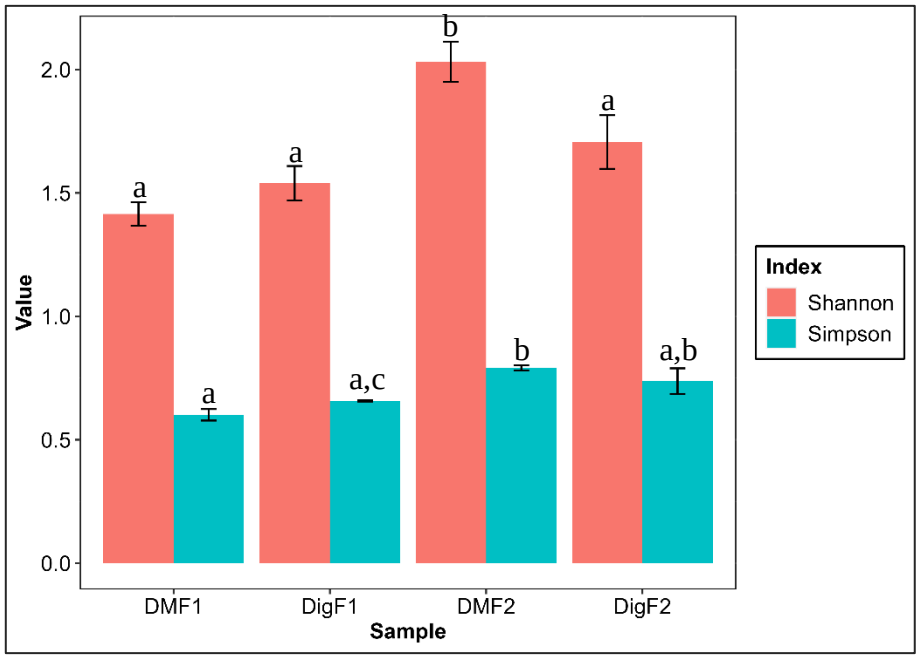

Figure 5.6 Shannon and Simpson diversity indices. Different letters in the same index bars indicate a statistically significant difference with 95% confidence.

The microbial richness and evenness of the different samples were evaluated with the Shannon and Simpsons diversity indices (Figure 5.6). The Shannon index evaluates diversity valuing more the richness and it increases as the diversity increases, whereas the Simpson index places a greater weight on species evenness, and it decreases as diversity increases (Kim et al. 2017). The indices showed a significantly richer (*p-value* < 0.05) and more even microbial diversity in DMF2 compared to DMF1. The microorganisms with higher abundance in DMF2 belonged to the phyla Proteobacteria (Rhizobacteriales, Pheseudomonadales, Rizhobiales, and Xanthomonadales) and Bacteroidetes (Sphingobacteriales and Flavobacteriales) (Figure 5.5). The variance in microbial diversity between the manures from the two farms might be attributed to their distinct manure management practices. The results might suggest that the recirculation of recovered solids in Farm 2, may induce the enrichment of Proteobacteria and Bacteroidetes in the manure. Since many Proteobacteria and Bacteroidetes have been identified as potential ARG

carriers in ruminant guts and manure (Gou et al. 2018; Hu et al. 2016b), it is possible that elevated presence in DMF2 might correlate with the increased ARG levels observed in this study. However, more comprehensive research is needed to validate this hypothesis.

On the other hand, the microbial composition of the digestate samples (Dig1 and Dig2) were comparable between the two farms but were different from the raw manure (Figure 5.5). The Shannon and Simpson indices (Figure 5.6) suggested that the diversity of DMF1 and its digestates (DigF1) had comparable biodiversity, whereas the digestate DigF2 was significative less diverse than DMF2 ($p\text{-}value < 0.05$). Since the anaerobic CSTR provided an engineered environment, the microbial diversity was expected to decrease because the anaerobic populations required in the AD process are favored. For instance, acetotrophic methanogens (acetate-utilizing methanogens), belonging to the order Methanosarcinales, such as *Methanosarcina* and *Methanosaeta*, were enriched as they usually comprise the majority of archaea present in anaerobic digesters (Zhang et al. 2018a). Similarly, anaerobic ammonium-oxidizing (anammox) bacteria of the order Pirellulales, Anaerolineales responsible for the fermentation of carbohydrates and proteinaceous materials (Petriglieri et al. 2018), Synergistales, and Bacteroidales, typically found in anaerobic digesters, were only detected in digestate samples. Nonetheless, hydrogenotrophic methanogens of the order Methanobacteriales, and some Clostridiales, were found in manures and digestates as they play an important role in the animal gut and anaerobic digesters.

The Pearson's correlation of the co-occurrence of the microbial orders in manure and digestate samples (Figure 5.7) demonstrates the microbial community shift after the AD process. As expected, anaerobic microorganisms (i.e., Anaerolineales, Methanosarcinales, Pirellulales, and some Bacteroidales) were negatively correlated with aerobes belonging to orders such as Coribacteriales, Bifidobacteriales, Lactobacteriales, Actinomycetales, and Xanthomonadales. The

typical anaerobic microorganisms found in anaerobic digesters (Methanosarcinales, Pirellulales, Synergistales, and Anaerolineales) had a strong positive correlation. Likewise, typical microorganisms found in dairy manure belonging to orders such as Erysipelotrichales, Rhizobiales, Burkholderiales, and Flavobacteriales, were positively correlated.

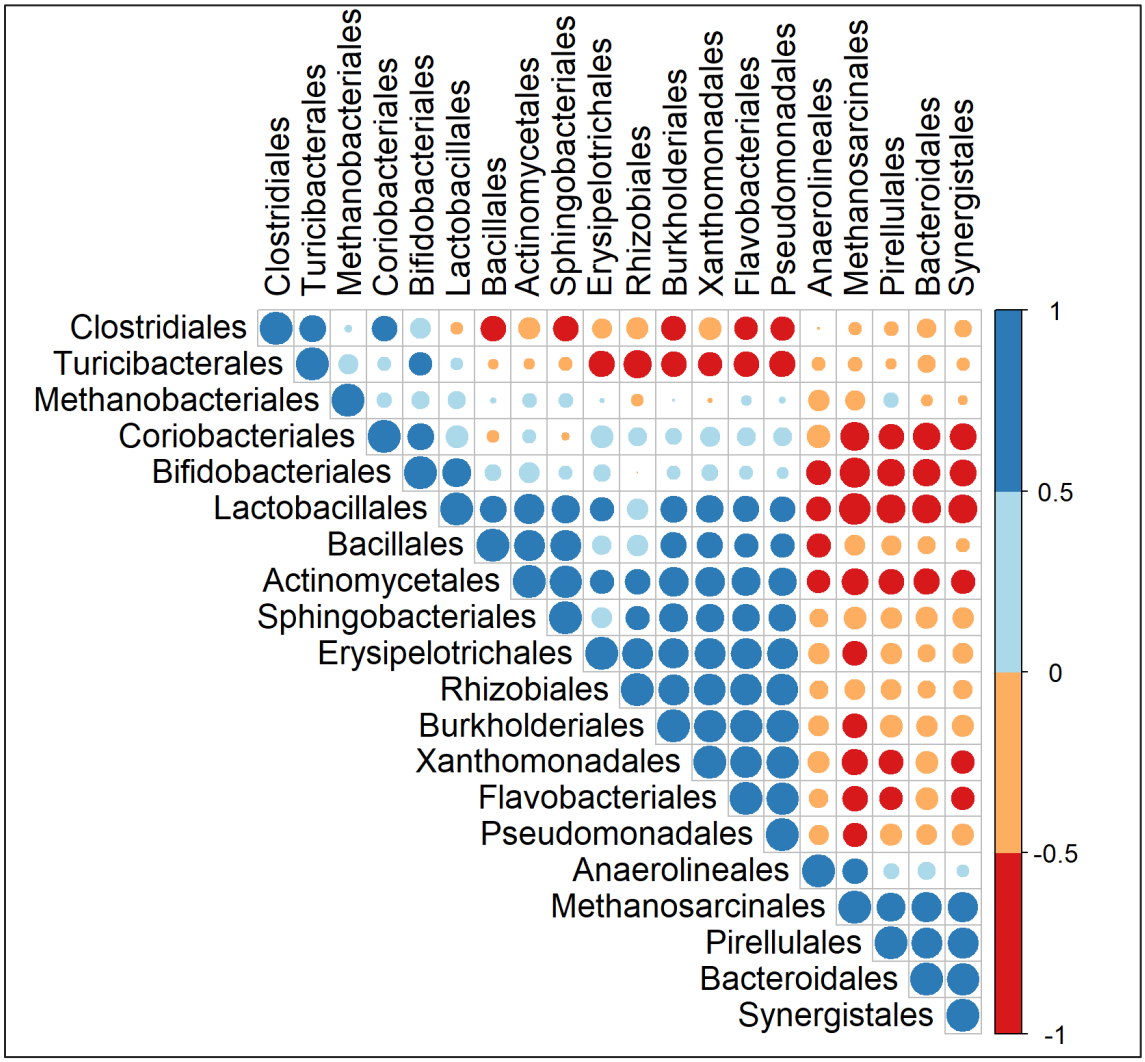

Figure 5.7 Pearson's correlations of the co-occurrence of the different groups of microorganisms (order level). Blue color indicates a positive correlation, whereas red negative correlation; size represents correlation value (0-1).

5.5.5. Relationships between resistomes and microbial community

The microbial composition and resistome profile (categorized by antibiotic class) were employed to ordinate the manure (DMF1 and DMF2) and digestate (DigF1 and DigF2) samples

using a PCoA based on Bray-Curtis dissimilarities (Figure 5.8). The analysis explained 80.2% of the variation of the data (61.3 PC1 and 18.9% PC2), which confirmed the efficacy of integrating resistome and microbial profiles for assessing sample similarities, given their intrinsic connection.

The PCoA (Figure 5.8) also revealed the following: (i) manure and digestate samples were clearly different as they clustered separately; (ii) manure batches form the same farm (i.e., DMF1or DMF2) were similar as they clustered together but were different from the manure from the other farm; (iii) digestate samples were similar as they clustered together regardless of the source of the manure. These findings confirmed that MAD could change and establish a stable microbial community and a resistome profile regardless of the source of the dairy manure. Futures studies should evaluate how changes in the microbial communities driven by changes in operational parameters of the AD process affect the evolution of ARGs.

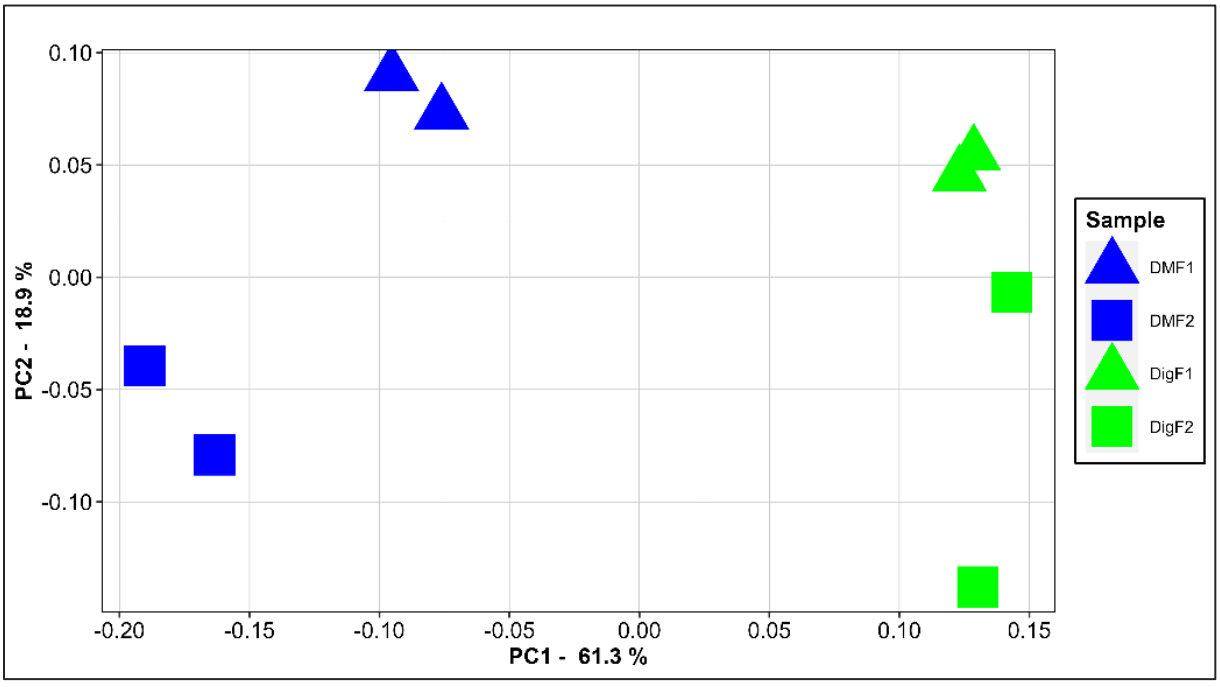

Figure 5.8 Principal Coordinate analysis (PCoA) based on the Bray-Curtis distance of the resistome and microbial community combination.

5.5.6. Putative ARGs carriers

The co-occurrence of ARGs and microorganisms in manures and digestates was evaluated in a correlation matrix using the Pearson's correlation coefficients (Figure 5.9). The results suggested that Proteobacteria from the Orders Burkholderiales, Pseudomonadales, Rhizobiales, and Xanthomonadales, Firmicutes such as Erysipelotrichales, and Lactobacilliales, and Bacteroidetes such as Flavobacteriales, were strongly correlated with ARGs conferring resistance to acridine dye, beta-lactams, multidrug resistance, phenicol, and diaminopyrimidine. ARGs for sulfonamides were correlated with Actinomycetales and Bacilliales, whereas Clostridiales had the highest correlation with ARGs for tetracyclines. These results are in line with previous studies that have suggested potential ARG carriers in different samples. Pseudomonadales, Xanthomonadales, Burkholderiales, and Flavobacteriales have been associated with ARGs for tetracyclines, fluoroquinolones, sulfonamides and several multidrug (Crossman et al. 2008; Liu et al. 2020; Sun et al. 2016); Actinomycetales with ARGs for fluoroquinolones (Liu et al., 2020); Pseudomonadales and Bacilliales with sulfonamides (Byrne-Bailey et al. 2009) and; Clostridiales and Bacteriodales with ARG for tetracyclines and MLS (Jia et al. 2017). ARGs encoding resistance to beta-lactams have been associated with several Bacteriodales, including *Prevotella* (Jia et al., 2017). Therefore, it would be reasonable to assume that the differences in ARGs levels observed in manures (Figure 5.1) was caused by the higher abundance of microbial groups harboring ARGs that were favored in each farm.

On the other hand, the correlation matrix (Figure 5.9) revealed a negative correlation between the typical anaerobes involved in mesophilic AD (i.e., Methanosarcinales, Pirellulales, Synergistales, and Anaerolineales) and most of the ARGs previously mentioned. This indicates that the reduction of ARGs observed after the mesophilic AD process was mainly driven by the

reduction of aerobic microorganisms and the selection of anaerobic microbial populations, as previous studies have also suggested (Sun et al. 2016). These microbial taxa were positively correlated with the presence of ARGs encoding resistance to aminoglycosides, peptides, glycopeptides, pleuromutilin, and nucleosides. Interestingly, Methanosarcinales, Pirellulales, and Synergistales seemed to be the microbial groups responsible for carrying the ARGs for pleuromutilin, nitroimidazole, and nucleoside, while Anaerolineales were the microbial group with the greatest correlation with ARGs for fluoroquinolones. Hence, the increase in ARG levels for these antibiotics observed after AD (Figures 5.3 and 5.4) may have been driven by the increase of these microbial groups in the anaerobic CSTR.

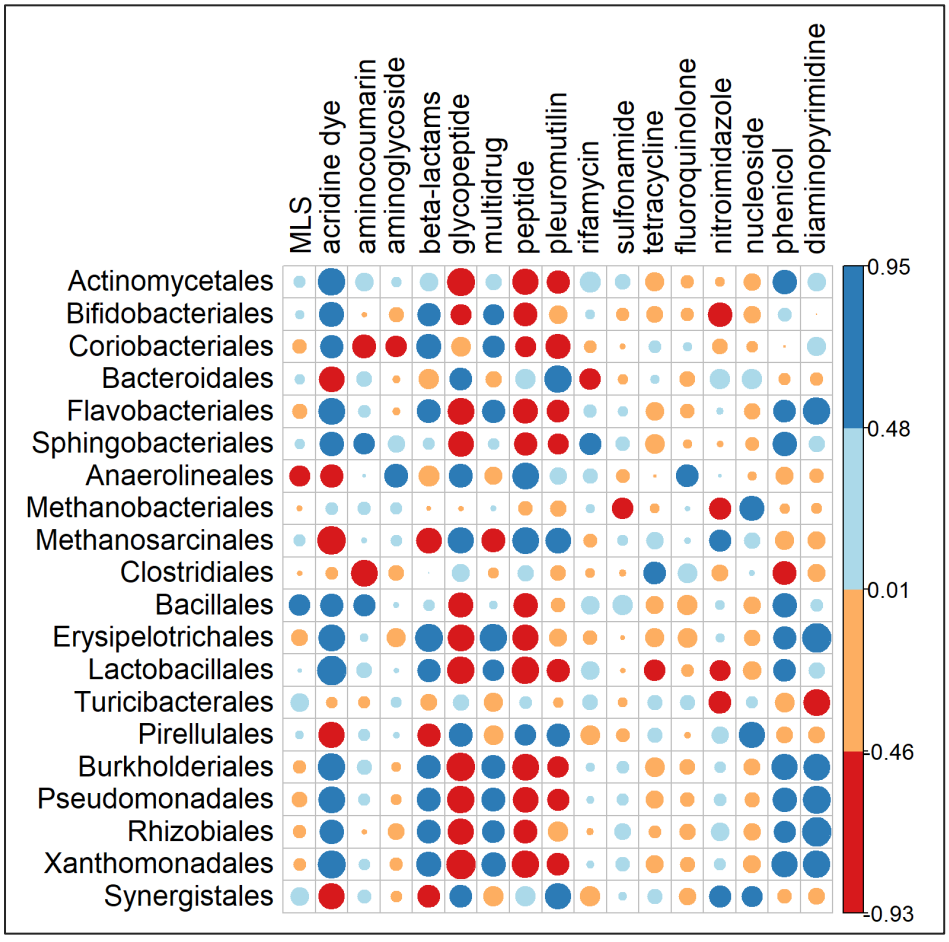

Figure 5.9 Pearson's correlation of the co-occurrence of ARGs by antibiotic class and microbial Orders. The size and color in correlograms represent the correlation direction and coefficient.

Together these results imply that the treated manure generated in the mesophilic AD process could have a lower risk of ARGs emission compared to raw manures when applied on land. Futures studies should compare the evolution of the resistome profile on land amended with raw manure and digestate to confirm this hypothesis.

5.5.7. Co-occurrence of different ARGs

Pearson's correlations of the co-occurrence of ARGs by antibiotic class in all samples (Figure 5.10) showed that some of the resistances were strongly correlated. ARGs for tetracyclines and sulfonamides, which are consistently detected in animal manures and wastewaters (Ma et al. 2011; Zou et al. 2020), were strongly correlated. ARGs for beta-lactams were positively correlated with ARGs encoding resistance to phenicol, diaminopyrimidine, acridine dye, and multidrug ARGs, while phenicol ARGs were strongly correlated with acridine dye, aminocumarin, and multidrug ARGs. Interestingly, some of the resistances were negatively correlated. For example, ARGs encoding multidrug resistance had a negative correlation with MLS, tetracyclines, glycopeptide, and peptide, whereas glycopeptide and peptide were also negatively correlated with diaminopyrimidine, acridine dye, beta-lactams, and phenicol ARGs. These negative correlations between ARGs for different antibiotics were attributed to the switch of the microbial community during the AD process that enriched microbial species strongly correlated with other types of ARGs.

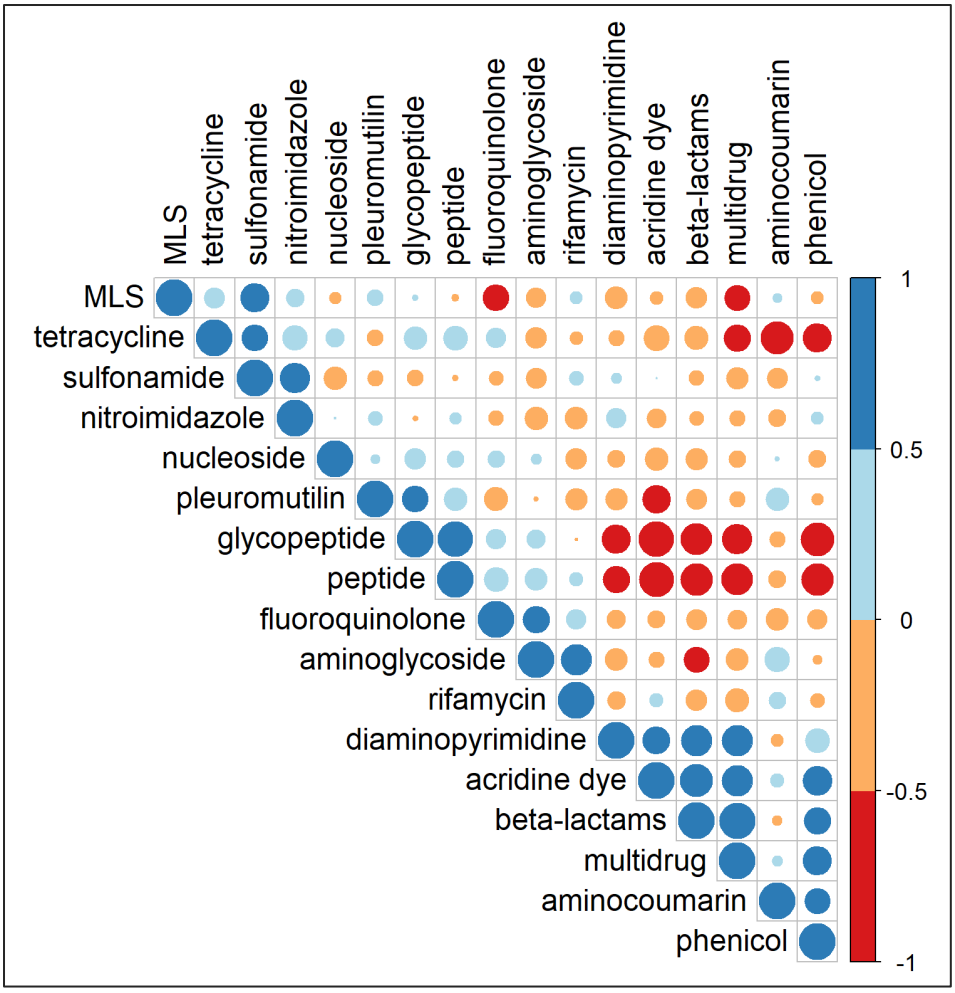

Figure 5.10 Pearson's correlation of the co-occurrence of ARGs by antibiotic class. The size and color in correlograms represent the correlation direction and coefficient.

The network analysis of the interactions between the ARGs detected in manures (Figure 5.11a) and digestate samples (Figure 5.11b), showed groups of several ARGs closely correlated, indicating that they could be part of the same elements (e.g., integrons, transposons, plasmids, and/or microbial genomes). In the manure network (Figure 5.11a), a higher number of clusters were observed compared to the digestate network. The clusters were richer in ARGs encoding different mechanisms of resistance for different antibiotics. This suggests that mesophilic AD not only reduced the total number of unique ARGs, but it also reduced the co-occurrence and interactions of different groups of ARGs potentially located in the same genetic elements or

microbial groups. Previous studies have observed a consistent reduction in ARGs for different antibiotics such as tetracyclines, sulfonamides, and MLS associated with MGEs such as the class 1 integron system (*intlI*) during AD (Cui et al. 2016; Zou et al. 2020). Therefore, it is suggested that the reduction in levels of ARGs in this study could also be attributed to MGEs removal.

The network of digestate samples (Figure 5.11b) also revealed intensive correlations between several groups of ARGs. Since the microbial communities in digestates were less diverse and more homogeneous than in manures (Figures 5.5 and 5.6), the clusters could represent more traceable elements. For example, the strong correlation between *aad(6)* and *ANT(6)-Ia* with and others ARGs such as *lsaE, ErmA, tetT, tetM, arlR, vatB*, and *LlmA*, could indicate the presence of plasmids carrying them since *ANT(6)-Ia* and *aad(6)* are well-known plasmid-encoded ARGs (Schwarz et al. 2001). Moreover, the intensive interactions between different van genes (e.g., *vanRI*, *vanHM*, *vanG*, *vanRC*, etc.) could be associated with the presence of van operons. Similarly, strong relationships between tetracyclines ARGs suggested the presence of specialized elements encoding this resistance. Futures studies should determine whether these ARGs clustered are part of MGEs that represent a risk of ARG transfer or if they are part of microbial genomes.

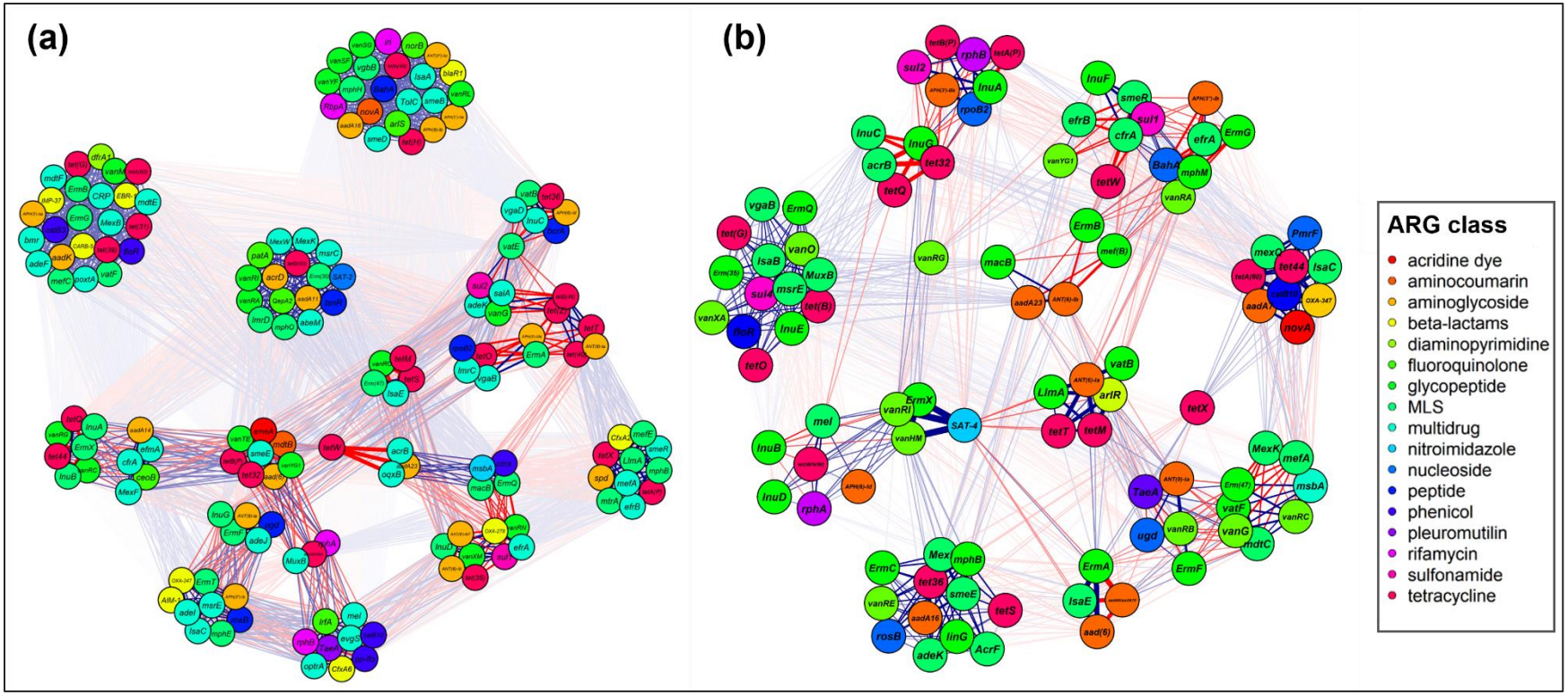

Figure 5.11 Network analysis of the co-occurrence of individual ARGs in (a) Manure samples and (b) Digestate samples. Line thickness indicates correlation (0-1). Blue lines indicate s a positive correlation; red lines indicate a negative correlation.

5.6. Conclusion

Using a metagenomic approach, this study demonstrated that mesophilic AD could change the resistome profile and reduce the relative abundance of several ARGs in dairy manures, although a complete removal was rarely achieved. The shift of the microbial community was strongly correlated with the changes in ARGs, suggesting this as one of the main drivers. The analyses showed several microbial groups in dairy manures and mesophilic digestates as potential ARG hosts. A network analysis suggested that mesophilic AD was also capable of reducing the co-occurrence of different groups of ARGs potentially located in the same genetic elements. Finally, this study demonstrated the reliability of this metagenomic approach to evaluate the complex interactions between microbial communities and ARGs.

5.7. Acknowledgments

This research work was financially supported by the National Sciences and Engineering Research Council of Canada (NSERC) through the Discovery Grants program [RGPIN-2016-05929].

Chapter 6: Effects of different manure treatments on resistomes and mobilomes

6.1. Preface

This chapter explores the resistome and mobilome profiles in bovine manures from three different farms in Manitoba, and how their manure management strategies influence ARG and MGE levels. Notably, one of these farms operated in an antibiotic-free environment, which served as a control to assess the impact of avoiding the use of antibiotic on ARGs. The work described in this chapter has been peer-reviewed and published as original research in the journal *Frontiers in Synthetic Biology* in 2023 in a manuscript entitled "*Influence of three different manure treatments on antimicrobial resistance genes and mobile genetic elements*" (https://doi.org/10.3389/fsybi.2023.1301879). I alone was responsible for the data collection and analysis, interpretation of the results, and the preparation of the manuscript. The other co-authors provided thoughtful and challenging discussions on the results and reviewed the manuscript prior to publication. Minor modifications were made to the original manuscript to adjust the style to this document and reduce redundancy.

6.2. Abstract

This study employed a metagenomic approach to investigate and compare the impact of common manure treatments, including aerobic storage, mesophilic anaerobic digestion (MAD), and solid-liquid separation, on the presence and abundance of ARGs, BacMet resistance genes, and MGEs in manure from three different farms, including one operating in an antibiotic-free environment. The results indicated that MAD was the best method to reduce the numbers of ARGs, BacMet, and MGEs, achieving reduction rates greater than 40%, 89%, and 68%, respectively. Manure storage significantly reduced BacMet levels (over 30%) and MGEs (28%) but had no significant effect on total ARG levels. Solids recovered through solid-liquid separation exhibited

elevated levels of ARGs, BacMet, and MGEs, while the liquid fraction displayed levels similar to untreated manures. Correlation and co-occurrence analyses indicated that changes in microbial communities, particularly fluctuations in aerobic and facultative communities belonging to the phyla Bacillota, Actinomycetota, and Pseudomonadota played a significant role in driving changes in ARGs, BacMet, and MGEs. The results also showed the presence of toxin-antitoxin and transposon systems near different ARGs. Overall, the results confirmed the widespread presence of genes conferring resistance to various antimicrobials and MGE capable of mobilizing them are widely spread in dairy farms. The results also suggested that even without antibiotics, the use of heavy metals and disinfectants might sustain ARGs and MGEs. Finally, this study corroborated that AD could be one of the best alternatives to reduce the risk of spread of AMR associated with livestock manure.

6.3. Introduction

In the last decade, several studies have evaluated the fate of various ARGs in different types of animal manures during common manure treatments, including composting (Cheng et al. 2019; Cui et al. 2016), aerobic and anaerobic storage (Duriez and Topp 2007; Wallace et al. 2018), and AD (Chapter 4 and Flores-Orozco et al. (2022)). Although all these studies have shown that manure treatments can influence the levels of ARGs and MGEs in manure thanks to the specific microbial successions involved (Cheng et al. 2019; Zhang et al. 2020c, 2020b), it has not been possible to draw solid conclusions due to the variability of the results. Also, the fate and evolution of ARGs and MGEs in novel manure treatments, such as the separation of solids from liquid manure (often used in cattle farms for recovering solids for animal bedding), have not been investigated. As the adoption of these treatments is expected to grow due to their various economic and environmental benefits, including increasing the value of manure and reducing the costs

related to bedding materials and the reduction of odors and nutrients (Wicks and Keener 2017), it is important to understand the dynamics of ARGs and MGEs in these contexts.

In this study, metagenomic techniques were utilized to evaluate the dynamics of resistomes (including BacMet resistance genes) and mobilomes, across various manure treatments. These treatments included open (aerobic) tank storage, solid-liquid separation within a bedding recovery unit (BRU), and MAD. The methodology involved collecting samples from both untreated and treated manures across three distinct dairy farms and then employing metagenomics for resistome and mobilome analysis. Notably, one of the farms operated without antibiotics, offering a unique perspective on the implications of reducing antibiotic usage on resistomes and mobilomes, as well as the potential effects of other antimicrobial agents, like foot bathing solutions. Additionally, this study delved into the co-occurrence patterns of microbial groups, ARGs, and MGEs to identify microbial shifts that might influence resistomes and mobilomes under different manure management practices. The main hypotheses were that untreated manure from the antibiotic-free farm would have lower levels of ARGs, and that the treatments that cause the reduction of aerobic communities would yield greater ARG reduction rates.

6.4. Materials and methods

6.4.1. Sampling

Untreated bovine manures were collected from the temporary manure pit of three dairy farms located in Manitoba, Canada, as follows: Two samples (4 months apart) of untreated manure (F1M1, F1M2) from a medium-size farm (~ 200 milking cows, Farm 1); Two samples (one year apart) of manure (F2M1, F2M2) from a small antibiotic-free dairy farm (< 100 milking cows, Farm 2); two samples of manure (F3M1, F3M2) from a large farm (> 500 milking cows, Farm 3).

Treated manures were sampled as follows: Untreated manures from Farm 1 were digested in the mesophilic anaerobic digester as described in Chapter 3. Hence, Farm 1 treated manures were the corresponding digestates (F1D1, F1D2). Farm 2 treated manures corresponded to manure stored in an open collection and storage tank sampled in two consecutive fall seasons (F2S1, F2S2). This tank was 5.5 m in height and 28 m in diameter open to atmosphere (aerobic) and was usually emptied twice a year during the spring and fall seasons. Farm 3 treated manures were the liquid (F3L1, F3L2) and solid (F3S1, F3S2) fractions of the BRU operated in the farm. In such systems, the solids and liquids are separated through a screw press and the solids are then passed through an in-vessel composter for approximately 24 h, reaching temperatures over 60 °C. The liquids are stored in lagoons for on-field agronomic applications. A detailed description of the operation of the BRU on this farm as well as the general physicochemical properties of the solids and liquids can be found in Ackerman et al. (2018). Farm 3 untreated manures were also digested (F3D1, F3D2) in a lab-scale mesophilic anaerobic digester similar to Farm 1 samples.

A schematic of the sampling points and general physicochemical properties of untreated and treated manures can be found in Appendix D (Table D6.1 and Figure D6.1). Note that all three farms reported the use of acidified copper sulfate solutions for foot bathing, typically composed of 80-90% copper sulfate mixed with 10-20% citric acid on a weekly basis. These solutions are commonly washed off and go to the main manure pits.

6.4.2. DNA isolation, sequencing, and metagenomics

The methodology of the DNA extraction, sequencing, and metagenomic analyses are described in detailed in Chapter 3.

6.4.3. Data analyses

Principal Coordinates Analyses (PCoA) based on Bray-Curtis were used to determine similarities between the different groups of samples in terms of ARGs, BacMet, MGEs, and microbial communities. The Chao, Shannon, and Simpson diversity indices were estimated using the R package *vegan*. The 95%-confidence intervals of the diversity indices were estimated via bootstrapping (n = 1500, sample size = 133). Mantel tests were used to determine the correlations between the total levels of ARGs, MGEs, and the microbial genera grouped by the type of respiration (i.e., aerobic, anaerobic, and facultative). The relationships between microbial genera and ARGs and MGEs were further explored with co-occurrence analyses as described in in Chapter 3 (Section 3.9.6). Statistically significant differences in the different parameters evaluated in this study were determined using t-tests with an alpha of 0.05.

6.5. Results and Discussion

6.5.1. Microbiomes in untreated and treated manures

6.5.1.1. Microbiomes in untreated manures

The microbial communities at the phylum and genus levels of untreated and treated manures from the three different farms are shown in Figures 6.1 and 6.2, respectively. The dominant phyla in untreated manure from Farm 1 (F1M1, F1M2) were Bacillota (51%), Actinomycetota (33%), Euryarchaeota (7.6%), Pseudomonadota (5.1%), and Bacteroidota (2.5%); in Farm 2 (F2M1, F2M2) Bacillota (49%), Actinomycetota (15%), Pseudomonadota (12.3%), Bacteroidota (11%), and Euryarchaeota (8.4%); and in Farm 3 (F3M1, F3M2) Bacillota (37%), Actinomycetota (22%), Pseudomonadota (17%), Bacteroidota (15.6%), and Euryarchaeota (24.8%). Although the dominant phyla were similar in all untreated manures, those from Farm 1 were characterized by higher levels of Actinomycetota (e.g., *Bifidobacterium*, *Corynebacterium*) and lower levels of

Bacteroidota (e.g., *Sphingobacterium*, *Phocaeeicola*, *Bacteroides*). The higher levels of Mycoplasmatota (e.g., *Haploplasma*, *Paracholeplasma*, *Acholeplasma*) were distinctive of untreated manures from Farm 2. Also, the microbiomes in manures from Farm 2 were more diverse than the other untreated manures (Figure 6.3), although they also had the lowest microbial richness indices (Figure 6.4). On the other hand, Farm 3 was characterized by a higher abundance of Pseudomonadota (e.g., *Acinetobacter*, *Pseudoxanthomonas*) and Bacteroidota (e.g., *Sphingobacterium, Bacteroides*). The diversity indices indicated that the microbiomes in manures from Farm 3 were less diverse than those in Farm 2 but similar to those in Farm 1 (Figure 6.3), although they had higher microbial richness indices (Figure 6.4).

To evaluate the overall similarity and dissimilarity of microbial communities among the different farms and manure samples, a PCoA was performed based on the phylum-level composition, as depicted in Figure 6.5A. The PCoA analysis explained 64.1% of the variation, with PC1 accounting for 48.6% and PC2 accounting for 15.5%. The PCoA plot revealed distinct clustering patterns, indicating that untreated manures from the same farm tended to group together and were distinguishable from manures obtained from the other farms. Notably, untreated manures from Farm 2 exhibited greater variability in the structure of their microbial communities. Specifically, F2M1 displayed a closer resemblance to the microbiome structure of manure from Farm 3, while F2M2 displayed a closer resemblance to the microbiomes of manures from Farm 1. These differences were primarily attributed to variations in the levels of Bacillota and Pseudomonadota between F2M1 and F2M2.

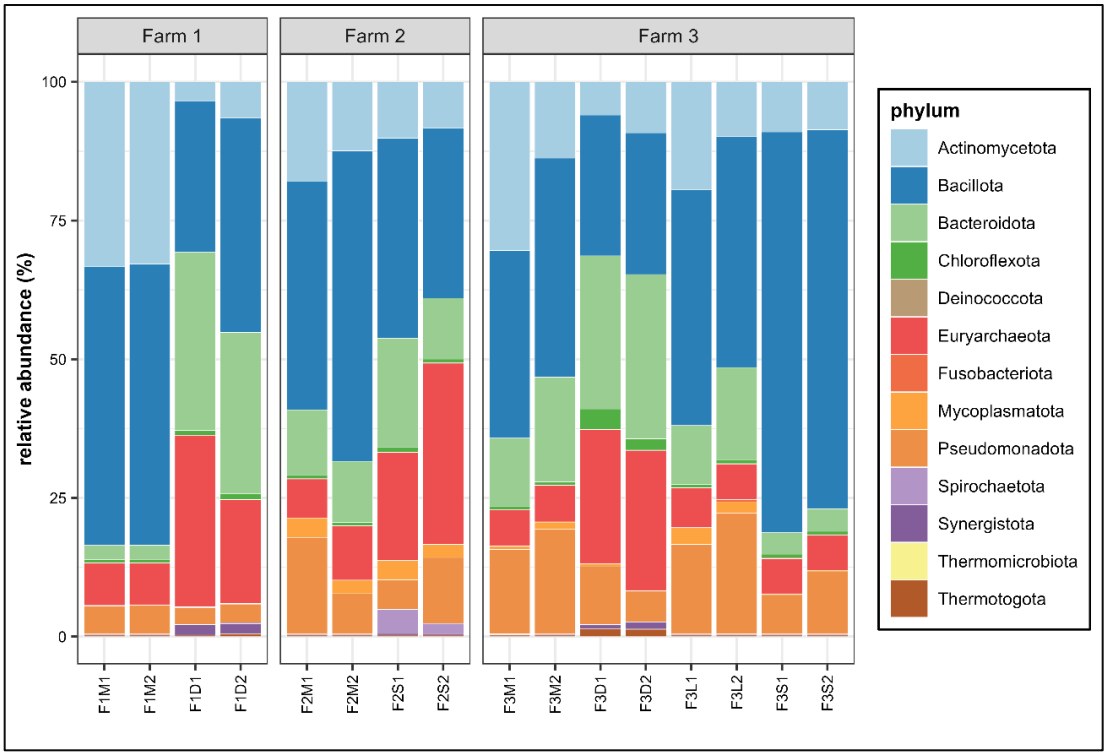

Figure 6.1 Microbial communities in untreated and treated manures at the Phylum level.

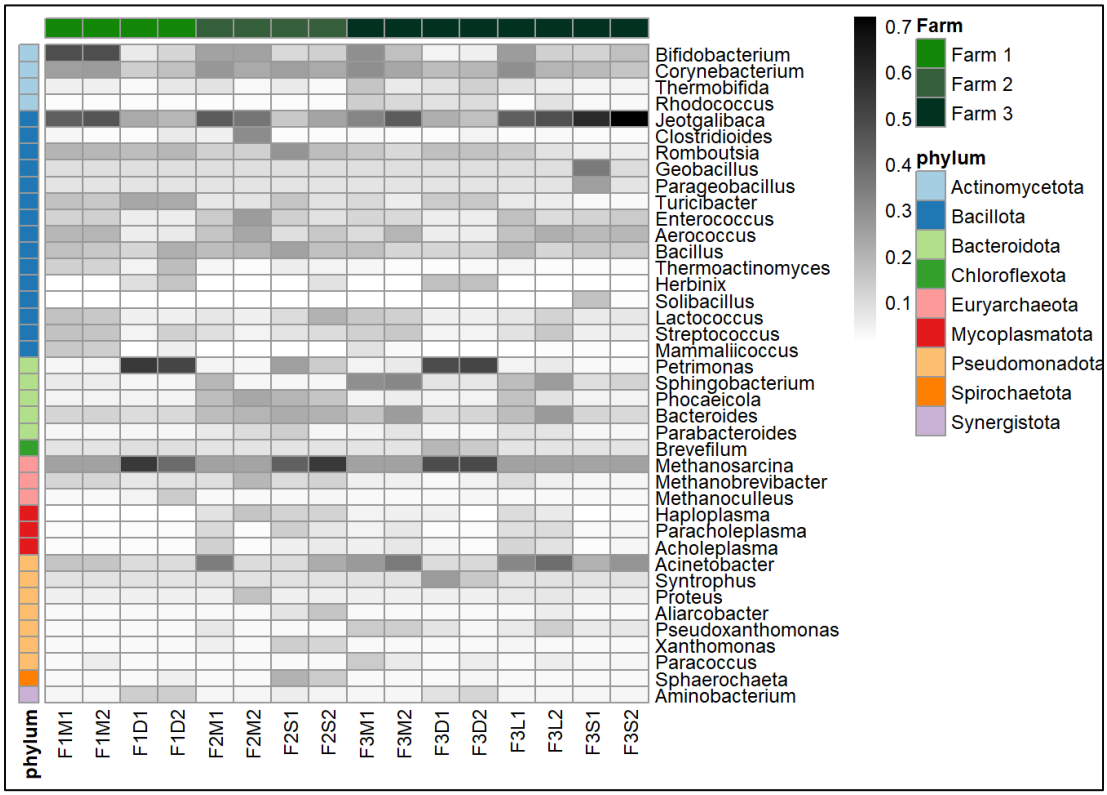

Figure 6.2 Top-40 microbial genera of untreated and treated manures.

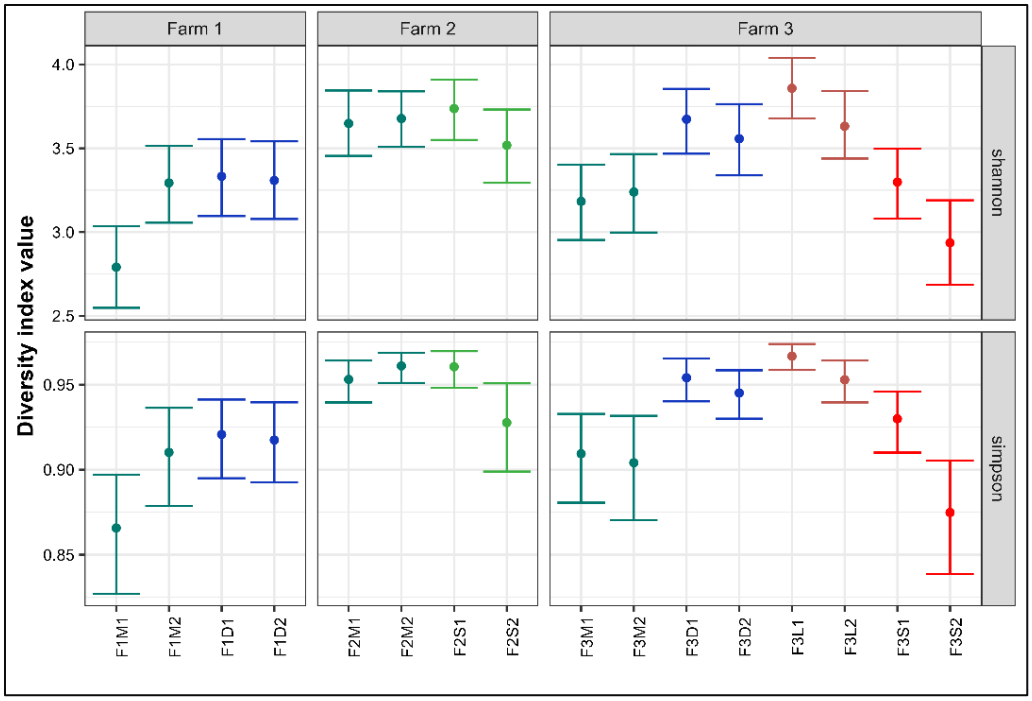

Figure 6.3 Shannon's and Simpsons' diversity indices. Bars represent the 95%-confidence intervals.

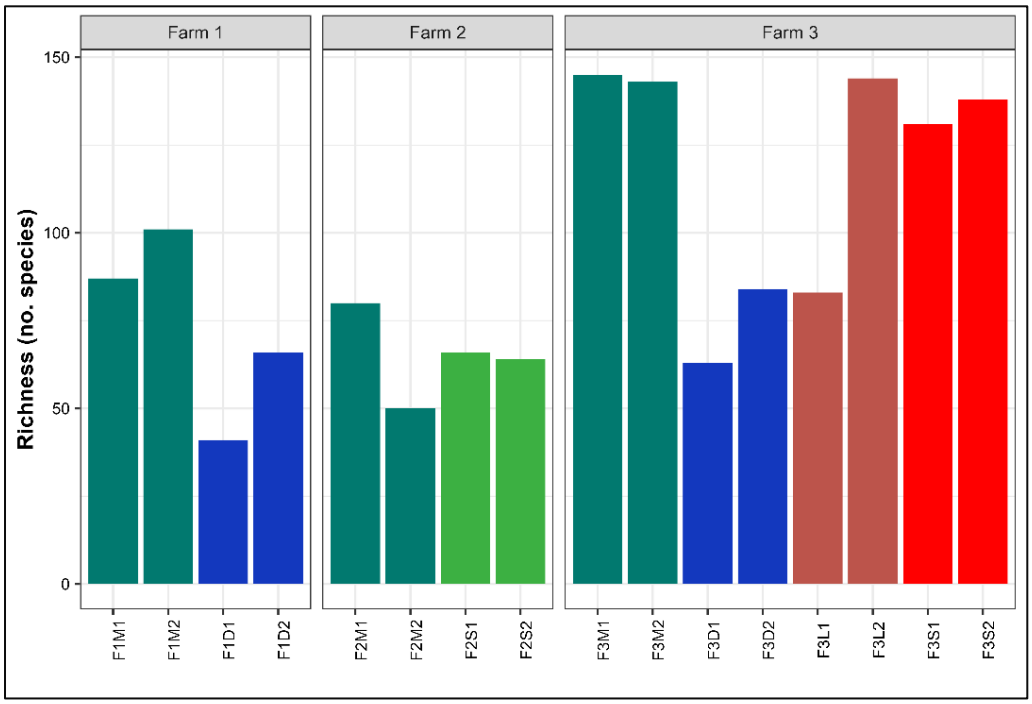

Figure 6.4 Chao index of microbiomes of untreated and treated manures.

The observed differences in the structures of microbial communities across the farms are likely influenced by a combination of factors, including each farm's specific manure management strategies, unique farm operations such as feeding practices and disinfection regimes. Additionally, environmental and physicochemical variables like temperature, humidity, nitrogen, and oxygen levels in the manure storage areas could also have significant impacts (Sun et al. 2020). In the case of Farm 3, the recirculation of solids from the BRU may have influenced the microbiomes in the temporary manure pit where the samples were collected. Previous studies have reported the enrichment of specific bacteria, such as *Streptococcus* and *Klebsiella*, in farms utilizing BRUs (Harrison et al. 2008). However, there is still limited knowledge regarding the impact of such practices on microbial communities in manure pits and the potential consequences they may have. In contrast, the microbiome of manures from the antibiotic-free farm (Farm 2) exhibited higher diversity but lower microbial richness compared to the other farms (Figures 6.3 and 6.4). Previous studies have reported that antibiotics can reduce the microbial diversity in complex microbiomes (Liu et al. 2020; Mazzurco Miritana et al. 2020). This suggests that the absence of residual antibiotics allowed natural competition that ultimately led to the establishment of more evenly distributed microbial communities.

Overall microbiome structure in untreated manures of the three survey farms corresponded to common manure microbiomes adapted to environmental conditions (e.g., higher O_2) and not gut-adapted manure microbiomes (Sukhum et al. 2021). Untreated bovine manures are commonly rich in Pseudomonadota and Bacteroidota (Pitta et al. 2020), whereas in this study, Bacillota stood as the dominant phyla. Also, the results highlight the potential influence of manure management strategies, such as the use of BRUs or the absence of antimicrobials, on the microbial composition of manures. Further research is necessary to gain a deeper understanding of how these practices

affect microbial communities in manure pits and the potential implications for overall ecosystem health and stability.

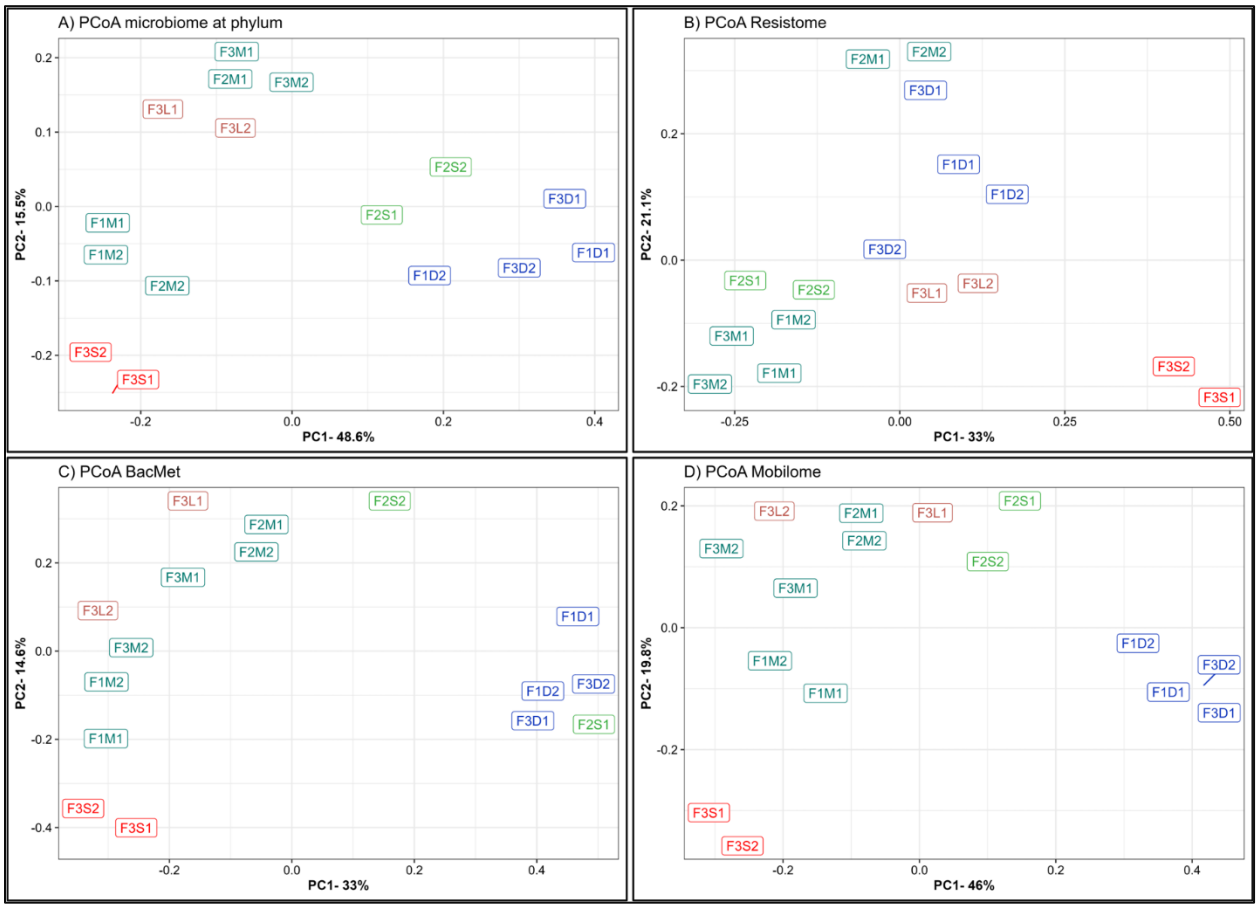

Figure 6.5 Principal coordinate analyses of microbiomes at phylum (A), ARGs (B), BacMet (C), and MGEs (D). Bray-Curtis distance was used to ordinate samples. Colors indicate the farm where the manure samples were collected.

6.5.1.2. Microbiomes in treated manures

The impact of manure treatments on microbial communities was evident, leading to distinct changes in composition. For instance, MAD samples (F1D1, F1D2, F3D1, F3D2) exhibited higher abundances of Euryarchaeota (e.g., *Methanosarcina*), Bacteroidota (e.g., *Petrimonas*), Synergistota (e.g., *Aminobacterium*), and Thermotogota (e.g., *Mesotoga*), and lower levels of Actinobacteria (e.g., *Bifidobacterium*), Bacillota (e.g., *Enterococcus*, *Aerococcus*, *Lactococcus*,

Streptococcus), and Pseudomonadota (e.g., *Acinetobacter*) (Figures 6.1 and 6.2). As expected, the digested manures had elevated levels of anaerobic microorganisms and reduced levels of facultative and aerobic species (Figure D6.2 in Appendix D). Also, these samples had lower levels of Gram-positive and higher levels of Gram-negative species (Figure D6.3 in Appendix D). Moreover, the results showed that various microbial groups (e.g., *Bifidobacterium*, *Enterococcus*, *Streptococcus*) known to host pathogenic species were reduced in MAD (Figure 6.2), indicating that digested manure would pose lower health risks. Although the microbial diversity in the digested manures was not significantly different to untreated manures, it tended to be higher and less rich (Figures 6.3 and 6.4). The PCoA plot (Figure 6.5A) demonstrated that despite originating from different farms, the microbial communities in the digested manures exhibited similarities. Overall, the microbial communities in the MAD samples aligned with those typically observed in healthy mesophilic anaerobic digesters (Khafipour et al. 2020).

Manure storage reduced the abundance of Bacillota (e.g., *Jeotgalibaca*, *Clostridioides*), Actinomycetota (e.g., *Bifidobacterium*, *Enterococcus*, *Aerococcus*), and Pseudomonadota (e.g., *Acinetobacter*) and enriched Bacteroidota (e.g., *Petrimonas*), Euryarchaeota (e.g., *Methanosarcina*), and Spirochaetota (e.g., *Sphaerochaeta*) (Figures 6.1 and 6.2). Some Bacillota genera, such as *Rombustia*, *Lactococcus*, and *Streptococcus*, and some Pseudomonadota, such as *Aliarcobacter*, *Xanthomonas*, and *Sphaerochaeta*, also tended to be higher in stored manure. (Figure 6.2). Although the microbial diversity of untreated and stored manures in the antibiotic-free farm was not significantly different (Figures 6.3 and 6.4), the second stored batch (F2S2) tended to be less diverse and rich than the untreated batch (F2M2). The PCoA plot (Figure 4.5A) revealed that the microbial communities in stored manures exhibited greater similarity to those of

digested manures, suggesting that manure storage facilitated the establishment of certain anaerobic communities commonly observed in anaerobic digesters (Figure D6.2 in Appendix D).

Some differences between the microbial communities in untreated manure (F3M1, F3M2) and the streams of the BRU system (solids and liquids) were observed. For example, the microbiomes in the liquid stream (F3L1, F3L2) tended to have a higher abundance of Mycoplasmatota (e.g., *Haploplasma*, *Paracholeplasma*, *Acholeplasma*), a slightly higher abundance of some Bacillota (i.e., *Jeotgalicoccus*, *Aerococcus*) and Psuodomonadota (i.e., *Acinetobacter*), and lower levels of Actinomycetota (e.g., *Thermobifida*, *Rhodococcus*) (Figure 6.1 and 6.2). However, the microbial richness and diversity indices were similar between the BRU-liquids and untreated manures. This similarity was further supported by the PCoA plot (Figure 6A), which demonstrated that these samples were closer to untreated manure (F3M1, F3M2). In a previous study, Ackerman et al. (2018) reported that the untreated manure and the liquids from the BRU of this farm had similar physicochemical properties, which could explain why the microbiomes were similar. In contrast, the microbiomes of the solids stream from the BRU (F3S1, F3S2) had a much higher abundance of Bacillota (e.g., *Jeotgalibaca*, *Geobacillus*, *Parageobacillus*, *Aerococcus*, *Solibacillus*), which represented 70% ± 3% of the microbial population. The levels of phyla, such as Actinomycetota (e.g., *Bifidobacterium*, *Corynebacterium*, *Thermobifida*, *Rhodococcus*), Pseudomonadota (e.g., *Pseudoxanthomonas*), and Bacteroidota (e.g., *Sphingobacterium*, *Bacteroides*), were found at lower concentrations in the BRU-solids samples compared to the levels in untreated manures. Additionally, while the microbial richness of the BRU-solids samples was comparable to that of untreated manures (Figure 6.5), they exhibited significantly lower evenness (Figure 6.4). These differences were evident in the PCoA plot, where the BRU-solids samples clustered distinctly apart from untreated manures and the

BRU-liquids (Figure 6.5A). Overall, these results indicate that the microbial populations in the solids obtained from BRU systems can substantially differ from those found in untreated dairy manures and in the BRU-liquid stream.

6.5.2. Resistomes and Mobilomes in untreated bovine manures

6.5.2.1. Resistomes in untreated manures

The read-based analysis revealed the presence of a substantial number of ARG-like sequences in untreated manures from the three surveyed farms. In Farm 1, 52 different ARGs were identified, while Farm 2 and Farm 3 had 77 and 86 different ARGs, respectively (Table D6.2 in Appendix D). Antibiotic inactivation, efflux pumps, and antibiotic target protection were the predominant modes of action of ARGs observed in all untreated manures. Regarding specific antibiotic resistances, the most abundant ARGs were associated with tetracycline, aminoglycoside, macrolide-lincosamide-streptogramin (mls), beta-lactams, and multidrug resistance. Additionally, ARGs related to sulfonamides (e.g., *sul1*, *sul2*) were detected in all manure samples. These findings confirm that untreated bovine manures serve as reservoirs for numerous ARGs, including those for critically important antibiotics, as previously reported (Lima et al. 2020).

In terms of total levels of ARGs (Figures 6.6 and 6.7), untreated manure from Farm 1 (666 ± 60 rpkm) tended to be slightly higher than those in manures from Farm 2 (519 ± 24 rpkm) and Farm 3 (558 ± 86 rpkm). These results suggested that the recovery and recirculation of solids in Farm 3 did not affect the total ARG levels, as they were similar to those from the other farms. Interestingly, the ARG levels in manures from the antibiotics-free farm (Farm 2) tended to be slightly lower, but they were not significantly different (p-value > 0.05). This was unexpected because one would anticipate lower ARG levels in the absence of selective pressure from antibiotics. For example, a previous study reported a lower abundance and diversity of ARGs in

manure from farms not using antibiotics compared to conventional farms (Pitta et al. 2020). This discrepancy may be the result of the different microbial communities as Pseudomonadota was the main phylum in manure microbiomes (accounting for over 55%) in such study, whereas in our study, the dominant phylum in the antibiotic-free farm was Bacillota (49%), and Pseudomonadota only accounted for around 12% of the microbiome. Given the co-location of ARGs and heavy metal resistance genes (Shintani and Nojiri 2013), it is possible that heavy metals from foot baths, like copper, may indirectly select for ARGs, as suggested by prior research (Mulder et al. 2018; Vats et al. 2022). Overall, the results confirmed the presence of relatively high levels of ARGs, potentially conferring resistance to tetracyclines, mls, and aminoglycosides in manure from antibiotic-free dairy farms.

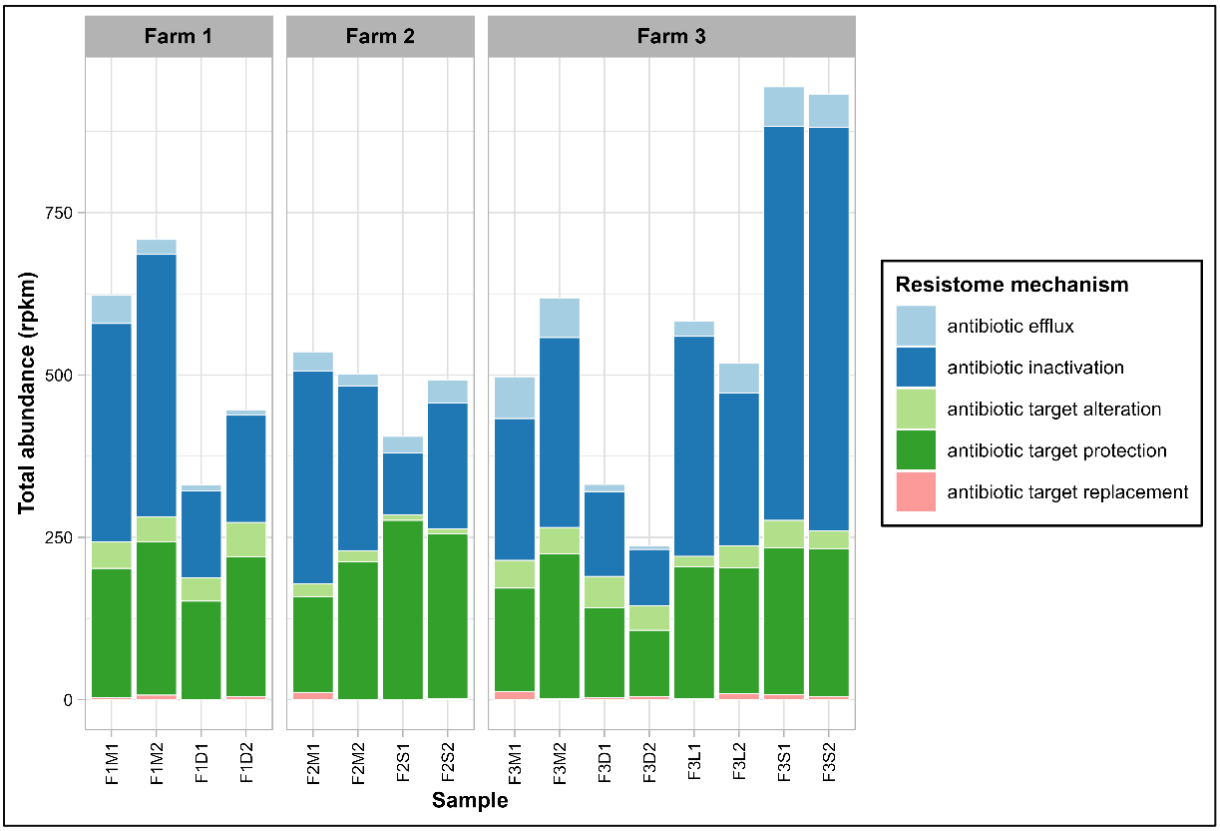

Figure 6.6 Total abundance of ARGs by mechanism.

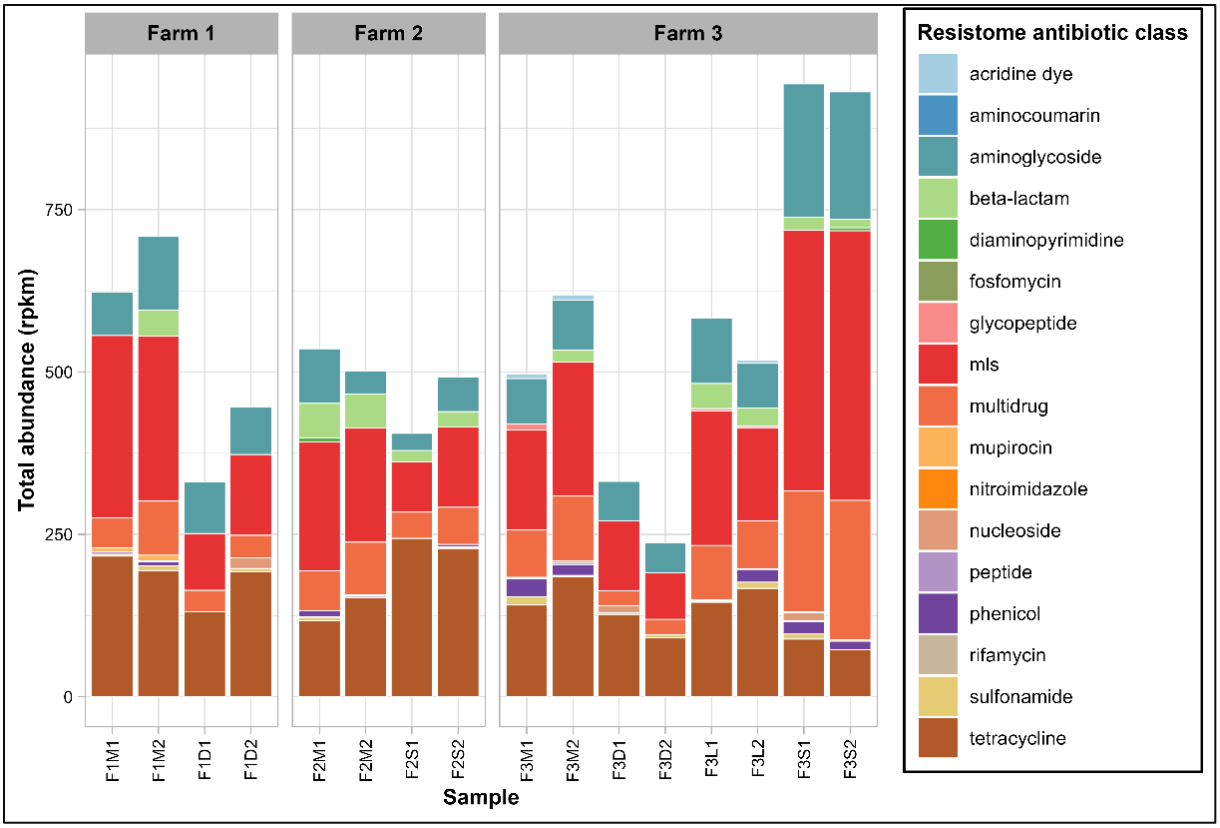

Figure 6.7 Total abundance of ARGs by antibiotic class. ARGs encoding resistance to more than one antibiotic were classified as multidrug. MLS stands for macrolide-lincosamide-streptogramin

The resistome PCoA (Figure 6.5B), explaining 54% of the variation (PC1 = 33%; PC2 = 21.1%), revealed distinct resistome profiles in manure from Farm 2 (F2M1, F2M2), indicating differences in ARG diversity. Cumulatively, these findings suggest that limiting the use of antibiotics may not be sufficient to minimize the risk of antibiotic resistance dissemination in manures. More in-depth studies on the long-term evolution of ARGs in antibiotic-free farms are required since other practices, such as the use of disinfectants or feed ingredients, could possibly cause the co-selection of ARGs.

6.5.2.2. Bactericides and heavy metal resistance in untreated manures

Genes encoding resistance to biocides and heavy metals (BacMet) were also found in untreated manures from the three farms. A total of 18 BacMet genes were found in Farm 1, 31 in

Farm 2, and 37 in Farm 3 (Table D6.3 in Appendix D). Genes encoding resistance to heavy metals (i.e., *copA, tcr, acn*) and multi-compounds (i.e., *ade*) were prevalent in all untreated manures. Additionally, genes linked to resistance to acids like sodium deoxycholate (e.g., *evgS, mdt, yeg*), and hydrochloric acid (e.g., *gad*) were also persistent in untreated manures. Farm 1 exhibited the highest overall levels of BacMet genes (154 ± 9 rpkm), while Farm 2 had the lowest values (89 ± 20 rpkm) (Figure 6.8). However, the overall levels did not exhibit significant differences across the three farms. Among the BacMet genes, those associated with heavy metals, particularly copper (e.g., *copA, tcrA, tcrB, tcrY*), and iron (e.g., *acn*), were the most abundant across all three farms. The use of copper-based solutions for foot-bathing is a common practice in dairy farms to prevent hoof diseases (Cook 2017), including the farms surveyed in this study, which reported using different copper sulphate solutions for this purpose. Therefore, it is plausible that this practice exerts selective pressure favoring the presence of heavy metal resistance genes in the microbiomes of manure. Similarly, using disinfectants like quaternary ammonium compounds (QACs) in daily farm operations may also contribute to selecting specific resistance genes (Mulder et al. 2018).

The PCoA based on BacMet-like genes revealed that untreated manures from Farm 1 and Farm 3 clustered closely together, while Farm 2 samples showed some differences (Figure 6.5C). Overall, these findings indicate that resistance genes associated with heavy metals and other compounds are prevalent in dairy farms. Further investigations are necessary to understand the impact of routine farm practices such as foot bathing and disinfection on the prevalence and spread of this type of resistance.

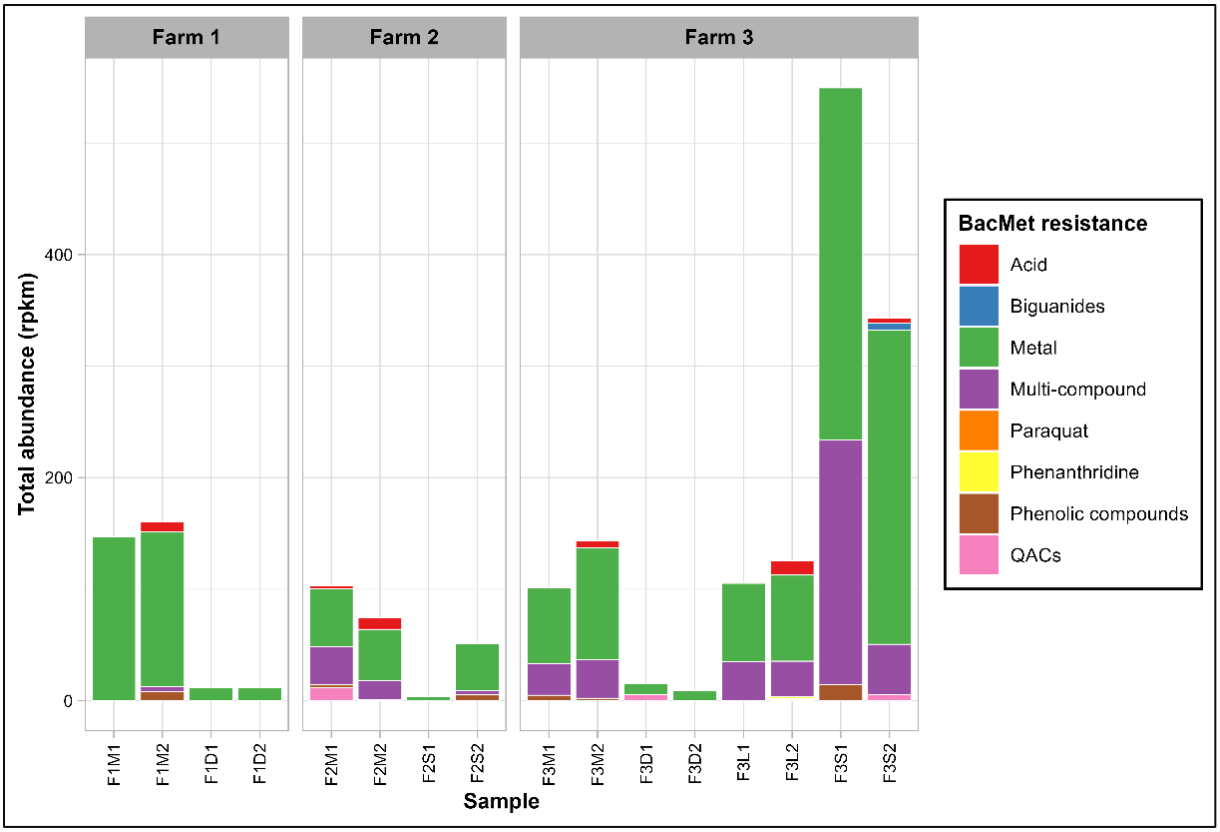

Figure 6.8 Total abundance of BacMet genes by category.

6.5.2.3. Mobilomes in untreated manures

Untreated manures were also rich in MGEs-like sequences. A total of 167, 169, and 231 different genes were detected in untreated manures from Farm 1, Farm 2, and Farm 3, respectively (Table D6.4 in Appendix D). On average, the total MGE levels in untreated manures were 3,123 ± 61 rpkm in Farm 1, 2,432 ± 46 rpkm in Farm 2, and 3,939 ± 1,322 rpkm in Farm 3 (Figure 6.9). The most common and abundant MGE groups in all untreated manures were replication/recombination/repair, integration/excision, and transfer. These results confirmed that bovine manures are important reservoirs of MGEs, as previous studies have suggested (Buta-Hubeny et al., 2022). The PCoA (Figure 6.5D), which explained 65.8% (PC1= 46%; PC2 = 19.8%) of the variability of the MGE profiles, showed that manure samples from different farms tended to cluster apart and exhibit distinct profiles. Although the total MGE levels of the three farms were

not significantly different, some patterns were observed. For example, the antibiotic-free farm (Farm 2) tended to have lower total MGE levels. Specifically, the integration/excision MGEs were significantly lower in Farm 2, whereas the phage group tended to be higher than in Farm 1 (Figure 6.5D). On the other hand, Farm 3, which utilized the BRU system, exhibited higher total MGE levels and richness. Specifically, phage related MGEs were significantly more abundant, while transfer and replication/recombination/repair MGEs also tended to be higher. These findings suggest that the utilization of BRU systems may lead to an enrichment of microbial communities carrying MGEs. A more detailed discussion of putative MGE carriers is presented in subsequent sections.

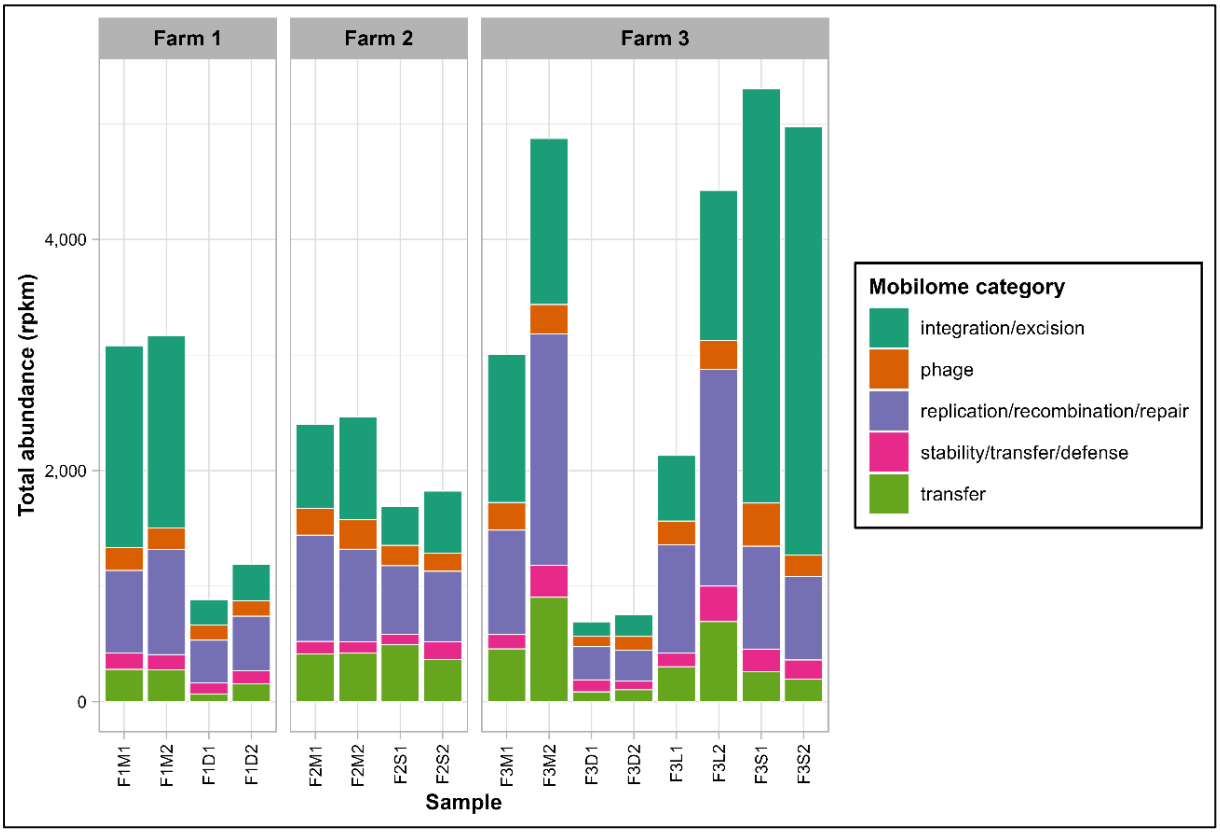

Figure 6.9 Total abundance of MGE categories.

Overall, the analysis of resistomes and mobilomes in the different farms confirmed the presence of various ARGs and MGE in animal manures, suggesting that manure from dairy farms

could provide favourable conditions for horizontal gene transfer of antimicrobial resistance elements. Also, the small difference in the total ARG and MGE levels in manure from the antibiotic-free farm (Farm 2) suggested that limiting the use of antibiotics may not be sufficient to minimize the levels of these antimicrobial resistance markers and associated risks.

6.5.3. Effect of manure treatments on resistomes

MAD achieved the highest reduction rates of total ARG levels, reaching over 40% reduction in manures from Farm 1 (-42% ± 7%) and Farm 3 (-47.5% ± 20%) (Figures 6.6 and 6.7). The PCoA (Figure 6.5B) indicated that MAD samples were similar between them and substantially different from untreated manures and other treated samples. The storage treatment showed no significant effect on the total ARG levels in untreated manures, although there was a slight decrease compared to the untreated samples. Similarly, the total ARG levels remained unchanged in the liquid stream of the BRU system, which is consistent with the minimum changes in microbial communities observed in this condition (Figures 6.1 and 6.2). In contrast, the solids stream of the BRU system saw a 70% increase in the total ARG levels. This increase was primarily observed in antibiotic inactivation mechanisms (+145% ± 46%) (Figure 6.6), as well as genes encoding resistance to aminoglycosides (+173% ± 28%), macrolide-lincosamide-streptogramin (mls) antibiotics (+131% ± 42%), and multidrug resistance (+135% ± 29%) (Figure 6.7). The PCoA analysis indicated that these samples (F3S1, F3S2) exhibited significant differences in ARG diversity compared to the other samples (Figure 6.5B). The rise in ARG levels in the BRU solids samples was likely associated with an increase in the abundance of Bacillota (Figure 6.1 and 6.2), a phylum known to potentially harbour various species carrying ARGs (Chapter 7 and Flores-Orozco et al. (2023)).

In terms of BacMet resistance genes, MAD reduced over 85% of the total levels in untreated manures from Farm 1 (-92% ± 1%) and Farm 3 (-89% ± 6%) (Figure 6.8). The remaining genes were primarily heavy metal resistance genes, present at low concentrations. Storage treatment (Farm 2) showed varying reduction rates of BacMet genes, ranging from 31% to 96%. While the majority of BacMet groups declined during storage, heavy metal resistance genes persisted in F2S2. The liquid fraction of the BRU system in Farm 3 exhibited reductions ranging from 12% to 5% in total BacMet levels. In contrast, the BRU-solids experienced a significant enrichment of BacMet genes, ranging from 140% to 440 %. Notably, genes encoding resistance to heavy metals (273% ± 129%) were the main group enriched in the solid fraction. This is likely the result of the concentration of solids and the related increase in the microbial density in the solids as well as the relative enrichment of some resistance genes due to water removal.

The analysis of ARG and BacMet profiles in the treated manures revealed distinct clustering patterns in the PCoA plot (Figures 6.5B and 6.5C), indicating that different manure treatments had specific influences on ARGs. These findings support previous studies suggesting that the microbial dynamics associated with each treatment process play a significant role (Cheng et al. 2019; Zhang et al. 2020b). Further sections provide detailed information on putative ARGs and BacMet carriers and the microbial dynamics involved.

Overall, all these findings emphasize MAD as the most effective method for reducing BacMet genes, followed by storage, although with variable outcomes. Conversely, the BRU system appeared to enrich genes conferring resistance to heavy metals and other compounds in the solid fraction. Further studies are warranted to assess the impact of solid recovery from manure on the evolution of these antimicrobial resistance markers in dairy farms, as this practice may be enriching different resistance genes.

6.5.4. Effect of manure treatments on mobilomes

MAD was the best alternative to reduce the total MGE levels from untreated manures, achieving a reduction of 68% ± 6% in Farm 1 and 81% ± 5% in Farm 2 (Figure 6.9). The MGE groups that saw the greatest reduction in MAD were integration/excision (-86% ± 4%), transfer (-73% ± 19%), and replication/recombination/repair (-63% ± 19). Storage treatment resulted in a 28% ± 3% reduction in total MGE-like sequences. Integration/excision, phage-like, and replication/recombination/repair MGEs were reduced by 47% ± 10%, 31% ± 11%, and 30% ±8%, respectively. The liquids of the BRU (F3L1, F3L2) saw a reduction of 19% ± 14% in MGE-like sequences, whereas they increased between 2% and 77% in the solids of the BRU (F3S1, F3S2). The variability of the results observed in Farm 3 was attributed to the high levels observed in F3M2, which was 60% higher than in F3M1. It is possible that this difference resulted from the differences in the microbial communities (i.e., Pseudomonadota) between the two samples. Despite this variability, some patterns emerged. For example, MGE-like sequences classified as integration/excision were the group that saw the greatest increase (169% ± 16%) in BRU-solids samples (Figure 6.9). Interestingly, MGEs directly associated with transfer processes (e.g., conjugation, secretion, and transformation machinery) decreased by around 61% ± 25% in BRU solid samples. This observation, combined with the PCoA (Figure 6.5D) suggested a substantial change in the mobilome of these samples, which likely corresponded to the substantial changes in the microbial communities.

Overall, MAD stood out as the most effective method for reducing the overall levels of MGE-like sequences, ARGs, and BacMet resistance genes in bovine dairy manure. This implies that digested manure could present a significantly lower risk of AMR spread compared to untreated, stored manures, and the outputs from BRU systems. Notably, the solids derived from

BRU exhibited elevated levels of total MGEs, highlighting potential concerns about an enhanced risk of AMR transmission in farms utilizing these systems. Previous studies have observed increased levels of residual antimicrobials in the solid fraction of manures (Wallace et al. 2018), thus, it is possible that the increased levels of MGEs and ARGs are the results of a stronger selective pressure in the solid fraction of the BRU. However, it's important to highlight that the solids analyzed in this investigation were directly sourced from the BRU, known to contain more readily digestible carbon and, consequently, heightened biological activity, compared to solids that have undergone extended composting (Ackerman et al. 2018). As a result, the microbiomes, resistomes, and mobilomes of freshly obtained solids might differ considerably from those in aged and complete composted solids. More comprehensive studies are essential to shed light on the behavior and progression of ARGs in farms that incorporate manure recirculation systems.

6.5.5. Relationship between microbial groups, ARGs, and MGEs

6.5.5.1. Correlation between microbiomes, resistomes, and mobilomes

Mantel tests were used to evaluate the relationship between the resistome and mobilome profiles with the microbial communities. The results suggested that the correlation between the microbial communities at the phylum level and ARGs ($R = 0.43$, p-value = 0.002) and MGEs ($R = 0.63$, p-value = 0.001) was significantly positive. The microbiome profile at the genera level was also positively and significantly correlated with ARGs ($R = 0.44$, p-value = 0.001) and MGEs ($R = 0.63$, p-value = 0.001). Interestingly, the Mantel test also revealed that the relative abundance of aerobic and anaerobic communities was significantly correlated with resistomes (aerobes: $R = 0.36$, p-value = 0.003; anaerobes: $R = 0.25$, p-value =0.04) and mobilomes (aerobes: $R = 0.54$, p-value = 0.001; anaerobes: $R = 0.41$, p-value = 0.003). Furthermore, a significant positive correlation was observed between the mobilomes and resistomes ($R = 0.84$, p-value = 0.008),

indicating that changes in the mobilome may contribute to variations in ARGs. These findings confirm the substantial influence of microbial communities on the dynamics of ARGs and MGEs in manure-related environments, as previous studies have indicated (Liu et al. 2020; Zhang et al. 2019a). The findings also suggested that microbial compositions, both at the phylum and genera levels, could serve as potential indicators to model and anticipate resistomes and mobilomes.

6.5.5.2. Microbial groups potentially carrying ARGs and MGEs

A model of co-occurrence combined with Pearson Correlation analyses was used to determine significant associations between microbial genera and ARGs, MGEs, and BacMet genes. The results indicated that 34 different ARGs were associated with 69 genera, primarily belonging to the phyla Bacillota (22 genera), Pseudomonadota (11), Actinomycetota (7), and Bacteroidota (6) (Figure 6.10). Bacillota were the main group significantly associated with all different ARG mechanisms, including efflux pumps (e.g., *efrB, adeJ*, *tet(40)*, *fexA*, *mefB*, *floR, pp-flo*), target alteration (e.g., *ileS, Erm*), target protection (e.g., *tetS, tet44, optrA, poxtA*), target replacement (i.e., *sul2*), and ARGs for mls (i.e., *lnuG, ErmF, mefB*), tetracyclines (i.e., *tetS, tet44, tet40*), and sulfonamides (i.e., *sul2*). On the other hand, Pseudomonadota stood as the primary phylum associated with ARGs for beta-lactams (e.g., *CARB*), phenicol (e.g., *floR, pp-flo, fexA*), and multidrug (e.g., *cfr(D), poxtA, smeE, efrB, optrA*).

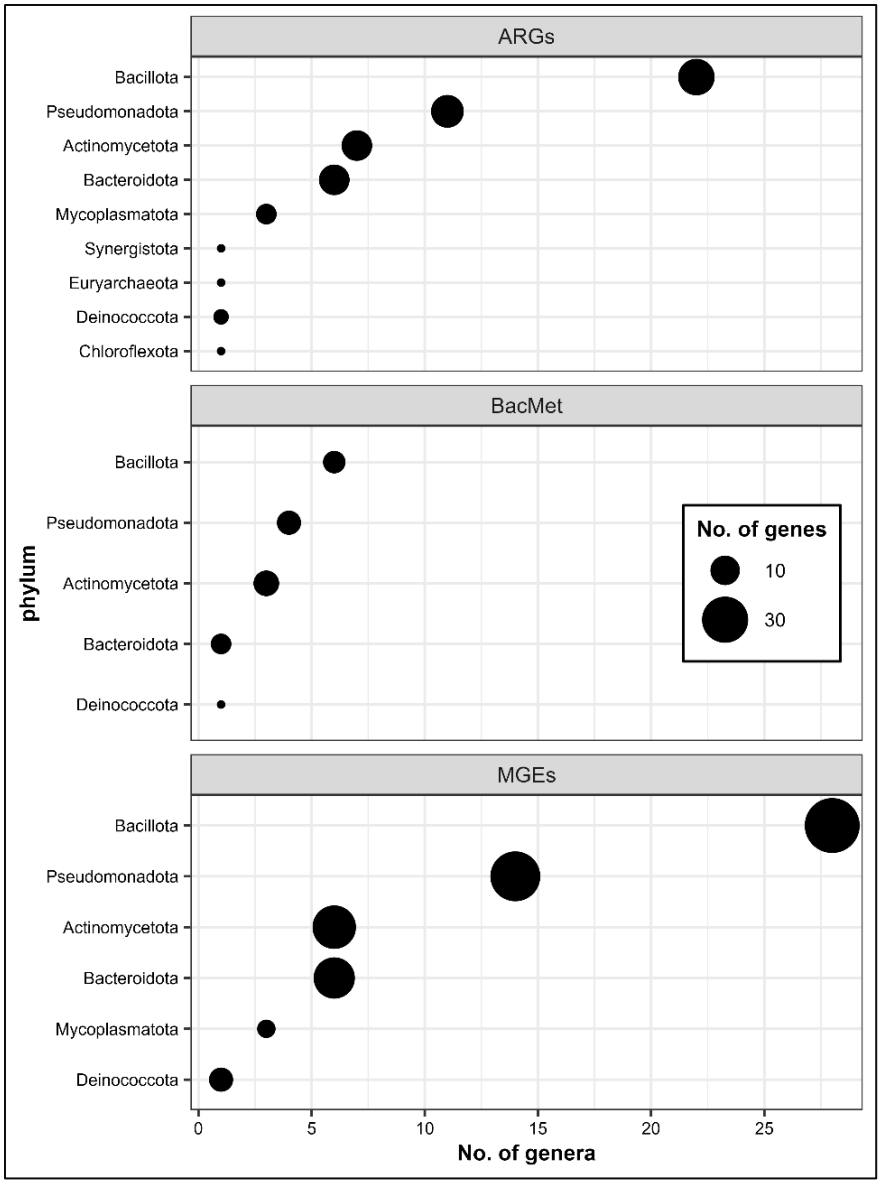

Figure 6.10 Number of microbial genera significantly associated with ARGs, BacMet, and MGEs.

In terms of BacMet, 12 genes were significantly associated with 28 different genera. Bacillota (e.g., *Amylolactobacillus*, *Carnobacterium*, *Erysipelothrix*, *Limosilactobacillus*, *Mammaliicoccus*, and *Staphylococcus*) was the main group associated with genes conferring resistance to heavy metals, including iron (i.e., *acn*), copper (i.e., *tcrY*), and arsenic (i.e., *arsB*).

Pseudomonadota (e.g., *Comamonas*, *Halopseudomonas*) was the main group associated with genes conferring resistance to multi compounds (e.g., *ruvB*, *rpoS*, *smeE*, *srpB*).

A total of 96 different MGEs were significantly associated with 58 genera, of which 28 were Bacillota, 14 Pseudomonadota, 6 Actinomycetota, and 6 Bacteroidota. *Staphylococcus*, *Amylolactobacillus*, and *Carnobacterium* were the top genera associated with integration/excision genes; *Comamonas* and *Glutamicibacter* with replication/recombination/repair; *Glutamicibacter* and *Psychrobacter* with transfer; *Myroides* and *Comamonas* with stability/transfer/defense; and *Carnobacterium*, *Comamonas*, *Erysipelothrix*, and *Jeotgalicoccus* with phage related MGEs.

A table with the list of bacterial genera linked to both ARGs and MGEs can be found in the supplementary material (Table D6.5 in Appendix D). *Glutamicibacter*, *Comamonas*, *Psychrobacter*, *Empedobacter*, *Advenella*, *Macrococcus*, *Carnobacterium*, *Moraxella*, *Petrocella*, and *Staphylococcus* stood as the genera associated with the highest number of ARGs and MGEs. Many of these genera are known to host important pathogenic species with high antimicrobial resistance potential (CDC 2019), confirming that livestock manure is an important reservoir of pathogenic bacteria with the genetic machinery to disseminate antimicrobial resistance.

6.5.5.3. Co-occurrence of ARGs and MGEs in co-assembled contigs

The co-occurrence of ARGs and MGEs was investigated by analyzing co-assembled contigs. Intriguingly, these analyses revealed the presence of structures resembling the transposon family Tn554, which encompassed the transposition genes *tnpB* and *tnpC*, along with different ARGs such as *ANT(9)-la*, *ErmA*, *LnuG*, and *LnuP* in samples obtained from Farm 2 and Farm 3 (Figure 6.11). These transposon structures are commonly associated with Bacillota genera, including *Staphylococcus*, *Enterococcus*, *Listeria*, and *Bacillus* (Li et al. 2019). Remarkably, these transposon structures were also observed in the antibiotic-free farm, indicating the widespread

distribution of horizontal gene transfer machinery for various antimicrobial resistance genes in dairy farms. Previous studies have proposed that ruminant guts could exert selective pressure favouring certain *tet* ARGs (Sabino et al. 2019). Therefore, it is possible that even in the absence of antibiotics, other selective pressures may be promoting the prevalence of mls and aminoglycoside ARGs.

Genes encoding the Zeta toxin and Epsilon antitoxin, which are part of a type II toxin-antitoxin (TA) system, were identified in a contig derived from a MAD sample obtained from Farm 1, in close proximity to the ARG *ErmB* (Figure 6.11). This TA type is commonly found in addiction plasmids, which ensure survival of only those cells containing the plasmid by producing an antitoxin that neutralizes the toxin encoded within the same genetic structure (Fraikin et al. 2020). A more detailed discussion on the significance of this finding is presented in Chapter 7.

Overall, the analysis of co-assembled contigs provided further confirmation of the findings obtained from the co-occurrence model, highlighting that genera from the phylum Bacillota are major carriers of ARGs and MGEs. These results suggest that the persistence of ARGs in untreated and treated manure, even in the absence of antimicrobial selective pressure, could be attributed to their proximity to systems such as type II TA systems that indirectly contribute to their maintenance. The identification of transposon genes in the vicinity of various ARGs (e.g., *Ant(9)-la, lnuP, lnuG*) provides additional evidence of the potential transmissibility of these genes in manure-related environments. However, further metagenomic studies with higher sequencing depths (e.g., tens of millions of reads per sample) are needed to comprehensively assess how these systems influence the preservation and dissemination of ARGs and antibiotic resistance in manure-related environments.

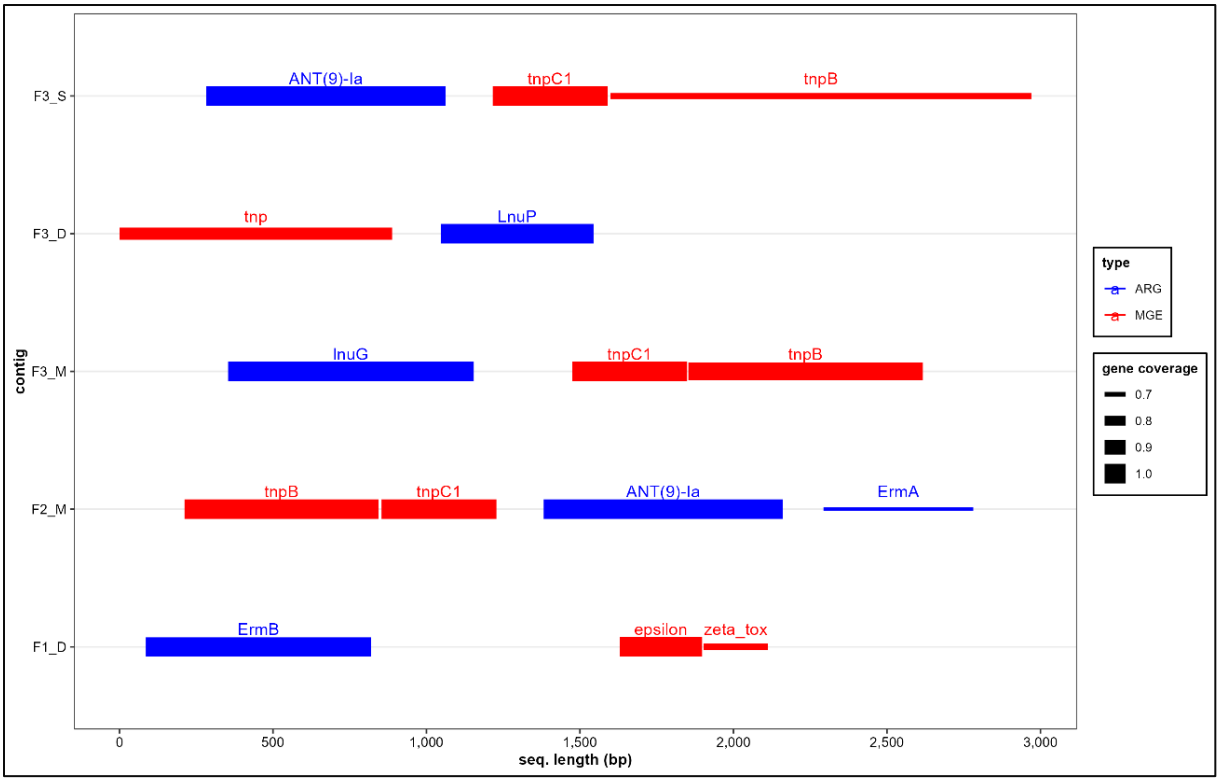

Figure 6.11 Co-occurrence of ARGs and MGEs in co-assembled contigs. The size of the segment indicates the percentage of the genes detected in the contig. F1_D: digested manure from Farm 1; F2_M: untreated manure from Farm 2; F3_M untreated manure from Farm 3; F3_D: digested manure from Farm 3; F3_S: BRU-solids from Farm 3.

6.5.6. Microbiome shifts potentially influencing resistomes and mobilomes in manure treatments

Several studies have emphasized the significant role of microbial communities in driving changes in ARGs and MGEs levels (Liu et al. 2020; Sun et al. 2016; Wu et al. 2020). These studies have shown that shifts in microbial populations with distinct resistomes and mobilomes can occupy ecological niches and influence resistance profiles. For example, during manure composting, the reduction in ARG levels has been associated with the establishment of thermophilic communities at the expense of original mesophilic consortia (Liu et al. 2020). Similarly, studies on pig manure have indicated that thermophilic anaerobic digestion is more effective than mesophilic digestion in reducing ARGs due to the elimination of mesophilic bacteria, particularly Bacteroidetes, and

Proteobacteria (Sun et al. 2016). The research study described in Chapter 7 linked the reduction of ARGs to the decline of facultative anaerobes, especially Lactobacilli, during MAD. In this study, the decline in ARG levels corresponded to the decrease in aerobic and facultative communities observed in untreated and digested manures, with a more pronounced effect observed in the digested sample (Figure 6.12).

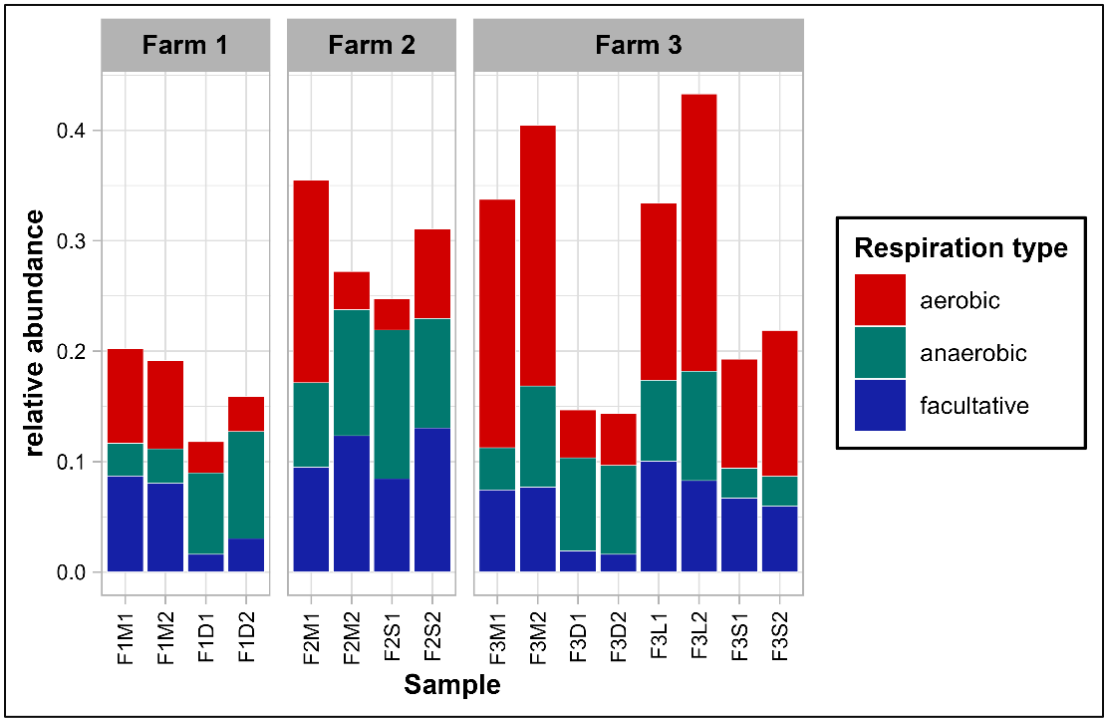

Figure 6.12 Relative abundance of genera associated with ARGs, BacMet, and MGEs by respiration phenotype. Significant associations were defined as co-occurrencewith a frequency higher than expected (p-values < 0.025) and positive Pearson's correlation coefficient (R > 0.50).

On the other hand, the increase of the aerobic communities in the solids recovered from the BRU (Figure D6.2 in Appendix D) appeared to be associated with increased levels of ARGs (Figures 6.6 and 6.7). Notably, although the relative abundance of the aerobic groups significantly associated with ARGs and MGEs was lower in the BRU-solids compared to those in the untreated samples (Figure 6.12), the total ARG and MGE levels were higher (Figures 6.6, 6.7, and 6.9). Since the resistome and mobilome profiles were different from those dominated by anaerobic

communities (e.g., F3D1 and F3D2), it is possible that the co-occurrence analysis was not able to detect aerobic groups carrying ARGs and MGEs exclusively present in the BRU-solids samples. Further investigations are necessary to comprehensively assess the dynamics of resistomes and mobilomes in manure solids recovery units like BRUs, as this practice may potentially contribute to elevated levels of various ARGs and MGEs in dairy farm settings.

Although the changes in the microbial communities during storage did not seem to have influenced the total ARG levels in untreated manure from the antibiotic-free farm, the overall profiles were substantially different. In fact, the resistome profiles of stored manure were more similar to digested manures than to untreated manure from Farm 2 (Figure 6.5B). For example, the levels of tetracycline ARGs tended to be higher in stored manure, whereas ARGs for mls and multidrug tended to be higher in untreated manures (Figure 6.6). These changes in the ARG profile were likely associated with the restructuring of microbial communities within the storage tank, characterized by a decline in aerobic populations and an enrichment of anaerobes (Figures 6.12 and D6.2 in Appendix D).

The PCoA of the abundance of genera significantly associated with ARGs and MGEs indicated that despite the differences in microbiomes, resistomes, and mobilomes, treated and untreated manures tended to be similar and clustered together (Figure 6.13). This suggested that there were some groups of microorganisms potentially carrying ARGs and MGEs persistent in untreated and treated manures. However, digested manures displayed a distinct profile of microbes associated with ARGs and MGEs, which suggested that MAD allowed the establishment of microbiomes with resistomes and mobilomes that differ from those in untreated manures. The discrepancies in the total levels of ARGs and MGEs and the abundance of microbial groups potentially carrying them demonstrate the complex relationship between antimicrobial resistance

markers and microbial communities. These findings emphasize the need for more comprehensive metagenomic studies to identify the specific microbial species carrying ARGs and elucidate the mechanisms underlying their maintenance and mobilization as the major sources for the antibiotic resistance load circulating through the animals and barn has not been determined accurately yet.

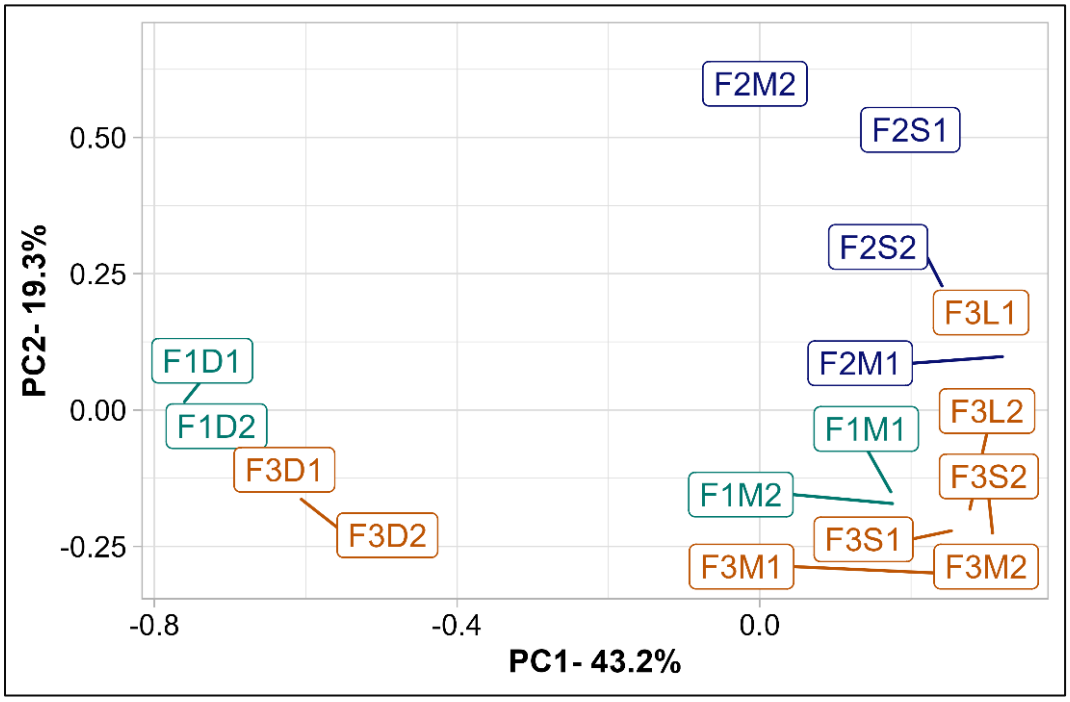

Figure 6.13 PCoA of genera associated with ARGs, BacMet, and MGEs.

6.6. Conclusions

This study demonstrated that bovine dairy manures are important reservoirs of genes conferring resistance to several different antimicrobials, including antibiotics and heavy metals, and of different MGEs that could potentially disseminate AMR. The results showed that manure storage, a widely used manure management strategy, has little effect on the total ARG and MGE levels, whereas MAD stood as the best alternative to reduce the levels and diversity of these elements. The results also showed that BRU systems caused an enrichment of ARGs and MGEs in the recovered solids, although it had little effect on the liquid stream. Changes in the microbial

community structure, particularly the decline of aerobic and facultative genera from Bacillota, Pseudomonadota, and Actinomycetota phyla, were key drivers influencing the changes in ARGs and MGEs across different treatments. This study also suggested that the use of heavy metals and disinfectants in dairy farms may promote the maintenance and possibly the amplification of ARGs and MGEs even in antibiotic-free environments. Lastly, the strong correlation between particular microbial groups and ARGs and MGEs suggested that these microbes could serve as potential indicators to model and predict resistomes and mobilomes.

6.7. Acknowledgments

This research work was financially supported by the National Sciences and Engineering Research Council of Canada (NSERC) through the Discovery Grants program [RGPIN-2022-03670].

Chapter 7: Metagenomics study of the long-term effects of MAD on resistomes and mobilomes in bovine manure

7.1. Preface

This chapters describes the comprehensive study on the long-term effects of MAD on resistomes and mobilomes. It represented one of the first comprehensive metagenomic studies on the fate and evolution of mobilomes during manure AD. It also provides interesting insights into the potential ARG and MGEs carriers present in animal manures. The work presented in this chapter was peer-reviewed and published in the journal *Environmental Technology & Innovation* in 2023 as original research in a manuscript entitled "*Metagenomic analyses reveal that mesophilic anaerobic digestion substantially reduces the abundance of antibiotic resistance genes and mobile genetic elements in dairy manures*" (https://doi.org/10.1016/j.eti.2023.103128). I alone was responsible for the data collection and analysis, interpretation of the results, and the preparation of the manuscript. Rakesh Patidar helped with the sample preparation and submission for metagenomic sequencings and the initial quality control tasks of the metagenomic analyses. The other co-authors provided thoughtful and challenging discussions on the results and reviewed the manuscript prior to publication. Section 7.5.8 and a few figures were added to the originally published manuscript. Some other modifications, such as section titles, the introduction, and writing style were modified to fit the style of the thesis and reduce redundancy.

7.2. Abstract

Animal manure is considered one of the main reservoirs of antibiotic resistance genes (ARGs) and mobile genetic elements (MGEs). There is increasing concern regarding the dissemination of AMR due to the application of manure as a soil amendment, and there is an urgent need to define alternatives to minimize this problem. While AD has shown the potential to reduce

the levels of ARGs present in manure, little is known about the effect of AD on the entire mobilomes, which play a crucial role in the dissemination of antibiotic resistance. In this study, we used a set of metagenomic and bioinformatics tools to evaluate the long-term effects of MAD on resistomes and mobilomes in bovine dairy manure and the potential mechanisms driving these changes. The results indicated that the average ARG and MGE levels were significantly reduced by 53% and 74 %, respectively, after AD. The results also suggested that microbial groups including Lactobacillales, Bacillales, Eubacteriales, Micrococcales, and Actinomycetales were main groups associated with ARGs and MGEs. The changes in ARG and MGE seemed to result from distinct microbial successions, such as the removal of aerobic species and the decline in facultative bacteria, which led to the establishment of typical microbial communities present in anaerobic digesters. The study also suggested that hydrolytic species are another important group that potentially harbors ARGs and MGEs. Overall, the results indicated that digested manure could have a reduced risk of dissemination of antibiotic resistance.

7.3. Introduction

The meta-analyses conducted in this research, presented in Chapter 4, highlighted a notable gap: the scarcity of long-term metagenomic studies exploring the fate and evolution of resistomes in long-term continuous anaerobic digesters. Notably, a significant proportion of the existing studies were conducted in batch systems with relatively short digestion times, typically less than 20 days. Since the microbial profiles in batch digesters might not consistently mirror those in continuous systems, extrapolating findings from the former to the latter could yield inaccurate results. Furthermore, at the beginning of this research, there was an absence of studies examining the comprehensive shifts and evolution of mobilomes during manure AD. Given the increased risk of ARG transmission due to the presence of MGEs, and the subsequent potential spread of AMR,

it becomes imperative to learn whether manure treatments, such as AD, can influence both resistomes and mobilomes. Equally crucial is the identification of microbial species that carry ARGs and MGEs, as they could be strategically targeted for mitigation in various manure treatments.

In response to these gaps, we performed a series of metagenomic analyses in a lab-scale mesophilic anaerobic digester fed with bovine dairy manure and operated for over four years (> 1,600 days) to determine the long-term effect of AD on resistomes and mobilomes and identify microbial groups potentially harboring ARGs and MGEs. The primary hypothesis of this study was that a long-term operating anaerobic digester would substantially decrease the levels of ARGs and MGEs. The secondary hypotheses were that this reduction in ARGs and MGEs would remain consistent irrespective of variations in the microbial communities present in the input manure and that the decline of aerobic and facultative communities would be significantly associated with the reduction of ARGs and MGEs. The results provide valuable insights into the reliability of the AD process to reduced ARGs and MGEs the potential microbial mechanisms driving these changes.

7.4. Material and methods

7.4.1. Mesophilic anaerobic digestion and dairy manures

The mesophilic anaerobic digester used in this study was the one described in Chapter 3, section 3.2. Briefly, it was a CSTR continuously operated at 35 °C for over four years (> 1600 days). It had a working volume of 8 L, an SRT of 30 days, and a continuous mixing rate of 120 rpm. The reactor's performance was evaluated in terms of biogas production yield (L/g-VS), biogas composition (CH_4 and CO_2), pH, and volatile fatty acids (VFAs) profile, as described in Chapter 3. During the time of operation several batches of manure were collected, processed, and fed to the digester as described in section 3.3.

7.4.2. Sample collection

For this long-term study, a total of 14 digestates (mesophilic anaerobic digestate, MAD) and their corresponding manures (M, 10 different batches) were sampled when the CSRT was operating under steady-state conditions. The set of samples (manures and digestates) were taken on the moths 11 (MAD1, M1), 17 (MAD2, M2), 20 (MAD3, M3), 23 (MAD4, M4), 27 (MAD5, M5), 39 (MAD6, M6), 43 (MAD7.1, MAD7.2 M7), 45 (MAD7.3, M7), 47 (MAD8, M8), 50 (MAD9, M9), and 52 (MAD10, M10). All samples were analyzed for COD, dissolved COD, total solids (TS), volatile solids (VS), alkalinity, pH, and VFAs as described in sections 4.5 and 4.6. Samples for DNA isolation and metagenomic sequencing were collected and stored at -20 °C.

7.4.3. DNA isolation and metagenomic sequencing

For the methodology pertaining to DNA isolation and metagenomic sequencing, please refer to sections 3.7 and 3.8 of Chapter 3, respectively. Briefly, the metagenomic analyses consisted of the taxonomic classification and functional annotation (for ARGs, BacMet genes, MGEs, and cazymes) of the metagenomic reads. Then, co-assembled contigs were generated and annotated to investigate the co-occurrence of ARGs and MGEs in these contigs.

7.4.4. Data analysis and visualization

The general microbiome structure at phylum levels was displayed in stacked bar plots generated in R with the package *ggplot2*. The differences in the structure of the microbial communities, at the different taxonomic levels, in raw manures and digestates were analyzed and visualized in a differential heat-tree generated in R with the package *MetaCoder* (Foster et al. 2017). For this, the $\log_2$ of the fold change ($\log_2$ FC) of the abundance of the microbial groups was estimated and then encoded in the color of the plot. The number of OTUs in each level was used

to define the size of the nodes and edges of the tree. Chao, Shannon, and Simpson diversity indices were calculated with the R package *vegan* (Oksanen et al. 2019).

ARGs detected in the metagenomic samples were classified according to the type of mechanism they encode and the type of antibiotic they exert resistance to. A differential heat-tree was also used to evaluate the abundance of the different types of ARGs. In this case, the ARG mechanisms were set as the first level, the type of antibiotic as the second level, and the ARG names as the third level. Individual MGEs were classified as integration/excision, phage, replication/recombination/repair, stability/transfer/defense, or transfer based on the molecular machinery described in the MobileOG database (Brown et al. 2021). Individual genes from the CAZY database detected in the metagenomic reads were classified into one of the six enzyme families: glycoside hydrolase (GH), glycosyltransferase (GT), polysaccharide lyase (PL), carbohydrate esterase (CE), carbohydrate-binding module (CBM), and auxiliary activities (AA). The relative abundance of the different enzyme families was calculated by dividing the total abundance of each family by the total abundance of all families in each sample.

7.4.5. Statistical analyses

Statistically significant difference in the different studied parameters between raw manures and digestates were determined using Wilcox tests with an alpha of 0.05. Principal coordinates analyses (PCoA) were applied to the microbiome, resistome, mobilome, and CAZy profiles to determine the similarities (defined as the Bray-Curtis distance) of individual manure and digestate samples. The analyses were performed with the R-package *vegan*. Co-occurrence analyses were carried out to evaluate the relationships of microbial species with ARGs and MGEs as described in Chapter 3 (Section 3.9.6). The results of these co-occurrence analyses were displayed in heatmaps generated in R. Mantel tests were used to determine the relationships between

physicochemical parameters (e.g., VS, dCOD, alkalinity, total VFAs), ARGs, and MGEs. The relationship of individual parameters with total ARG and MGE levels were further explored using Pearson Correlations.

7.5. Results and Discussion

7.5.1. Manure and digestate properties

The digester performance in terms of biogas production, biogas methane concentration and pH as well as the sampling points are shown in Figure 7.1. Overall, the digester performance was very stable during the time of operation with only minor temporary disturbances. For instance, due to a problem with the gas chromatogram, very low levels of CH_4 were registered during the first months. Once the method was adjusted, expected CH_4 levels were observed. The disturbance between days 500 and 600 can likely be traced back to elevated copper sulfate levels in the manure used during that period. This inference is supported by the simultaneous drop in pH and CH_4 levels (Figure 7.1) and a spike in VFAs (data not shown), a pattern consistent with such scenarios as noted by Jordaan et al. (2019). Under steady state operation, the average biogas production yield was 321.3 ± 108.3 mL/g-VS_{added}, the CH_4/CO_2 ratio was 2 ± 0.3, and the pH was 7.5 ± 0.1.

The physicochemical properties of fresh raw manures and digestates are shown in Figures E7.1 and E7.2 in Appendix E. The organic matter parameters COD, dCOD, TS, and VS were significantly lower in the digestates than in the fresh raw manures. On average, COD was reduced 39% (± 6.4%), dCOD 56.1% (± 4.0%), TS 27.4% (± 7.0%), and VS 33% (± 7.1%). The pH of the manures ranged from 6.9 to 7.3, whereas the pH of the digestate in the reactor remained stable around 7.5 ± 0.1 during steady-state operation. The alkalinity in digestates (13.4 ± 4.4 g/L $CaCO_3$) was significantly higher than manures (8.6 ± 2.8 g/L). The total VFAs levels were much higher in raw manures (5,890 ± 1,696 mg/L) compared to those in digestates (193 ± 240 mg/L). The most

abundant VFAs in raw manures were acetate, propionate, and butyrate, whereas acetate, formate, and butyrate were dominant in digestates. The lower VFA levels in digestates combined with the other physicochemical properties indicated a healthy microbiome in the anaerobic digester.

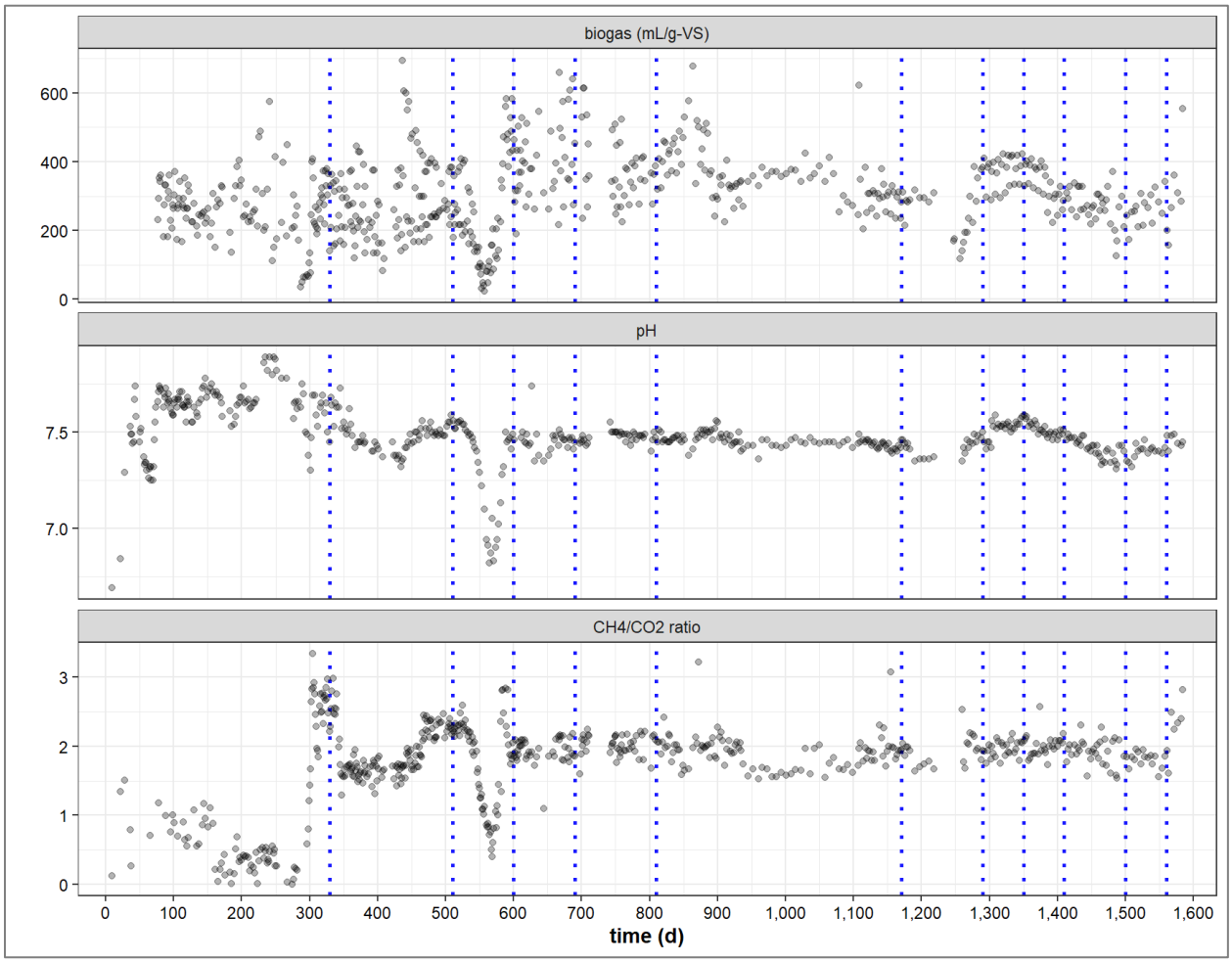

Figure 7.1 Mesophilic anaerobic digester performance over time. The dotted blue lines represent the time when manure and digestates were sampled for metagenomic analyses.

7.5.2. Resistome and mobilome profiles in bovine manures

A total of 146 different ARGs encoding five different mechanisms, including antibiotic inactivation (62), efflux pump (39), antibiotic target alteration (22), antibiotic target protection (17), and antibiotic target replacement (6) were detected in the fresh manure samples. These ARGs encoded resistance to 14 antibiotic classes, including multidrug (31), mls (30), aminoglycosides

(29), tetracyclines (26), beta-lactams (11), phenicol (6), diaminopyrimidines (4), glycopeptides (2), sulfonamides (2), acridines (1), aminocoumarin (1), mupirocin (1), nucleoside (1), and peptide (1). The number of different ARGs in individual manure samples range from 32-68 (Table E7.1 in Appendix E).

Figure 7.2 presents the abundance of various ARG mechanisms across individual samples. There was a notable variation in total ARG levels among different manure batches, ranging from 503 to 920 rpkm. Specifically, batches M3 and M4 exhibited total ARG levels nearly double those found in M5. This variability was not attributed to he examined physicochemical parameters like solids, COD, VFAs, alkalinity, or pH, as these parameters remained consistent across manure samples. Thus, other unexamined factors, such as manure biodegradability and micronutrient content, might have influenced these levels. However, despite these differences, the overall resistome profiles were similar since the dominant ARG groups in all raw manures were antibiotic inactivation, antibiotic target protection, and efflux pumps. These results confirmed that dairy manures are important ARG reservoirs, as previous studies had suggested (Buta-Hubeny et al. 2022; Munir and Xagoraraki 2011; Qiu et al. 2022).

The raw manures used in this study were also rich in MGEs. A total of 348 different MGE-related genes of which 101 were integration/excision, 96 replication/transfer/defense, 66 transfer, 53 phages, and 45 stability/transfer defense, were detected. The MGEs in individual samples is shown in Table E7.2 in Appendix E. The total MGE abundance in all manure samples was fairly constant and ranged between 2,772-4,931 rpkm (Figure 7.3). The dominant MGE groups were integration/excision (47.1%), replication/recombination/repair (29.6%), and transfer (11.9%) (Figure 7.3).

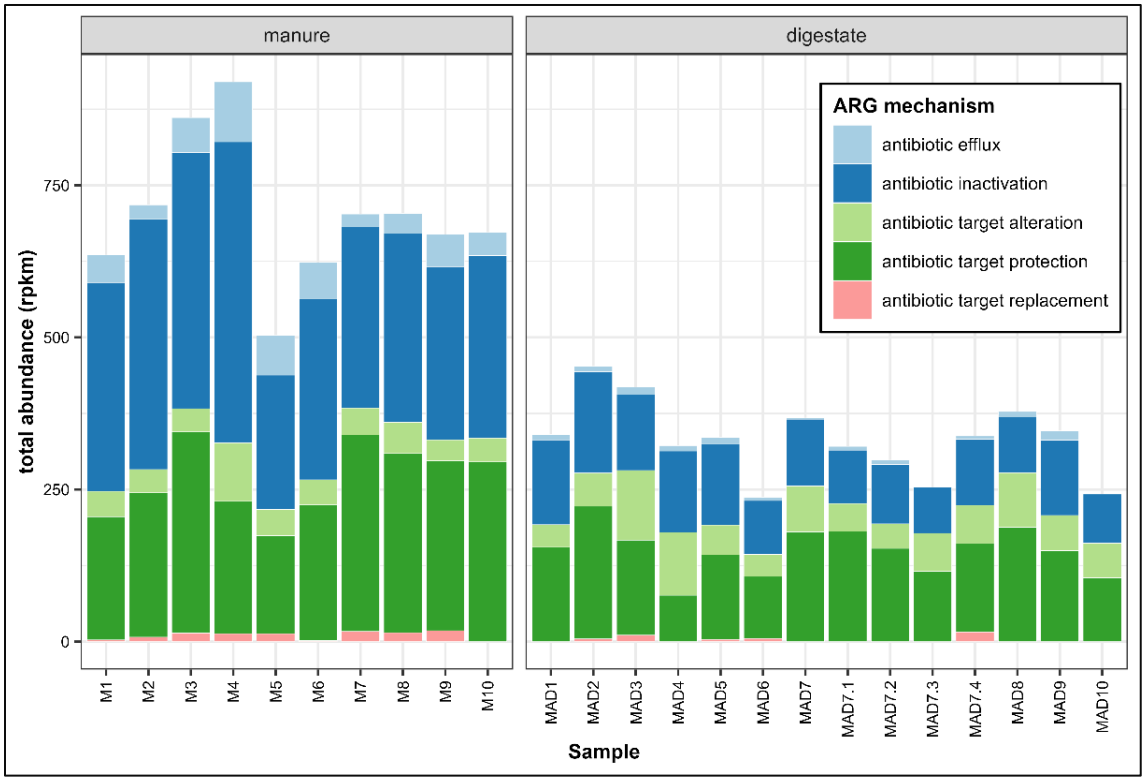

Figure 7.2 Total abundance of ARG mechanisms in manure and digestates.

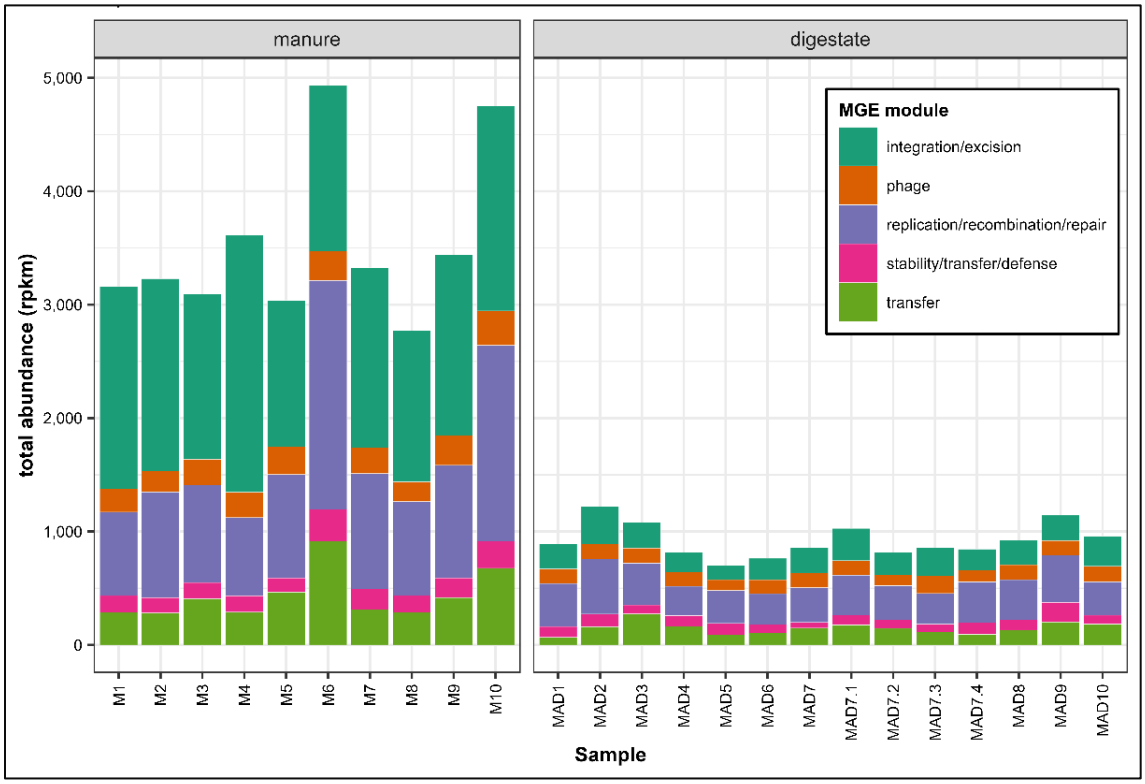

Figure 7.3 Total abundance of MGE categories in manures and digestates.

Although several studies have documented the presence of different types of MGEs, including integrons, transposons, and conjugative plasmids (Sun et al. 2019; Yang et al. 2020a; Zhang et al. 2018b), only a handful of studies have evaluated whole mobilome profiles using metagenomics (Buta-Hubeny et al. 2022). Our study confirmed that dairy manures not only serve as repositories for antibiotic resistance genes (ARGs) but also encompass a broad spectrum of functional modules pertinent to MGEs. These modules are intrinsically involved in the life cycles of MGEs, addressing facets such as integration (integration/excision), replication (replication/recombination/repair), transfer mechanisms, and defense strategies (stability/transfer/defense). Furthermore, the study also confirmed the presence of phage-associated attributes, including structural proteins and lysogenic mechanisms, associated with transduction processes. These results provide evidence of the high risk of HGT of ARGs and the potential spread of AMR into the environment dairy manures could pose.

7.5.3. Effect of MAD on resistomes

The mesophilic AD process reduced the number of unique ARGs in the different batches of dairy manure (Table E7.1 in Appendix E). For instance, the number of unique ARGs detected in digestate samples was 90, which represented a reduction of 38% compared to those in raw manures. These ARGs encoded different mechanisms including antibiotic inactivation (42), target alteration (19), and target protection (16), efflux (11), and target replacement (2). In terms of antibiotic resistance, 25 were *mls*, 23 tetracyclines, 19 aminoglycosides, 10 multidrug, beta-lactams, 3 glycopeptides, 2 sulfonamides, one nucleoside, and one rifamycin. The most abundant ARGs were target protection (147 ± 38 rpkm) and inactivation (111 ± 26 rpkm), and tetracyclines (131 ±39 rpkm) and *mls* (108 ± 30 rpkm) (Figure 7.2).

The overall ARG levels in digestates (332 ± 62 rpkm) were significantly lower (Figure 7.2), averaging a reduction of 53%. The total ARG levels in digestates remained relatively stable during the length of the experiment (237-452 rpkm). They did not seem to be affected by the variation in the levels of ARGs present in the manures used as feed (Figure 7.2). This observed reduction in ARGs aligns closely with the estimates from the meta-analysis presented in Chapter 4, where a log2FC of -1.11 (or 46% reduction) was noted, further affirming the findings of that study. These outcomes not only corroborate the efficacy of AD in diminishing ARGs in animal manure, as highlighted by prior research (Gurmessa et al. 2020; Youngquist et al. 2016), including the metanalysis discussed in Chapter 4, but also emphasize the consistency and reliability of AD as a method to manage and reduce AMR associated with livestock manure.

The PCoA (Figure 7.4A), revealed that digestate and manure samples distinctly clustered at the extremes of the principal coordinate (PC) 1. This analysis accounted for 56.5% of the data variation (38.2% for PC1 and 18.3% for PC2), highlighting the efficacy of resistome profiles in differentiating the samples. These findings indicate that, regardless of the source, varying physicochemical properties, and the diversity in microbiome and resistome profiles of the manure, the microbial communities within the digester consistently sustain a stable resistome profile over time. Recognizing this stability is crucial as it underscores the digester's ability to provide consistent treatment outcomes, which is vital for ensuring the safe use and disposal of digestate.

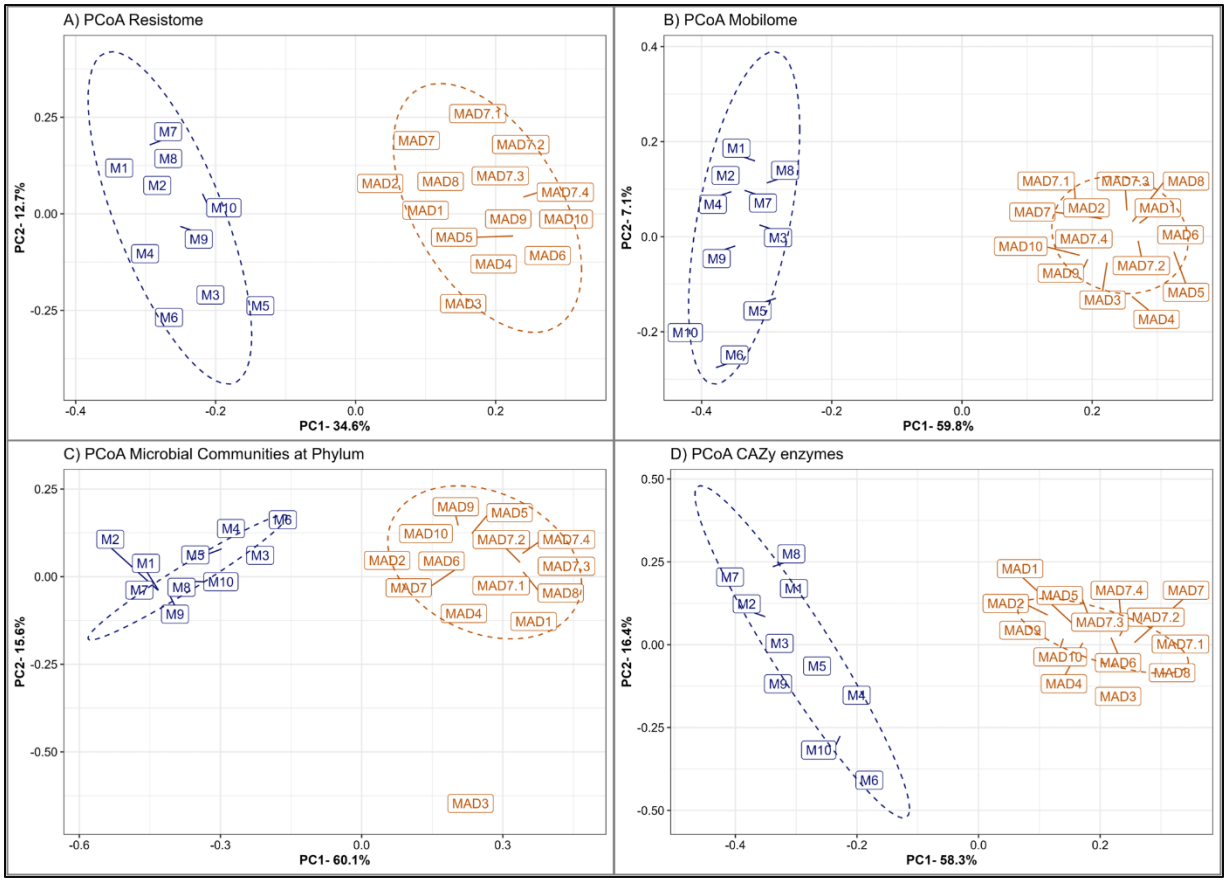

Figure 7.4 Principal coordinates analyses (PCoA): (A) resistomes; (B) mobilomes; (C) microbiomes, and (D) cazymes. Ellipses represent the 95%-confidence intervals.

The changes in the levels of the different ARGs during the AD process were evaluated using a differential heat tree (Figure 7.5). Heat trees offer an innovative approach to visualizing multi-level data and are commonly used to evaluate microbiomes (Foster et al. 2017). This study demonstrated that this tool could also be used to evaluate resistomes. The results indicated that different groups of ARGs were significantly reduced during the mesophilic AD process. These ARGs included antibiotic efflux pumps for tetracyclines, phenicol and multidrug, antibiotic inactivation for mls, beta-lactams, tetracyclines, and aminoglycosides, target protection for tetracyclines and multidrugs, target alteration for multidrug and target replacement for sulfonamides (i.e., sul1).

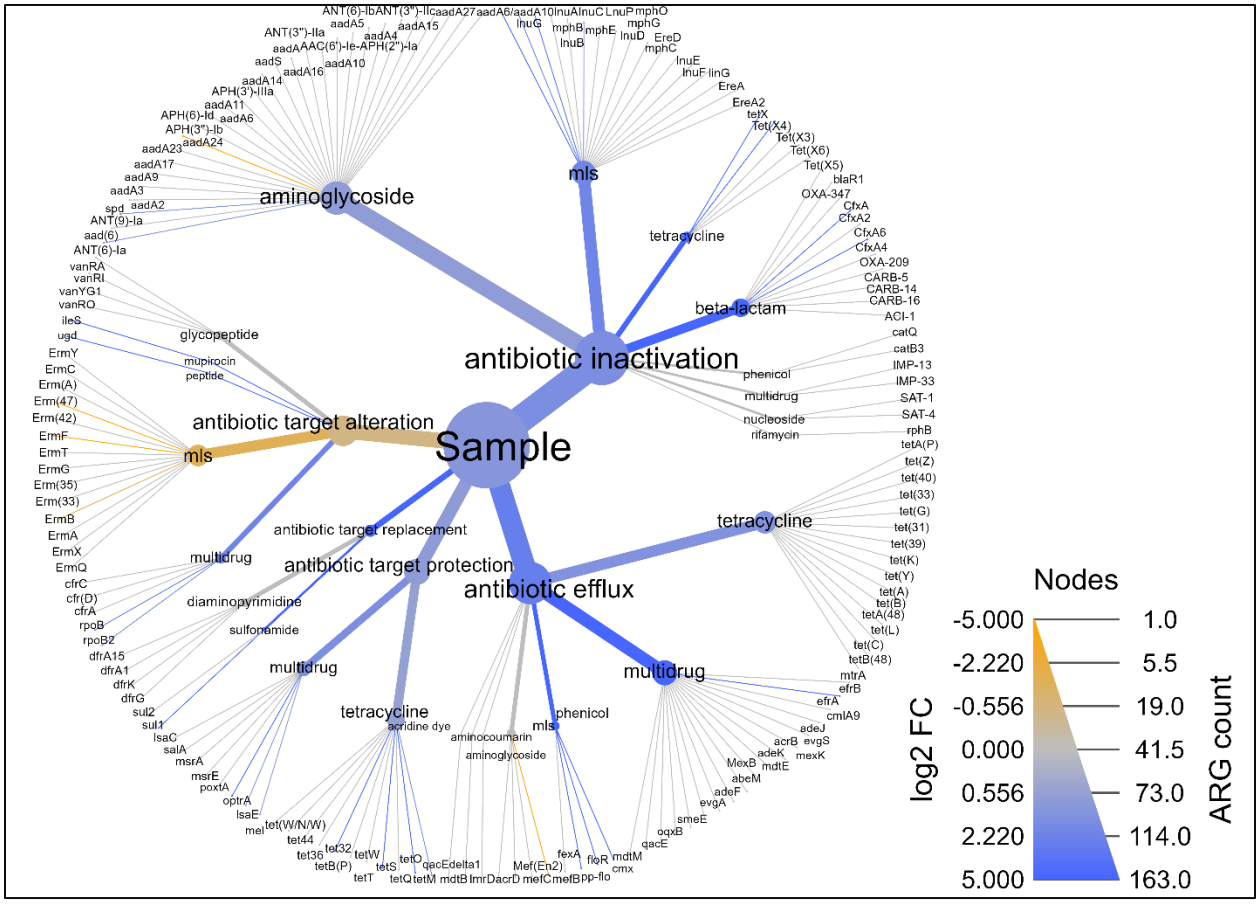

Figure 7.5 Differential heat tree of average ARG abundance in manures and digestates. Color encodes the log2 of the fold change (FC) defined as the abundance in digestate divided by the abundance in manure; blue indicates significantly (p-value < 0.05) higher abundance in manure while orange significantly (p-value < 0.05) higher abundance in digestate, gray indicates no significant difference; edge size indicates the number of ARGs in each group.

The results also indicated that the levels of specific ARGs were not affected during the AD process. For example, sul2, which encodes resistance to sulfonamides via antibiotic target replacement, and ARGs encoding resistance to glycopeptides via antibiotic target alteration (e.g., *vanRA*, *vanRI*, *vanYG1*, *vanRO*) did not significantly change during AD (Figure 7.5). Similarly, ARGs encoding antibiotic inactivation for multidrug, phenicol, nucleoside, and rifamycin were found at comparable levels in fresh and digested manures.

On the other hand, some ARGs encoding resistance to *mls* antibiotics via antibiotic target alteration (i.e., *ErmF*, *ErmB*, *Erm47*) and aminoglycosides via efflux pumps (i.e., *mefB*) were

found at significantly higher levels in digestates, suggesting they were enriched during the AD process (Figure 7.5). A possible explanation for this is that some microbial groups commonly found in manure anaerobic digesters harbor this type of ARG, which is supported by previous studies having made similar observations (Syafiuddin and Boopathy 2021; Zhang et al. 2020a). More details about the putative carries of these ARGs is presented in subsequent sections. Overall, these results provide valuable insights into the expected resistome dynamics during MAD that could serve to develop strategies to minimize the abundance of ARG for critically important antibiotics.

7.5.4. Effect of mesophilic AD on mobilomes

The MAD process substantially reduced the number and levels of MGE-related modules in raw manures: 188 different MGEs were detected in digestates, which represented the removal of 46.9% of those observed in raw manures. The MGE modules in digestates included 56 replication/recombination/repair, 51 integration/excision, 33 transfer, 31 stability/transfer/defense, and 23 phage-related genes. The total MGE abundance was also dramatically reduced after AD (Figure 7.3). On average, total MGE abundance in digestates was 921 rpkm, which represented a reduction of 74% of the levels observed in raw manures (Figure 7.3). The PCoA on the mobilomes (Figure 4.B) showed that digestates were substantially different from raw manures as they clustered in the extremes of the PC1. The PCoA also explained 76.7% of the variability of the data (67% PC1, 9.7% PC2), confirming that the mobilome profiles were significantly distinct before and after the AD process.

As seen in Figure 7.6, all different MGE groups were significantly reduced after AD. On average, the integration/excision MGE group was reduced 99%, the phage group was reduced by 46%, the replication/recombination/repair group was reduced by 69%, the

stability/transfer/defense group was reduced by 46%, and the transfer group was reduced by 66%. Previous studies reported the reduction of the levels of a few specific MGEs (e.g., integrons, transposons/transposases, plasmids) in animal manure during AD (Sun et al. 2019; Yang et al. 2020a; Zhang et al. 2018b). The results of the metagenomic analysis confirmed that mesophilic AD was capable of effectively reducing the diversity and total abundance of MGEs and related modules present in dairy manure. Overall, these findings suggest that digested manures, with their reduced MGE content, may present a diminished risk for the propagation of AMR compared to untreated manure, given the lower potential for ARG mobilization through HGT.

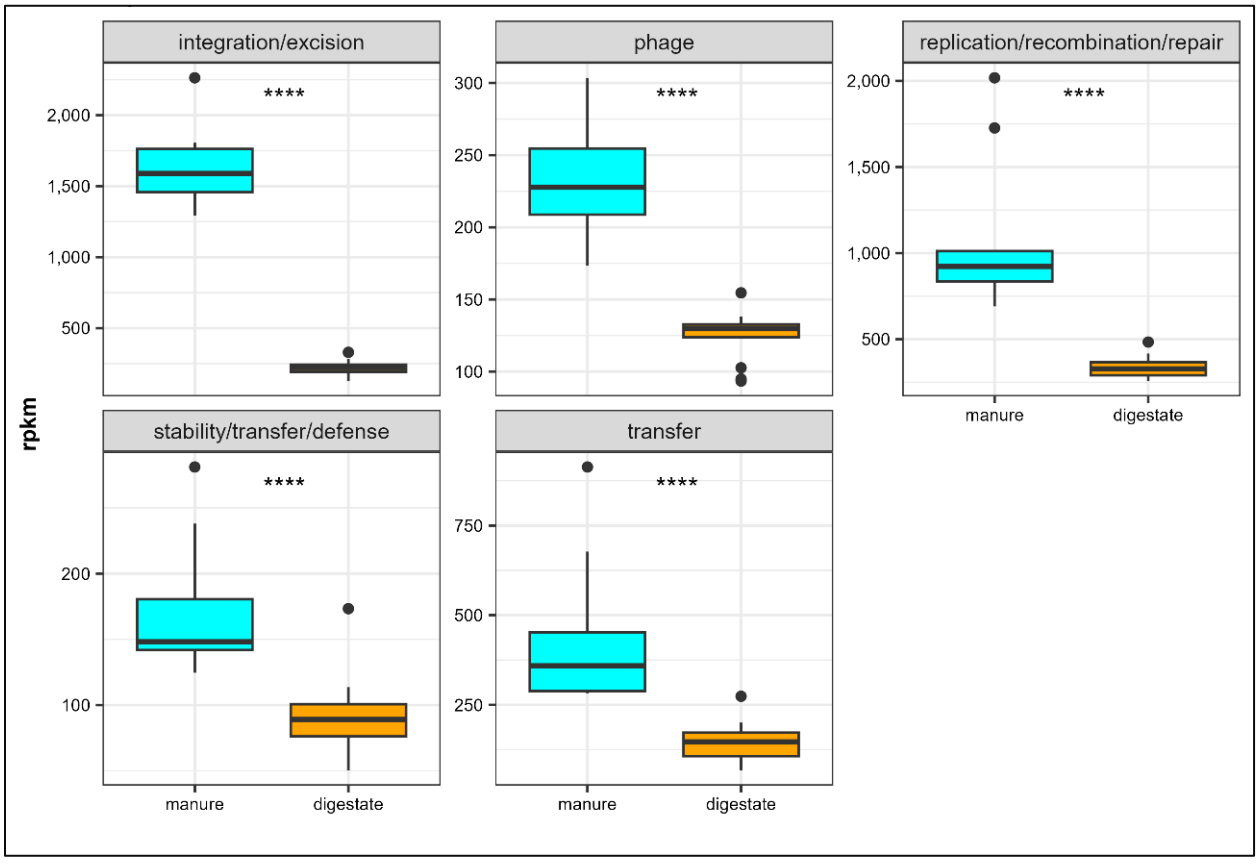

Figure 7.6 Total abundance of different MGE modules. **** indicates significant difference from Wilcox tests with alpha = 0.0001.

7.5.5. Effect of mesophilic AD on microbiomes

The microbial community composition at the phylum level in raw manure exhibited slight variations across different batches, as seen in Figure 7.7. The main differences were the levels of Pseaudomonadota and Bacteroidota, which were considerably higher in M3, M4, M5, and M6. These differences could be the result of the different feeds used on the farms that lead to distinctive microbial communities or other changes in the farm's daily operations. Nonetheless, on average, the dominant phyla in raw manures were Bacillota (49.3%), Actinomycetota (30.3%), and Pseudomonadota (12.2%) (Figure 7.7).

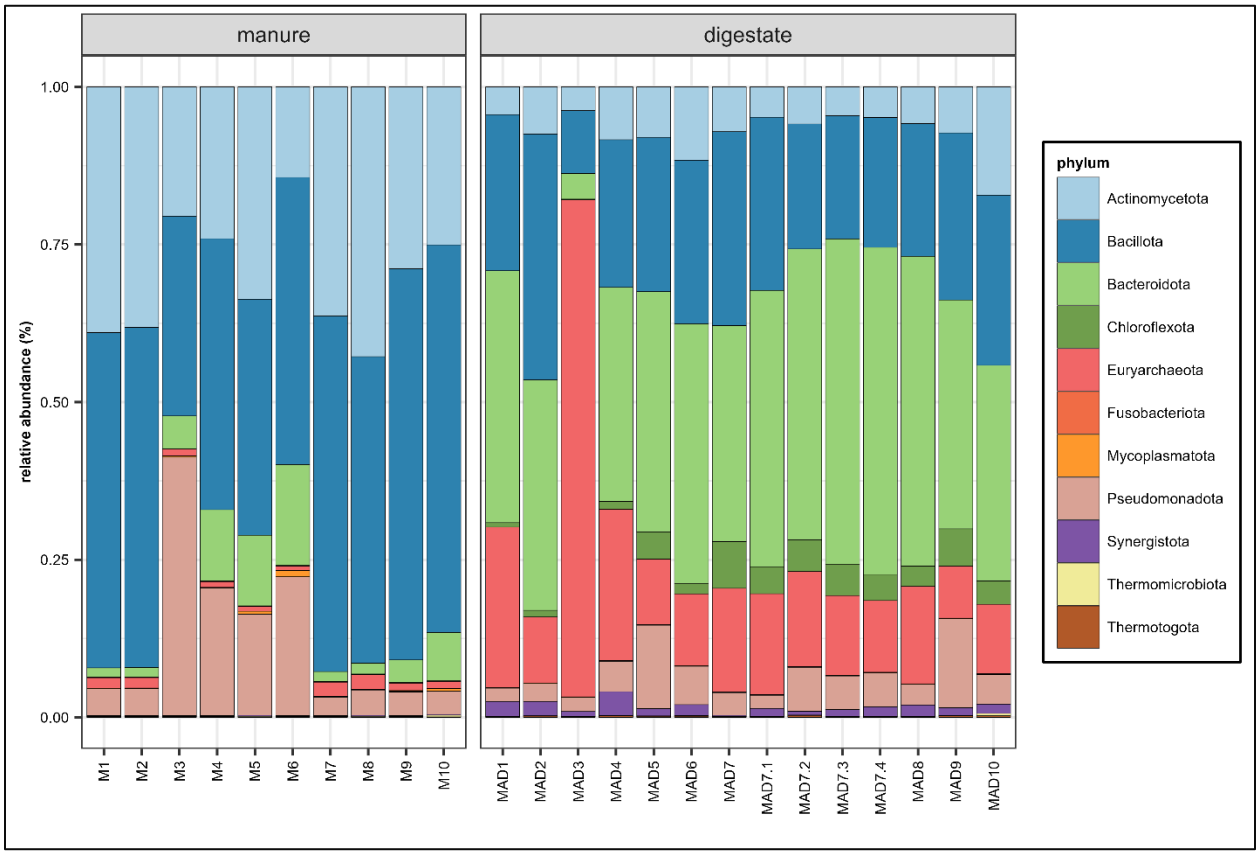

Figure 7.7 Microbiome structure at Phylum level in manures and digestates.

The microbial communities in digestates were more homogeneous, indicating that the digester remained stable throughout the study (Figure 7.7). The only exception was MAD3, which

had higher levels of Euryarchaeota species (i.e., methanogens). This fluctuation was likely caused by an operational disturbance a few weeks before the sample was taken (Figure 7.1, days 500 to 600), which led to an accumulation of VFAs and, ultimately, the temporary enrichment of methanogens. Since the digester performance and the other physicochemical properties were stable, sample was included as part of the overall analysis. Despite this outlier, the dominant phyla in all digestate samples were Bacteroidota (38.7%), Bacillota (24.3%), and Euryarchaeota (19.1%) (Figure 7.7). Species from other phyla, such as Thermotogae, Synergistetes, and Chloroflexi, were also distinctive of digestates (Figure 7.7). The overall consistency of the microbial communities within the digestates, despite the variations in the fed manure, underscores the resilience and stability of the microbial populations in the anaerobic digester.

The microbial composition at the phylum level was utilized to differentiate manure and digestate samples using PCoA (Figure 7.4C). The analysis indicated that 74.7% (54.8% PC1 + 19.9% PC2) of the variation in the data could be explained by the microbial composition. The analysis also showed that manure and digestate samples were substantially different as they clustered independently in the extremes of the PC1. The results indicated that microbial communities among manures were similar. Likewise, digestate samples were comparable, although the MAD3 was slightly different as it was richer in methanogens for the reasons previously discussed.

The Shannon and Simpsons were used to compare the microbial diversity of manures and digestates (Figure 7.8). These diversity indices were significantly higher in manure samples, which indicated that the microbial communities in fresh manures were richer and more even than those in digestates. Moreover, the chao indices also indicated that microbiomes in manure (161 ± 0.50) were more diverse than digestates (99 ± 10). The lower microbial diversity in digestate was

expected since the AD process involves a controlled environment that promotes the establishment of well-defined microbial populations.

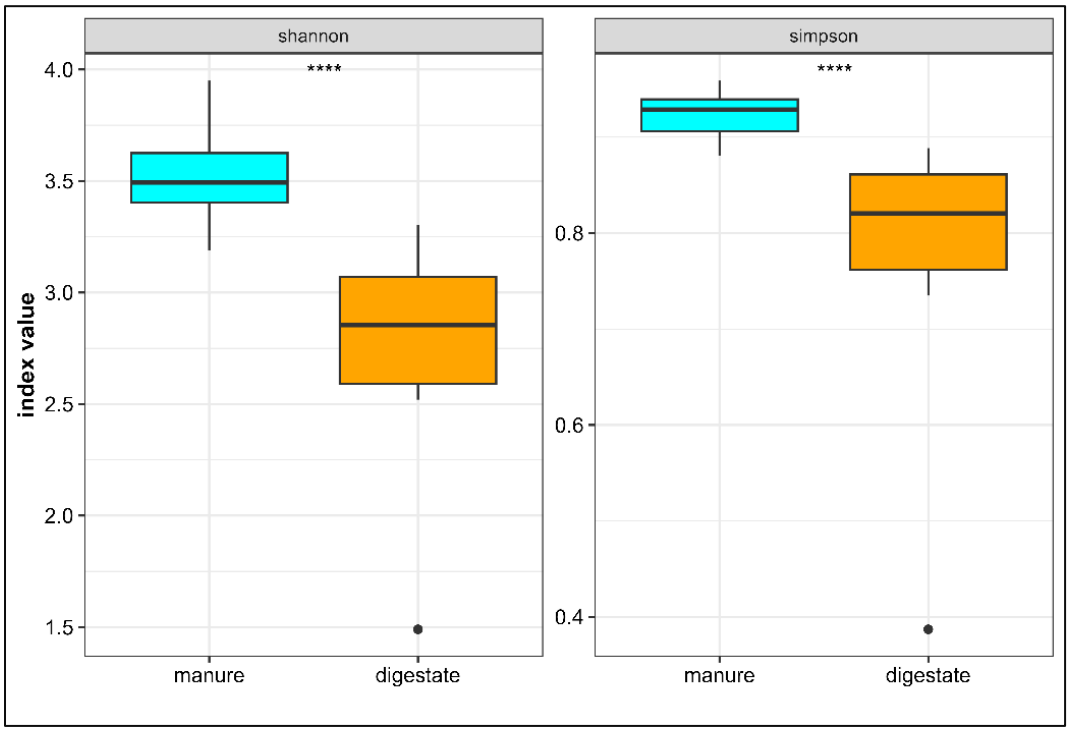

Figure 7.8 Shannon and Simpson diversity indices (Species levels). **** indicate significant difference with alpha = 0.0001.

The differences in the abundance of the microbial communities at the different taxonomic levels, before and after AD, are displayed in the form of heat trees in Figure 7.9. In general, fresh manures were richer in Pseudomonadota, including Gammaproteobacteria (e.g., Acinetobacter), Betaproteobacteria (e.g., Burkholderiales), Actinomycetota including Cornybacterales (e.g., Corynebacterium, Dietzia), Bifidobacterales (e.g., Bifidobacterium), Micrococcales (e.g., Brevibacterium, Microbacterium) and Actinomycetales (e.g., Flaviflexus, Trueperella), Bacillota such as Bacillales (i.e., Staphylococcus, Ureibacillus, lysinibacillus), Lactobacillales (e.g., Enterococcus, Lactococcus, Ligilactobacillus, Streptococcus, Aerococcus, Wisella, Jeotgalibaca), and some Methanobacteria species (e.g., Methanobrevibacter).

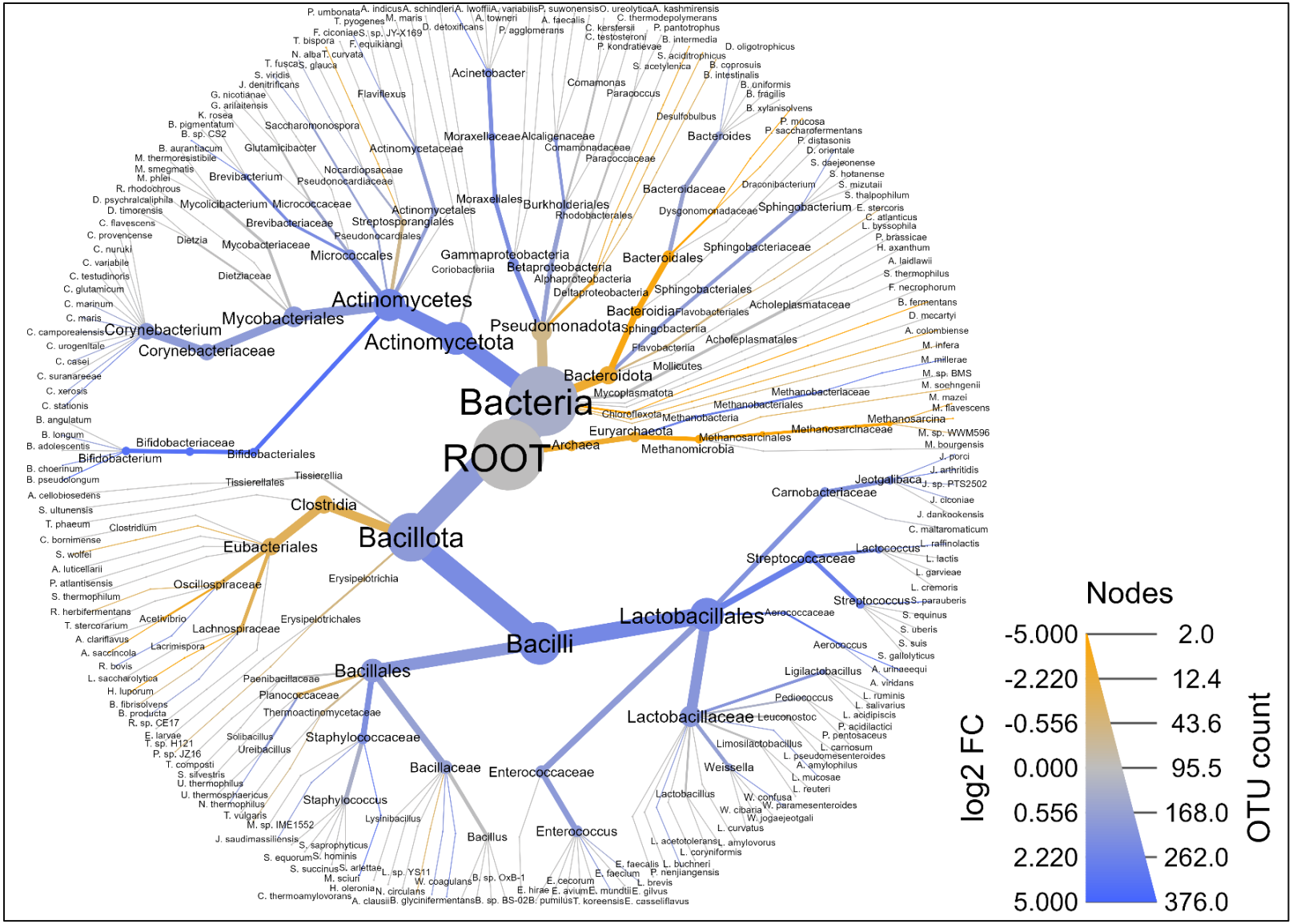

Figure 7.9 Differential heat tree of manure and digestate microbiomes. Color indicates differences in the average abundance of the microbial taxon. Blue indicates higher abundance in manure while orange indicates higher abundance in digestates.

On the other hand, digestates were richer in methanogens such as *Methanosarcina* and *Methanoculleus*; Bacteroidota such as Bacteroidales and Marinilabiliales; Bacillota such as Eubacteriales (e.g., *Acetivibrio*) and Erysipelotrichales; Chloroflexi (i.e., *Brevefilum, Dehalococcoides*); some Deltaproteobacteria including Desulfuromonadales (i.,e., *Syntrophotalea*), Desulfobacterales (i.e., *Desulfobulbus*), and Syntrophales (i.e., *Syntrophus*); Thermotogae (i.e., *Mesotoga*); and Synergistetes (i.e., *Aminobacterium*). These microbial groups are typically found in healthy anaerobic digesters, and their abundance could serve as indicators of the status of the AD process (Khafipour et al. 2020; Wolak et al. 2022).

7.5.6. Cazymes in manures and digestates

The results of meta-analyses described in Chapter 4 suggested hydrolytic communities as one of the main ARG carriers in animal manures and that reducing these microbial groups during AD could lead to the reduction of ARGs. To further investigate this observation, carbohydrate-active enzymes (Cazymes) from the CAZY database present in the metagenomes of manure and digestate samples were analyzed and contrasted.

A total of 580 distinct cazymes genes were identified in raw manures, compared to 439 in digestates. The relative abundance of the different enzyme families is shown in Figure 10. The results indicated that the cazymes profiles in manures and digestates were different. For instance, the relative abundance of auxiliary activities (AA), carbohydrate-binding modules (CBM), carbohydrate esterases (CE), and glycosyl hydrolases (GH) were significantly higher in fresh manures than in digestates (Figure 7.11). The most abundant GH in manure samples were α-glycosidases (GH13) and β-glycosidases (GH3) (data not shown), which are known for hydrolyzing starch and cellulose. On the other hand, glycosyltransferases (GT) were found at significantly higher levels in digestates (Figure7.11). These enzymes catalyze the biosynthesis of

glycosides and are also involved in glycosylation processes (Magidovich and Eichler 2009). The PCoA confirmed that the cazyme profiles in fresh and digested manures were substantially different as they clustered independently in the extremes of the PC1 (Figure 7.4D). Also, the PCoA indicated that the CAZY profile could explain 85.2% (72.5% PC1, 12.7% PC2) of the variability of the data.

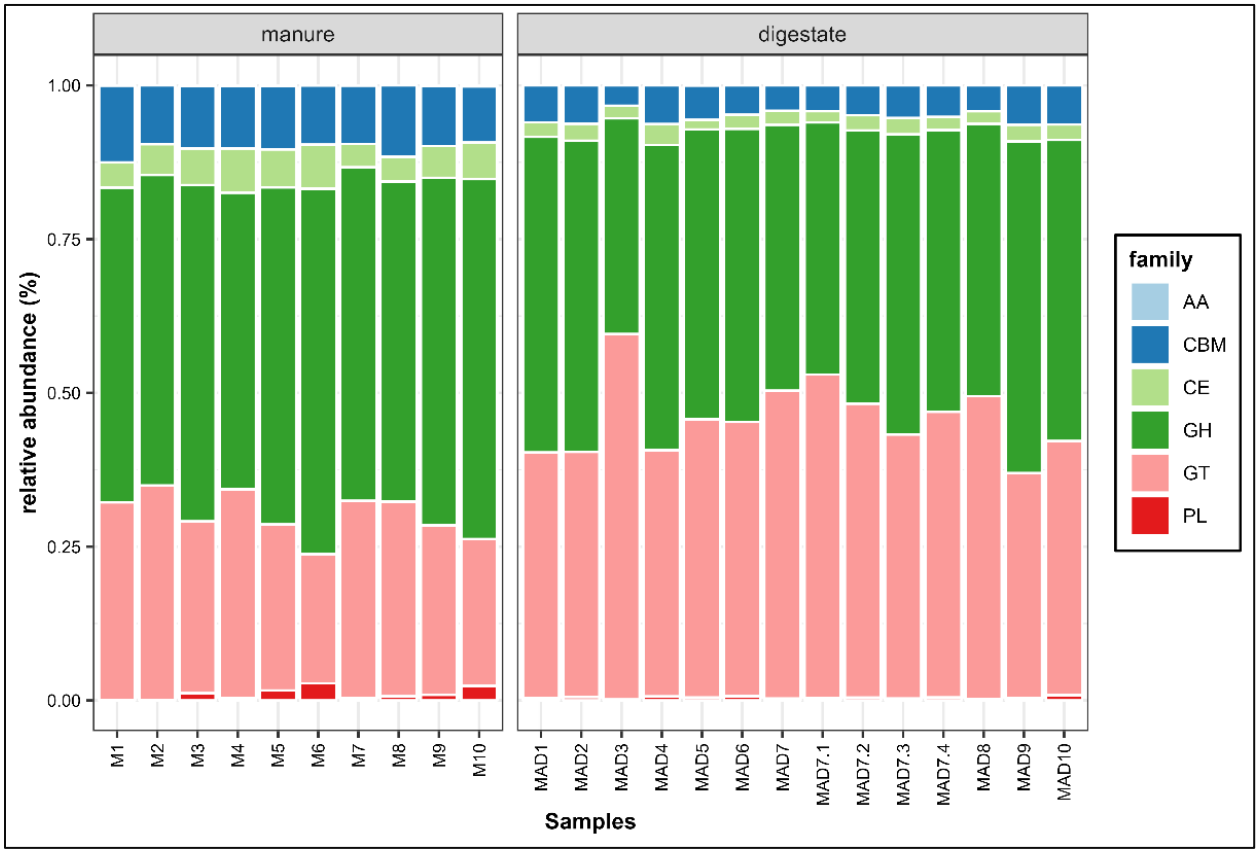

Figure 7.10 Relative abundance of Cazymes. The abbreviations in the legends are are glycoside hydrolases (GH), glycosyl transferases (GT), polysaccharide lyases (PL), carbohydrate esterases (CE), carbohydrate binding modules (CBM), and auxiliary activities (AA).

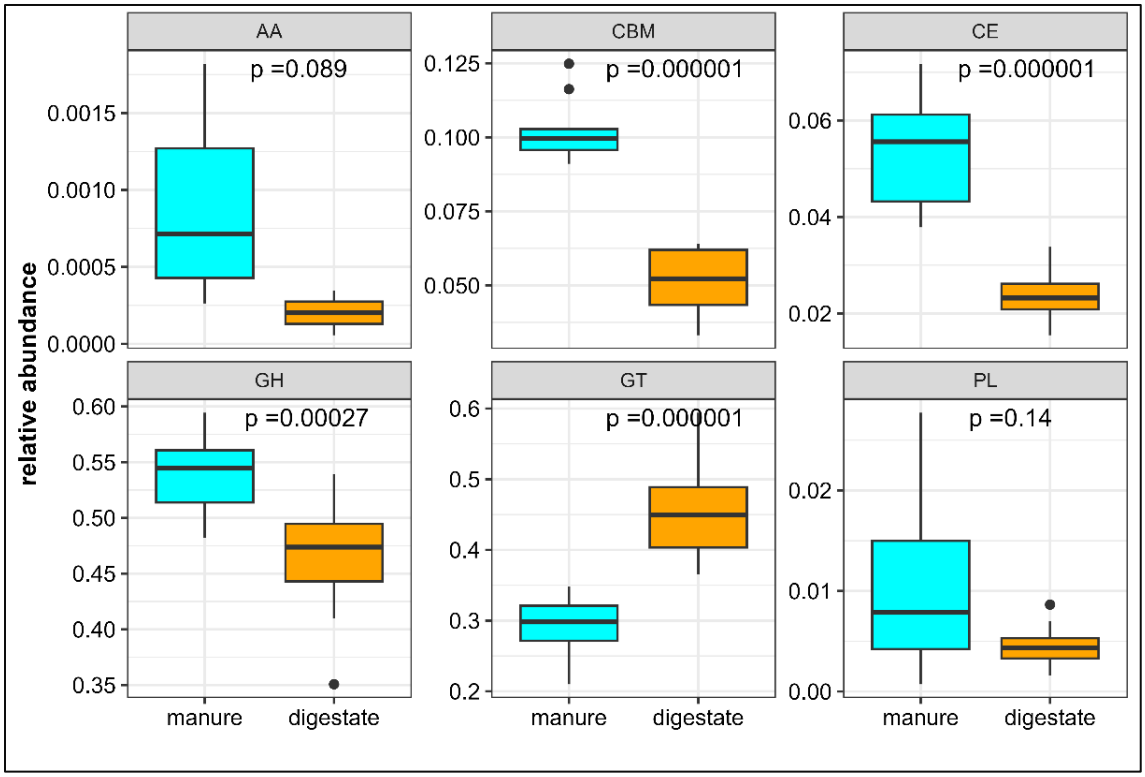

Figure 7.11 Boxplot of relative abundance of cazymes in manure and digestate. p indicates p-values from Wilcox test.

The diminished presence of hydrolytic CAZY enzymes in digestate metagenomes implies that the hydrolytic communities in anaerobic digesters may be less prevalent than in raw manures. Coupled with the observed reduction in ARGs (Figure 7.2) and MGEs (Figure 7.3), this strengthens the hypothesis that hydrolytic communities in raw manures might be significant reservoirs for both ARGs and MGEs. This insight emphasizes the importance of understanding microbial dynamics in waste treatment processes to mitigate the spread of antibiotic resistance.

7.5.7. Relationship between microbiomes, resistomes, and mobilomes

7.5.7.1. Microbial groups potentially harboring ARGs

Spearman correlations combined with a probabilistic model of co-occurrence (Veech 2013) were used to evaluate the relationship between ARGs and microbial communities. The significant association of microbial genera with ARGs are shown in Figure 7.12. The results indicated that 52

different genera were significantly associated with 41 ARGs. The phylum Bacillota (e.g., Bacillales, Lactobacillales, Eubacteriales) accounted for the great majority of these genera (27), followed by Actinomycetota (7) from Orders like Micrococcales, Actinomycetales, and Mycobacteriales; Pseudomonadota (7) from Orders including Burkholderiales, Moraxellales, and Xanthomonadales; and Bacteroidota (7) including Flavobacteriales, Bacteroidales, and Sphingobacteriales. The genera *Jeotgalicoccus*, *Amylolactobacillus*, *Lentilactobacillus*, *Streptococcus*, *Enterococcus*, *Mammaliicoccus*, *Weissella*, *Brevibacterium*, and *Lactococcus*, all Bacillota, stood as the main groups associated with more than 10 different ARGs. *Staphylococcus* (Bacillota) and *Acinetobacter* (Pseudomonadota), known to include pathogenic species, were also strongly associated with ARGs encoding resistance to different antibiotic including tetracyclines and sulfonamides.

The ARGs associated with the different microbial groups included inactivation (15), efflux (10), target alteration (7), target protection (7), and target replacement (2) mechanisms. In terms of antibiotic groups, these ARGs were mainly mls (9) tetracyclines (9), multidrug (8), aminoglycoside (4), phenicol (3), beta-lactams (2), and sulfonamides (2). Bacillota genera were the primary group associated with the different types of ARG mechanisms and antibiotic class resistance.

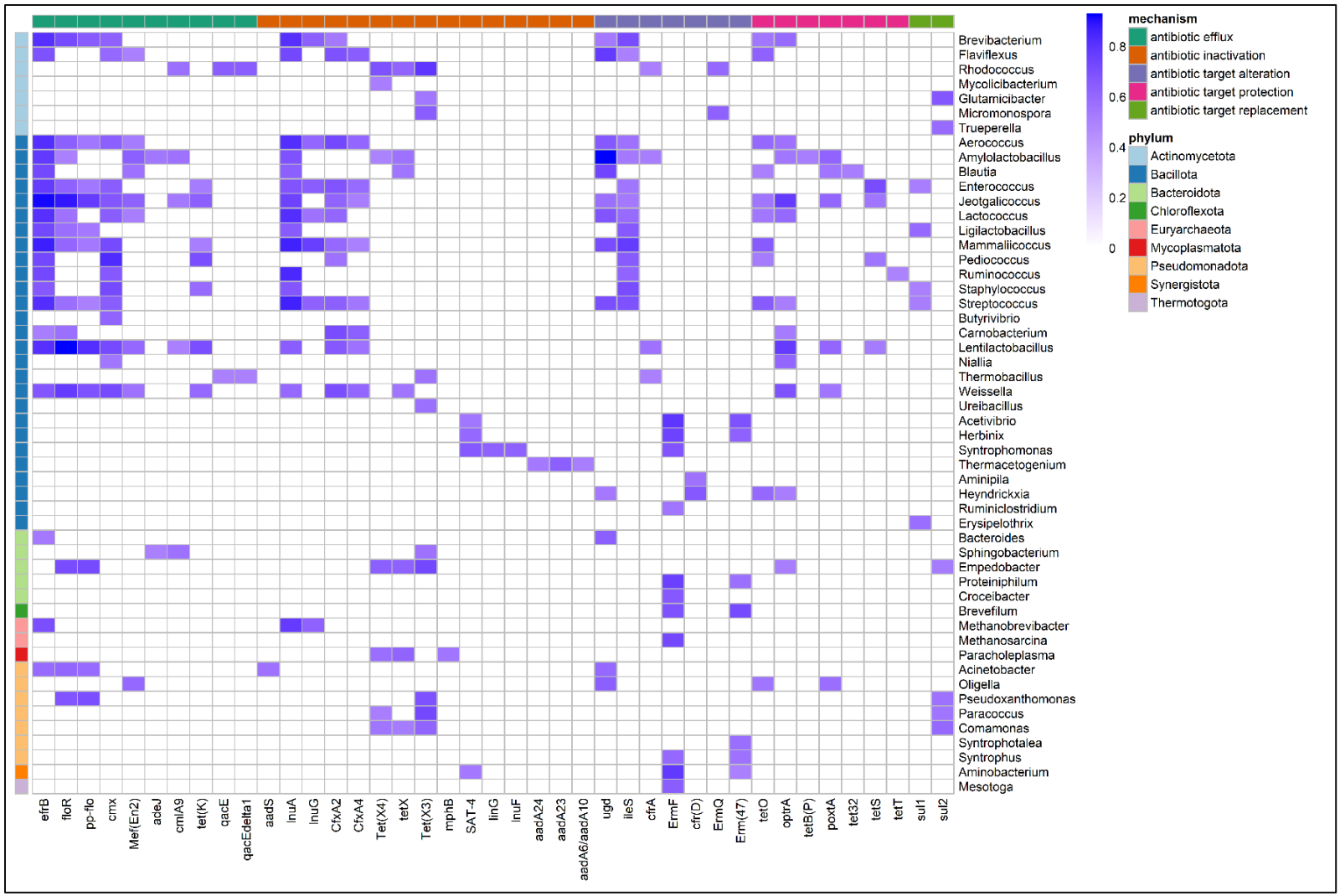

Figure 7.12 Relationship between microbial groups and ARGs. Showing the significant associations from the co-occurrence model that had positive (R > 0.50) and significant (p-value < 0.05) Spearman correlation coefficients. The correlation coefficients are encoded by the intensity of the colors. Colors on top the columns indicates the ARG mechanism. Row colors indicate the Phylum of the microbial genera.

Figure 7.13 Relationship between microbial groups and MGEs. Showing the significant associations from the co-occurrence model that had positive (R > 0.50) and significant (p-value < 0.05) Spearman correlation coefficients. The correlation coefficients are encoded by the intensity of the colors. Colors on top the columns indicates the ARG mechanism. Row colors indicate the Phylum of the microbial genera.

The presence of ARGs encoding resistance to several antibiotics in Xanthomonadales, Burkholderiales, Pseudomonadales, Moraxellales, Flavobacteriales, Bacilliales, and Lactobacillales species have been well documented in previous studies (Anisimova and Yarullina 2019; Crossman et al. 2008; Liu et al. 2020; Sun et al. 2016), including the research in Chapter 5 (Flores-Orozco et al. 2020a). Many of these species are known pathogens (e.g., *Staphylococcus*, *Acinetobacter*) capable of acquiring and mobilizing ARGs from and towards different species. The coexistence of these pathogenic bacteria, known ARG carriers, and elevated MGE levels underscores the heightened risk of antibiotic resistance spread in dairy manures. However, this study also suggested that MAD is capable of reducing the abundance of most of these concerning microbial species and potentially minimizing the risk of mobilization of ARGs into pathogenic bacteria.

An intriguing result was the strong correlation of methanogens (i.e., *Methanosarcina*) with *ErmF* (antibiotic target alteration), one of mls ARGs enriched during the AD process. Previous studies have reported similar results (Sun et al. 2019). The mode of action of mls antibiotics involves the interruption of the protein synthesis by binding to the bacterial 50s ribosomal subunit. Thus, it seems unlikely that methanogens harbor these types of ARGs because Archaea are naturally resistant to mls, as their 50S subunit does not interact with this type of antibiotic (Dridi et al. 2011). In order to explore this finding further, the *Methanosarcina mazei* and *Methanosarcina flavescens* genomes, available in Genebank (accession numbers NZ_CP009509.1 and NZ_CP032683.1, respectively), were analyzed with the Resistance Gene Identifier (RGI) available in the CARD webpage. Interestingly, the genomes of these two methanogens had loose hits to a variety of *Erm* genes. Therefore, it is possible that the enrichment of these types of ARGs observed during AD was related to the presence of similar sequences in the genomes of the

different methanogens. Nonetheless, it is also possible that other anaerobic microbial groups common in anaerobic digesters (e.g., *Ruminiclostridium*, *Proteiniphilum*, *Syntrophus*, *Herbinix*, *Aminobacterium*) host this type of ARGs as they had strong associations. Since mls antibiotics are often used in livestock production, more detailed studies are required to identify the microbial groups harboring these ARGs in manure anaerobic digesters and determine the risk of antibiotic resistance they could represent.

7.5.7.2. Microbial groups potentially harboring MGEs

The analysis of co-occurrence indicated that a total of 62 genera were significantly associated with 124 MGEs (Figure 7.13). These genera were mainly Bacillota (e.g., Lactobacillales, Bacillales, Eubacteriales, Erysipelotrichales, Tissierellales), Actinomycetota (e.g., Bifidobacteriales, Micrococcales, Eggerthellales, Actinomycetales, Mycobacteriales, Streptosporangiales), Bacteroidota (Bacteroidales, Sphingobacteriales, Flavobacteriales), and Pseudomonadota (e.g., Moraxellales, Burkholderiales, Rhodobacterales, Xanthomonadales, Desulfuromonadales). Lactobacillales and Bacillales were the microbial groups with the largest number of genera associated with the different types of MGEs.

Lactobacillales stood as one of the groups with the highest number of species potentially carrying MGEs and MGE-related modules. Lactobacilli are part of the lactic acid consortia commonly found in the gastrointestinal tract of different animals and are known to carry a variety of MGEs, including phages, integrative and conjugative elements, and conjugative plasmids (van Reenen and Dicks 2011; Tanizawa et al. 2015). *Acinetobacter* species (Moraxellales) were also strongly correlated with MGEs, especially integration/excision and replication/recombination/repair modules. The *Acinetobacter* genus includes species (e.g., *A. baumannii*) characterized by their genome plasticity and the presence of several different MGEs

that allow them to acquire and disseminate ARGs (Pagano et al. 2016; Veress et al. 2020). In environments rich in ARGs, like manure-related settings, the presence of all these microbial species increases the risk of mobilization of ARGs. Therefore, the removal of these microbial groups from manures before they reach the environment is essential to prevent the dissemination of antibiotic resistance into the environment.

7.5.8. Co-occurrence of ARGs and MGEs in co-assembled contigs

To further explore the relationship between ARGs and MGEs, the metagenomic reads of manure and digestate samples were co-assembled to create longer sequences, known as contigs. These longer contigs were then annotated and evaluated to determine if ARGs and MGEs appeared together (Figure 7.14). This analysis showed the presence of ARGs and MGEs in arrangements that resembled structures involved in the mobilization of ARGs. For example, in manure contigs, *tetW* was found in a manure contigs near the *tndx* and *mobC* genes, kwon to be part of the transposon family Tn5397 (Lyras et al. 2004), commonly found in Bacillota species. Notably, Tn5397 has been linked to the intergeneric transfer of tetracycline ARGs (Roberts et al. 1999). The *tetM* ARG was found in a contigs containing the *orf20*, *ftsk*, *int*, and *immR* genes, kwon to be part of ICEs in Bacilli species (Lee and Grossman 2007).

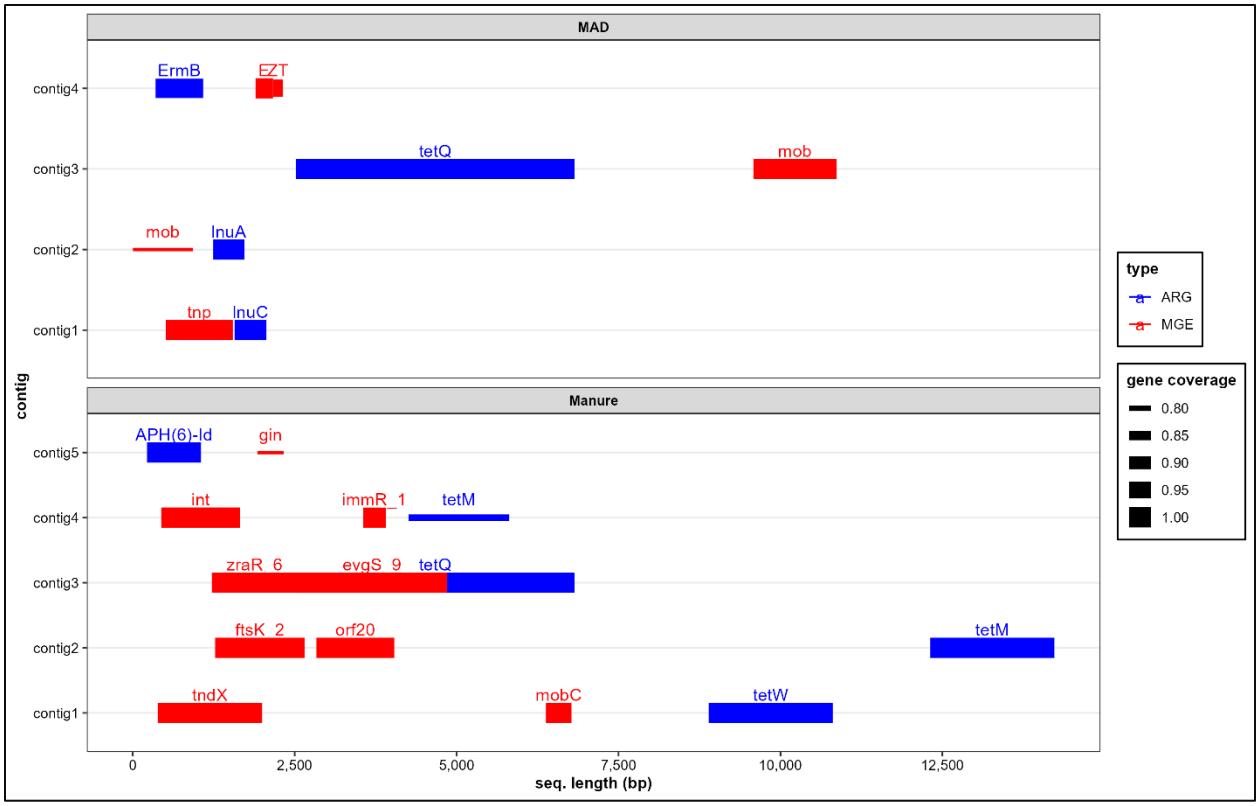

Figure 7.14 Co-occurrence of ARGs and MGEs in manure and MDAAD contigs. In MAD contig1, E represent the epsilon antitoxin and ZT the zeta toxin.

In MAD contigs, the *lnuC* ARG was found near a *tnp* gene were found in close proximity. This aligns with the understanding that *lnuC* is a transposon-mediated nucleotidyl transferase found in Streptococcus, as per the CARD database. The *lnuA*, an ARG commonly found in plasmids, was found near *mob*, a plasmid recombination protein. Similarly, another tetracycline ARG (*tetQ*) was also found near *mob*. Notably, the *ErmB* gene was located close to a type II toxin-antitoxin (TA) system, consisting of the zeta toxin (ZT) and the epsilon antitoxin (E). Type II TA systems are genetic elements present in low-copy plasmids and bacterial and archaeal chromosomes and are involved in different biological roles, including stress responses, and plasmid and genome stabilization (Fraikin et al. 2020). TA systems function by producing a toxin and its corresponding antitoxin, which neutralizes the toxin, ensuring the survival of cells containing the system. These systems are often associated with MGEs and have been linked to

ARGs conferring resistance to erythromycin (Zielenkiewicz and Cegłowski 2005). Interestingly, ARGs encoding resistance to this type of antibiotic are persistently found in manure anaerobic digesters (Tran et al. 2021), where there should be minimum selective pressure in favor of these ARGs. Therefore, this finding suggested that *Erm* genes may be preserved due to the indirect effect of nearby TA systems present in microbial communities in anaerobic digester-related environments. According to the mobileOG, the Zeta toxin and Epsilon antitoxin found in the co-assembled contig belonged to the Lactobacilli genera (i.e., *Streptococcus*, *Enterococcus*). Since the abundance of Lactobacilli was reduced during AD, but *Erm* ARGs persisted, it is possible that these elements were transferred to another group of closely related microorganisms (e.g., Bacilli) that remained in the anaerobic digester.

7.5.9. Factors driving changes in ARGs and MGEs

7.5.9.1. Physicochemical properties

The relationships between physicochemical properties (such as dCOD, VS, and total VFAs), resistomes, and mobilomes were examined using Mantel. The results showed a strong correlation between physicochemical properties, ARGs ($r = 0.74$), and MGEs ($r = 0.83$). Furthermore, Pearson correlations (Figure 7.15) revealed that the total ARGs and MGEs levels were positively correlated with VS ($R_{ARG} = 0.62$, $R_{MGE} = 0.66$), dCOD ($R_{RG} = 0.83$, $R_{MGE} = 0.82$) and total VFAs ($R\text{-}_{ARG} = 0.83$, $R_{MGE} = 0.86$). Alkalinity levels were negatively correlated with total MGEs ($R = -0.55$). Additionally, the abundances of some cazyme families were also significantly correlated with ARGs and MGEs (Figure 7.15). For example, higher levels of AA, CBM, and CE were associated with higher levels of ARGs and MGE, while GT levels had the opposite effect. All this provides further evidence for the potential role of hydrolytic species in harboring ARGs and MGEs. Thus, seems to be plausible to reduce ARGs and MGEs from manure by reducing the abundance of

hydrolytic communities. In this study, several known hydrolytic species, such as Bacteroides, *Staphylococcus* and *Bacillus*, were strongly correlated with different ARGs, which seems to support this hypothesis.

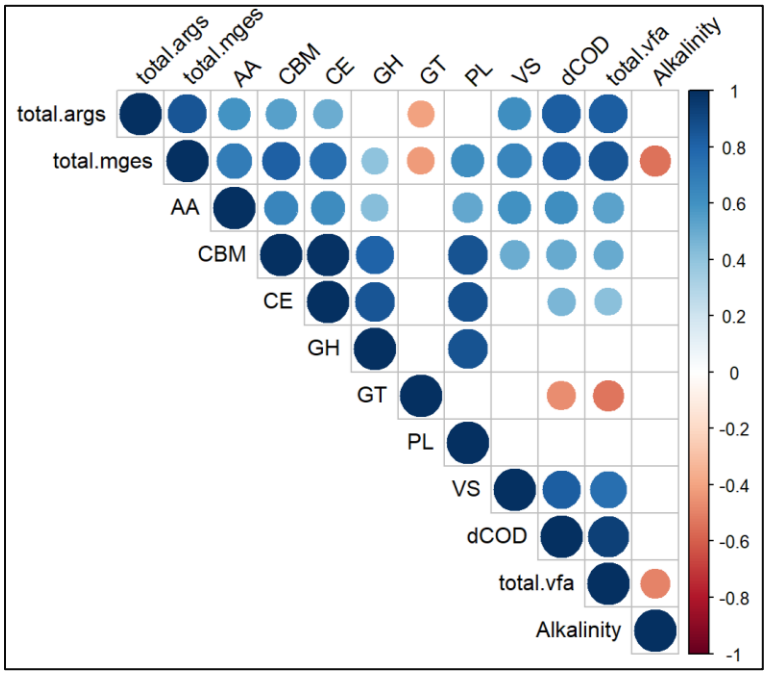

Figure 7.15 Correlation of total ARG and MGE levels with different physicochemical properties and CAZymes.

To further explore this hypothesis, the manure batches used as feed were classified according to the VS concentration into 3 categories: low (M2, M6, M8, M9), mid (M3, M5, M7, M10), and high (M1, M4), as shown in Figure E7.4 in Appendix E. Then, the changes in ARG levels after MAD were compared using Wilcox tests. Although the results indicated no significant differences between the tree VS groups in the ARG (Figure 7.16) and MGE (Figure 7.17) reduction rates, these values tended to be higher in the groups with higher VS content. This trend seems to contradict the results obtained with the meta-analysis (Chapter 4). However, a more detailed examination of the meta-analysis reveals that the diminished reduction rates were associated with digesters supplemented with an additional source of solids. In contrast, in this study, the variations

in solid content were inherent to the manures themselves. Introducing extra solids to a digester might lead to an enrichment of hydrolytic communities, which could hypothetically elevate the ARG levels in the digester, resulting in reduced ARG reduction rates. Conversely, introducing manure with a higher solid content, and potentially more hydrolytic communities, might not necessarily lead to a significant increase in these microbial groups due to the dilution effect. While the observed trends provide insights into the relationship between hydrolytic communities, and ARG and MGE levels, further research is essential to fully understand implications of these interactions in anaerobic digesters.

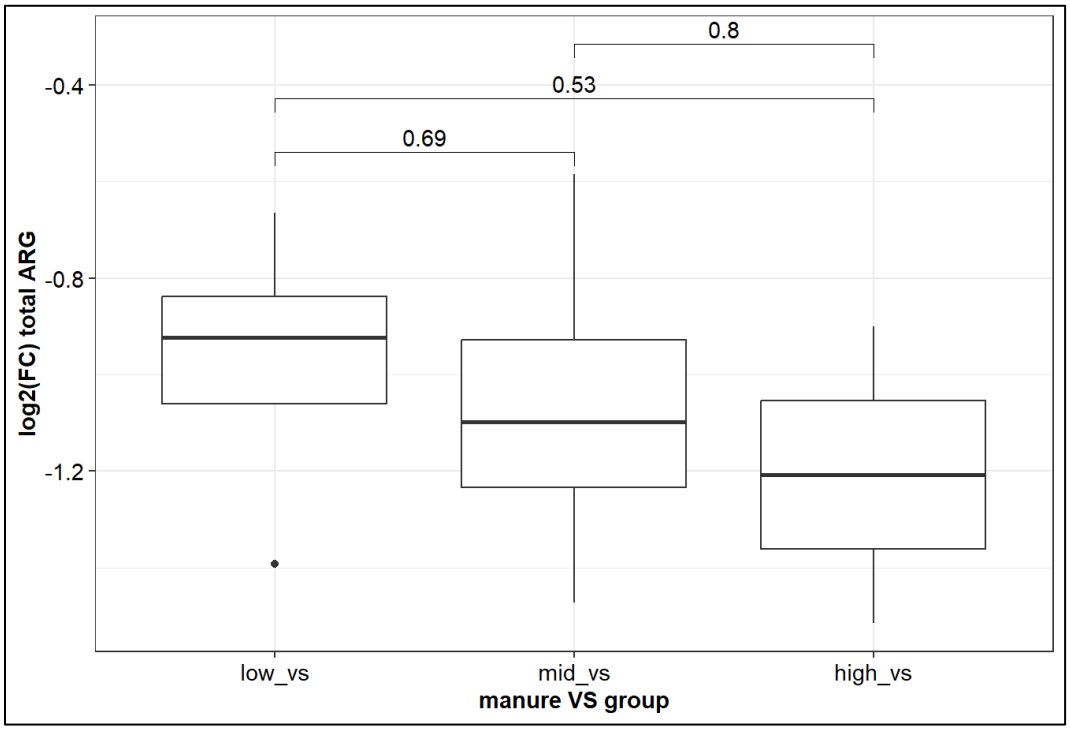

Figure 7.16 Changes in ARG levels by manure VS group. The numbers indicate the p-values of the Wilcox test.

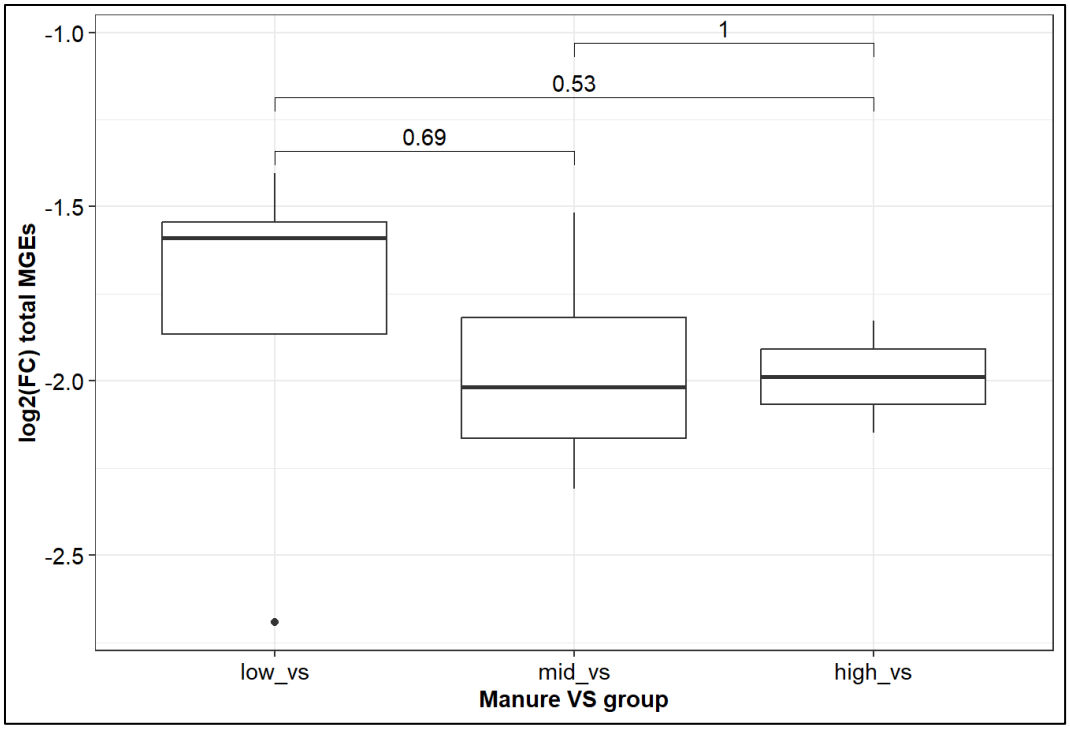

Figure 7.17 Changes in MGE levels by manure VS group. The numbers indicate the p-values of the Wilcox test.

7.5.9.2. Microbial shifts

The mantel tests also indicated a strong correlation between microbiomes and ARG (r = 0.64) and MGE profiles (r = 0.66). Microbial successions and the establishment of distinct microbial communities have been suggested as one of the main drivers of the changes in ARG and MGE levels during different manure treatments, as described in Chaper 6. One of the main factors driving the changes in the microbial communities and, ultimately, the levels of ARGs and MGE during manure AD is the transition towards a controlled anaerobic environment. Under these conditions, the abundance of typical anaerobic communities such as methanogens and other syntrophic bacteria is expected to increase at the expense of the aerobic and non-fermentative communities in raw manures. In this study, this transition resulted in a decline in the overall microbial diversity and the establishment of a homogeneous microbiome in the digester. Consequently, the reduction of aerobic microorganisms present in raw manures (Figure 7.9),

including *Acinetobacter* (Moraxellales), *Psychrobacter* (Moraxellales), *Luteimonas* (Xanthomonadales), *Comamonas* (Burkholderiales), *Brevibacterium* (Micrococcales), *Dietzia* (Corynebacteriales), and *Corynebacterium* (Corynebacteriales), was likely one of the primary reasons for the decline in ARG and MGE levels after the AD process as these microbial groups were strongly correlated with the different types of ARGs (Figure 7.12) and MGEs (Figure 7.13).

What appeared to be the main driver of the changes in MGE and ARG levels during the manure AD process was the reduction of facultative acidogenic microorganisms such as Lactobacilli. Lactobacilli species occupy an important niche in the gastrointestinal tract of dairy cows and are often enriched to improve dairy production (Wang et al. 2021). Hence, it is no surprise to find them at relatively high levels in dairy manures. However, Lactobacilli species are also prone to host a variety of ARGs and MGEs (van Reenen and Dicks 2011; Tanizawa et al. 2015), which could lead to an increased risk of ARG horizontal gene transfer and the eventual dissemination of antibiotic resistance. In this study, the abundance of all Lactobacilli species was significantly reduced after AD (Figure 7.9), which seemed to correspond to the substantial drop in the number and abundance of MGEs and ARGs. Further studies are needed to explore the role these lactic acid bacteria play in harboring ARGs and MGEs and confirm that lowering their abundance would indeed result in a reduced risk of spread of antibiotic resistance.

7.6. Conclusion

This study represents the first-of-its-kind in-depth evaluation of the long-term effect of mesophilic AD on the resistome and mobilome profiles in dairy manures. Results indicated AD significantly reduced the levels of all different groups of MGEs and some types of ARGs. These changes seemed to correspond to distinct microbial successions, such as the removal of aerobic and facultative communities and the establishment of typical AD communities. Hydrolytic

communities were suggested as another microbial group potentially harboring ARGs and MGEs. Moreover, the result suggested the presence of distinct genetic structure potentially linked to the mobilization and maintenance of different ARGs in these types of environments. Understanding these associations is crucial as it offers insights into the mechanisms driving antibiotic resistance, aiding in the development of strategies to mitigate its spread.

7.7. Acknowledgments

This research work was financially supported by the National Sciences and Engineering Research Council of Canada (NSERC) through the Discovery Grants program [RGPIN-2022-03670].

Chapter 8: Metagenomic comparison of the effects of MAD and TAD on resistomes and mobilomes in bovine manure

8.1. Preface

This Chapter represents the last experimental study of this research. Here, one thermophilic anaerobic digester was set up and operated side by side with the mesophilic anaerobic digester to explore the similarities and differences on theirs resistomes. This work has been peer-reviewed and published in the journal *Environmental Advances* in a manuscript titled "*Metagenomic comparison of effects of mesophilic and thermophilic manure anaerobic digestion on antimicrobial resistance genes and mobile genetic elements*" (https://doi.org/10.1016/j.envadv.2023.100472). I alone was responsible for the data collection and analysis, interpretation of the results, and the preparation of the manuscript. The other co-authors provided thoughtful and challenging discussions on the results and reviewed the manuscript prior to publication. Minor modifications were made to the original manuscript to adjust the style to this document and reduce redundancy.

8.2. Abstract

This study employed a metagenomic approach to assess the long-term effects of MAD and TAD on the resistomes and mobilomes in bovine manure. The results indicated that both MAD and TAD lowered ARG levels in fresh cattle manure by over 50% and MGEs by over 65%. Notably, the reduction levels between MAD and TAD were statistically comparable. Co-occurrence analysis suggested facultative anaerobic species belonging to the Bacillota and Actinomycetota phyla as the primary potential hosts of ARGs and MGEs. The decline in facultative species closely related to pathogenic bacteria, were identified as key drivers behind the observed changes in ARG and MGE levels. Further analysis identified the proximity of transposon

and toxin-antitoxin systems to some ARGs typically found in anaerobic digesters. This is particularly significant, as it suggests a potential mechanism for the persistence and spread of ARGs in such environments. Overall, the results indicated that digested cattle manure (whether under mesophilic or thermophilic conditions) would pose a much lower risk of dissemination of antimicrobial resistance than untreated manures. Since TAD did not outperform MAD at reducing ARGs and MGEs, thermophilic temperatures may not be necessary to improve ARG reduction rates in cattle manure AD. These valuable insights could help develop strategies to reduce the dissemination of antibiotic resistance due to manure treatment and disposal.

8.3. Introduction

AD can be performed under different temperature ranges, including psychrophilic (15-25 °C), mesophilic (32-38 °C), and thermophilic (50-60 °C) conditions (Amani et al. 2010; McKeown et al. 2011). However, anaerobic digesters are predominantly operated at mesophilic temperatures due to the high stability of the process (Cheng 2010). The higher stability of MAD is often attributed to the higher microbial diversity, which makes the population more resilient to process disturbances (Wang et al. 2018). Nonetheless, TAD has several potential advantages. For example, higher temperatures increase the reaction rates, which translates into shorter HRTs and SRTs and smaller digester volumes (Cheng 2010). Also, higher methane yields can be achieved due to the increased organic matter degradation at thermophilic temperatures (Amani et al. 2010). Moreover, TAD can also achieve higher pathogen reduction, making digestate more suitable for land applications (Amani et al. 2010; Cheng 2010). Yet, the broader adoption of TAD is constrained by challenges in its initiation and potential stability issues (Amani et al. 2010).

While it may be reasonable to expect higher ARG removal rates in TAD compared to MAD due to the decline in microbial diversity and pathogens, the results of the meta-analyses discussed

in Chapter 4 indicated that this is not necessarily the case for bovine manure. Thus, further research was needed to corroborate this finding. Moreover, there has been a noticeable lack of long-term studies comparing resistomes in continuously operated mesophilic and thermophilic digesters and the potential influence of MGEs in the HGT of ARGs.

In this study, we used metagenomics to evaluate and compare the long-term effects of MAD and TAD on the resistome and mobilome profiles of bovine manure. By integrating a probabilistic co-occurrence model with correlation tests, the study delved into identifying microbial groups that might harbor ARGs and MGEs, as well as understanding the microbial population shifts influencing these elements. The main hypothesis was that under a steady state, TAD would not outperform MAD at reducing the levels of ARGs and MGEs. It was also hypothesized that the microbial dynamics during the transition to thermophilic conditions, would improve our ability to identify microbial groups associated with ARGs and MGEs. This study offers a deeper understanding of how microbial diversity and community dynamics influence the evolution of resistomes and mobilomes during manure digestion.

8.4. Material and methods

8.4.1. Anaerobic digesters setup and operation

8.4.1.1. Initial setup and operation

In this study, two anaerobic digesters were set up and operated. The anaerobic digester previously described on Chapter 3, was used in this study as the mesophilic digester (MD). A second CSTR (Applikon Biotechnology- EZ Controller), which eventually became the thermophilic digester (TD), was set up and initially operated under the same conditions as the MD (Figures 8.1). The TD was first inoculated with 4 L of the MD digestate and one manure dose (~ 0.62 L fresh manure). During the following two weeks, the feed of the TD consisted of mixture

1:1 of the MD digestate and fresh manure, aiming to develop microbial populations similar to those in the MD. After this, the volume of the TD was adjusted to 8L, and the two digesters were fed cattle manure on a regular basis for 120 days.

Figure 8.1 Thermophilic (TD) and mesophilic (MD) anaerobic digesters. The temperature of the TD (left) was maintained with a heating jacket and a extra layer of foil bubble wrap.

The performance of the two digesters, in terms of biogas production (L/g-VS added), biogas composition (CH_4/CO_2 ratio), pH, VFAs profile, alkalinity, and other organic matter properties (e.g., COD, dCOD, TS, VS) was evaluated to ensure steady operation. The biogas production of the digesters was monitored with in-line wet-tip meters and the biogas composition using a gas chromatograph (Agilent Micro GC 490, USA). The methodology for the biogas and physicochemical analyses are described in detail on Chapter 3.

8.4.1.2. Transition to thermophilic conditions

After 154 days of operation, when the biogas production and other biochemical parameters were comparable between the two digesters (i.e., no statistically significant difference), the

temperature of the TD (performing MAD at the time) was increased to 55 °C in one step. The TD was maintained at this condition and operated side-by-side with the MD for an additional 400 days. (Figure 8.1).

8.4.2. Sample collection

Several samples of the MD and TD digestates and their corresponding manures were taken at different time points and used for metagenomic analyses. The first samples corresponded to the mesophilic stage of the two digesters (MD-in, TD-in) and were taken 25 days before the transition to thermophilic temperatures (Figure 8.2). The manure batch from this period was defined as M-in. During the transition to the thermophilic stage, where presumably the microbial communities in TD were adjusting to the new conditions, samples were taken on days 8 (TD-T1, MD-T1), day 22 (TD-T2, MD-T2), day 53 (TD-T3, MD-T3), and day 60 (TD-T4, MD-T4). The manure fed during this period was defined as M0. The digestates of the steady state of the MD and TD were sampled on days 120 (TD1, MD1), 210 (TD2, MD2), and 270 (TD3, MD3). The corresponding manures of the steady states were labeled as M1, M2, and M3, respectively. Figure 8.2 shows the time and overall digesters performance when the samples were taken.

Manure and digestate samples (n = 4) were analyzed for chemical oxygen demand (COD, dissolved COD (dCOD), total solids (TS), volatile solids (VS), alkalinity, pH, and VFAs (i.e., propionic, acetic, butyric, isobutyric, isovaleric, and valeric acids) following standard methods (APHA, 1995) as described in Chapter 3.

8.4.3. DNA isolation and metagenomics

The methodology of the DNA isolation process, the whole genome sequencing, and metagenomic analyses are described in Chapter 3.

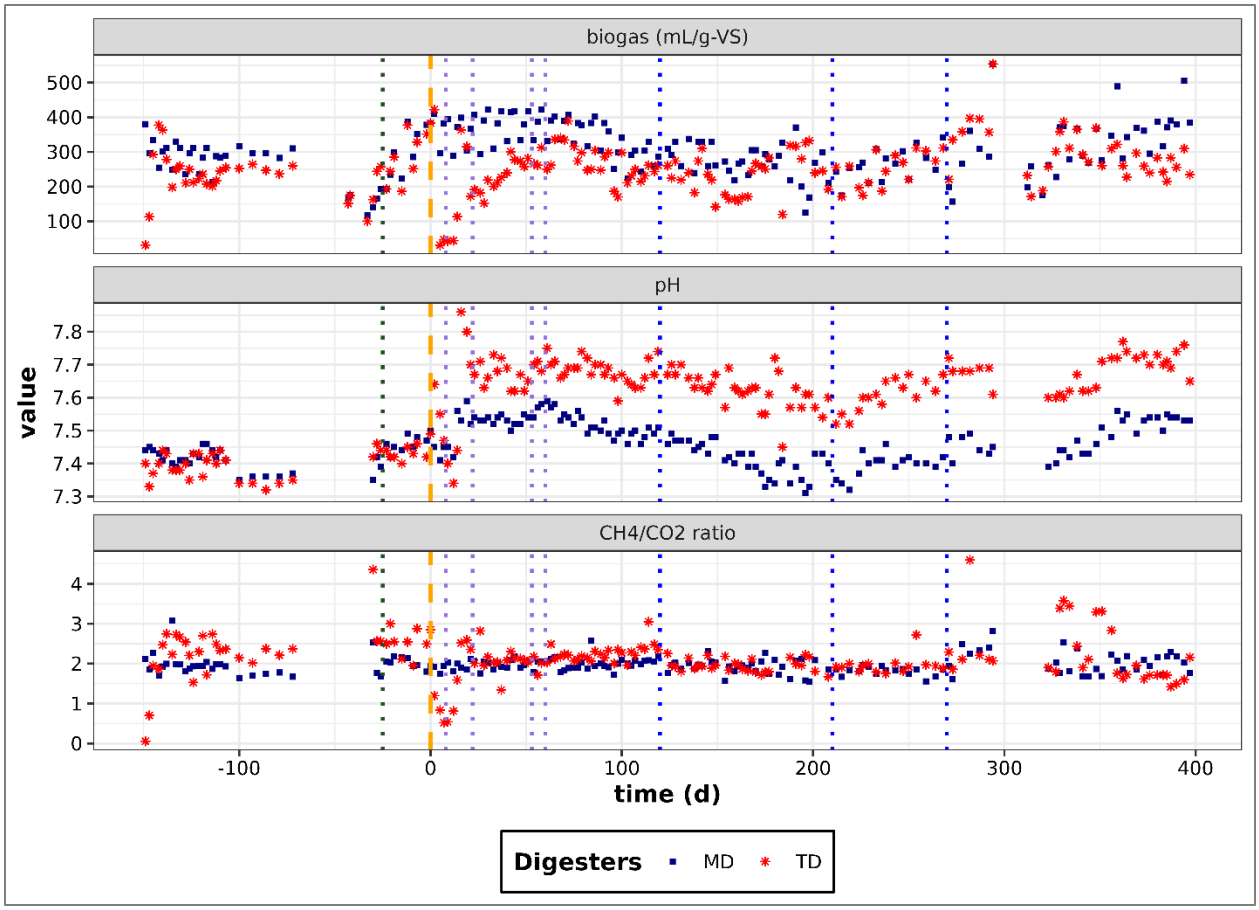

Figure 8.2 MD and TD overall performance and sampling points. Vertical, dashed, and orange line indicates the start of the thermophilic stage. The time before the first red line represents the start-up time when both digesters were operated at 35 °C. The green dotted vertical line represents the sample of the initial mesophilic stage of MD and TD reactors. Vertical, dotted blue lines indicate the sampling points (light blue are transition samples; dark blue are steady-state samples.

8.4.4. Data and statistical analysis

All statistical analyses were performed in *R*. Total levels of A RGs, MGEs, and BacMet genes of each group of samples (i.e., manure, TD, MD) in the different stages were averaged and compared. Statistically significant differences in all studied parameters were determined using non-parametric tests (e.g., Wilcox, Kruskal-Walis, Dunn) with an alpha of 0.05. Only differences where statistical tests had p-values < 0.05 were stated as significant. The Chao, Shannon, and Simpson indices were calculated using the R package *vegan*. The 95% confidence intervals of the

diversity indices were estimated via bootstrapping (n = 1,300, sample size = 133) using the microbiome at the genus level.

The dissimilarities of the resistome, mobilome, microbiome, and BacMet between samples were evaluated by principal coordinate analysis (PCoA) based on *Bray-Curtis* distance. Mantel and partial Mantel tests based on Spearman correlations were performed to determine if the microbial population dynamics were associated with changes in ARGs, MGEs, and BacMet genes. Potential ARG carriers were determined by performing co-occurrence analyses as described in Chapter 3 (Section 3.9.6). The results of this analysis were displayed in a network generated with the R package *igraph*.

8.5. Results and discussion

8.5.1. Digesters performance

The digesters performance during operation is shown in Figure 8.2. During the start-up stage (first 154 days), where the two digesters were operated at mesophilic temperatures, the biogas production and pH of the MD (253 ± 64 mL/g-VS_{added}, pH 7.42 ± 0.04) and TD (228 ± 51 mL/g-VS_{added}, pH = 7.40 ± 0.04) were comparable, although the CH_4 concentration was slightly but significantly higher in the TD (CH_4/CO_2 ratio = 2.4 ± 0.5). However, this difference was more prominent during the first weeks of operation and gradually decreased to levels similar to those in the MD (CH_4/CO_2 ratio = 1.9 ± 0.2). The COD, dCOD, VS, and TS were comparable between the MD and TD, and significantly lower than the fed manure (Figure 8.3). In this stage, the VS removal in the MD and TD ranged between 30.5% – 34.4%. The VFAs concentrations in the MD and TD were very low (< 100 mg/L) compared to the levels in the fed manure (MD-in, > 5,000 mL) (Figure 8.4). On the other hand, the alkalinity of the MD (11.5 ± 0.1 g/L) and TD (11.4 ± 0.1 g/L) were comparable and significantly higher than the fresh manure (5.2 ± 0.1 g/L).

During the transition stage, the biogas production of the TD decreased dramatically during the first eight days. It slowly increased in the following days until reaching levels comparable to those in the MD by around day 60 (Figure 8.2). The pH also sharply decreased in the first 10 days and then increased until reaching 7.63 ± 0.12, which was significantly higher than the MD (7.52 ± 0.05). The CH_4/CO_2 ratio decreased during the first eight days, but it reached levels comparable to the MD after two weeks. This stage was also characterized by the significant increase in dCOD, COD, and VFA levels in the TD (Figures 8.3 and 8.4).

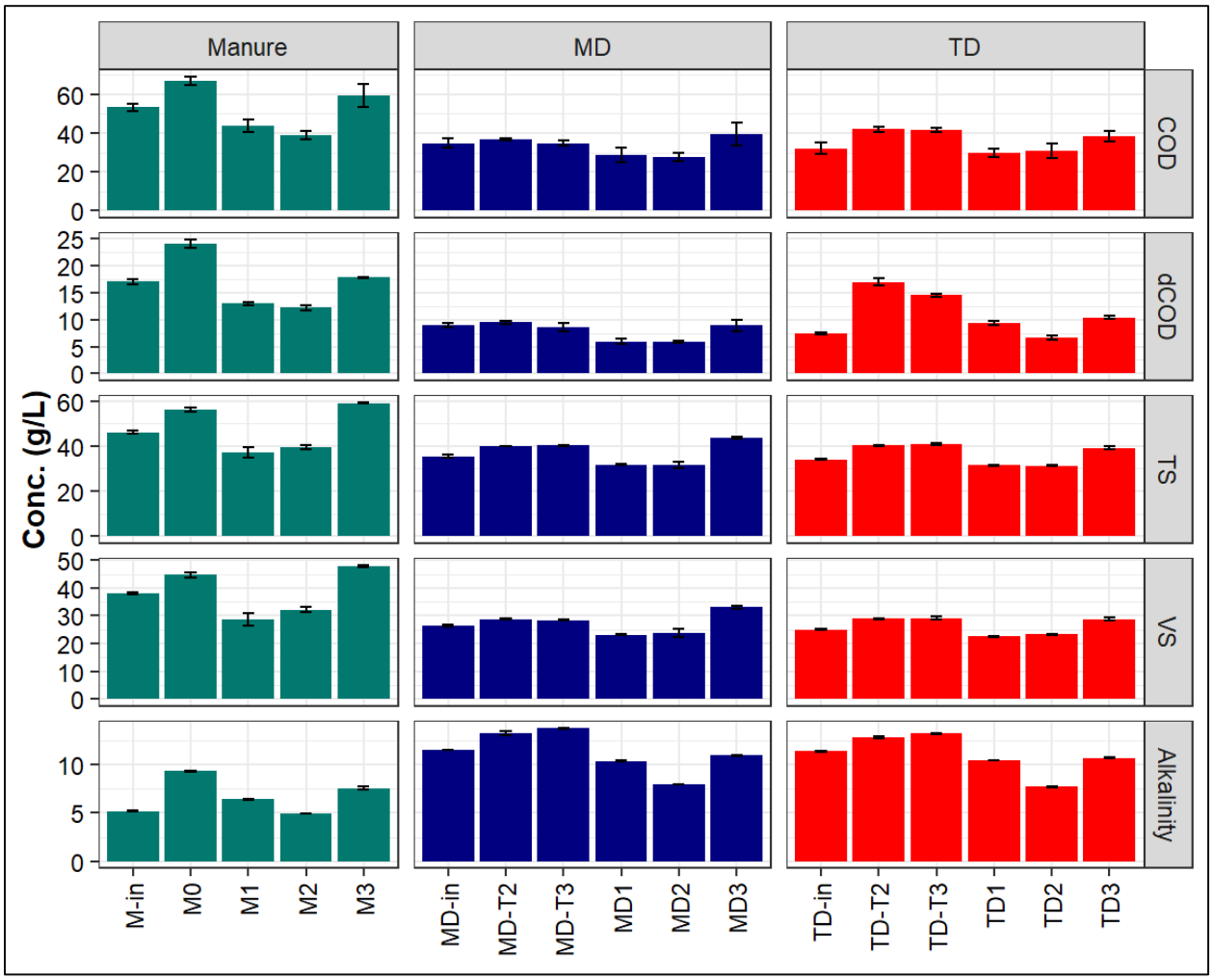

Figure 8.3 Manure and digestates physicochemical properties. Bars represents standard deviations.

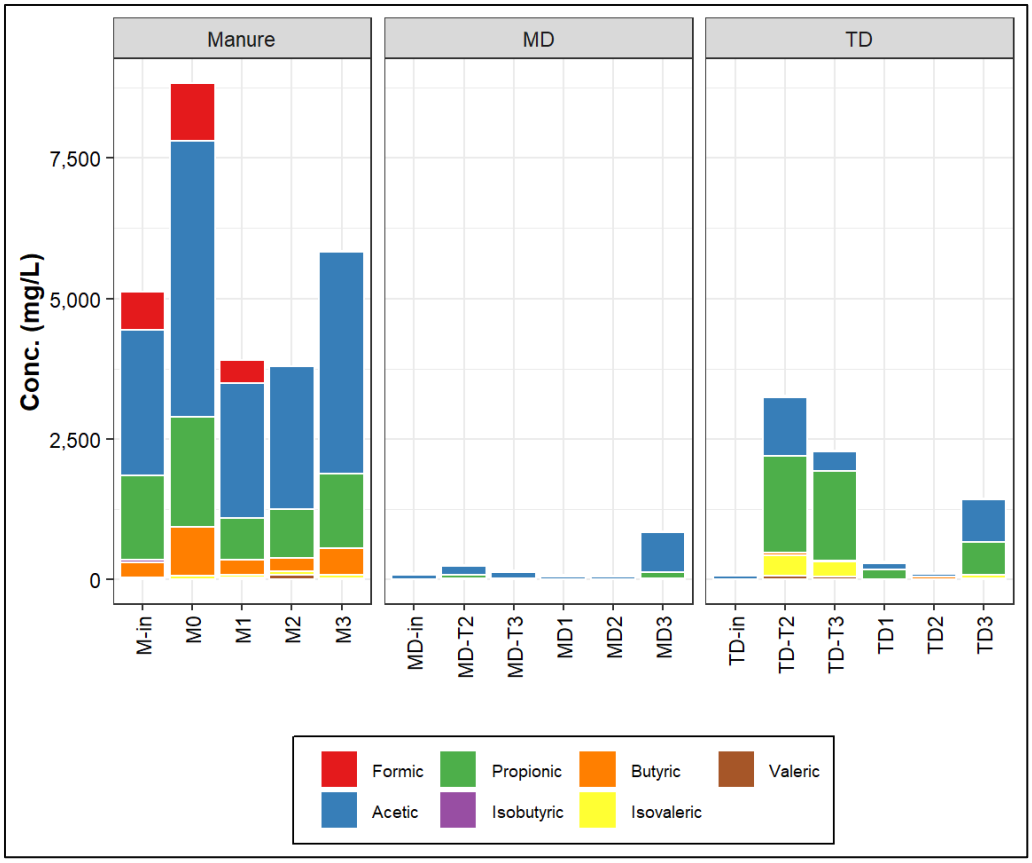

Figure 8.4 VFA profiles of manures and digestates.

The steady state of the TD was achieved after 60 days of the temperature change. After this time, the biogas production of the TD (258 ± 69 mL/g-VS) was significantly lower than the MD (285 ± 66 ml/g-VS). In contrast, the pH and CH_4/CO_2 ratio were significantly higher in the TD (pH = 7.64 ± 0.06, CH_4/CO_2 ratio = 2.1 ± 0.37) compared to those in the MD (pH = 7.44 ± 0.06, CH_4/CO_2 ratio = 1.95 ± 0.22). The physicochemical properties of the MD and TD digestates were similar and significantly different than those in manure (Figure 8.3). The VS removal was 27% for MD and 31.2% for TD, while the COD removal was 33% and 30% for MD and TD, respectively. In terms of VFAs, the MD and TD had similarly low levels (total VFAs < 500 mg/L) at the thermophilic steady state (Figure 8.4). In general, the TD was more sensitive to small disturbances (e.g., small temperature changes), which was reflected in the difference in biogas production rates,

as previous studies have reported (Labatut et al. 2014). However, an overall steady state was achieved and maintained during the thermophilic period of the study.

8.5.2. Effect of MAD and TAD on resistomes

8.5.2.1. Effects on ARGs

A total of 100 different ARGs were detected in the fresh manure samples encoding resistance to ten different antibiotics, including aminoglycosides (21), macrolide-lincosamide-streptogramin (*mls*, 19), tetracyclines (18), beta-lactams (9), diaminopyrimidine (4), phenicol (4), sulfonamides (2), glycopeptides (1), mupirocin (1), peptides (1) and others classified as multidrug (14). These ARGs encoded five different mechanisms of resistance, including antibiotic inactivation (42), target protection (16), efflux pumps (15), antibiotic target alteration (15), and antibiotic target replacement (6). However, it is worth mentioning that the number of different ARGs in individual manure batches ranged from 47-58 (M0 = 48; M1 = 47; M2 = 53; M3 = 58). A table with all different ARGs found in individual manures and digestates is shown in the appendices (Table F8.1 in Appendix F).

During the start-up stage, when both the MD and TD were operating at mesophilic temperatures, the number of distinct ARGs in the two digesters was similar, with 35 in the MD and 39 in the TD. The total levels of ARGs, as shown in Figures 8.5 and 8.6, were also comparable (366 rpkm for MD and 351 rpkm for TD), suggesting that both digesters had analogous resistome profiles prior to the temperature adjustment. In the initial eight days of the transition stage, there was a significant decrease in the total ARG levels in the TD. For the remainder of the transition stage, the total ARG levels in the TD tended to be both higher and more variable (378 ± 114 rpkm) compared to the more consistent levels in the MD (301 ± 37.5 rpkm). Given that shifts in microbial communities have been identified as primary drivers for changes in ARGs (Cheng et al. 2019; Lu

et al. 2021; Zhang et al. 2017), it is plausible that the variations in ARG levels during the transition stage were a consequence of the transitional shifts in microbial communities within the TD.

During the steady state period, both mesophilic and thermophilic AD exhibited a reduction in ARG richness, with the number of distinct ARGs generally being lower in the TD digestates. Specifically, in the MD, a total of 51 unique ARGs were identified across the samples (MD-1 had 34; MD-2 had 37; MD-3 had 31). These ARGs conferred resistance to six different antibiotic families, encompassing aminoglycosides (14), beta-lactams (2), mls (12), tetracyclines (15), glycopeptides (2), and an additional six ARGs that encoded resistance to multiple drugs. Notably, no ARGs associated with sulfonamides were detected in the MD samples. The mechanisms encoded in the MD ARGs included antibiotic inactivation (21), target protection (14), target alteration (10), and efflux pump (6).

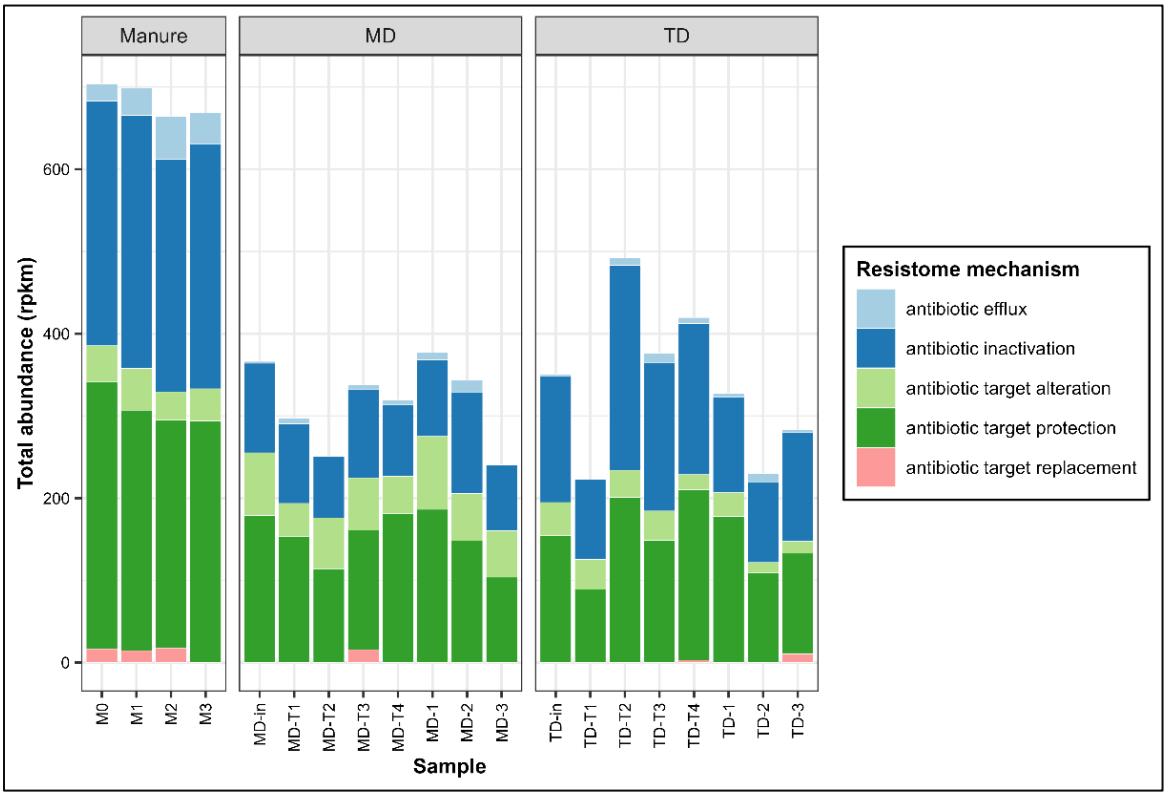

Figure 8.5 Total abundance of ARG mechanisms in manure and MD and TD digestates.

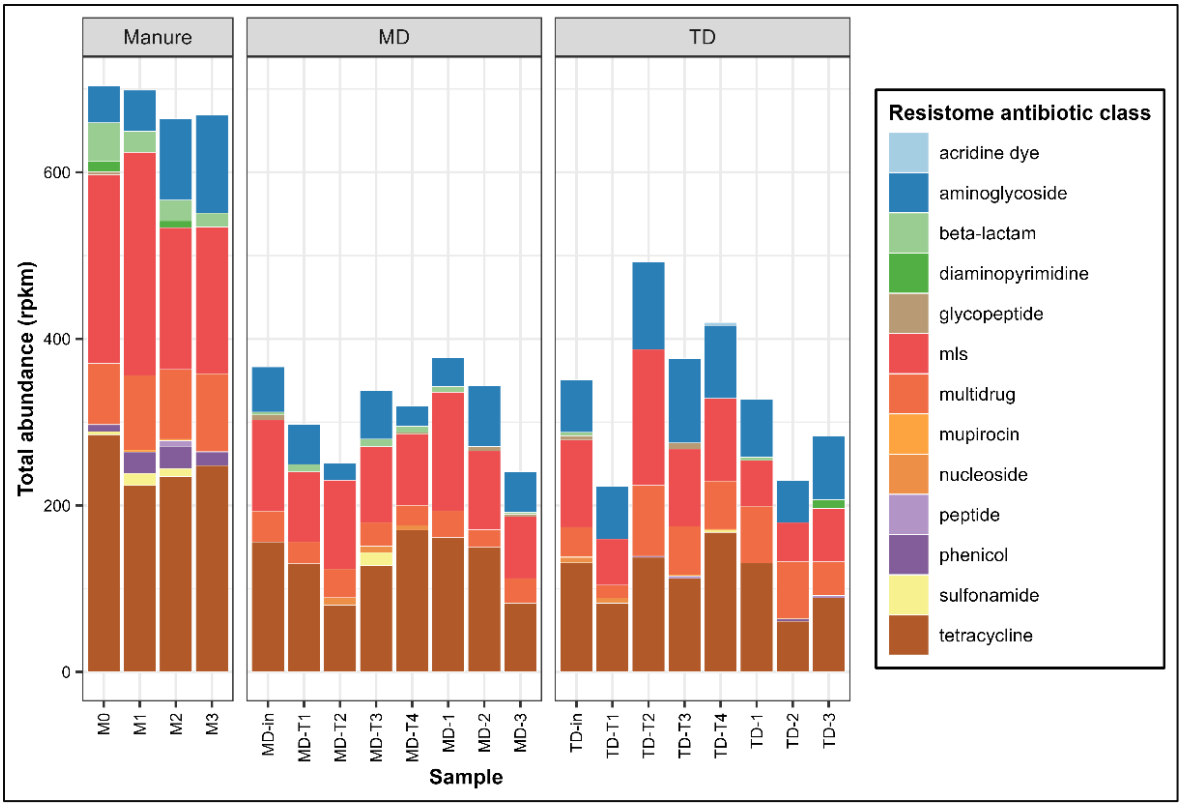

Figure 8.6 Total abundance of ARG antibiotic class in manures and MD and TD digestates. ARGs encoding resistance to more than one antibiotic were classified as multidrug. MLS stands for macrolide-lincosamide-streptogramin.

On the other hand, only 41 different ARGs were detected in TD digestates (TD-1 = 23; TD-2 = 25; TD-3 = 24), encoding resistance to eight different antibiotic families, including tetracyclines (11), MLS (9), multidrug (9), aminoglycosides (5), beta-lactams (2), diaminopyrimidine (2), mupirocin (1), peptide (1), phenicol (1) and nine more encoding resistance to multidrug. The ARG mechanisms included antibiotic inactivation (13), target protection (11), target alteration (8), efflux pumps (7), and target replacement (2).

Despite the observed reduction in ARGs during both MAD and TAD processes, 26 distinct ARGs initially detected in fresh manures continued to persist in both TD and MD digesters. These ARG encoding resistance to various antibiotics, including tetracyclines (*tetM, tetO, tetQ, tetS, tetT, tetW, tetB(P), tet44, tet(W/N/W), tet(Z)*), mls *(ErmB, lnuA, lnuB, lnuC, lnuG, LnuP, mefB*),

aminoglycosides (*ANT(6)-Ia, aad(6), ANT(9)-Ia, APH(6)-Id, APH(3')-IIIa*), and multidrug (*rpoB2, mel, lsaE, rpoB*). Consistent with these findings, prior research has identified the presence of these and related ARGs in digested cattle and dairy manure (Sun et al. 2016; Tian et al. 2016), suggesting that microbiomes in MAD and TAD are likely carrying these ARGs.

At the steady state stage, both MAD and TAD significantly decreased the total levels of ARGs found in fresh manures, with reductions of 53% (320 ± 71 rpkm) and 59% (280 ± 49 rpkm) respectively, from an initial level of 677 ± 19 rpkm (Figures 8.5 and 8.6). Although the total levels of ARGs tended to be lower in the TD, this difference was not statistically significant (p-value = 0.364). The analysis of the ARG mechanisms indicated that MAD and TAD significantly reduced the average levels of efflux pumps by 79% and 83% respectively, and antibiotic target protection by 49% and 54% respectively. Additionally, MAD also significantly reduced ARGs encoding antibiotic inactivation mechanisms by 67%. On the other hand, TAD exhibited significantly lower levels of target alteration ARGs (19 ± 9 rpkm) when compared to fresh manures (42 ± 7 rpkm) and MAD (61 ± 16 rpkm). The differential reduction rates of these ARG categories can likely be attributed to the unique microbial communities present in MD and TD, a topic elaborated upon in subsequent sections.

In general, the results indicated that TAD was able to reduce the ARG richness (number of different ARGs) to a greater extent, although the remaining total ARG levels were similar to those in MAD. The PCoA (Figure 8.7A) further accentuated this observation, with MD and TD digestates clustering closely together, indicating similar resistome profiles. This aligned with the results of the meta-analysis (Chapter 4) and other prior studies (Zou et al. 2020) that indicated that TAD does not necessarily outperform MAD in reducing total ARG levels in bovine manures. Intriguingly, some studies have found TAD to be superior to MAD in reducing overall ARG levels

in pig and bovine manure as well as municipal waste-activated sludge(Tian et al. 2016; Wen et al. 2021; Yang et al. 2020b; Zhang et al. 2015, 2021a). The reduction in ARGs is often associated with a decrease in microbial diversity. Distinct conditions in certain thermophilic studies, such as variations in nutrient and carbon availability, might have resulted in less diverse microbial communities. For instance, in one study where a thermophilic digester treating pig manure exhibited higher microbial diversity compared to its mesophilic counterpart, the ARG reduction rates were found to be comparable (Huang et al. 2019). Another potential reason for the varying results across studies could be the experimental setup. Many of these investigations were conducted as short-term batch experiments, typically lasting less than 60 days. Therefore, it is possible that the observed microbiomes and resistomes might not have fully captured the dynamics of a digester in continuous operation.

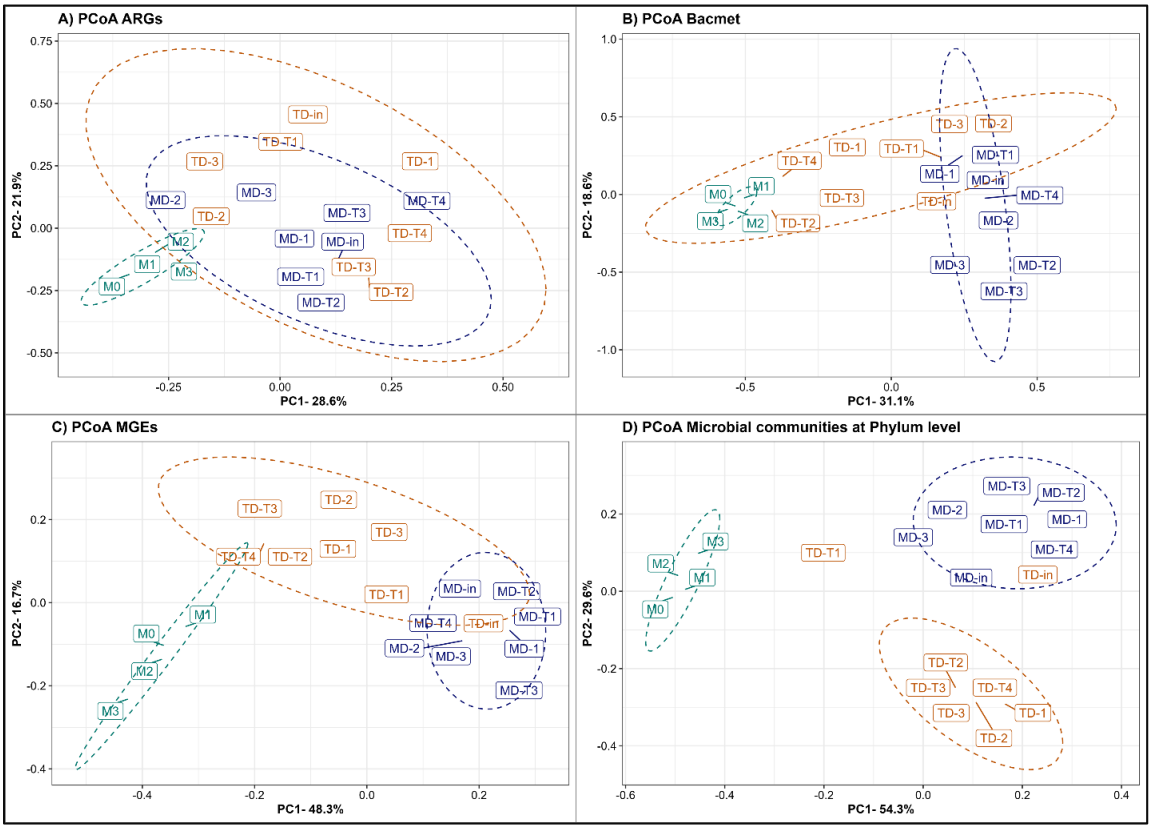

Figure 8.7 Principal Coordinates analyses (PCoA). Resistomes (A), BacMet genes (B), mobilomes (C), and microbiomes (D).

8.5.2.2. Effects on BacMet genes

Figure 8.8 illustrates the levels of BacMet resistance genes across various samples. In the different manures, a total of 17 distinct BacMet genes were identified. These genes cause resistance to heavy metals (10), quaternary ammonium compounds (QACs, 1), and multi-compounds (6). In contrast, MD and TD digestates contained only 14 and eight different BacMet genes, respectively. Overall, fresh manures exhibited significantly higher total levels of these genes compared to MD and TD digestates. Heavy metal resistance genes predominated in fresh manures, MD, and TD, though multi-compound resistance genes also played a significant role in steady MD digestates. The list of the different genes detected in individual samples can be found in Table F8.2 in appendix F.

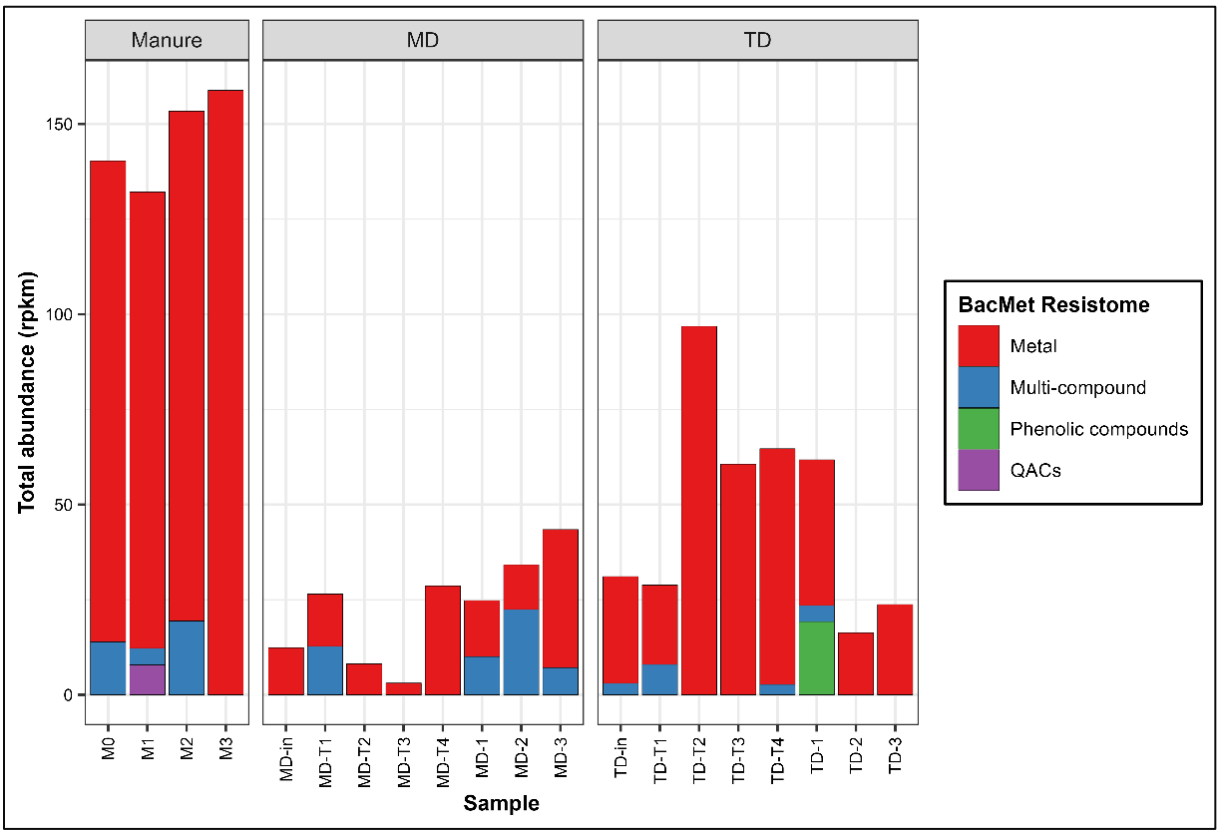

Figure 8.8 Total abundance of BacMet categories in manures and MD and TD digestates.

The *tcrA* and *tcrB* genes, which encode resistance to copper (Cu), remained in steady state MD and TD digestates suggesting that Cu resistance may persist in mesophilic and thermophilic digested manures, as other studies have reported (Agga et al. 2020). The use of copper sulfate solutions for foot bathing is common in dairy farms (Cook 2017). In fact, acidified copper sulfate is used on a regular basis in the farm that provided the manure for this study. Thus, it is possible that this caused a positive selective pressure for copper resistance genes, and this remained in the digesters. Overall, under steady-state conditions, both MAD and TAD significantly reduced the total levels of metal resistance genes in manures by 85% and 81%, respectively. There was no significant difference observed between the levels of BacMet genes in MAD and TAD digestates. This observation is further supported by the PCoA, where MD and steady TD samples clustered closely on the ordination plot, as shown in Figure 8.7B.

During the transition stage, the total BacMet levels in TD were twice as high as the ones of the initial stage, which was likely attributed to the rapid changes in the microbial communities caused by the increase in temperature. The PCoA (Figure 8.7B) showed that transition TD samples were closer to fresh manures than TD or MD digestates. This suggests that the transitional microbial population in TD contained microbial groups that harbored heavy metal resistance genes similar to those in fresh manure. However, these groups appeared to decrease once a steady state was reached. Notably, multi-compound resistance genes for heavy metals (e.g., mercury), aromatics (e.g., toluene, xylene), and quaternary ammonium compounds persisted in the steady-state MD digestates but were absent in TD. This pattern indicates that TAD might be more effective than MAD in reducing this type of resistance. While the exact reason for this remains undetermined, it's possible that the reduced levels of these genes in TD are linked to the decreased

presence of Bacilli species (see section 8.5.4), which have been shown to have the potential to degrade aromatic compounds (Kong et al. 2022).

8.5.3. Effects of MAD and TAD on mobilomes

A total of 237 MGE-related genes were detected in fresh manures, including replication/recombination/repair (77), integration/excision (66), transfer (44), phage (30), and stability/transfer/defense (29). However, the number of different MGEs in each batch of manure ranged from 115-155 genes. A list with all MGEs detected in this study can be found in Table F8.3 in Appendix F. Interestingly, the number of different MGEs increased to 143 during the transition stage of the TD. Similarly, the total MGE abundance increased by around 90% of the levels seen at the mesophilic stage. The increase in MGEs during this stage was likely the results of the microbial shifts caused by the instability of the processes. However, it is worth mentioning that despite this increment in MGE diversity, the total MGE levels in TD were still significantly lower than the fresh manure by around 50%, as seen in Figure 8.9.

At the steady stage, 108 MGEs were detected in MD digestates and only 96 in TD, suggesting both processes were able to reduce the richness of these elements. Yet, 59 of the MGEs detected in manure, mainly replication/recombination/repair (27) and integration/excision (17), remained in the MD and TD digestates. At steady-state, MD and TD significantly reduced the MGE levels present in fresh manures (Figure 8.9). Specifically, MD achieved a 73% reduction, whereas the TD achieved 65% reduction. The total MGE levels in MD and TD were not significantly different (p-value = 0.139), although they tended to be slightly higher in TD.

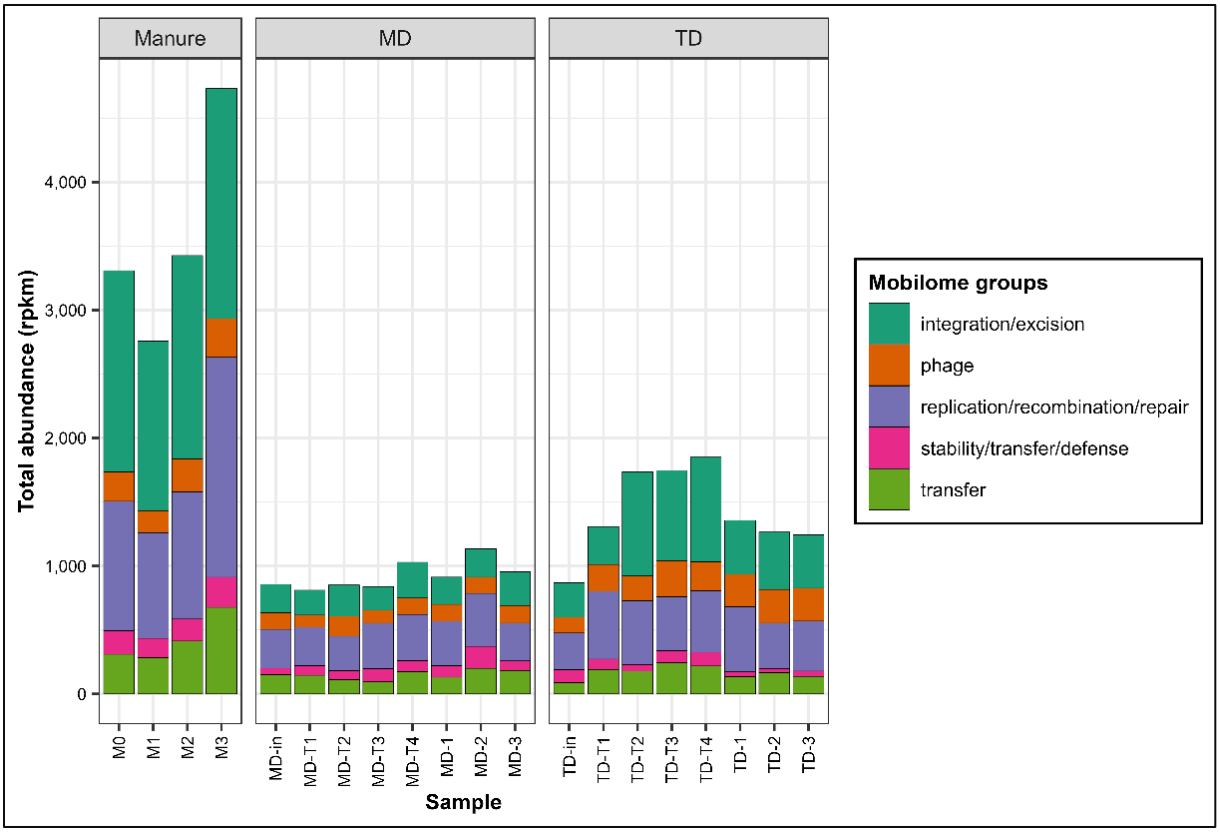

Figure 8.9 Total abundance of MGE-related genes in manures and MD and TD digestates.

However, despite the similar MGE reduction rates, the PCoA suggested different steady state mobilome profiles in MD and TD samples as they formed separate clusters in the ordination plot (Figure 8.7C). The analysis of the changes in the different MGE categories revealed distinctive patterns. Specifically, MD significantly reduced integration/excision by 85%, phage by 48%, replication/recombination/repair by 71%, and transfer by 65%. Conversely, TD significantly reduced stability/transfer/defense by 81% and transfer by 65%. Notably, the levels of phage-related MGEs were significantly higher in TD digestates, registering at 258 rpkm, compared to MD's 126 rpkm. This suggests a propensity of the thermophilic consortia to retain and accumulate these elements. Overall, the results indicated that, regardless of the temperature, AD could reduce the diversity and total abundance of MGEs in fresh cattle manures. This confirmed that digested

manure could have a lower potential risk of spreading antimicrobial resistance via horizontal gene transfer, as discussed in Chapters 4, 5, 6, and 7 (Flores-Orozco et al. 2023a, 2022, 2023b).

8.5.4. Microbial communities in manures and MD and TD digestates

The microbial communities of fresh manures and the MD and TD digestates at the phylum and genera levels are shown in Figures 8.10 and 8.11, respectively. The microbiomes in fresh manures, MD, and TD were substantially different, as seen in the ordination plot derived from the PCoA (Figure 8.7D). Bacillota and Actinomycetota emerged as the predominant phyla, accounting for 55.7% and 29%, respectively. The dominant genera in fresh manures were *Jeotgalibaca* (13.6%), *Corynebacterium* (13%), *Bifidobacterium* (12.4%), *Staphylococcus* (5.5%) and *Lactococcus* (5.3%). Overall, while there were some variations in the microbial communities of fresh manures, they were relatively constant across all fresh manure samples.

The microbial communities in the MD remained consistent throughout the study and were characterized by higher levels of the phyla Bacteroidota (31.7%), Euryarchaeota (30.8%), Chloroflexota (4.5%), and Synergistota (1.0%). The abundance of the phylum Bacillota saw a substantial reduction after MAD, accounting for only 22.4% of the microbiome. The dominant genera in the MD microbiome were *Methanosarcina* (29.7%), *Petrimonas* (29.2%), *Jeotgalibaca* (4.6%), *Brevefilum* (4.5%), and *Romboutsia* (2.8%) (Figure 8.11). Overall, the microbial communities of the MD resembled those from healthy mesophilic anaerobic digesters treating bovine manures (Khafipour et al. 2020).

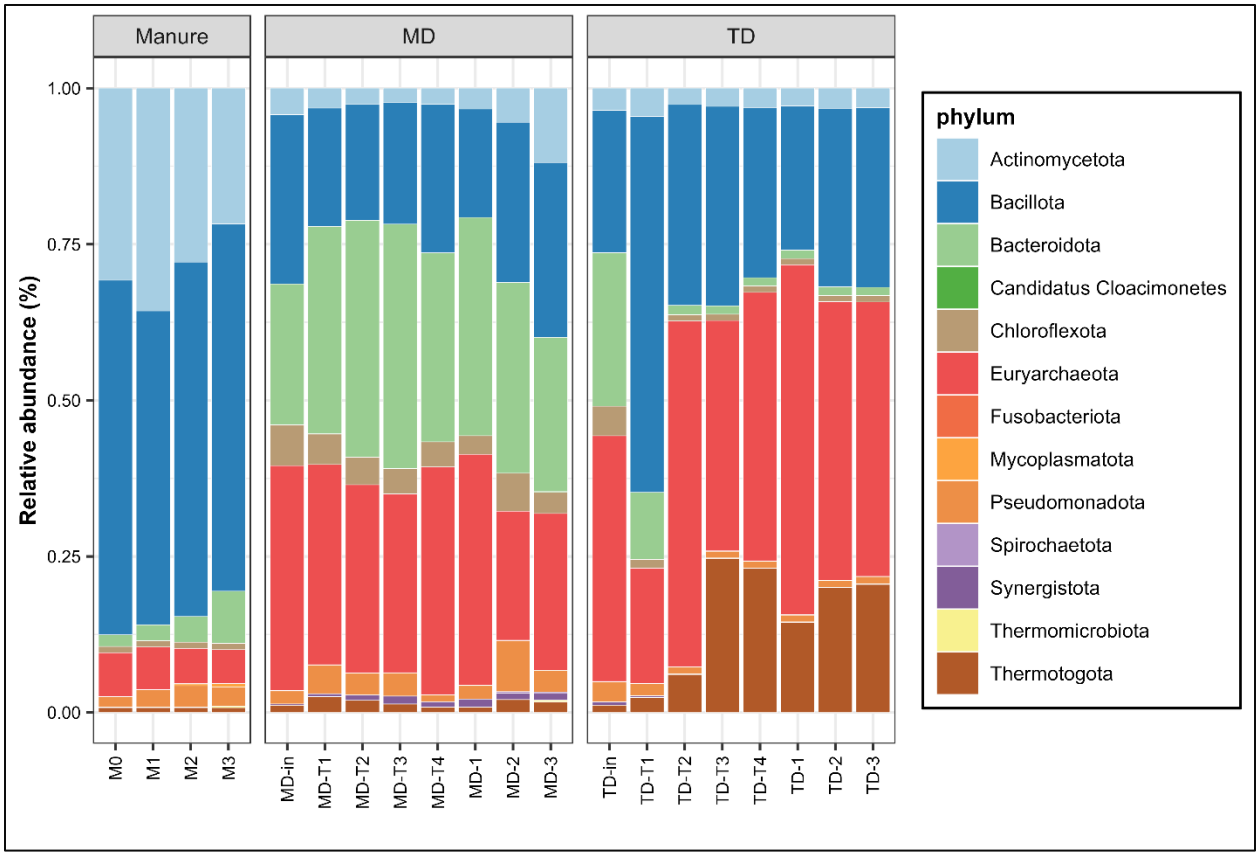

Figure 8.10 Microbiome structures at Phylum level in manures and MAD and TD digestates.

On the other hand, the microbial communities within the TD experienced more pronounced shifts across the different stages. In the mesophilic phase (TD-in), the TD microbiome mirrored that of the MD, with Euryarchaeota (39.3%), Bacteroidota (24.5%), and Bacillota (22.8%) as the dominant phyla. As the transition stage began with the temperature increase, there was a noticeable rise in the relative abundance of Thermotogota (i.e., thermophilic species) from 1.1% to 14.1% and Bacillota from 22.8% to 38%. This increase came at the decline of phyla such as Pseudomonadota (-50.8%), Chloroflexota (-76.8%), Synergistota (-82.4%), and Bacteroidota (-85%). The microbial composition during the thermophilic steady state also diverged from the transition phase. Notably, there was an upsurge in phyla like Thermotogota (+30%), Euryarchaeota (+25.5%), and Thermomicrobiota (+11.6%), while Bacillota (-29.2%), Bacteroidota (-63.7%), and

Synergistota (-75.4%) saw significant reductions. Yet, dominant genera such as *Methanosarcina*, *Acetivibrio*, *Defluviitoga*, *Methanothermobacter*, *Thermoclostridium*, and *Corynebacterium* remained consistent in both the transition and steady stages of the TD microbiomes (Figure 8.11). Overall, the TD microbial communities adapted to the temperature shift, eventually stabilizing into a distinct microbiome.

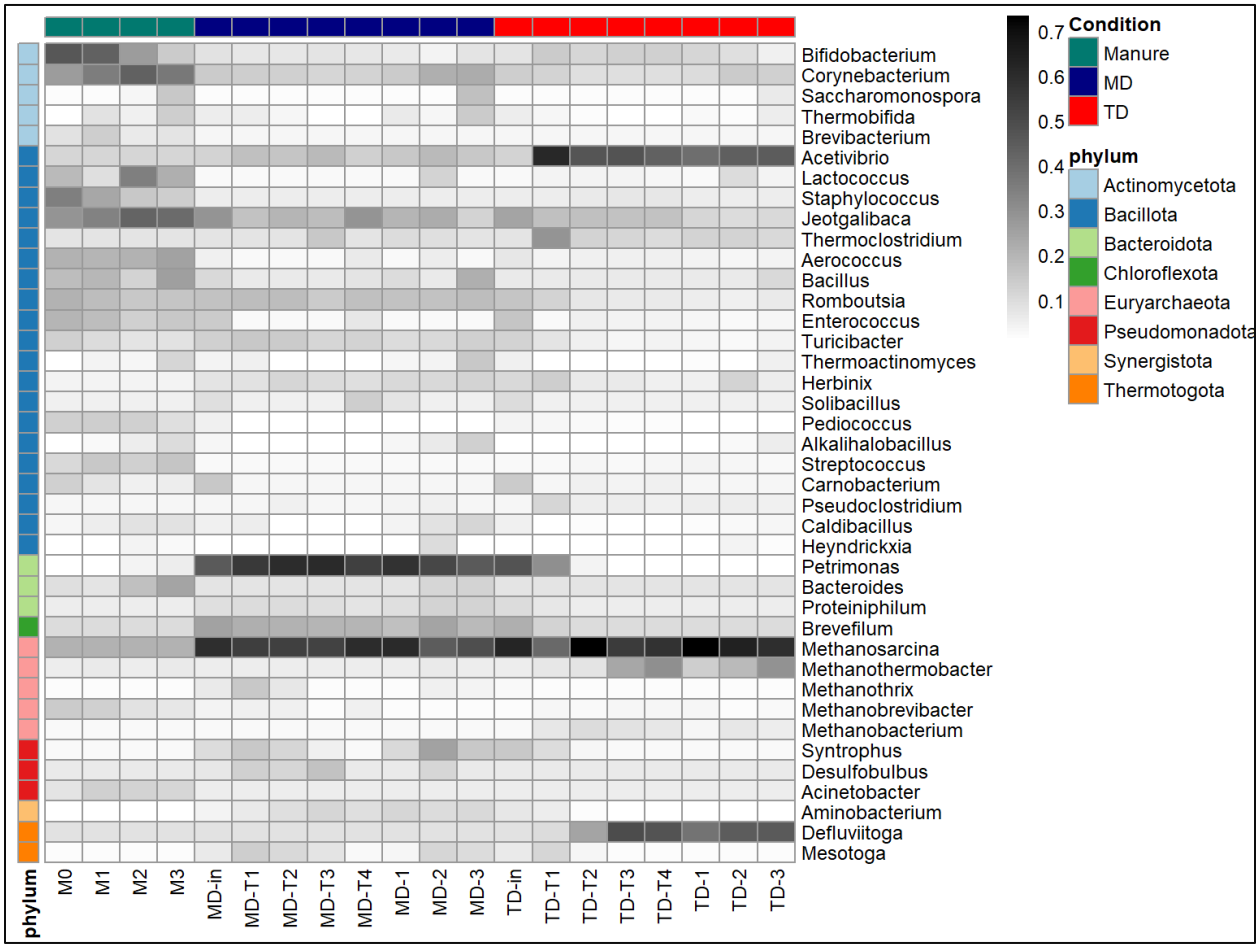

Figure 8.11 Relative abundance of top-40 microbial genera. Shades represents the squared root of the relative abundance.

The distribution of aerobic, anaerobic, and facultative microorganisms varied notably between fresh manure and the MD and TD digestates, as shown in Figure F8.1 in Appendix 8. Fresh manure exhibited significantly higher levels of aerobic and facultative species, while its

anaerobic microbial content was notably lower compared to the MD and TD digestates. This observation aligns with the understanding that manure's exposure to air likely promotes the proliferation of aerobic communities. In contrast, the TD microbiomes saw a significantly increased presence of anaerobic species, accounting for 91.9%, in comparison to MD's 84.3%. While TD microbiomes also displayed a trend towards reduced levels of facultative microorganisms (3.2%) relative to MD (5.4%), this variation was not statistically significant.

The Shannon, Simpson, and Chao diversity indices were consistently higher in manure samples compared to those in MD and TD, as seen in Figures 8.12 and 8.13. This suggested that the microbial communities in fresh manures were richer and more even than those in digestates. The lower microbial diversity in the digesters was expected since the controlled anaerobic environment promotes the establishment of well-defined microbial communities involved in the AD process. Notably, while the microbial diversity appeared comparable between MD and TD in the initial and transition phases, the last samples from the steady stage revealed a marked decrease in microbial diversity in TD compared to MD. This trend is anticipated in TD, as elevated temperatures inherently favor the growth of specific microbial groups, particularly thermophiles. Overall, the diversity indices also indicated stable microbial populations in the MD and TD, validating the stability of the processes.

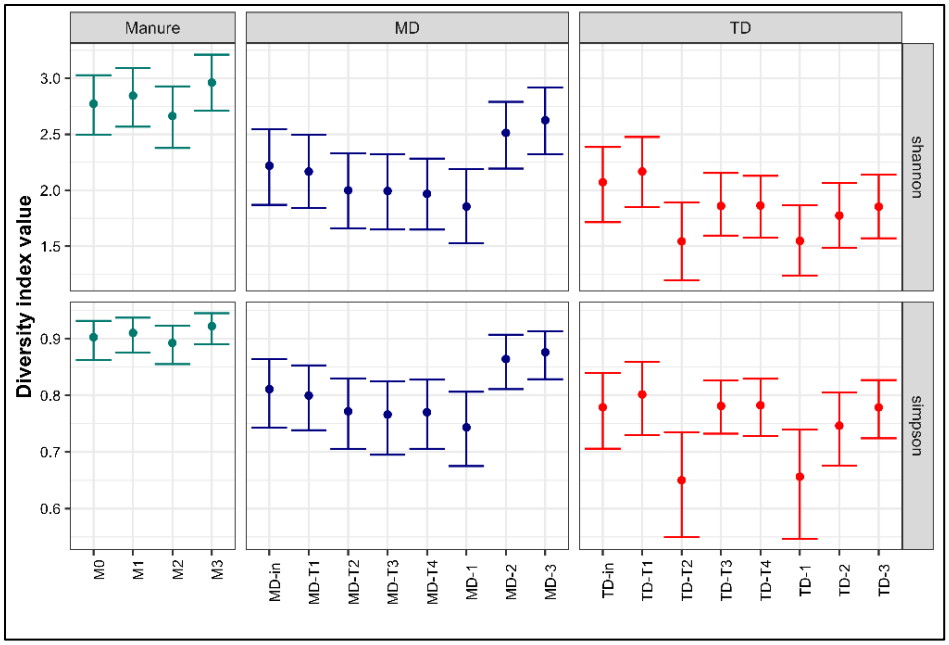

Figure 8.12 Shannon and Simpson diversity indices (at genus level). Bars represent the 95%-confidence intervals.

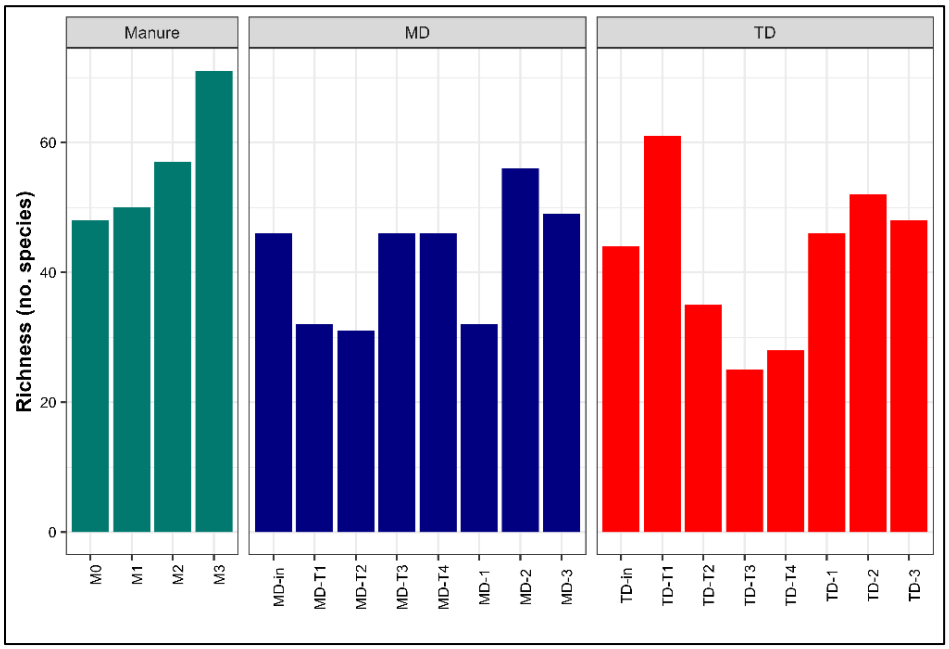

Figure 8.13 Chao diversity index at genus level.

8.5.5. Relationships between microbial dynamics, resistomes, and mobilomes

8.5.5.1. Correlations between the changes resistomes, mobilomes, and microbiomes

Mantel tests were used to the relationship between resistomes, mobilomes, and microbiomes across various taxonomic levels. Significant correlations between microbial communities at the phylum ($r = 0.39$), order ($r = 0.40$), genus ($r = 0.40$), and species ($r = 0.62$) levels and the shifts in resistome profiles. These observations are consistent with the insights presented in Chapter 7 (Flores-Orozco et al. 2023b) and with prior research that identified notable correlations between alterations in microbial communities and the behavior of various ARGs during AD (Lu et al. 2020; Zhang et al. 2019a). Interestingly, when microbial communities were categorized based on their respiratory type (e.g., aerobic, anaerobic, facultative), significant correlations with resistome profiles were still evident. Pearson's product-moment correlation indicated that facultative microorganisms had the strongest significant and positive correlation ($R = 0.88$) with the total levels of ARGs followed by aerobic species ($R = 0.78$), while anaerobic species negatively correlated with ARGs ($R = -0.86$).

The MGE profiles were also significantly correlated with the microbial communities at phylum ($r = 0.77$), order ($r = 0.75$), genus ($r = 0.77$), and species ($r = 0.26$) levels. Changes in the abundance of aerobic, anaerobic, and fermentative species were also significantly associated with changes in MGE. For instance, facultative ($R = 0.87$) and aerobic ($R = 0.81$) microorganisms displayed positive correlations with MGEs, while anaerobic species showed a negative correlation ($R = -0.86$) with overall MGE levels. Mantel tests ($r = 0.24$) and Pearson's correlations ($R = 0.87$) revealed a significant correlation between resistomes and mobilomes. Furthermore, the results also indicated that MGE categories such as integration/excision, replication/recombination/repair, and stability/transfer/defense were significantly correlated with efflux pumps, inactivation, and target

protection ARGs. Phage-related MGEs were only significantly correlated with ARG encoding inactivation mechanisms. These results represent valuable insights into the potential pathways and mechanisms for the transmission of certain AMR markers.

Overall, the results confirmed that facultative microorganisms are associated with ARGs and MGEs and that they could be one of the main groups involved in the dissemination of antimicrobial resistance in manure-related environments. It is worth noting that previous studies have suggested that facultative consortia play a substantial role in the dissemination of AMR in municipal wastewater (Hembach et al. 2019). Therefore, the reduction of facultative bacteria stands as a promising alternative to reduce the risk of the spread of AMR.

8.5.5.2. Co-occurrence of ARG, MGEs, and microbial groups

8.5.5.2.1. Analysis of co-occurrence

A probabilistic model of co-occurrence (Veech 2013) combined with Spearman correlations ($r > 0.5$, alpha = 0.05) was used to determine microbial groups potentially carrying ARGs and MGEs. This approach allows for the detection of patterns of co-occurrence and correlations that are less likely to occur by chance, reducing the risk of false positive results. The results indicated that 35 microbial genera co-occurred and had positive significant correlations with both ARGs and MGEs (Figures 8.14 and 8.15). They belonged to eight phyla, including Bacillota (21), Actinomycetota (5), Pseudomonadota (3), Bacteroidota (2), Euryarchaeota (1), Chloroflexota (1), Synergistota (1), Thermotogota (1). Also, 24 of these genera were Gram-positive, and only 10 were Gram-negative (one was an Archaea). Moreover, 17 were facultative anaerobes or aerotolerant, 12 anaerobic, and only six were aerobic. The microbial genera significantly associated with ARGs and MGEs can be found in Tables F8.4 and F8.5 in Appendix F.

Genera within the phylum Bacillota were predominantly linked to the different ARG mechanisms. Specifically, 25 Bacillota genera were correlated with antibiotic efflux pump (i.e., *cmx, efrB, floR, tet(K)*) ARGs, five with inactivation (i.e., *CfxA2*, *lnuA*, *SAT-4*), eight with target alteration (i.e., *ileS*, *ugd*, *cfr(D)*, *Erm47*, *ErmF*), nine with target protection (i.e., *tetO*, *tet44*, *poxtA*, *tetS*, *tetB(P)*), and five with target replacement (*sul1*). Genera from the Actinomycetota were also significantly associated with all different ARG mechanisms. Pseudomonadota genera were correlated with ARGs for all types of mechanisms except antibiotic target replacement. Notably, microbial groups present in MD and TD, such as Bacteroidota (i.e., *Petrimonas* and *Proteiniphilum*), Chloroflexota (i.e., *Brevefilum*), Euryarchaeota (i.e., *Methanothrix*), Synergistota (i.e., *Aminobacterium*), and Thermotogota (i.e., *Mesotoga*) were associated with target alteration ARGs (*Erm47, ErmF*).

Genes encoding resistance to heavy metals were mainly correlated with Bacillota genera, including *Ruminococcus*, *Staphylococcus*, *Streptococcus*, and *Enterococcus*. On the other hand, *Jeotgalicoccus*, *Amylolactobacillus*, *Flaviflexus*, *Ligilactobacillus*, *Staphylococcus*, *Brevibacterium*, *Erysipelothrix*, *Paeniclostridium*, and *Acinetobacter* were the main genera correlated with ARGs encoding resistance to a variety of antibiotics, including beta-lactams, tetracyclines, sulfonamides, macrolides, fluoroquinolones, MLS, multidrug and even heavy metals.

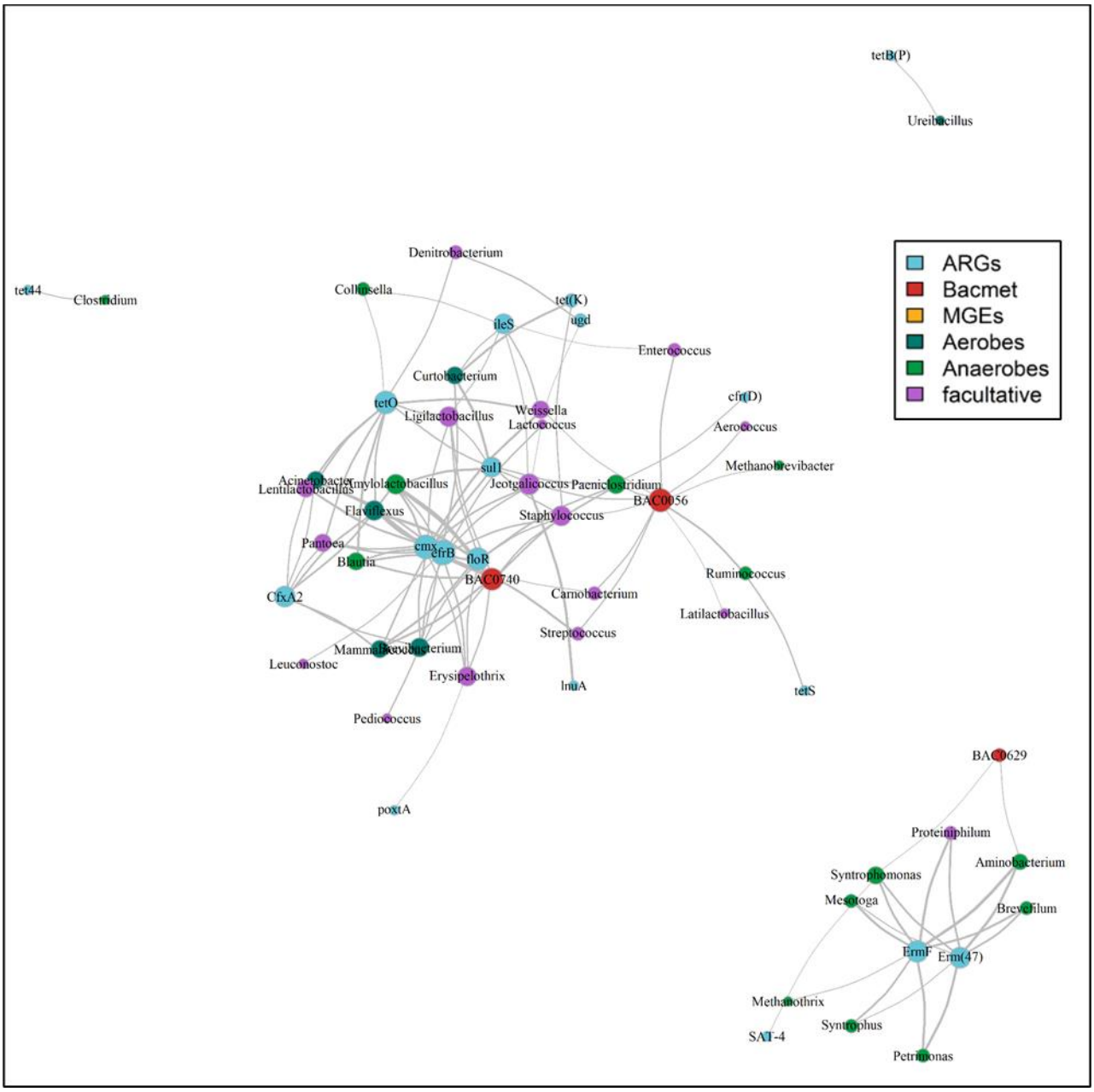

Figure 8.14 Network of co-occurrence of ARGs, BacMet, and microbial genera. The width of the edges is proportional to the correlation coefficient.

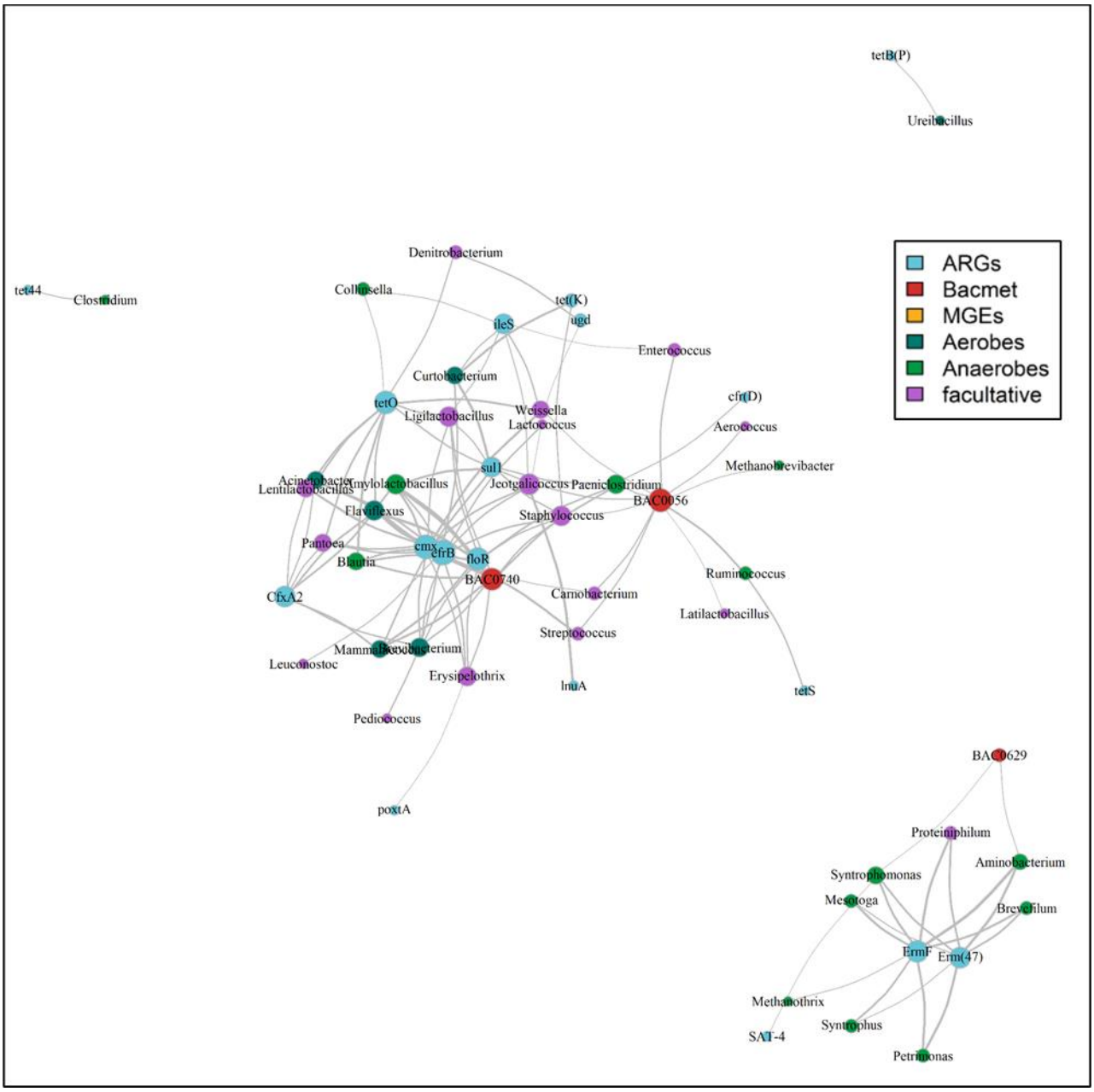

Figure 8.15 Network of co-occurrence of MGEs and microbial genera. The width of the edges is proportional to the correlation coefficient.

Following the intricate relationships between specific microbial taxa and resistance mechanisms, Bacillota genera also emerged as the primary group linked with various MGE categories. Specifically, 29 genera had significant associations with 59 distinct MGEs. Of these, 27 were categorized under replication/recombination/repair, 16 fell under integration/excision, 10

were related to transfer, five were phage-related genes, and four pertained to stability/transfer/defense. Other notable phyla with a significant number of genera associated with MGEs included Actinomycetota, represented by genera such as *Brevibacterium*, *Collinsella*, *Curtobacterium*, *Denitrobacterium*, and *Flaviflexus*, and Bacteroidota, with genera like *Parabacteroides*, *Petrimonas*, and *Proteiniphilum*. These genera collectively were linked to 30 different MGE-related genes.

Overall, these results suggested microbial taxa within the phyla Bacillota and Actinomycetota, as the main groups potentially harboring ARGs and MGEs. Many of these microbial taxa are known to include species considered pathogenic (e.g., *Staphylococcus, Erysipelothrix, Streptococcus, Enterococcus*) and are typically found in animal manures. An environment with a high abundance of MGEs and these microbial groups could create optimal conditions for the spread of AMR to clinically significant bacteria. However, as demonstrated in the study, both MAD and TAD processes effectively reduce the abundance of ARGs, MGEs, and their potential carriers. This suggests that digested manure may pose a reduced risk for the dissemination of AMR markers.

8.5.5.2.2. Co-occurrence of ARGs and MGEs in co-assembled contigs

In order to further explore the co-occurrence of ARGs and MGEs in microbial species, co-assembled contigs with more than 4,000 bp of steady-state samples were analyzed. One contig containing ARGs was identified in manure, one in MAD, and one in TAD samples (Figure 8.16). This analysis revealed the presence of *ANT(6)-Ia* and *lsaE*, in a contig belonging to *Staphylococcus aureus* (Bacillota) from manure samples. Interestingly, the Serine recombinase *pinR* (MGE) was found in this contig between the two ARGs. Serine recombinases are enzymes that are involved in the process of DNA recombination, which allows for the exchange of genetic material between

different organisms (Durrant et al. 2022). Interestingly, *ANT(6)-Ia* and *tetW* were located in a TD contig near *mobC*, an auxiliary transfer protein that stimulates transfer efficiency (Godziszewska et al. 2014). Tetracycline ARGs (e.g., *tetW*) are commonly found in animal manures and digestates. Recently, one study reported the presence of a variety of *tet* ARGs in novel integrative and conjugative elements in the microbiomes of ruminants' guts and suggested that this type of ARG could be under positive selective pressure in these types of environments (Sabino et al. 2019). Thus, the presence of MGEs close to tetracycline ARGs could result in the mobilization of these genes and could explain why they are persistently found in digestates.

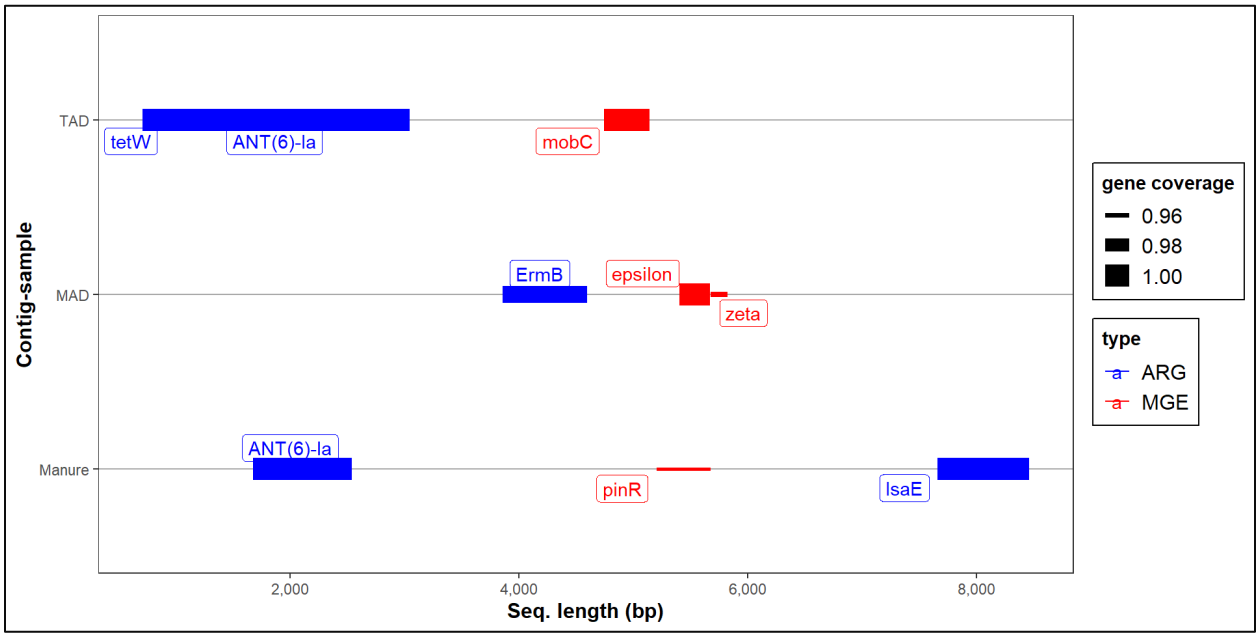

Figure 8.16 Co-occurrence of ARGs and MGEs in co-assembled contigs.

The ARG *ErmB* was detected in an MD contig nearby a type II toxin-antitoxin (TA) system composed of the zeta toxin and the epsilon antitoxin. The consistent presence of this TA near *Erm* genes in contigs from MAD microbiomes throughout various studies in this research strongly indicates that such ARGs, frequently observed in anaerobic digesters (Tran et al. 2021), as seen in Chapters 4 to 7, might persist and proliferate due to their proximity to TA systems. Although it

was challenging to pinpoint the exact microbial group carrying this contig, co-occurrence analyses suggested it's likely associated with microbial groups characteristic of mesophilic anaerobic digestion, such as *Petrimonas*, *Proteiniphilum*, *Brevefilum*, *Aminobacterium*, and *Mesotoga*. Further research is essential to understand and delineate the potential impacts of these systems on the selection and co-selection of ARGs in similar environments.

8.5.6. Microbial dynamics likely driving changes in resistomes and mobilomes

Prior research, including the worked described in Chapter 6 (Flores-Orozco et al. 2023b), has indicated that microbial dynamics significantly influence the fate and evolution of ARGs and MGEs in AD and other manure treatments (Cheng et al. 2019; Lu et al. 2021; Zhang et al. 2017). In some instances, microbial dynamics seem to have a greater impact than the presence of antimicrobials themselves, as seen in Chapter 4 and Flores-Orozco et al. (2022). In this study, the differences in the microbial populations in fresh manures compared to those in MD and TD were strongly correlated with the changes in resistomes and mobilomes. Notably, under steady state conditions, the microbiomes of MAD and TAD exhibited lower microbial diversity indices than those of fresh manures (Figure 8.12). This trend was consistent with the decrease in ARGs and MGEs observed in Figures 8.5, 8.8, and 8.9, which aligns with previous findings that have linked a decline in microbial diversity to a reduction in ARGs (Tian et al. 2016; Wen et al. 2021; Zhang et al. 2021a). In this study, the decline of microbial diversity during MAD and TAD could be attributed to the establishment of the microbial communities required for the processes.

The PCoA analysis on microbial genera significantly associated with both ARGs and MGEs during the steady state stage (Figure 8.17), revealed distinct clustering patterns for manure, MD, and TD. Each formed separate clusters in the ordination plot, underscoring significant differences in their microbial groups and associated resistomes and mobilomes. This suggests that, while both

MD and TD treatments led to comparable reductions in ARGs and MGEs, their final resistome and mobilome profiles diverged. Notably, during the transition phase, the TD microbiome exhibited variability in ARG and MGE levels, as shown in Figures 8.6-8.8. This observation underscores the criticality of allowing microbial communities in AD processes to mature, especially when conducting resistome-focused studies.

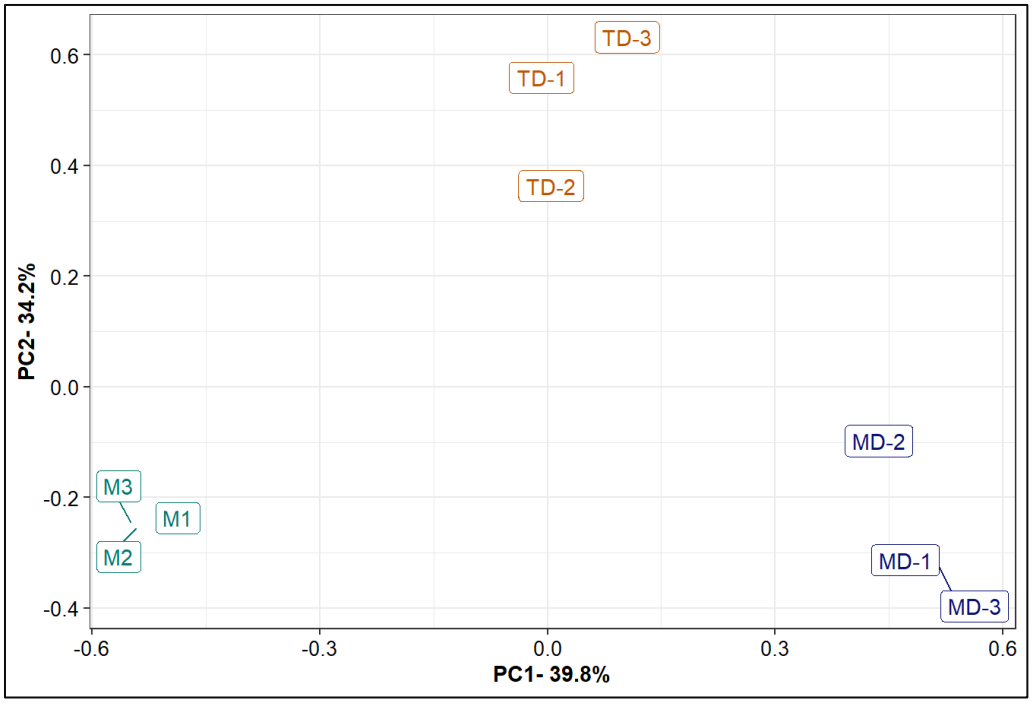

Figure 8.17 PCoA of the microbial genera significantly associated with ARGs and MGEs.

The analysis of the co-occurrence and correlation of microbial groups with ARGs and MGEs revealed that microbial groups from the phyla Bacillota and Actinomycetota, particularly Gram-positive facultative anaerobes, exhibited the highest degree of association with ARGs and MGEs. Notably, these microbial groups encompass genera known to contain pathogens, such as *Staphylococcus*, *Streptococcus*, *Enterococcus*, *Clostridium*, *Aerococcus*, *Lactococcus*, and other *lactobacilli*. Additionally, other genera, like *Acinetobacter* and *Pantoea* from the Phylum Pseudomonadota, were strongly associated with ARGs and MGEs. These groups of

microorganisms were more prevalent in fresh manures, and their decline in abundance correlated strongly with changes in ARGs and MGEs. Facultative pathogenic bacteria present in animal manures have been previously identified as carriers of various ARGs (Hembach et al. 2022), aligning with the findings of this study. Based on this, one of the main microbial shifts potentially driving the reduction of ARGs and MGEs during MAD and TAD was the decline of these facultative communities. By exploring ways to alter the microbial communities in bovine manure, especially promoting the decline of aerobic and facultative anaerobic groups from the phyla Bacillota, Actinomycetota, and Pseudomonadota, there is potential not only to reduce ARG levels but also to decrease the risk of HGT as MGE levels would also diminish.

Another interesting finding was that TAD outperformed MAD in reducing antibiotic inactivation ARGs, such as *ErmB*, *ErmF*, and *Erm47*. Surprisingly, the overall levels of these ARGs were significantly higher in the MD digestate compared to fresh manures, as depicted in Figure 8.7. The analyses of co-occurrence revealed that the abundance of the microbial genera associated with these ARGs (e.g., *Aminobacterium*, *Brevefilum*, *Mesotoga*, *Petrimonas*, *Proteiniphilum*, *Syntrophomonas*, *Syntrophus*, *Methanothrix*) was much higher in the MD digester (Figure 8.11). This suggests that the formation of microbiomes abundant in these groups likely contributed to the disparities in the abundance of antibiotic target alteration ARGs. Furthermore, the continued presence of *Erm* genes (related to antibiotic target alteration for MLS antibiotics) in MAD might be influenced by a nearby TA complex associated with these genes.

Overall, the results of this long-term study, combined with previous results, suggest that the levels of ARGs and MGEs could be significantly reduced by shaping the microbial communities via different manure treatments or management strategies. In particular, the reduction of facultative species, closely related to pathogenic bacteria, seemed to be one of the main drivers of

the decline of ARG and MGE diversity and abundance. These findings also confirmed that digested manure would have reduced risks of disseminating antibiotic resistance due to the lower levels of pathogenic species, MGEs, and ARGs. Finally, this study suggested no advantage of TAD over MAD in reducing ARG and MGE levels in fresh cattle manure when operating at similar HRTs, suggesting thermophilic temperatures may be unnecessary to mitigate the risk of antibiotic resistance dissemination. Future studies are encouraged to evaluate shorter HRTs and compare their performance.

8.6. Conclusion

This study revealed that both MAD and TAD of cattle manure significantly reduced ARGs and MGEs. Interestingly, TAD did not offer a superior advantage over MAD in diminishing these elements. Therefore, high temperatures may not be necessary to improve ARG reduction rates in AD process. The observed changes in ARG and MGE levels during MAD and TAD were largely attributed to shifts in microbial dynamics, especially the reduction in Gram-positive facultative species from phyla such as Bacillota and Actinomycetota. Furthermore, the persistence of specific ARGs in MAD, likely influenced by proximate TA complexes, warrants further exploration. In essence, the findings from this study provides valuable insights into formulating strategies to mitigate the risk of antibiotic resistance dissemination through manure application to land.

8.7. Acknowledgments

This research work was financially supported by the National Sciences and Engineering Research Council of Canada (NSERC) through the Discovery Grants program [RGPIN-2022-03670].

Chapter 9: Significance of the work and future work

9.1. Significance of the work

This multidisciplinary research made significant contributions to the scientific understanding of AMR in the context of anaerobic digestion of animal manure in different ways. Firstly, the systematic review of the available literature, in the form of a series of meta-analyses, revealed the existence of several gaps, including the variability of the results, the need for long-term AD studies and the limited application of metagenomics to evaluate resistomes and mobilomes. Additionally, the study confirmed the comparability between metagenomic results and qPCR-derived data. Identifying these gaps and validating the comparability of metagenomic results are valuable to promote further research in this field.

Secondly, this research provided quantitative insights into the expected ARG reduction rates during manure AD. Specifically, the research revealed that around 56% of the ARGs detected in manures could be reduced and that a decline of about 50% of the total ARG levels could be expected after AD. These quantifiable results are valuable for researchers, policymakers, and industry professionals, as they provide a clear benchmark against which the efficiency of various AD processes can be compared. Moreover, this study demonstrated TAD did not outperform MAD at reducing ARGs and MGEs from bovine manure. This finding has practical implications because thermophilic processes can be more expensive and challenging to maintain due to the need for higher temperatures and potential instabilities. The research suggests that such investments might not be essential for achieving optimal ARG and MGE reduction rates. This could lead to cost savings and more stable AD operations, making the technology more accessible and appealing to a broader range of users.

Thirdly, this research provided valuable insights into microbial groups potentially harboring ARGs and MGEs, and the molecular and microbial mechanisms driving the changes in resistomes. By pinpointing facultative groups within the phyla Bacillota and Actinomycetota as potential primary carriers of these AMR markers, the study provides a more detailed understanding of the microbial landscape of AMR in these types of environments. This knowledge can result in the development of more targeted interventions to manage and reduce AMR in animal manures. Moreover, the identification of ARGs typically found in anaerobic digesters in genetic cassettes containing toxin-antitoxin systems sheds light on the resilience and persistence mechanisms of these genes. This knowledge can pave the way for the development of innovative strategies aimed at blocking these systems. By targeting the mechanisms that allow these ARGs to survive, it may become possible to more effectively minimize the risk of dissemination of ARGs, especially those encoding resistance to commonly used antibiotics.

This research also provides insights into the current status of microbial community-based AMR in manures from local dairy farms, including one working with an antibiotic-free regime. By studying the resistomes in an antibiotic-free farm, this study provides evidence of the presence of selective forces other than antibiotics, possibly heavy metals-based solutions, directly or indirectly driving AMR in barns and animal manures. Moreover, by studying the effects of different treatments, this research provides valuable insights that can help decide which manure treatment to implement to minimize ARGs and MGEs. This is important as local policymakers and farmers can use this information to implement measures to reduce the risk of dissemination of AMR in farms and agricultural fields.

Lastly, this research successfully used novel tools designed to display hierarchical data (heat trees) for the analysis of resistome profiles in these complex microbiomes. Traditional methods of

data representation often do not capture all the complexities of hierarchical data. By pioneering the use of heat trees in this context, this study not only enhanced the clarity of data interpretation but also unveiled detailed patterns within the resistomes that might have been missed using traditional visualization approaches. This has also set a precedent for future studies, emphasizing the importance of innovative data visualization techniques in extracting meaningful insights from multifaceted datasets.

Overall, this research has made several important contributions to the scientific understanding of AMR in the context of anaerobic digestion of animal manures that could be extrapolated to other manure treatments. These contributions not only bridge existing gaps in the literature but also pave the way for future research, providing valuable insights that can be used to inform the development of more effective strategies to mitigate the dissemination of AMR associated with manure management, application, and disposal.

9.2. Future research

Future research from this thesis can go in several directions. From Chapter 4, metagenomic analyses that focus on the long-term evolution of resistomes and mobilomes in thermophilic anaerobic digesters treating pig manure could be valuable. Such studies could help elucidate the reasons for the higher ARG removal rates and clarify why thermophilic temperatures are not as effective with bovine manures. This could also provide insights into the microbial groups potentially harboring ARGs and the microbial shifts driving the changes in resistomes and mobilomes in animal manures.

One of the main limitations faced in this research was the difficulty in assembling long contigs and performing metagenomic analyses on them due to the sequencing depth. Future work studying resistomes and mobilomes in these complex environments should use deeper

metagenomic sequencing (e.g., tens of millions of read per sample) to generate more metagenomic data per sample. This would facilitate the assembly of longer contigs, which can then be annotated for ARGs and MGEs, allowing for a more detailed co-occurrence analysis. This approach would provide more genomic context to the ARGs identified in these types of microbiomes. For instance, longer contigs would enable a comprehensive study of the entire genetic cassette containing the TA systems and *Emr* genes (commonly found in manure anaerobic digesters), identifying the microbial groups potentially harboring them in AD microbiomes. Moreover, the isolation of resistance bacteria from these microbial communities would further strengthen such studies.

Lastly, future research should aim to establish a framework to evaluate, in a quantitative or at least semi-quantitative manner, the risk of ARG transmission. This would be based on the co-occurrence of ARGs, MGEs, pathogenic bacteria, and other related microbial groups. Such a framework would be instrumental in assessing the effectiveness of different treatments in reducing the potential risk of AMR dissemination in specific contexts.

References

Abbasi, T. and S.A. Abbasi. 2011. Formation and impact of granules in fostering clean energy production and wastewater treatment in upflow anaerobic sludge blanket (UASB) reactors. *Renewable and Sustainable Energy Reviews* 16: 1696–1708. https://doi.org/10.1016/j.rser.2011.11.017

de Abreu, V.A.C., J. Perdigão and S. Almeida. 2021. Metagenomic Approaches to Analyze Antimicrobial Resistance: An Overview. *Frontiers in Genetics* 11. https://doi.org/10.3389/fgene.2020.575592

Ackerman, J., E. Khafipour and N. Cicek. 2018. Sustainable re-use of dairy cow manure as bedding and compost: Nutrients and self-heating potential. *Canadian Biosystems Engineering / Le Genie Des Biosystems Au Canada* 60: 61–67. https://doi.org/10.7451/CBE.2018.60.6.1.

Afgan, E., D. Baker, B. Batut, M. Van Den Beek, D. Bouvier, M. Ech, J. Chilton, D. Clements, N. Coraor, B.A. Grüning, A. Guerler, J. Hillman-Jackson, S. Hiltemann, V. Jalili, H. Rasche, N. Soranzo, J. Goecks, J. Taylor, A. Nekrutenko and D. Blankenberg. 2018. The Galaxy platform for accessible, reproducible and collaborative biomedical analyses: 2018 update. *Nucleic Acids Research* 46(W1): W537–W544. https://doi.org/10.1093/nar/gky379

Agga, G.E., J. Kasumba, J.H. Loughrin and E.D. Conte. 2020. Anaerobic Digestion of Tetracycline Spiked Livestock Manure and Poultry Litter Increased the Abundances of Antibiotic and Heavy Metal Resistance Genes. *Frontiers in Microbiology* 11: 614424. https://doi.org/10.3389/fmicb.2020.614424

Alcock, B.P., W. Huynh, R. Chalil, K.W. Smith, A.R. Raphenya, M.A. Wlodarski, A. Edalatmand, A. Petkau, S.A. Syed, K.K. Tsang, S.J.C. Baker, M. Dave, M.C. McCarthy, K.M. Mukiri, J.A. Nasir, B. Golbon, H. Imtiaz, X. Jiang, K. Kaur, M. Kwong, Z.C. Liang, K.C. Niu, P.

Shan, J.Y.J. Yang, K.L. Gray, G.R. Hoad, B. Jia, T. Bhando, L.A. Carfrae, M.A. Farha, S. French, R. Gordzevich, K. Rachwalski, M.M. Tu, E. Bordeleau, D. Dooley, E. Griffiths, H.L. Zubyk, E.D. Brown, F. Maguire, R.G. Beiko, W.W.L. Hsiao, F.S.L. Brinkman, G. Van Domselaar and A.G. McArthur. 2023. CARD 2023: expanded curation, support for machine learning, and resistome prediction at the Comprehensive Antibiotic Resistance Database. *Nucleic Acids Research* 51(D1): D690–D699. https://doi.org/10.1093/nar/gkac920

Amani, T., M. Nosrati and T.R. Sreekrishnan. 2010. Anaerobic digestion from the viewpoint of microbiological, chemical, and operational aspects — a review. *Environmental Reviews* 18: 255–278. https://doi.org/10.1139/A10-011.

Aminov, R.I. 2010. A brief history of the antibiotic era: Lessons learned and challenges for the future. *Frontiers in Microbiology* 1(DEC): 134. https://doi.org/10.3389/fmicb.2010.00134

Anisimova, E.A. and D.R. Yarullina. 2019. Antibiotic Resistance of LACTOBACILLUS Strains. *Current Microbiology* 76(12): 1407–1416. https://doi.org/10.1007/s00284-019-01769-7.

APHA. 1995. *Standard Methods*. 19th edition. Maryland: American Public Health Association.

Arango-Argoty, G., G. Singh, L.S. Heath, A. Pruden, W. Xiao and L. Zhang. 2016. MetaStorm: a public resource for customizable metagenomics annotation. *PLoS ONE* 11(9). https://doi.org/10.1371/journal.pone.0162442

Bayr, S., M. Rantanen, P. Kaparaju and J. Rintala. 2012. Mesophilic and thermophilic anaerobic co-digestion of rendering plant and slaughterhouse wastes. *Bioresource Technology* 104: 28–36. https://doi.org/10.1016/j.biortech.2011.09.104

Bolger, A.M., M. Lohse and B. Usadel. 2014. Trimmomatic: A flexible trimmer for Illumina sequence data. *Bioinformatics* 30(15): 2114–2120. https://doi.org/10.1093/bioinformatics/btu170

Boulter, N., F.G. Suarez, S. Schibeci, T. Sunderland, O. Tolhurst, T. Hunter, G. Hodge, D. Handelsman, U. Simanainen, E. Hendriks and K. Duggan. 2016. A simple, accurate and universal method for quantification of PCR. *BMC Biotechnology* 16(1): 1–14. https://doi.org/10.1186/S12896-016-0256-Y/TABLES/1

Bragg, L. and G.W. Tyson. 2014. Metagenomics using next-generation sequencing. *Methods in Molecular Biology* 1096: 183–201. https://doi.org/10.1007/978-1-62703-712-9_15/TABLES/4

Brown, C.L., J. Mullet, F. Hindi, J.E. Stoll, S. Gupta, M. Choi, I. Keenum, P. Vikesland, A. Pruden and L. Zhang. 2021. mobileOG-db: a manually curated database of protein families mediating the life cycle of bacterial mobile genetic elements. *BioRxiv* 2021.08.27.457951. https://doi.org/10.1101/2021.08.27.457951

Buchfink, B., C. Xie and D.H. Huson. 2014. Fast and sensitive protein alignment using DIAMOND. *Nature Methods 2014 12:1* 12(1): 59–60. https://doi.org/10.1038/NMETH.3176

Burch, T.R., M.J. Sadowsky and T.M. Lapara. 2016. Modeling the fate of antibiotic resistance genes and class 1 integrons during thermophilic anaerobic digestion of municipal wastewater solids. *Applied Microbiology and Biotechnology* 100(3): 1437–1444. https://doi.org/10.1007/s00253-015-7043-x

Buta-Hubeny, M., E. Korzeniewska, J. Hubeny, W. Zieliński, D. Rolbiecki, M. Harnisz and Ł. Paukszto. 2022. Structure of the manure resistome and the associated mobilome for assessing the risk of antimicrobial resistance transmission to crops. *Science of The Total Environment* 808: 152144. https://doi.org/10.1016/j.scitotenv.2021.152144

Byrne-Bailey, K.G., W.H. Gaze, P. Kay, A.B.A. Boxall, P.M. Hawkey and E.M.H. Wellington. 2009. Prevalence of sulfonamide resistance genes in bacterial isolates from manured

agricultural soils and pig slurry in the United Kingdom. *Antimicrobial Agents and Chemotherapy* 53(2): 696–702. https://doi.org/10.1128/AAC.00652-07

CDC. 2019. Antibiotic resistance threats in the United States, 2019. Atlanta, Georgia. https://doi.org/10.15620/cdc:82532 (2023 /5/22)

Chen, B., R. He, K. Yuan, E. Chen, L. Lin, X. Chen, S. Sha, J. Zhong, L. Lin, L. Yang, Y. Yang, X. Wang, S. Zou and T. Luan. 2017. Polycyclic aromatic hydrocarbons (PAHs) enriching antibiotic resistance genes (ARGs) in the soils. *Environmental Pollution* 220: 1005–1013. https://doi.org/10.1016/j.envpol.2016.11.047

Chen, C., C.A. Pankow, M. Oh, L.S. Heath, L. Zhang, P. Du, K. Xia and A. Pruden. 2019. Effect of antibiotic use and composting on antibiotic resistance gene abundance and resistome risks of soils receiving manure-derived amendments. *Environment International* 128: 233–243. https://doi.org/10.1016/j.envint.2019.04.043

Cheng, D., Y. Feng, Y. Liu, J. Xue and Z. Li. 2019. Dynamics of oxytetracycline, sulfamerazine, and ciprofloxacin and related antibiotic resistance genes during swine manure composting. *Journal of Environmental Management* 230: 102–109. https://doi.org/10.1016/j.jenvman.2018.09.074

Cheng, J. 2010. *Biomass to Renewable Energy Processes*. CRC Press.

Conrad, R. 1999. Contribution of hydrogen to methane production and control of hydrogen concentrations in methanogenic soils and sediments. *FEMS Microbiology Ecology* 28(3): 193–202. https://doi.org/10.1111/j.1574-6941.1999.tb00575.x

Cook, N.B. 2017. A Review of the Design and Management of Footbaths for Dairy Cattle. *Veterinary Clinics of North America: Food Animal Practice* 33(2): 195–225. https://doi.org/10.1016/j.cvfa.2017.02.004

Crossman, L.C., V.C. Gould, J.M. Dow, G.S. Vernikos, A. Okazaki, M. Sebaihia, D. Saunders, C. Arrowsmith, T. Carver, N. Peters, E. Adlem, A. Kerhornou, A. Lord, L. Murphy, K. Seeger, R. Squares, S. Rutter, M.A. Quail, M.A. Rajandream, D. Harris, C. Churcher, S.D. Bentley, J. Parkhill, N.R. Thomson and M.B. Avison. 2008. The complete genome, comparative and functional analysis of Stenotrophomonas maltophilia reveals an organism heavily shielded by drug resistance determinants. *Genome Biology* 9(4): R74. https://doi.org/10.1186/gb-2008-9-4-r74

Cui, E., Y. Wu, Y. Zuo and H. Chen. 2016. Effect of different biochars on antibiotic resistance genes and bacterial community during chicken manure composting. *Bioresource Technology* 203: 11–17. https://doi.org/10.1016/j.biortech.2015.12.030

Czaplicki, L.M. and C.K. Gunsch. 2016. Reflection on Molecular Approaches Influencing State-of-the-Art Bioremediation Design: Culturing to Microbial Community Fingerprinting to Omics. *Journal of Environmental Engineering* 142(10): 03116002. https://doi.org/10.1061/(ASCE)EE.1943-7870.0001141.

Data M Intelligence. 2021. Veterinary Antibiotics Market, Size, Share, Growth, Trends, Insight and Industry Forecast, 2021-2028. https://www.datamintelligence.com/research-report/veterinary-antibiotics-market (2021 /11/2)

Davies, J. and D. Davies. 2010. Origins and Evolution of Antibiotic Resistance. *Microbiology and Molecular Biology Reviews* 74(3): 417–433. https://doi.org/10.1128/MMBR.00016-10

Demirel, B. 2014. Major Pathway of Methane Formation From Energy Crops in Agricultural Biogas Digesters. *Critical Reviews in Environmental Science and Technology* 44(3): 199–222. https://doi.org/10.1080/10643389.2012.710452.

DerSimonian, R. and N. Laird. 1986. Meta-analysis in clinical trials. *Controlled Clinical Trials* 7(3): 177–188. https://doi.org/10.1016/0197-2456(86)90046-2

DeSantis, T.Z., P. Hugenholtz, N. Larsen, M. Rojas, E.L. Brodie, K. Keller, T. Huber, D. Dalevi, P. Hu and G.L. Andersen. 2006. Greengenes, a chimera-checked 16S rRNA gene database and workbench compatible with ARB. *Applied and Environmental Microbiology* 72(7): 5069–5072. https://doi.org/10.1128/AEM.03006-05

Dionisio, F., I.C. Conceição, A.C.R. Marques, L. Fernandes and I. Gordo. 2005. The evolution of a conjugative plasmid and its ability to increase bacterial fitness. *Biology Letters* 1(2): 250–252. https://doi.org/10.1098/rsbl.2004.0275

Dridi, B., M.L. Fardeau, B. Ollivier, D. Raoult and M. Drancourt. 2011. The antimicrobial resistance pattern of cultured human methanogens reflects the unique phylogenetic position of archaea. *Journal of Antimicrobial Chemotherapy* 66(9): 2038–2044. https://doi.org/10.1093/jac/dkr251

Drula, E., M.L. Garron, S. Dogan, V. Lombard, B. Henrissat and N. Terrapon. 2022. The carbohydrate-active enzyme database: Functions and literature. *Nucleic Acids Research* 50(D1): D571–D577. https://doi.org/10.1093/nar/gkab1045

Duan, M., J. Gu, X. Wang, Y. Li, R. Zhang, T. Hu and B. Zhou. 2019. Factors that affect the occurrence and distribution of antibiotic resistance genes in soils from livestock and poultry farms. *Ecotoxicology and Environmental Safety* 180: 114–122. https://doi.org/10.1016/j.ecoenv.2019.05.005

Duriez, P. and E. Topp. 2007. Temporal dynamics and impact of manure storage on antibiotic resistance patterns and population structure of Escherichia coli isolates from a commercial

swine farm. *Applied and Environmental Microbiology* 73(17): 5486–5493. https://doi.org/10.1128/AEM.00218-07

Durrant, M.G., A. Fanton, J. Tycko, M. Hinks, S.S. Chandrasekaran, N.T. Perry, J. Schaepe, P.P. Du, P. Lotfy, M.C. Bassik, L. Bintu, A.S. Bhatt and P.D. Hsu. 2022. Systematic discovery of recombinases for efficient integration of large DNA sequences into the human genome. *Nature Biotechnology 2022* 1–12. https://doi.org/10.1038/s41587-022-01494-w

Egorov, A.M., M.M. Ulyashova and M.Y. Rubtsova. 2018. Bacterial Enzymes and Antibiotic Resistance. *Acta Naturae* 10(4): 33. https://doi.org/10.32607/20758251-2018-10-4-33-48

Fan, H., S. Wu, J. Woodley, G. Zhuang, Z. Bai, S. Xu, X. Wang and X. Zhuang. 2020. Effective removal of antibiotic resistance genes and potential links with archaeal communities during vacuum-type composting and positive-pressure composting. *Journal of Environmental Sciences (China)* 89: 277–286. https://doi.org/10.1016/j.jes.2019.09.006

Fanning, S., S. Proos, K. Jordan and S. Srikumar. 2017. *A review on the applications of next generation sequencing technologies as applied to food-related microbiome studies*. *Frontiers in Microbiology* SEP, Frontiers Media S.A., 21 September 2017. https://doi.org/10.3389/fmicb.2017.01829 (2020 /11/26)

FDA. 2018. 2018 Summary Report On Antimicrobials Sold or Distributed for Use in Food-Producing Animals. https://www.fda.gov/media/133411/download (2023 /6/1)

Flores-Orozco, D., D. Levin, A. Kumar, R. Sparling and N. Cicek. 2022. A meta-analysis reveals that operational parameters influence levels of antibiotic resistance genes during anaerobic digestion of animal manures. *Science of The Total Environment* 814: 152711. https://doi.org/10.1016/j.scitotenv.2021.152711

Flores-Orozco, D., D. Levin, A. Kumar, R. Sparling and N. Cicek. 2023a. Influence of three different manure treatments on antimicrobial resistance genes and mobile genetic elements. *Frontiers in Synthetic Biology* 1. https://doi.org/10.3389/fsybi.2023.1301879.

Flores-Orozco, D., R. Patidar, D. Levin, A. Kumar, R. Sparling and N. Cicek. 2023b. Metagenomic analyses reveal that mesophilic anaerobic digestion substantially reduces the abundance of antibiotic resistance genes and mobile genetic elements in dairy manures. *Environmental Technology & Innovation* 30: 103128. https://doi.org/10.1016/j.eti.2023.103128.

Flores-Orozco, D., R. Patidar, D.B. Levin, R. Sparling, A. Kumar and N. Çiçek. 2020a. Effect of mesophilic anaerobic digestion on the resistome profile of dairy manure. *Bioresource Technology* 315: 123889. https://doi.org/10.1016/j.biortech.2020.123889.

Flores-Orozco, D., R. Patidar, D.B. Levin, R. Sparling, A. Kumar and N. Çiçek. 2020b. Effect of ceftiofur on mesophilic anaerobic digestion of dairy manure and the reduction of the cephalosporin-resistance gene cmy-2. *Bioresource Technology* 301: 122729. https://doi.org/10.1016/j.biortech.2019.122729

Foster, Z.S.L., T.J. Sharpton and N.J. Grünwald. 2017. Metacoder: An R package for visualization and manipulation of community taxonomic diversity data. *PLoS Computational Biology* 13(2). https://doi.org/10.1371/journal.pcbi.1005404

Fraikin, N., F. Goormaghtigh and L. Van Melderen. 2020. Type II Toxin-Antitoxin Systems: Evolution and Revolutions. *Journal of Bacteriology* 202(7). https://doi.org/10.1128/JB.00763-19

Franco, B.E., M.A. Martínez, M.A. Sánchez Rodríguez and A.I. Wertheimer. 2009. The determinants of the antibiotic resistance process. *Infection and Drug Resistance* 2(1): 1–11. https://doi.org/10.2147/IDR.S4899

Frost, L.S., R. Leplae, A.O. Summers and A. Toussaint. 2005. Mobile genetic elements: the agents of open source evolution. *Nature Reviews Microbiology* 3(9): 722–732. https://doi.org/10.1038/nrmicro1235.

Godziszewska, J., A. Kulińska and G. Jagura-Burdzy. 2014. MobC of conjugative RA3 plasmid from IncU group autoregulates the expression of bicistronic mobC-nic operon and stimulates conjugative transfer. *BMC Microbiology* 14(1): 235. https://doi.org/10.1186/s12866-014-0235-1

Gou, M., H.W. Hu, Y.J. Zhang, J.T. Wang, H. Hayden, Y.Q. Tang and J.Z. He. 2018. Aerobic composting reduces antibiotic resistance genes in cattle manure and the resistome dissemination in agricultural soils. *Science of the Total Environment* 612: 1300–1310. https://doi.org/10.1016/j.scitotenv.2017.09.028

Goulas, A., D. Belhadi, A. Descamps, A. Andremont, P. Benoit, S. Courtois, C. Dagot, N. Grall, D. Makowski, S. Nazaret, S. Nélieu, D. Patureau, F. Petit, C. Roose-Amsaleg, M. Vittecoq, B. Livoreil and C. Laouénan. 2020. *How effective are strategies to control the dissemination of antibiotic resistance in the environment? A systematic review*. *Environmental Evidence* 1, 2020. https://doi.org/10.1186/s13750-020-0187-x (2020 /3/25)

Gurmessa, B., E.F. Pedretti, S. Cocco, V. Cardelli and G. Corti. 2020. Manure anaerobic digestion effects and the role of pre- and post-treatments on veterinary antibiotics and antibiotic resistance genes removal efficiency. *Science of the Total Environment* 721: 137532. https://doi.org/10.1016/j.scitotenv.2020.137532

Hamza, R.A., O.T. Iorhemen and J.H. Tay. 2016. Advances in biological systems for the treatment of high-strength wastewater. *Journal of Water Process Engineering* 10: 128–142. https://doi.org/10.1016/j.jwpe.2016.02.008

Harirchi, S., S. Wainaina, T. Sar, S.A. Nojoumi, M. Parchami, M. Parchami, S. Varjani, S.K. Khanal, J. Wong, M.K. Awasthi and M.J. Taherzadeh. 2022. Microbiological insights into anaerobic digestion for biogas, hydrogen or volatile fatty acids (VFAs): a review. *Bioengineered* 13(3): 6521–6557. https://doi.org/10.1080/21655979.2022.2035986

Harrer, M. and P. Cuijpers. 2019. Dmetar: Companion R Package For The Guide "Doing Meta-Analysis in R"R package version 0.0.9000, 2019. http://dmetar.protectlab.org/.

Harrison, E., J. Bonhotal, M. Schwarz Prepared and T. Fiesinger. 2008. Using Manure Solids as Bedding. https://ecommons.cornell.edu/handle/1813/44571 (2023 /4/26)

Haug, R.T. 1993. *The Practical Handbook of Compost Engineering*. The Practical Handbook of Compost Engineering. CRC Press. https://doi.org/10.1201/9780203736234

Hembach, N., J. Alexander, C. Hiller, A. Wieland and T. Schwartz. 2019. Dissemination prevention of antibiotic resistant and facultative pathogenic bacteria by ultrafiltration and ozone treatment at an urban wastewater treatment plant. *Scientific Reports* 9(1): 12843. https://doi.org/10.1038/s41598-019-49263-1

Hembach, N., G. Bierbaum, C. Schreiber and T. Schwartz. 2022. Facultative pathogenic bacteria and antibiotic resistance genes in swine livestock manure and clinical wastewater: A molecular biology comparison. *Environmental Pollution* 313: 120128. https://doi.org/10.1016/j.envpol.2022.120128

Heuer, H., H. Schmitt and K. Smalla. 2011. Antibiotic resistance gene spread due to manure application on agricultural fields. *Current Opinion in Microbiology* 14(3): 236–243. https://doi.org/10.1016/j.mib.2011.04.009

Hu, H.W., X.M. Han, X.Z. Shi, J.T. Wang, L.L. Han, D. Chen and J.Z. He. 2016a. Temporal changes of antibiotic-resistance genes and bacterial communities in two contrasting soils

treated with cattle manure. *FEMS Microbiology Ecology* 92(2): 1–13. https://doi.org/10.1093/femsec/fiv169.

Hu, Y., X. Yang, J. Li, N. Lv, F. Liu, J. Wu, I.Y.C. Lin, N. Wu, B.C. Weimer, G.F. Gao, Y. Liu and B. Zhu. 2016b. The bacterial mobile resistome transfer network connecting the animal and human microbiomes. *Applied and Environmental Microbiology* 82(22): 6672–6681. https://doi.org/10.1128/AEM.01802-16.

Huang, X., J. Zheng, S. Tian, C. Liu, L. Liu, L. Wei, H. Fan, T. Zhang, L. Wang, G. Zhu and K. Xu. 2019. Higher temperatures do not always achieve better antibiotic resistance gene removal in anaerobic digestion of swine manure. *Applied and Environmental Microbiology* 85(7): 2878–2896. https://doi.org/10.1128/AEM.02878-18

Jang, Y.N., O. Hwang, M.W. Jung, B.K. Ahn, H. Kim, G. Jo and Y.M. Yun. 2021. Comprehensive analysis of microbial dynamics linked with the reduction of odorous compounds in a full-scale swine manure pit recharge system with recirculation of aerobically treated liquid fertilizer. *Science of the Total Environment* 777. https://doi.org/10.1016/j.scitotenv.2021.146122

Jia, S., X.X. Zhang, Y. Miao, Y. Zhao, L. Ye, B. Li and T. Zhang. 2017. Fate of antibiotic resistance genes and their associations with bacterial community in livestock breeding wastewater and its receiving river water. *Water Research* 124: 259–268. https://doi.org/10.1016/j.watres.2017.07.061

Jjemba, P.K. 2002. The potential impact of veterinary and human therapeutic agents in manure and biosolids on plants grown on arable land: A review. *Agriculture, Ecosystems and Environment* 93: 267–278. https://doi.org/10.1016/S0167-8809(01)00350-4

Jordaan, E.M., D.B. Levin, R. Sparling, E. Khafipour and N. Çiçek. 2019. Microbial Population Change in Anaerobic Digestion during Copper Sulfate Inhibition and Recovery. *Transactions of the ASABE* 62(5): 1231–1241. https://doi.org/10.13031/trans.13462

Kasman, L.M. and L.D. Porter. 2022. Bacteriophages. *Brenner's Encyclopedia of Genetics: Second Edition* 280–283. https://doi.org/10.1016/B978-0-12-374984-0.00131-5

Kelleher Environmental. 2013. Canadian Biogas Study. https://biogasassociation.ca/images/uploads/documents/2014/biogas_study/Canadian_Biogas_Study_Technical_Document_Dec_2013.pdf (2019 /2/24)

Khafipour, A., E.M. Jordaan, D. Flores-Orozco, E. Khafipour, D.B. Levin, R. Sparling and N. Cicek. 2020. Response of Microbial Community to Induced Failure of Anaerobic Digesters Through Overloading With Propionic Acid Followed by Process Recovery. *Frontiers in Bioengineering and Biotechnology* 8. https://doi.org/10.3389/fbioe.2020.604838.

Khan, Z.A., M.F. Siddiqui and S. Park. 2019. Current and Emerging Methods of Antibiotic Susceptibility Testing. *Diagnostics 2019, Vol. 9, Page 49* 9(2): 49. https://doi.org/10.3390/DIAGNOSTICS9020049

Khanal, S.K., B. Giri, S. Nitayavardhana and V. Gadhamshetty. 2016. Anaerobic Bioreactors/Digesters: Design and Development. In *Current Developments in Biotechnology and Bioengineering*, 261–279. Elsevier. https://doi.org/10.1016/B978-0-444-63665-2.00010-2

Kim, B.R., J. Shin, R.B. Guevarra, J.H. Lee, D.W. Kim, K.H. Seol, J.H. Lee, H.B. Kim and R.E. Isaacson. 2017. Deciphering diversity indices for a better understanding of microbial communities. *Journal of Microbiology and Biotechnology* 27(12): 2089–2093. https://doi.org/10.4014/jmb.1709.09027

Knapp, G. and J. Hartung. 2003. Improved tests for a random effects meta-regression with a single covariate. *Statistics in Medicine* 22(17): 2693–2710. https://doi.org/10.1002/sim.1482

Komilis, D., R. Barrena, R.L. Grando, V. Vogiatzi, A. Sánchez and X. Font. 2017. *A state of the art literature review on anaerobic digestion of food waste: influential operating parameters on methane yield*. *Reviews in Environmental Science and Biotechnology* 2, pp. 347–360, 2017. https://doi.org/10.1007/s11157-017-9428-z (2018 /3/12)

Kong, X., R. Dong, T. King, F. Chen and H. Li. 2022. Biodegradation Potential of Bacillus sp. PAH-2 on PAHs for Oil-Contaminated Seawater. *Molecules* 27(3): 687. https://doi.org/10.3390/molecules27030687

Kraemer, S.A., A. Ramachandran and G.G. Perron. 2019. Antibiotic pollution in the environment: From microbial ecology to public policy. *Microorganisms* 7(6). https://doi.org/10.3390/microorganisms7060180

Kumar, M.S., E. V. Slud, K. Okrah, S.C. Hicks, S. Hannenhalli and H. Corrada Bravo. 2018. Analysis and correction of compositional bias in sparse sequencing count data. *BMC Genomics* 19(1): 799. https://doi.org/10.1186/s12864-018-5160-5

Kumar, R.R., J.T. Lee and J.Y. Cho. 2012. *Fate, occurrence, and toxicity of veterinary antibiotics in environment*. *Journal of the Korean Society for Applied Biological Chemistry*, pp. 701–709, 2012. https://doi.org/10.1007/s13765-012-2220-4 (2019 /2/26)

De la Rubia, M.A., V. Riau, F. Raposo and R. Borja. 2012. Thermophilic anaerobic digestion of sewage sludge: focus on the influence of the start-up. A review. *Critical Reviews in Biotechnology* 33(4): 448–460. https://doi.org/10.3109/07388551.2012.726962.

Labatut, R.A., L.T. Angenent and N.R. Scott. 2014. Conventional mesophilic vs. thermophilic anaerobic digestion: A trade-off between performance and stability? *Water Research* 53: 249–258. https://doi.org/10.1016/j.watres.2014.01.035

Lee, C.A. and A.D. Grossman. 2007. Identification of the Origin of Transfer (*oriT*) and DNA Relaxase Required for Conjugation of the Integrative and Conjugative Element ICE *Bs1* of *Bacillus subtilis*. *Journal of Bacteriology* 189(20): 7254–7261. https://doi.org/10.1128/JB.00932-07

Lee, J., J.H. Jeon, J. Shin, H.M. Jang, S. Kim, M.S. Song and Y.M. Kim. 2017. Quantitative and qualitative changes in antibiotic resistance genes after passing through treatment processes in municipal wastewater treatment plants. *Science of the Total Environment* 605–606: 906–914. https://doi.org/10.1016/j.scitotenv.2017.06.250

Leng, L., P. Yang, S. Singh, H. Zhuang, L. Xu, W.-H. Chen, J. Dolfing, D. Li, Y. Zhang, H. Zeng, W. Chu and P.-H. Lee. 2018. A review on the bioenergetics of anaerobic microbial metabolism close to the thermodynamic limits and its implications for digestion applications. *Bioresource Technology* 247: 1095–1106. https://doi.org/10.1016/j.biortech.2017.09.103

Li, D., X.-Y. Li, S. Schwarz, M. Yang, S.-M. Zhang, W. Hao and X.-D. Du. 2019. Tn6674 Is a Novel Enterococcal optrA-Carrying Multiresistance Transposon of the Tn554 Family. *Antimicrobial Agents and Chemotherapy* 63(9). https://doi.org/10.1128/AAC.00809-19

Li, D., C.-M. Liu, R. Luo, K. Sadakane and T.-W. Lam. 2015. MEGAHIT: an ultra-fast single-node solution for large and complex metagenomics assembly via succinct *de Bruijn* graph. *Bioinformatics* 31(10): 1674–1676. https://doi.org/10.1093/bioinformatics/btv033.

Li, M.M., P. Ray, K.F. Knowlton, A. Pruden, K. Xia, C. Teets and P. Du. 2020. Fate of pirlimycin and antibiotic resistance genes in dairy manure slurries in response to temperature and pH

adjustment. *Science of the Total Environment* 710. https://doi.org/10.1016/j.scitotenv.2019.136310

Li, X.-Z. and H. Nikaido. 2004. Efflux-Mediated Drug Resistance in Bacteria. *Drugs* 64(2): 159–204. https://doi.org/10.2165/00003495-200464020-00004

Li, X.Z. and H. Nikaido. 2009. Efflux-mediated drug resistance in bacteria: An update. *Drugs* 69(12): 1555–1623. https://doi.org/10.2165/11317030-000000000-00000

Lima, T., S. Domingues and G.J. Da Silva. 2020. Manure as a potential hotspot for antibiotic resistance dissemination by horizontal gene transfer events. *Veterinary Sciences* 7(3): 110. https://doi.org/10.3390/VETSCI7030110

Lindmark, J., E. Thorin, R.B. Fdhila and E. Dahlquist. 2014. Effects of mixing on the result of anaerobic digestion: Review. *Renewable and Sustainable Energy Reviews* 40: 1030–1047. https://doi.org/10.1016/j.rser.2014.07.182

Liu, Y., D. Cheng, J. Xue, L. Weaver, S.A. Wakelin, Y. Feng and Z. Li. 2020. Changes in microbial community structure during pig manure composting and its relationship to the fate of antibiotics and antibiotic resistance genes. *Journal of Hazardous Materials* 389. https://doi.org/10.1016/j.jhazmat.2020.122082

Lu, J., F.P. Breitwieser, P. Thielen and S.L. Salzberg. 2017. Bracken: Estimating species abundance in metagenomics data. *PeerJ Computer Science* 2017(1): e104. https://doi.org/10.7717/peerj-cs.104

Lu, T., J. Zhang, P. Li, P. Shen and Y. Wei. 2020. Enhancement of methane production and antibiotic resistance genes reduction by ferrous chloride during anaerobic digestion of swine manure. *Bioresource Technology* 298. https://doi.org/10.1016/j.biortech.2019.122519

Lu, Y., R. Sun, C. Zhang, S. Ding, M. Ying and S. Shan. 2021. In situ analysis of antibiotic resistance genes in anaerobically digested dairy manure and its subsequent disposal facilities. *Bioresource Technology* 333: 124988. https://doi.org/10.1016/j.biortech.2021.124988

Lyras, D., V. Adams, I. Lucet and J.I. Rood. 2004. The large resolvase TnpX is the only transposon-encoded protein required for transposition of the Tn4451/3 family of integrative mobilizable elements. *Molecular Microbiology* 51(6): 1787–1800. https://doi.org/10.1111/j.1365-2958.2003.03950.x

Ma, C., P.K. Lo, J. Xu, M. Li, Z. Jiang, G. Li, Q. Zhu, X. Li, S.Y. Leong and Q. Li. 2020. Molecular mechanisms underlying lignocellulose degradation and antibiotic resistance genes removal revealed via metagenomics analysis during different agricultural wastes composting. *Bioresource Technology* 314. https://doi.org/10.1016/j.biortech.2020.123731

Ma, J., J. Gu, X. Wang, H. Peng, Q. Wang, R. Zhang, T. Hu and J. Bao. 2019. Effects of nano-zerovalent iron on antibiotic resistance genes during the anaerobic digestion of cattle manure. *Bioresource Technology* 289. https://doi.org/10.1016/j.biortech.2019.121688

Ma, Y., C.A. Wilson, J.T. Novak, R. Riffat, S. Aynur, S. Murthy and A. Pruden. 2011. Effect of various sludge digestion conditions on sulfonamide, macrolide, and tetracycline resistance genes and class i integrons. *Environmental Science and Technology* 45(18): 7855–7861. https://doi.org/10.1021/es200827t

Madison, F., K. Kelling, L. Massie and L.W. Good. 1995. Guidelines for Applying Manure to Cropland and Pasture in Wisconsin.

Magidovich, H. and J. Eichler. 2009. Glycosyltransferases and oligosaccharyltransferases in Archaea: putative components of the N-glycosylation pathway in the third domain of life.

FEMS Microbiology Letters 300(1): 122–130. https://doi.org/10.1111/j.1574-6968.2009.01775.x

Mai, D.T., D.C. Stuckey and S. Oh. 2018. Effect of ciprofloxacin on methane production and anaerobic microbial community. *Bioresource Technology* 261: 240–248. https://doi.org/10.1016/j.biortech.2018.04.009

Mazel, D. 2006. Integrons: Agents of bacterial evolution. *Nature Reviews Microbiology* 4(8): 608–620. https://doi.org/10.1038/nrmicro1462

Mazzurco Miritana, V., G. Massini, A. Visca, P. Grenni, L. Patrolecco, F. Spataro, J. Rauseo, G.L. Garbini, A. Signorini, S. Rosa and A. Barra Caracciolo. 2020. Effects of Sulfamethoxazole on the Microbial Community Dynamics During the Anaerobic Digestion Process. *Frontiers in Microbiology* 11: 537783. https://doi.org/10.3389/fmicb.2020.537783

McKeown, R.M., D. Hughes, G. Collins, T. rè se Mahony, by C. Terry Hazen and S. Wuertz. 2011. Low-temperature anaerobic digestion for wastewater treatment. *Current Opinion in Biotechnology* 23: 444–451. https://doi.org/10.1016/j.copbio.2011.11.025

Milligan, E.G., J. Calarco, B.C. Davis, I.M. Keenum, K. Liguori, A. Pruden and V.J. Harwood. 2023. A Systematic Review of Culture-Based Methods for Monitoring Antibiotic-Resistant Acinetobacter, Aeromonas, and Pseudomonas as Environmentally Relevant Pathogens in Wastewater and Surface Water. *Current Environmental Health Reports* 10(2): 154–171. https://doi.org/10.1007/S40572-023-00393-9/FIGURES/4

Möller, K. and T. Müller. 2012. Effects of anaerobic digestion on digestate nutrient availability and crop growth: A review. *Engineering in Life Sciences* 12(3): 242–257. https://doi.org/10.1002/elsc.201100085

Mulder, I., J. Siemens, V. Sentek, W. Amelung, K. Smalla and S. Jechalke. 2018. *Quaternary ammonium compounds in soil: implications for antibiotic resistance development*. *Reviews in Environmental Science and Biotechnology* 1, pp. 159–185. Springer, 5 December 2018. https://doi.org/10.1007/s11157-017-9457-7 (2022 /4/21)

Munir, M. and I. Xagoraraki. 2011. Levels of Antibiotic Resistance Genes in Manure, Biosolids, and Fertilized Soil. *Journal of Environment Quality* 40(1): 248–255. https://doi.org/10.2134/jeq2010.0209

Murray, C.J., K.S. Ikuta, F. Sharara, L. Swetschinski, G. Robles Aguilar, A. Gray, C. Han, C. Bisignano, P. Rao, E. Wool, S.C. Johnson, A.J. Browne, M.G. Chipeta, F. Fell, S. Hackett, G. Haines-Woodhouse, B.H. Kashef Hamadani, E.A.P. Kumaran, B. McManigal, R. Agarwal, S. Akech, S. Albertson, J. Amuasi, J. Andrews, A. Aravkin, E. Ashley, F. Bailey, S. Baker, B. Basnyat, A. Bekker, R. Bender, A. Bethou, J. Bielicki, S. Boonkasidecha, J. Bukosia, C. Carvalheiro, C. Castañeda-Orjuela, V. Chansamouth, S. Chaurasia, S. Chiurchiù, F. Chowdhury, A.J. Cook, B. Cooper, T.R. Cressey, E. Criollo-Mora, M. Cunningham, S. Darboe, N.P.J. Day, M. De Luca, K. Dokova, A. Dramowski, S.J. Dunachie, T. Eckmanns, D. Eibach, A. Emami, N. Feasey, N. Fisher-Pearson, K. Forrest, D. Garrett, P. Gastmeier, A.Z. Giref, R.C. Greer, V. Gupta, S. Haller, A. Haselbeck, S.I. Hay, M. Holm, S. Hopkins, K.C. Iregbu, J. Jacobs, D. Jarovsky, F. Javanmardi, M. Khorana, N. Kissoon, E. Kobeissi, T. Kostyanev, F. Krapp, R. Krumkamp, A. Kumar, H.H. Kyu, C. Lim, D. Limmathurotsakul, M.J. Loftus, M. Lunn, J. Ma, N. Mturi, T. Munera-Huertas, P. Musicha, M.M. Mussi-Pinhata, T. Nakamura, R. Nanavati, S. Nangia, P. Newton, C. Ngoun, A. Novotney, D. Nwakanma, C.W. Obiero, A. Olivas-Martinez, P. Olliaro, E. Ooko, E. Ortiz-Brizuela, A.Y. Peleg, C. Perrone, N. Plakkal, A. Ponce-de-Leon, M. Raad, T. Ramdin, A. Riddell, T. Roberts, J.V.

Robotham, A. Roca, K.E. Rudd, N. Russell, J. Schnall, J.A.G. Scott, M. Shivamallappa, J. Sifuentes-Osornio, N. Steenkeste, A.J. Stewardson, T. Stoeva, N. Tasak, A. Thaiprakong, G. Thwaites, C. Turner, P. Turner, H.R. van Doorn, S. Velaphi, A. Vongpradith, H. Vu, T. Walsh, S. Waner, T. Wangrangsimakul, T. Wozniak, P. Zheng, B. Sartorius, A.D. Lopez, A. Stergachis, C. Moore, C. Dolecek and M. Naghavi. 2022. Global burden of bacterial antimicrobial resistance in 2019: a systematic analysis. *The Lancet* 399(10325): 629–655. https://doi.org/10.1016/S0140-6736(21)02724-0

Nguyen, A.Q., H.P. Vu, L.N. Nguyen, Q. Wang, S.P. Djordjevic, E. Donner, H. Yin and L.D. Nghiem. 2021. *Monitoring antibiotic resistance genes in wastewater treatment: Current strategies and future challenges*. *Science of the Total Environment*, 2021. https://doi.org/10.1016/j.scitotenv.2021.146964 (2021 /5/27)

Oksanen, J., F.G. Blanchet, M. Friendly, R. Kindt, P. Legendre, D. Mcglinn, P.R. Minchin, R.B. O'hara, G.L. Simpson, P. Solymos, M. Henry, H. Stevens, E. Szoecs and H.W. Maintainer. 2019. Vegan: Community Ecology Package2019. https://cran.r-project.org/package=vegan (2020 /12/7)

Pagano, M., A.F. Martins and A.L. Barth. 2016. Mobile genetic elements related to carbapenem resistance in Acinetobacter baumannii. *Brazilian Journal of Microbiology* 47(4): 785–792. https://doi.org/10.1016/j.bjm.2016.06.005

Pal, C., J. Bengtsson-Palme, E. Kristiansson and D.G.J. Larsson. 2015. Co-occurrence of resistance genes to antibiotics, biocides and metals reveals novel insights into their co-selection potential. *BMC Genomics* 16(1). https://doi.org/10.1186/s12864-015-2153-5

Pal, C., J. Bengtsson-Palme, C. Rensing, E. Kristiansson and D.G.J. Larsson. 2014. BacMet: antibacterial biocide and metal resistance genes database. *Nucleic Acids Research* 42(D1): D737–D743. https://doi.org/10.1093/nar/gkt1252

Palarea-Albaladejo, J. and J.A. Martín-Fernández. 2015. zCompositions — R package for multivariate imputation of left-censored data under a compositional approach. *Chemometrics and Intelligent Laboratory Systems* 143: 85–96. https://doi.org/10.1016/j.chemolab.2015.02.019

Parkin, G.F. and W.F. Owen. 1986. Fundamentals of Anaerobic Digestion of Wastewater Sludges. *Journal of Environmental Engineering* 112(5): 867–920. https://doi.org/10.1061/(ASCE)0733-9372(1986)112:5(867)

Partridge, S.R., S.M. Kwong, N. Firth and S.O. Jensen. 2018. *Mobile genetic elements associated with antimicrobial resistance*. *Clinical Microbiology Reviews* 4, American Society for Microbiology, 1 October 2018. https://doi.org/10.1128/CMR.00088-17 (2021 /5/19)

Paukner, S. and R. Riedl. 2017. Pleuromutilins: Potent drugs for resistant bugs-mode of action and resistance. *Cold Spring Harbor Perspectives in Medicine* 7(1). https://doi.org/10.1101/cshperspect.a027110

Peces, M., S. Astals, P.D. Jensen and W.P. Clarke. 2018. Deterministic mechanisms define the long-term anaerobic digestion microbiome and its functionality regardless of the initial microbial community. *Water Research* 141: 366–376. https://doi.org/10.1016/j.watres.2018.05.028

Petriglieri, F., M. Nierychlo, P.H. Nielsen and S.J. McIlroy. 2018. In situ visualisation of the abundant Chloroflexi populations in full-scale anaerobic digesters and the fate of immigrating species. *PLoS ONE* 13(11): e0206255. https://doi.org/10.1371/journal.pone.0206255

Pitta, D.W., N. Indugu, J.D. Toth, J.S. Bender, L.D. Baker, M.L. Hennessy, B. Vecchiarelli, H. Aceto and Z. Dou. 2020. The distribution of microbiomes and resistomes across farm environments in conventional and organic dairy herds in Pennsylvania. *Environmental Microbiome* 15(1): 21. https://doi.org/10.1186/s40793-020-00368-5

Public Health Agency Canada. 2018. *Canadian Antimicrobial Resistance Surveillance System Report 2017*. https://www.wormsandgermsblog.com/files/2017/11/CARSS-Report-2017-EN.pdf (2018 /7/4)

Qiu, T., L. Huo, Y. Guo, M. Gao, G. Wang, D. Hu, C. Li, Z. Wang, G. Liu and X. Wang. 2022. Metagenomic assembly reveals hosts and mobility of common antibiotic resistome in animal manure and commercial compost. *Environmental Microbiome* 17(1): 42. https://doi.org/10.1186/s40793-022-00437-x

Qiu, X., G. Zhou, L. Chen and H. Wang. 2021. Additive quality influences the reservoir of antibiotic resistance genes during chicken manure composting. *Ecotoxicology and Environmental Safety* 220: 112413. https://doi.org/10.1016/j.ecoenv.2021.112413

Quintela-Baluja, M., M. Abouelnaga, J. Romalde, J.Q. Su, Y. Yu, M. Gomez-Lopez, B. Smets, Y.G. Zhu and D.W. Graham. 2019. Spatial ecology of a wastewater network defines the antibiotic resistance genes in downstream receiving waters. *Water Research* 162: 347–357. https://doi.org/10.1016/j.watres.2019.06.075

van Reenen, C.A. and L.M.T. Dicks. 2011. Horizontal gene transfer amongst probiotic lactic acid bacteria and other intestinal microbiota: what are the possibilities? A review. *Archives of Microbiology* 193(3): 157–168. https://doi.org/10.1007/s00203-010-0668-3

Resende, J.A., C.G. Diniz, V.L. Silva, M.H. Otenio, A. Bonnafous, P.B. Arcuri and J.J. Godon. 2014. Dynamics of antibiotic resistance genes and presence of putative pathogens during

ambient temperature anaerobic digestion. *Journal of Applied Microbiology* 117(6): 1689–1699. https://doi.org/10.1111/jam.12653

Reygaert, W. 2018. An overview of the antimicrobial resistance mechanisms of bacteria. *AIMS Microbiology* 4(3): 482–501. https://doi.org/10.3934/microbiol.2018.3.482

Riaz, L., Q. Wang, Q. Yang, X. Li and W. Yuan. 2020. Potential of industrial composting and anaerobic digestion for the removal of antibiotics, antibiotic resistance genes and heavy metals from chicken manure. *Science of the Total Environment* 718. https://doi.org/10.1016/j.scitotenv.2020.137414

Roberts, A.P., J. Pratten, M. Wilson and P. Mullany. 1999. Transfer of a conjugative transposon, Tn5397 in a model oral biofilm. *FEMS Microbiology Letters* 177(1): 63–66. https://doi.org/10.1111/J.1574-6968.1999.TB13714.X

Rohatgi, A. 2021. WebPlotDigitizer: Version 4.5. https://automeris.io/WebPlotDigitizer (2021/8/23)

Ruuskanen, M., J. Muurinen, A. Meierjohan, K. Pärnänen, M. Tamminen, C. Lyra, L. Kronberg and M. Virta. 2016. Fertilizing with animal manure disseminates antibiotic resistance genes to the farm environment. *Journal of Environmental Quality* 45(2): 488–493. https://doi.org/10.2134/jeq2015.05.0250

Sabino, Y.N.V., M.F. Santana, L.B. Oyama, F.G. Santos, A.J.S. Moreira, S.A. Huws and H.C. Mantovani. 2019. Characterization of antibiotic resistance genes in the species of the rumen microbiota. *Nature Communications 2019 10:1* 10(1): 1–11. https://doi.org/10.1038/s41467-019-13118-0

Schwarz, F. V., V. Perreten and M. Teuber. 2001. Sequence of the 50-kb conjugative multiresistance plasmid pRE25 from Enterococcus faecalis RE25. *Plasmid* 46(3): 170–187. https://doi.org/10.1006/plas.2001.1544

Shen, Z., C.M. Tang and G.Y. Liu. 2022. Towards a better understanding of antimicrobial resistance dissemination: what can be learnt from studying model conjugative plasmids? *Military Medical Research* 9(1): 1–11. https://doi.org/10.1186/S40779-021-00362-Z/FIGURES/2

Shintani, M. and H. Nojiri. 2013. Mobile Genetic Elements (MGEs) carrying catabolic genes. In *Management of Microbial Resources in the Environment*, 167–214. Springer Netherlands. https://doi.org/10.1007/978-94-007-5931-2_8/TABLES/6

Singer, R.S., L.J. Porter, D.U. Thomson, M. Gage, A. Beaudoin and J.K. Wishnie. 2019. Raising Animals Without Antibiotics: U.S. Producer and Veterinarian Experiences and Opinions. *Frontiers in Veterinary Science* 6: 452. https://doi.org/10.3389/fvets.2019.00452

Sirohi, S.K., N. Pandey, B. Singh and A.K. Puniya. 2010. Rumen methanogens: A review. *Indian Journal of Microbiology* 50(3): 253–262. https://doi.org/10.1007/s12088-010-0061-6

Smith, T.C., W.A. Gebreyes, M.J. Abley, A.L. Harper, B.M. Forshey, M.J. Male, H.W. Martin, B.Z. Molla, S. Sreevatsan, S. Thakur, M. Thiruvengadam and P.R. Davies. 2013. Methicillin-Resistant Staphylococcus aureus in Pigs and Farm Workers on Conventional and Antibiotic-Free Swine Farms in the USA. *PLoS ONE* 8(5). https://doi.org/10.1371/journal.pone.0063704

Solomon, J.M. and A.D. Grossman. 1996. Who's competent and when: regulation of natural genetic competence in bacteria. *Trends in Genetics* 12(4): 150–155. https://doi.org/10.1016/0168-9525(96)10014-7

Song, W., X. Wang, J. Gu, S. Zhang, Y. Yin, Y. Li, X. Qian and W. Sun. 2017. Effects of different swine manure to wheat straw ratios on antibiotic resistance genes and the microbial community structure during anaerobic digestion. *Bioresource Technology* 231: 1–8. https://doi.org/10.1016/j.biortech.2017.01.054

Sukhum, K. V., R.C. Vargas, M. Boolchandani, A.W. D'Souza, S. Patel, A. Kesaraju, G. Walljasper, H. Hegde, Z. Ye, R.K. Valenzuela, P. Gunderson, C. Bendixsen, G. Dantas and S.K. Shukla. 2021. Manure Microbial Communities and Resistance Profiles Reconfigure after Transition to Manure Pits and Differ from Those in Fertilized Field Soil. *MBio* 12(3). https://doi.org/10.1128/mBio.00798-21.

Sun, L., X. Han, J. Li, Z. Zhao, Y. Liu, Q. Xi, X. Guo and S. Gun. 2020. Microbial Community and Its Association With Physicochemical Factors During Compost Bedding for Dairy Cows. *Frontiers in Microbiology* 11: 484346. https://doi.org/10.3389/FMICB.2020.00254/BIBTEX

Sun, W., J. Gu, X. Wang, X. Qian and H. Peng. 2019. Solid-state anaerobic digestion facilitates the removal of antibiotic resistance genes and mobile genetic elements from cattle manure. *Bioresource Technology* 274: 287–295. https://doi.org/10.1016/j.biortech.2018.09.013

Sun, W., X. Qian, J. Gu, X.J. Wang and M.L. Duan. 2016. Mechanism and effect of temperature on variations in antibiotic resistance genes during anaerobic digestion of dairy manure. *Scientific Reports* 6. https://doi.org/10.1038/srep30237

Syafiuddin, A. and R. Boopathy. 2021. *Role of anaerobic sludge digestion in handling antibiotic resistant bacteria and antibiotic resistance genes – A review*. *Bioresource Technology*, p. 124970, 2021. https://doi.org/10.1016/j.biortech.2021.124970 (2021 /4/7)

Tanizawa, Y., M. Tohno, E. Kaminuma, Y. Nakamura and M. Arita. 2015. Complete genome sequence and analysis of Lactobacillus hokkaidonensis LOOC260T, a psychrotrophic lactic

acid bacterium isolated from silage. *BMC Genomics* 16(1): 240. https://doi.org/10.1186/s12864-015-1435-2

Thomas, C.M. and K.M. Nielsen. 2005. Mechanisms of, and Barriers to, Horizontal Gene Transfer between Bacteria. *Nature Reviews Microbiology 2005 3:9* 3(9): 711–721. https://doi.org/10.1038/NRMICRO1234

Thomas, T., J. Gilbert and F. Meyer. 2012. Metagenomics - a guide from sampling to data analysis. *Microbial Informatics and Experimentation* 2(1): 3. https://doi.org/10.1186/2042-5783-2-3

Tian, G., B. Yang, M. Dong, R. Zhu, F. Yin, X. Zhao, Y. Wang, W. Xiao, Q. Wang, W. Zhang and X. Cui. 2018. The effect of temperature on the microbial communities of peak biogas production in batch biogas reactors. *Renewable Energy* 123: 15–25. https://doi.org/10.1016/j.renene.2018.01.119

Tian, Z., Y. Zhang, B. Yu and M. Yang. 2016. Changes of resistome, mobilome and potential hosts of antibiotic resistance genes during the transformation of anaerobic digestion from mesophilic to thermophilic. *Water Research* 98: 261–269. https://doi.org/10.1016/j.watres.2016.04.031

Tran, T.T., A. Scott, Y.-C. Tien, R. Murray, P. Boerlin, D.L. Pearl, K. Liu, J. Robertson, J.H.E. Nash and E. Topp. 2021. On-Farm Anaerobic Digestion of Dairy Manure Reduces the Abundance of Antibiotic Resistance-Associated Gene Targets and the Potential for Plasmid Transfer. *Applied and Environmental Microbiology* 87(14): 1–20. https://doi.org/10.1128/AEM.02980-20

Vats, P., U.J. Kaur and P. Rishi. 2022. Heavy metal-induced selection and proliferation of antibiotic resistance: A review. *Journal of Applied Microbiology* 132(6): 4058–4076. https://doi.org/10.1111/jam.15492

Veech, J.A. 2013. A probabilistic model for analysing species co-occurrence. *Global Ecology and Biogeography* 22(2): 252–260. https://doi.org/10.1111/J.1466-8238.2012.00789.X

Veress, A., T. Nagy, T. Wilk, J. Kömüves, F. Olasz and J. Kiss. 2020. Abundance of mobile genetic elements in an Acinetobacter lwoffii strain isolated from Transylvanian honey sample. *Scientific Reports* 10(1): 2969. https://doi.org/10.1038/s41598-020-59938-9.

Viechtbauer, W. 2010. Conducting Meta-Analyses in R with the metafor Package. *Journal of Statistical Software* 36(3): 1–48. https://doi.org/10.18637/jss.v036.i03.

Villar, I., D. Alves, J. Garrido and S. Mato. 2016. Evolution of microbial dynamics during the maturation phase of the composting of different types of waste. *Waste Management* 54: 83–92. https://doi.org/10.1016/j.wasman.2016.05.011

Wallace, J.S., E. Garner, A. Pruden and D.S. Aga. 2018. Occurrence and transformation of veterinary antibiotics and antibiotic resistance genes in dairy manure treated by advanced anaerobic digestion and conventional treatment methods. *Environmental Pollution* 236: 764–772. https://doi.org/10.1016/j.envpol.2018.02.024

Wang, F., W. Han, S. Chen, W. Dong, M. Qiao, C. Hu and B. Liu. 2020. Fifteen-Year Application of Manure and Chemical Fertilizers Differently Impacts Soil ARGs and Microbial Community Structure. *Frontiers in Microbiology* 11. https://doi.org/10.3389/fmicb.2020.00062

Wang, G., Y. Kong, Y. Yang, R. Ma, L. Li, G. Li and J. Yuan. 2022. Composting temperature directly affects the removal of antibiotic resistance genes and mobile genetic elements in livestock manure. *Environmental Pollution* 303: 119174. https://doi.org/10.1016/j.envpol.2022.119174

Wang, P., H. Wang, Y. Qiu, L. Ren and B. Jiang. 2018. Microbial characteristics in anaerobic digestion process of food waste for methane production: A review. *Bioresource Technology* 248: 29–36. https://doi.org/10.1016/j.biortech.2017.06.152

Wang, W.-K., W.-J. Li, Q.-C. Wu, Y.-L. Wang, S.-L. Li and H.-J. Yang. 2021. Isolation and Identification of a Rumen Lactobacillus Bacteria and Its Degradation Potential of Gossypol in Cottonseed Meal during Solid-State Fermentation. *Microorganisms* 9(11): 2200. https://doi.org/10.3390/microorganisms9112200.

Wen, Q., S. Yang and Z. Chen. 2021. Mesophilic and thermophilic anaerobic digestion of swine manure with sulfamethoxazole and norfloxacin: Dynamics of microbial communities and evolution of resistance genes. *Frontiers of Environmental Science and Engineering* 15(5): 1–12. https://doi.org/10.1007/s11783-020-1342-x

WHO. 2018a. Antibiotic resistance. *World Health Organization*. https://www.who.int/news-room/fact-sheets/detail/antibiotic-resistance (2019 /3/19)

WHO. 2018b. Critically Important Antimicrobials for Human Medicine. https://apps.who.int/iris/bitstream/handle/10665/312266/9789241515528-eng.pdf (2023 /6/1)

Wickham, H. 2016. *Ggplot2: Elegant Graphics for Data Analysis*. New York: Springer-Verlag. https://ggplot2.tidyverse.org..

Wicks, M. and H. Keener. 2017. Manure Processing Technologies. *The Ohio State University*. https://ocamm.osu.edu/sites/ocamm/files/imce/Manure/MM-Resources/MPT_3.2_separation.pdf (2023 /10/14)

Wilson, D.N., V. Hauryliuk, G.C. Atkinson and A.J. O'Neill. 2020. Target protection as a key antibiotic resistance mechanism. *Nature Reviews Microbiology 2020 18:11* 18(11): 637–648. https://doi.org/10.1038/S41579-020-0386-Z

Wohde, M., S. Berkner, T. Junker, S. Konradi, L. Schwarz and R.-A. Düring. 2016. Occurrence and transformation of veterinary pharmaceuticals and biocides in manure: a literature review. *Environmental Science Europe* 1–25. https://doi.org/10.1186/s12302-016-0091-8

Wolak, I., M. Czatzkowska, M. Harnisz, J. Paweł, J. Ebski, Ł. Paukszto, P. Rusanowska, E. Felis and E. Korzeniewska. 2022. Metagenomic Analysis of the Long-Term Synergistic Effects of Antibiotics on the Anaerobic Digestion of Cattle Manure. *Energies 2022, Vol. 15, Page 1920* 15(5): 1920. https://doi.org/10.3390/EN15051920

Wong, J.J.W., J. Lu and J.N.M. Glover. 2012. Relaxosome function and conjugation regulation in F-like plasmids - a structural biology perspective. *Molecular Microbiology* 85(4): 602–617. https://doi.org/10.1111/j.1365-2958.2012.08131.x

Wood, D.E., J. Lu and B. Langmead. 2019. Improved metagenomic analysis with Kraken 2. *Genome Biology* 20(1): 1–13. https://doi.org/10.1186/s13059-019-1891-0

Wu, X., Z. Tian, Z. Lv, Z. Chen, Y. Liu, X. Yong, J. Zhou, X. Xie, H. Jia and P. Wei. 2020. Effects of copper salts on performance, antibiotic resistance genes, and microbial community during thermophilic anaerobic digestion of swine manure. *Bioresource Technology* 300. https://doi.org/10.1016/j.biortech.2019.122728

Xia, J., H. Sun, X. xiang Zhang, T. Zhang, H. Ren and L. Ye. 2019. Aromatic compounds lead to increased abundance of antibiotic resistance genes in wastewater treatment bioreactors. *Water Research* 166. https://doi.org/10.1016/j.watres.2019.115073

Xiang, Y., Z. Yang, Y. Zhang, R. Xu, Y. Zheng, J. Hu, X. Li, M. Jia, W. Xiong and J. Cao. 2019. Influence of nanoscale zero-valent iron and magnetite nanoparticles on anaerobic digestion performance and macrolide, aminoglycoside, β-lactam resistance genes reduction. *Bioresource Technology* 294. https://doi.org/10.1016/j.biortech.2019.122139

Xu, M., R.D. Stedtfeld, F. Wang, S.A. Hashsham, Y. Song, Y. Chuang, J. Fan, H. Li, X. Jiang and J.M. Tiedje. 2019. Composting increased persistence of manure-borne antibiotic resistance genes in soils with different fertilization history. *Science of the Total Environment* 689: 1172–1180. https://doi.org/10.1016/j.scitotenv.2019.06.376

Yang, F., B. Han, Y. Gu and K. Zhang. 2020a. Swine liquid manure: a hotspot of mobile genetic elements and antibiotic resistance genes. *Scientific Reports* 10(1): 15037. https://doi.org/10.1038/s41598-020-72149-6

Yang, S., Q. Wen and Z. Chen. 2020b. Impacts of Cu and Zn on the performance, microbial community dynamics and resistance genes variations during mesophilic and thermophilic anaerobic digestion of swine manure. *Bioresource Technology* 312. https://doi.org/10.1016/j.biortech.2020.123554

Yang, W., I.F. Moore, K.P. Koteva, D.C. Bareich, D.W. Hughes and G.D. Wright. 2004. TetX Is a Flavin-dependent Monooxygenase Conferring Resistance to Tetracycline Antibiotics* □ S. *Journal of Biological Chemistry* 279: 52346–52352. https://doi.org/10.1074/jbc.M409573200

Youngquist, C.P., S.M. Mitchell and C.G. Cogger. 2016. Fate of Antibiotics and Antibiotic Resistance during Digestion and Composting: A Review. *Journal of Environmental Quality* 45(2): 537–545. https://doi.org/10.2134/jeq2015.05.0256.

Yuan, W., T. Tian, Q. Yang and L. Riaz. 2020. Transfer potentials of antibiotic resistance genes in Escherichia spp. strains from different sources. *Chemosphere* 246. https://doi.org/10.1016/j.chemosphere.2019.125736

Yue, Z., J. Zhang, Z. Zhou, C. Ding, T. Zhang, L. Wan and X. Wang. 2022. Antibiotic degradation dominates the removal of antibiotic resistance genes during composting. *Bioresource Technology* 344: 960–8524. https://doi.org/10.1016/j.biortech.2021.126229

Zhang, J., C. Buhe, D. Yu, H. Zhong and Y. Wei. 2020a. Ammonia stress reduces antibiotic efflux but enriches horizontal gene transfer of antibiotic resistance genes in anaerobic digestion. *Bioresource Technology* 295. https://doi.org/10.1016/j.biortech.2019.122191

Zhang, J., T. Lu, P. Shen, Q. Sui, H. Zhong, J. Liu, J. Tong and Y. Wei. 2019a. The role of substrate types and substrate microbial community on the fate of antibiotic resistance genes during anaerobic digestion. *Chemosphere* 229: 461–470. https://doi.org/10.1016/j.chemosphere.2019.05.036

Zhang, J., F. Mao, K.C. Loh, K.Y.H. Gin, Y. Dai and Y.W. Tong. 2018a. Evaluating the effects of activated carbon on methane generation and the fate of antibiotic resistant genes and class I integrons during anaerobic digestion of solid organic wastes. *Bioresource Technology* 249: 729–736. https://doi.org/10.1016/j.biortech.2017.10.082

Zhang, J., Z. Wang, Y. Wang, H. Zhong, Q. Sui, C. Zhang and Y. Wei. 2017. Effects of graphene oxide on the performance, microbial community dynamics and antibiotic resistance genes reduction during anaerobic digestion of swine manure. *Bioresource Technology* 245: 850–859. https://doi.org/10.1016/j.biortech.2017.08.217

Zhang, K., J. Gu, X. Wang, X. Zhang, T. Hu and W. Zhao. 2019b. Analysis for microbial denitrification and antibiotic resistance during anaerobic digestion of cattle manure

containing antibiotic. *Bioresource Technology* 291. https://doi.org/10.1016/j.biortech.2019.121803

Zhang, L., J. Gu, X. Wang, R. Zhang, X. Tuo, A. Guo and L. Qiu. 2018b. Fate of antibiotic resistance genes and mobile genetic elements during anaerobic co-digestion of Chinese medicinal herbal residues and swine manure. *Bioresource Technology* 250: 799–805. https://doi.org/10.1016/j.biortech.2017.10.100

Zhang, L., L. Li, G. Sha, C. Liu, Z. Wang and L. Wang. 2020b. Aerobic composting as an effective cow manure management strategy for reducing the dissemination of antibiotic resistance genes: An integrated meta-omics study. *Journal of Hazardous Materials* 386. https://doi.org/10.1016/j.jhazmat.2019.121895

Zhang, Q., J. Xu, X. Wang, W. Zhu, X. Pang and J. Zhao. 2021a. Changes and distributions of antibiotic resistance genes in liquid and solid fractions in mesophilic and thermophilic anaerobic digestion of dairy manure. *Bioresource Technology* 320: 124372. https://doi.org/10.1016/j.biortech.2020.124372

Zhang, R., J. Gu, X. Wang and Y. Li. 2020c. Antibiotic resistance gene transfer during anaerobic digestion with added copper: Important roles of mobile genetic elements. *Science of the Total Environment* 743: 140759. https://doi.org/10.1016/j.scitotenv.2020.140759

Zhang, R.M., X. Liu, S.L. Wang, L.X. Fang, J. Sun, Y.H. Liu and X.P. Liao. 2021b. Distribution patterns of antibiotic resistance genes and their bacterial hosts in pig farm wastewater treatment systems and soil fertilized with pig manure. *Science of the Total Environment* 758: 143654. https://doi.org/10.1016/j.scitotenv.2020.143654

Zhang, T., Y. Yang and A. Pruden. 2015. Effect of temperature on removal of antibiotic resistance genes by anaerobic digestion of activated sludge revealed by metagenomic approach. *Applied*

Microbiology and Biotechnology 99(18): 7771–7779. https://doi.org/10.1007/s00253-015-6688-9

Zhang, T., X.X. Zhang and L. Ye. 2011. Plasmid metagenome reveals high levels of antibiotic resistance genes and mobile genetic elements in activated sludge. *PLoS ONE* 6(10): 26041. https://doi.org/10.1371/journal.pone.0026041

Zhao, J., Y. Li, Y. Li, K. Zhang, H. Zhang and Y. Li. 2021. Effects of humic acid on sludge performance, antibiotics resistance genes propagation and functional genes expression during Cu(II)-containing wastewater treatment via metagenomics analysis. *Bioresource Technology* 323: 124575. https://doi.org/10.1016/j.biortech.2020.124575

Zhu, H., H. Zhang, Y. Xu, S. Laššáková, M. Korabečná and P. Neužil. 2020. PCR past, present and future. *BioTechniques* 69(4): 317–325. https://doi.org/10.2144/BTN-2020-0057.

Zielenkiewicz, U. and P. Cegłowski. 2005. The Toxin-Antitoxin System of the Streptococcal Plasmid pSM19035. *Journal of Bacteriology* 187(17): 6094–6105. https://doi.org/10.1128/JB.187.17.6094-6105.2005

Zinder, S.H., T. Anguish and S.C. Cardwell. 1984. Effects of Temperature on Methanogenesis in a Thermophilic (58°C) Anaerobic Digestor. *APPLIED AND ENVIRONMENTAL MICROBIOLOGY* 47(4): 808–813. https://www-ncbi-nlm-nih-gov.uml.idm.oclc.org/pmc/articles/PMC239768/pdf/aem00161-0220.pdf

Zou, Y., Y. Xiao, H. Wang, T. Fang and P. Dong. 2020. New insight into fates of sulfonamide and tetracycline resistance genes and resistant bacteria during anaerobic digestion of manure at thermophilic and mesophilic temperatures. *Journal of Hazardous Materials* 384. https://doi.org/10.1016/j.jhazmat.2019.121433

Appendices

Appendix A: Chapter 3 supplementary materials

Supplementary Figures

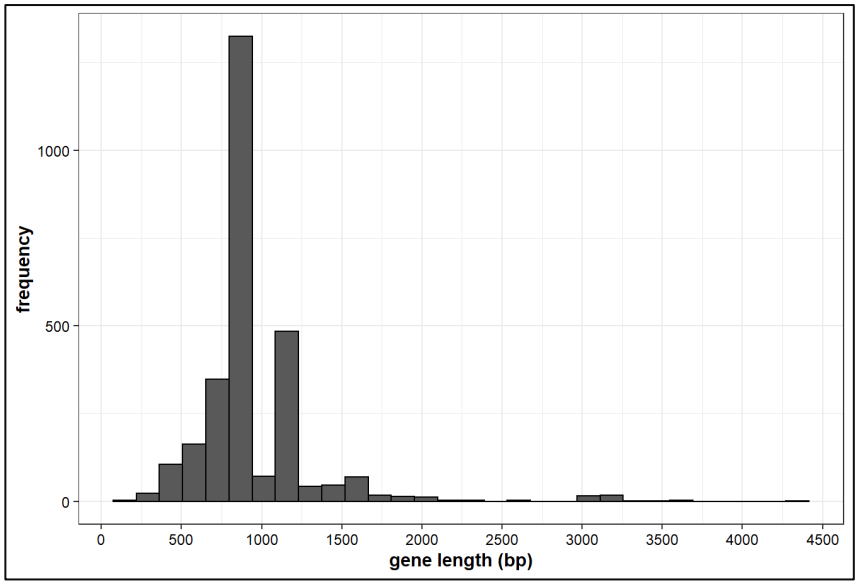

Figure A3.1 Distribution of gene lengths in CARD v3.1 after curation.

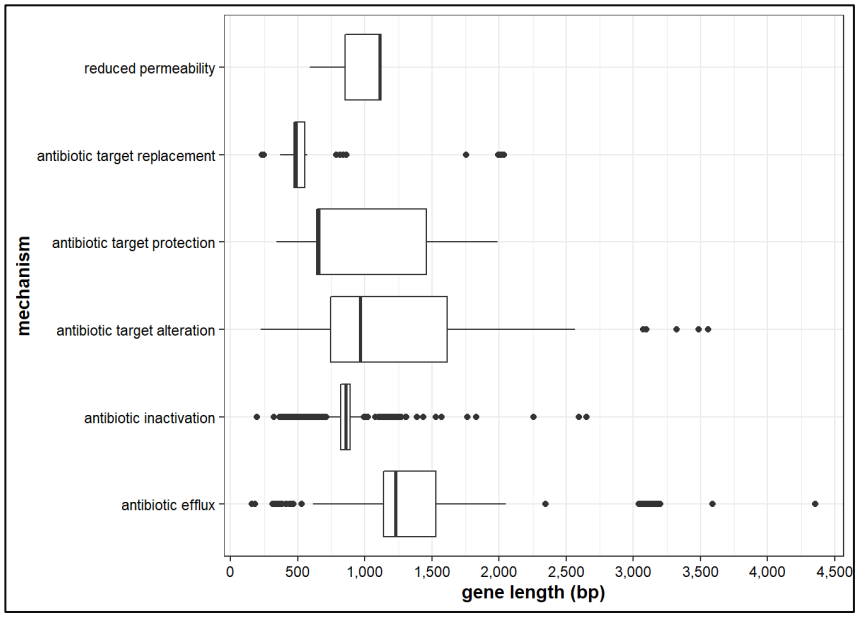

Figure A3.2 CARD gene length distribution by resistance mechanisms.

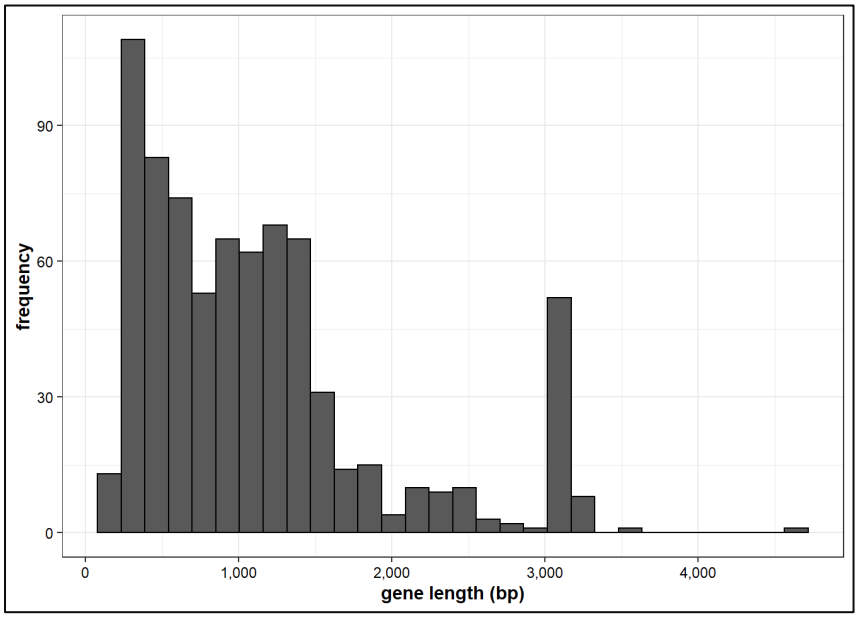

Figure A3.3 Distribution of gene lengths in BacMet2 database.

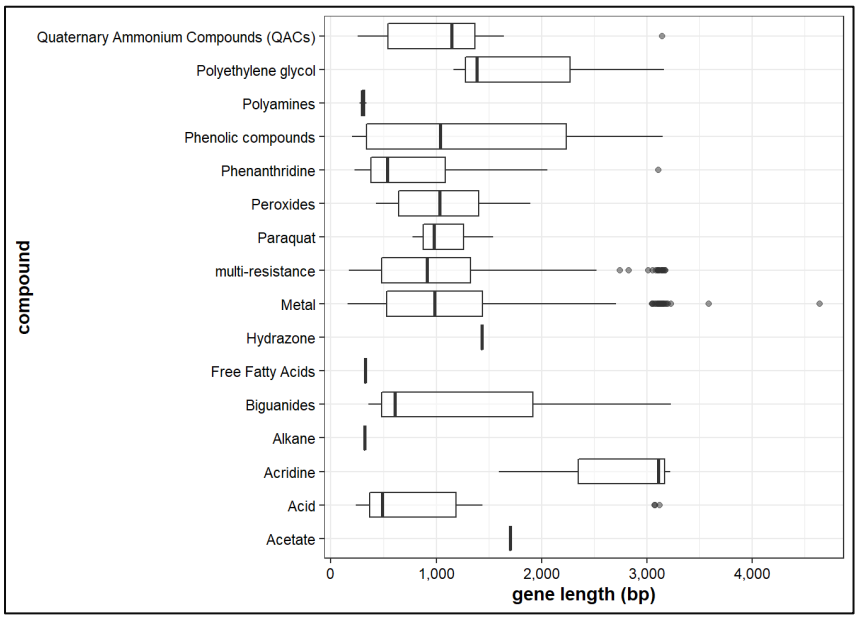

Figure A3.4 Distribution of gene lengths in BacMet2 by compound class.

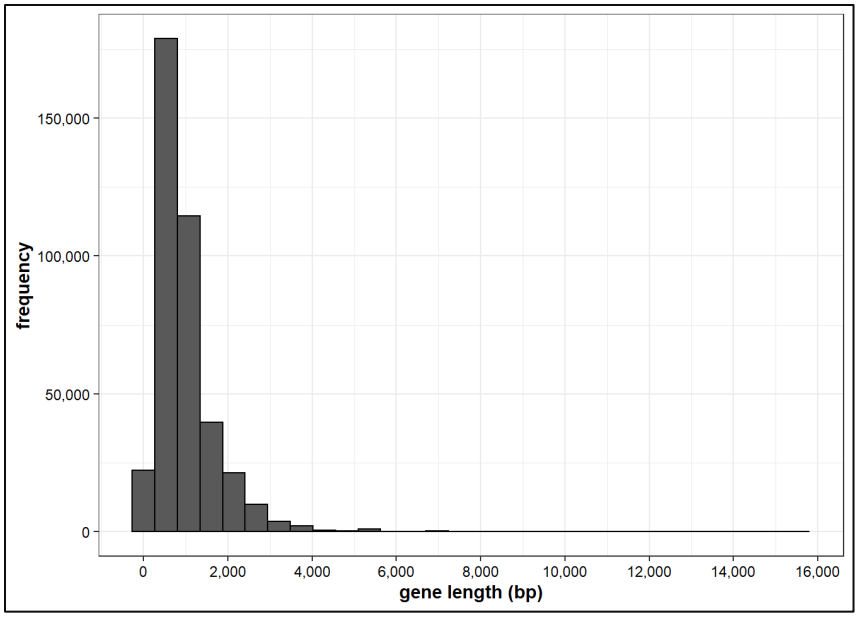

Figure A3.5 Distribution of gene lengths in mobileOG database

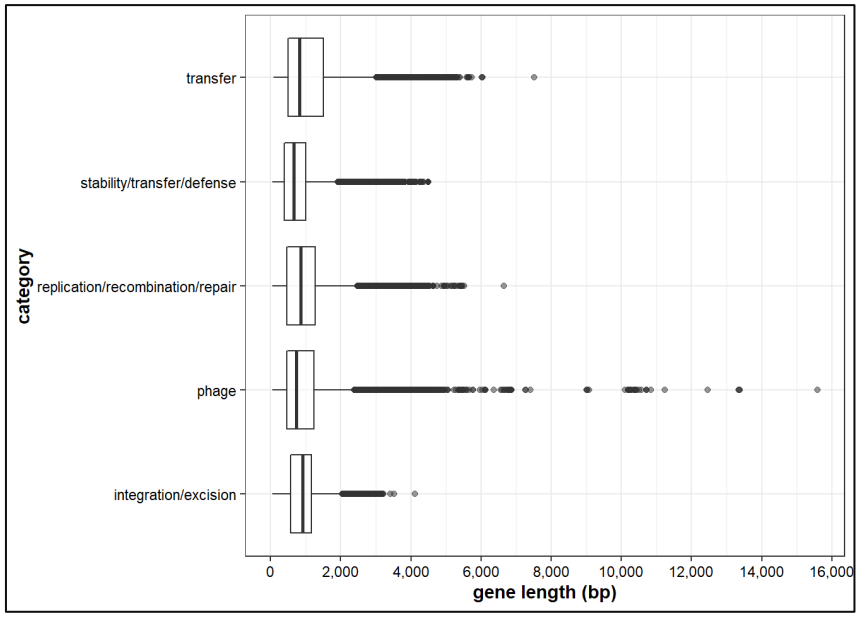

Figure A3.6 Distribution of gene lengths in mobileOG database by category

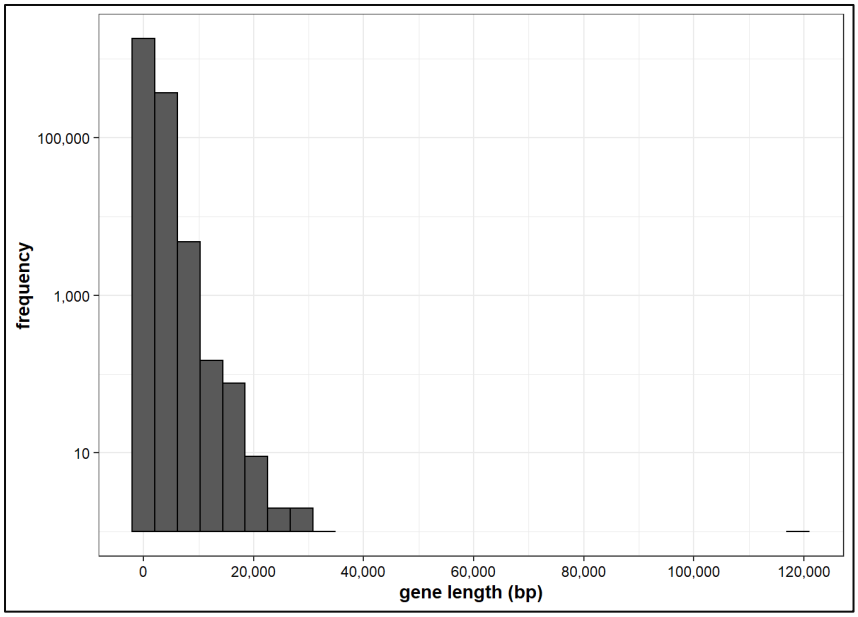

Figure A3.7 Distribution of of gene lengths in CAZy database.

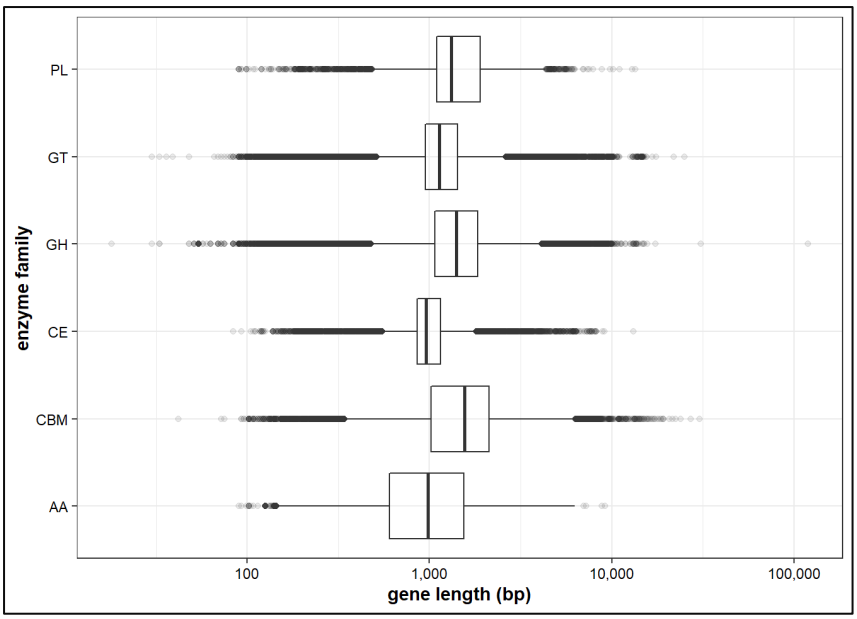

Figure A3.8 Distribution of of gene lengths in CAZy database by enzyme family.

Supplementary Tables

Table A3.1 Compounds and compound classes of genes listed in the BacMet2 database

Compound	Class
1a-62/JC-1-127	Guanylhydrazones
1i-39/JC-1-134	Guanylhydrazones
2-Chlorophenylhydrazine	Hydrazine
2-nitroimidazole	imidazole
2,6-dichloroindophenol	Phenolic Compounds
4,6-diamidino-2-phenylindole (DAPI)	Diamidine
4,6-diamidino-2-phenylindole (DAPI)	Diamindine
Acridine orange	Acridine
Acridine Orange	Acridine
Acriflavine	Acridine
Alexidine	Biguanides
Aluminium (Al)	Metal
Amicarbalide	Diamidine
Antimony (Sb)	Metal
Arsenic (As)	Metal
Benzylkonium Chloride (BAC)	Quaternary Ammonium Compounds (QACs)
Bismuth (Bi)	Metal
Cadmium (Cd)	Metal
Carbonyl cyanide 3-chlorophenylhydrazone (CCCP)	Hydrazone
Carbonylcyanide m-chlorophenyl hydrazone (CCCP)	Hydrazone
Cetrimide (CTM)	Quaternary Ammonium Compounds (QACs)
Cetylpyridinium Chloride (CPC)	Quaternary Ammonium Compounds (QACs)
Cetyltrimethylammonium bromide (CTAB)	Quaternary Ammonium Compounds (QACs)
Chlorhexidine	Biguanides
Chromium (Cr)	Metal
Clorine Dioxide (ClO2) [class: Halogens]	Halogens
Cobalt (Co)	Metal
Copper (Cu)	Metal
Crystal Violet	Triarylmethane
Cyclohexane	Cycloalkane
Dequalinium	Quaternary Ammonium Compounds (QACs)
Diamidinodiphenylamine	Diamidine
Diaminodiphenylamine	Diamidine
Dibrompropamidine	Diamidine
Dimethylphthalate	Pthalate
Diphenyl Ether	Phenyl
Dodine	Acetate
Empigen	Amine betaine
Ethidium Bromide	Phenanthridine
Ethylbenzene	Aromatic hydrocarbons

Compound	Class
Ethylmercury chloride	Organo-mercury
Fluorescein mercuric acetate	Organo-mercury
Gallium (Ga)	Metal
Glycerol	Alcohol
Gold (Au)	Metal
Hexamidine	Diamidine
Hoechst 33342	Bisbenzimide
Hydrochloric acid (HCl)	Acid
Hydrochloric Acid (HCl)	Acid
Hydrogen Peroxide (H2O2)	Peroxides
Iron (Fe)	Metal
Lead (Pb)	Metal
Linoleic acid	Free Fatty Acids
m-xylene	Aromatic hydrocarbons
Magnesium (Mg)	Metal
Manganese (Mn)	Metal
Menadione	Naphthoquinone
Mercury (Hg)	Metal
Methyl Viologen	Paraquat
Methylene Blue	Thiazinium
Methylmercury Acetate	Organo-mercury
Methylmercury chloride	Organo-mercury
Molybdenum (Mo)	Metal
n-hexane	Alkane
Nickel (Ni)	Metal
Oleic acid	Free Fatty Acids
p-chloro-mercuribenzoic acid	Organo-mercury
p-xylene	Aromatic hydrocarbons
Palmitic acid	Free Fatty Acids
Pentadiamine	Diamidine
Pentamidine	Diamidine
Pentane	Alkane
Phenamidine	Diamidine
Phenol	Phenolic compounds
Phenylmercury Acetate	Organo-mercury
Plumbagin	Naphthoquinone
Proflavin	Acridine
Propamidine	Diamidine
Propylbenzene	Aromatic hydrocarbons
Pyronin Y	Xanthene
Quinaldine red	Quinolines
Rhodamine 123	Xanthene
Rhodamine 6G	Xanthene

Compound	Class
Safranin O	Azin
Selenium (Se)	Metal
Silver (Ag)	Metal
Sodium acetate	Acetate
Sodium azide	Azide
Sodium Chenodeoxycholate	Acid
Sodium Cholate	Acid
Sodium Deoxycholate (SDC)	Acid
Sodium Deoxycholate	Acid
Sodium Dodecyl Sulfate (SDS)	Organo-sulfate
Sodium Glycocholate	Acid
Sodium hydroxide (NaOH)	Base
Sodium Hydroxide (NaOH)	Base
Sodium Nitrite (NaNo2)	Nitrites
Sodium Taurocholate	Acid
Sodium Taurodeoxycholate	Acid
Spermidine	Polyamines
Spermine	Polyamines
Stilbamidine	Diamidine
Styrene	Polystyrenes
Synergise	Metal
Synergize	QAC-Glutaraldehyde
Tellurium (Te)	Metal
Tetrachlorosalicylanilide (TCS)	Salicylanilide
Tetraphenylarsonium (TPA)	Quaternary Ammonium Compounds (QACs)
Tetraphenylphosphonium (TPP)	Quaternary Ammonium Compounds (QACs)
Thimerosal	Organo-mercury
Toluene	Aromatic hydrocarbons
Toluene	Aromatic hydrocarbons Aromatic hydrocarbons
Tributyltin (TBT)	Organo-tin
Triclosan	Phenolic compounds
Trimethylamine-diphenylhexatriene (TMA-DPH)	Diphenylhexatriene
Triton X-100	Polyethylene glycol
Tungsten (W)	Metal
Tween 20	Polyoxyethylene
Vanadium (V)	Metal
Virkon S	Peroxysulfate
Wex-cide-128	Phenyl
Zinc (Zn)	Metal

Table A3.2 Distribution of samples in repositories and samples IDs.

BioProject	Accession	Sample	Sample ID:1	Sample ID:2	Sample ID3
PRJNA1020798	SAMN37528980	F1M1	Chapter 6: F1M1	Chapter 7: M1	Chapter 5: DMF1_1
	SAMN37528981	F1D1	Chapter 6: F1D1	Chapter 7: MAD1	Chapter 5: DigF1_1
	SAMN37528982	F1M2	Chapter 6: F1M2	Chapter 7: M2	Chapter 5: DMF1_2
	SAMN37528983	F1D2	Chapter 6: F1D2	Chapter 7: MAD2	Chapter 5: DigF1_2
	SAMN37528984	F2M1	Chapter 6: F2M1		
	SAMN37528985	F2S1	Chapter 6: F2S1		
	SAMN37528986	F2M2	Chapter 6: F2M2		
	SAMN37528987	F2S2	Chapter 6: F2S2		
	SAMN37528988	F3M1	Chapter 6: F3M1	Chapter 7: M5	Chapter 5: DMF2_1
	SAMN37528989	F3D1	Chapter 6: F3D1	Chapter 7: MAD5	Chapter 5: DigF2_1
	SAMN37528990	F3S1	Chapter 6: F3S1		
	SAMN37528991	F3L1	Chapter 6: F3L1		
	SAMN37528992	F3M2	Chapter 6: F3M2	Chapter 7: M6	Chapter 5: DMF2_2
	SAMN37528993	F3D2	Chapter 6: F3D2	Chapter 7: MAD6	Chapter 5: DigF2_2
	SAMN37528994	F3S2	Chapter 6: F3S2		
	SAMN37528995	F3L2	Chapter 6: F3L2		
PRJNA1031688	SAMN37977631	M-3		Chapter 7: M3	
	SAMN37977632	M-4		Chapter 7: M4	
	SAMN37977633	MAD-3		Chapter 7: MAD3	
	SAMN37977634	MAD-4		Chapter 7: MAD4	
	SAMN37953781	M0	Chapter 8: M0	Chapter 7: M7	
	SAMN37953782	M1	Chapter 8: M1	Chapter 7: M8	
	SAMN37953783	M2	Chapter 8: M2	Chapter 7: M9	
	SAMN37953784	M3	Chapter 8: M3	Chapter 7: M10	
	SAMN37953785	MD_in	Chapter 8: MD_in	Chapter 7: MAD7	
	SAMN37953786	MD_T1	Chapter 8: MD_T1	Chapter 7: MAD7.1	
	SAMN37953787	MD_T2	Chapter 8: MD_T2	Chapter 7: MAD7.2	
	SAMN37953788	MD_T3	Chapter 8: MD_T3	Chapter 7: MAD7.3	
	SAMN37953789	MD_T4	Chapter 8: MD_T4	Chapter 7: MAD7.4	
	SAMN37953790	MD1	Chapter 8: MD1	Chapter 7: MAD8	
	SAMN37953791	MD2	Chapter 8: MD2	Chapter 7: MAD9	
	SAMN37953792	MD3	Chapter 8: MD3	Chapter 7: MAD10	
	SAMN37953793	TD_in	Chapter 8: TD_in		
	SAMN37953794	TD_T1	Chapter 8: TD_T1		
	SAMN37953795	TD_T2	Chapter 8: TD_T2		
	SAMN37953796	TD_T3	Chapter 8: TD_T3		
	SAMN37953797	TD_T4	Chapter 8: TD_T4		
	SAMN37953798	TD1	Chapter 8: TD1		
	SAMN37953799	TD2	Chapter 8: TD2		
	SAMN37953800	TD3	Chapter 8: TD3		

Appendix B: Chapter 4 supplementary materials

List of references used in meta-analyses.

1. Flores-Orozco et al. (2020a): Chapter 6
2. Flores-Orozco et al. (2020b)
3. Flores-Orozco et al. (Unpublished at the time of publication): Chapter 7
4. Guo et al. (2020)
5. Lu et al. (2020)
6. Luo et al. (2020)
7. Ma et al. (2019)
8. Mazzurco-Miritana et al. (2020)
9. Schueler et al. (2021)
10. Song et al. (2017)
11. Sun et al. (2016)
12. Sun et al. (2019)
13. Turker et al. (2018)
14. Wallace et al. (2018)
15. Wen et al. (2021)
16. Wu et al. (2020)
17. Zhang et al. (2018)
18. Zhang et al. (2017)
19. Zhang et al. (2020)
20. Zhang R.M. et al. (2021)

Figures

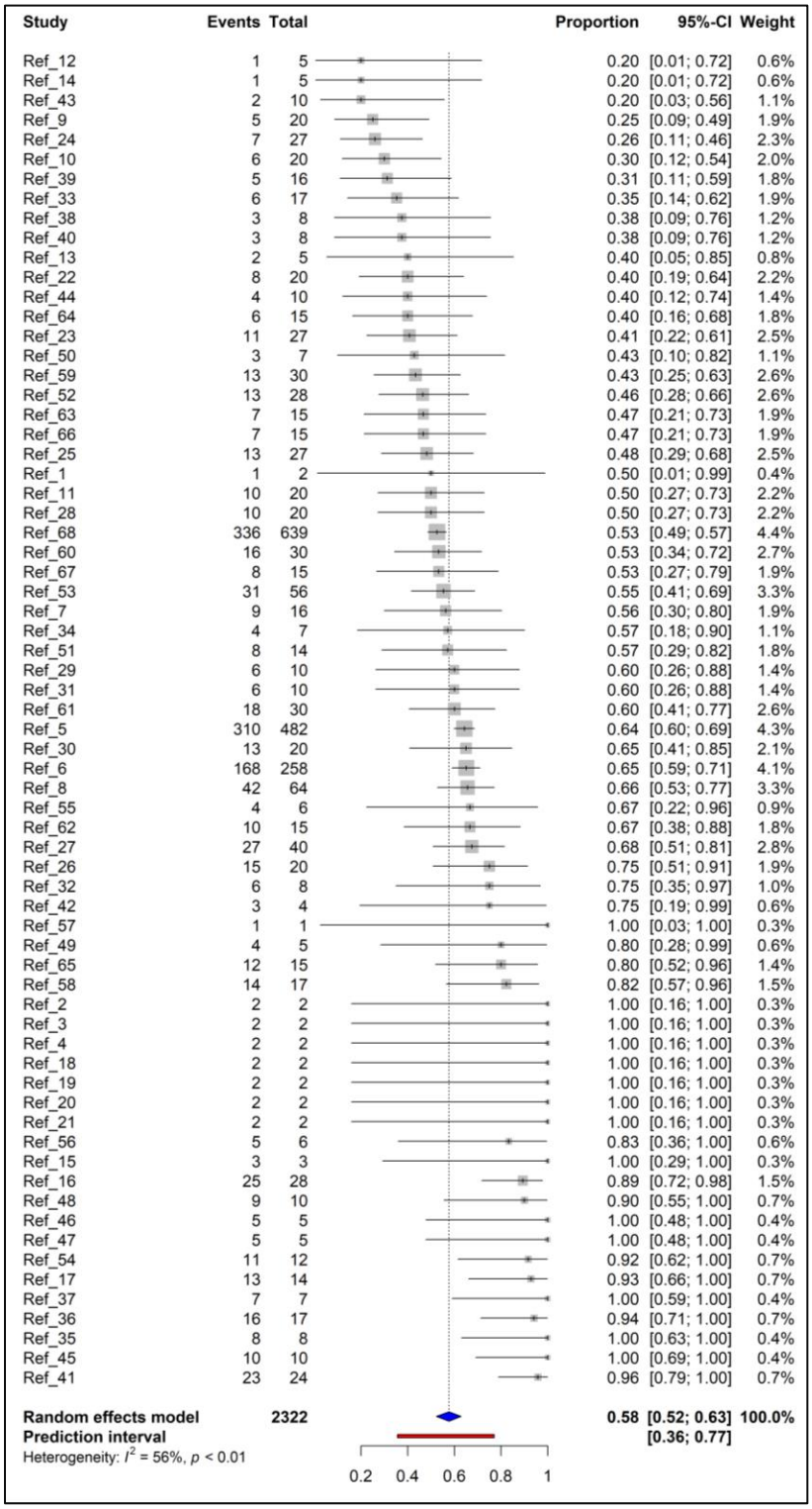

Figure B4.1 Forest plot of the general meta-analyses in term of the proportion of ARG reduced (P_{red}). References ID can be found in Table A3.1.

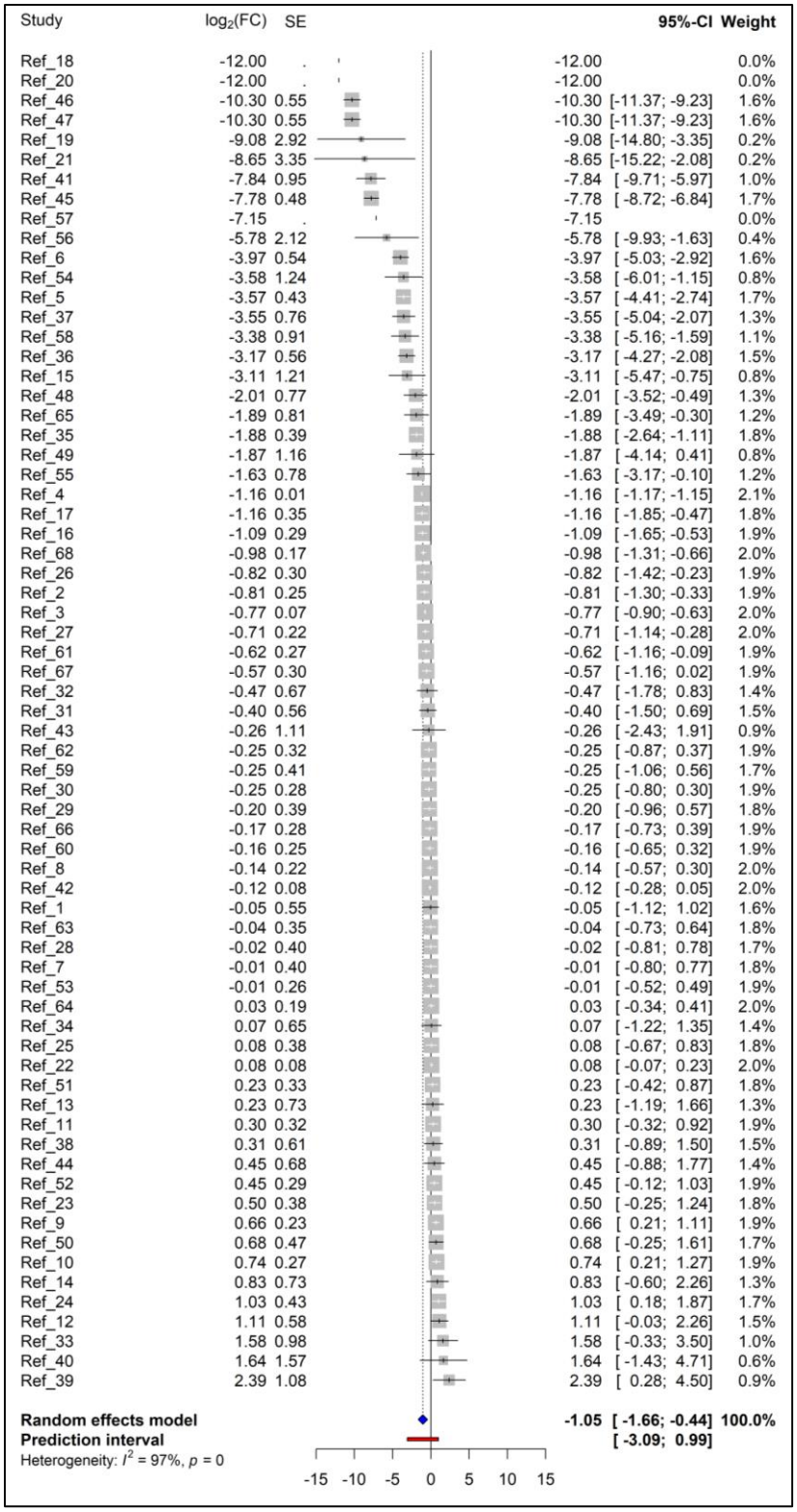

Figure B4.2 Forest plot of the general meta-analyses in term of the ARG log2 FC. References ID can be found in Table A3.1

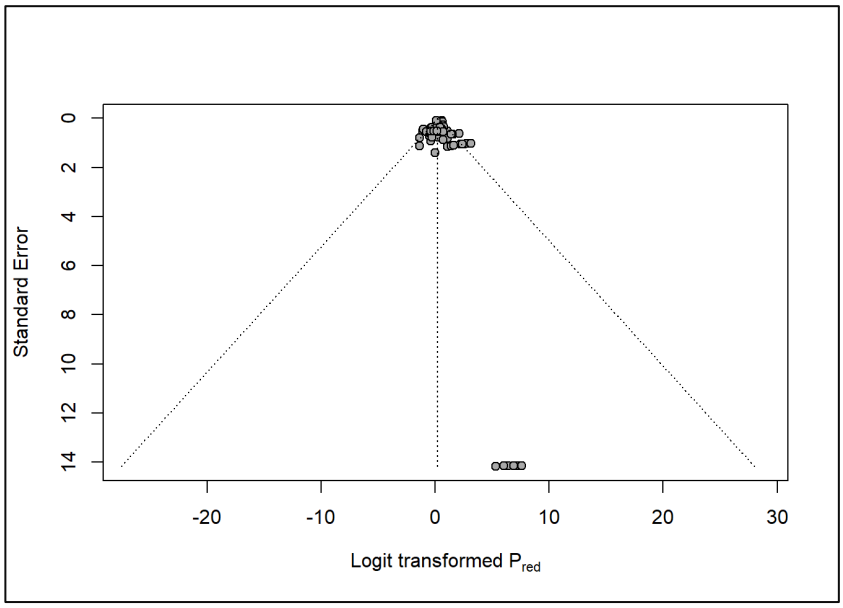

Figure A3.3 Funnel plot of P_{red} meta-analysis. Egger's test indicated no significant bias (p-values > 0.05).

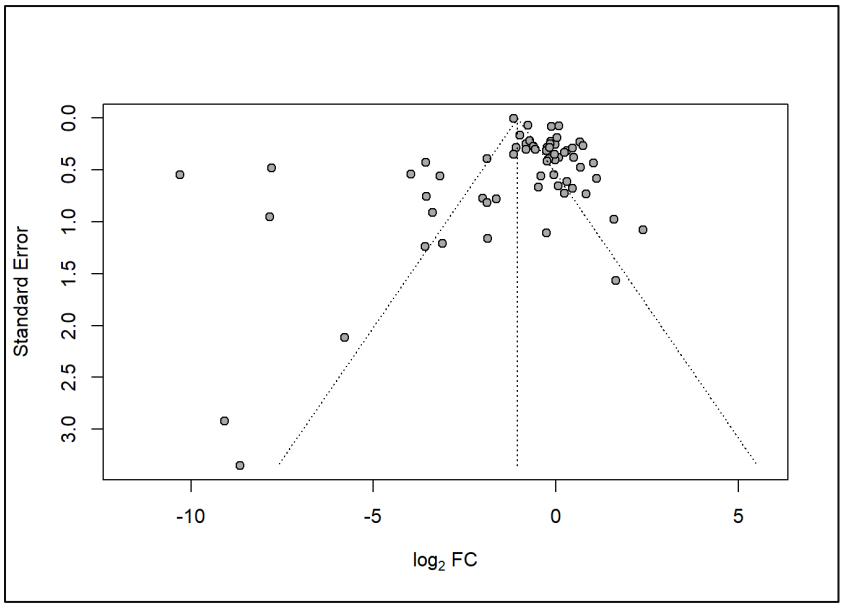

Figure B4.4 Funnel plot of log_2FC meta-analysis. Egger's test indicated no significant bias (p-values > 0.05).

Table B4.1 List of references and specific conditions.

Reference ID	Study	Quant. Method	Manure	Temperature	Setting	Treatment	HRT	pH	Vol
Ref_1	Flores-Orozco et al. (2020b)	qPCR	Cattle Manure	mesophilic	batch	antibiotic	hrt_g1	7	small
Ref_2	Flores-Orozco et al. (2020b)	qPCR	Cattle Manure	mesophilic	batch	antibiotic	hrt_g2	7	small
Ref_3	Flores-Orozco et al. (2020b)	qPCR	Cattle Manure	mesophilic	batch	NT	hrt_g1	7	small
Ref_4	Flores-Orozco et al. (2020b)	qPCR	Cattle Manure	mesophilic	batch	NT	hrt_g2	7	small
Ref_5	Flores-Orozco et al. (2020a)	metagenomics	Cattle Manure	mesophilic	continuous	NT	hrt_g2	7	lab_scale
Ref_6	Flores-Orozco et al. (UP)	metagenomics	Cattle Manure	mesophilic	continuous	NT	hrt_g2	7	lab_scale
Ref_7	Guo et al. (2020)	qPCR	Pig Manure	mesophilic	batch	NT	hrt_g2	7	small
Ref_8	Guo et al. (2020)	qPCR	Pig Manure	mesophilic	batch	other	hrt_g2	7	small
Ref_9	Lu et al. (2020)	qPCR	Pig Manure	mesophilic	batch	metal	hrt_g1	nd	small
Ref_10	Lu et al. (2020)	qPCR	Pig Manure	mesophilic	batch	metal	hrt_g2	nd	small
Ref_11	Lu et al. (2020)	qPCR	Pig Manure	mesophilic	batch	metal	hrt_g3	nd	small
Ref_12	Lu et al. (2020)	qPCR	Pig Manure	mesophilic	batch	NT	hrt_g1	nd	small
Ref_13	Lu et al. (2020)	qPCR	Pig Manure	mesophilic	batch	NT	hrt_g2	nd	small
Ref_14	Lu et al. (2020)	qPCR	Pig Manure	mesophilic	batch	NT	hrt_g3	nd	small
Ref_15	Luo et al. (2020)	qPCR	Pig Manure	mesophilic	continuous	antibiotic	hrt_g3	5	full_scale
Ref_16	Ma et al. (2019)	qPCR	Cattle Manure	mesophilic	batch	metal	hrt_g3	nd	small
Ref_17	Ma et al. (2019)	qPCR	Cattle Manure	mesophilic	batch	NT	hrt_g3	nd	small
Ref_18	Mazzurco Miritana et al. (2020)	qPCR	Cattle Manure	mesophilic	batch	antibiotic	hrt_g2	6	small
Ref_19	Mazzurco Miritana et al. (2020)	qPCR	Cattle Manure	mesophilic	batch	antibiotic	hrt_g4	5	small
Ref_20	Mazzurco Miritana et al. (2020)	qPCR	Cattle Manure	mesophilic	batch	NT	hrt_g2	5	small
Ref_21	Mazzurco Miritana et al. (2020)	qPCR	Cattle Manure	mesophilic	batch	NT	hrt_g4	5	small
Ref_22	Schueler et al. (2021)	qPCR	Cattle Manure	mesophilic	batch	antibiotic	hrt_g3	7	small
Ref_23	Song et al. (2017)	qPCR	Pig Manure	mesophilic	batch	solids	hrt_g1	7	small
Ref_24	Song et al. (2017)	qPCR	Pig Manure	mesophilic	batch	solids	hrt_g2	7	small
Ref_25	Song et al. (2017)	qPCR	Pig Manure	mesophilic	batch	solids	hrt_g4	7	small
Ref_26	Sun et al. (2019)	qPCR	Cattle Manure	mesophilic	batch	NT	hrt_g1	6	small
Ref_27	Sun et al. (2019)	qPCR	Cattle Manure	mesophilic	batch	NT	hrt_g2	6	small
Ref_28	Sun et al. (2019)	qPCR	Cattle Manure	mesophilic	batch	NT	hrt_g4	6	small
Ref_29	Sun et al. (2019)	qPCR	Cattle Manure	thermophilic	batch	NT	hrt_g1	6	small
Ref_30	Sun et al. (2019)	qPCR	Cattle Manure	thermophilic	batch	NT	hrt_g2	6	small
Ref_31	Sun et al. (2019)	qPCR	Cattle Manure	thermophilic	batch	NT	hrt_g4	6	small
Ref_32	Sun et al. (2016)	qPCR	Cattle Manure	mesophilic	batch	NT	hrt_g1	7	small
Ref_33	Sun et al. (2016)	qPCR	Cattle Manure	mesophilic	batch	NT	hrt_g2	7	small
Ref_34	Sun et al. (2016)	qPCR	Cattle Manure	mesophilic	batch	NT	hrt_g4	7	small
Ref_35	Sun et al. (2016)	qPCR	Cattle Manure	thermophilic	batch	NT	hrt_g1	7	small
Ref_36	Sun et al. (2016)	qPCR	Cattle Manure	thermophilic	batch	NT	hrt_g2	7	small
Ref_37	Sun et al. (2016)	qPCR	Cattle Manure	thermophilic	batch	NT	hrt_g4	7	small

Reference ID	Study	Quant. Method	Manure	Temperature	Setting	Treatment	HRT	pH	Vol
Ref_38	Sun et al. (2016)	qPCR	Cattle Manure	psychrophilic	batch	NT	hrt_g1	7	small
Ref_39	Sun et al. (2016)	qPCR	Cattle Manure	psychrophilic	batch	NT	hrt_g2	7	small
Ref_40	Sun et al. (2016)	qPCR	Cattle Manure	psychrophilic	batch	NT	hrt_g4	7	small
Ref_41	Turker et al. (2018)	qPCR	Cattle Manure	mesophilic	batch	NT	hrt_g2	nd	small
Ref_42	Wallace et al. (2018)	qPCR	Cattle Manure	mesophilic	continuous	antibiotic	hrt_g2	7	full_scale
Ref_43	Wen et al. (2021)	qPCR	Pig Manure	mesophilic	batch	antibiotic	hrt_g4	8	small
Ref_44	Wen et al. (2021)	qPCR	Pig Manure	mesophilic	batch	solids	hrt_g4	7	small
Ref_45	Wen et al. (2021)	qPCR	Pig Manure	thermophilic	batch	antibiotic	hrt_g4	8	small
Ref_46	Wen et al. (2021)	qPCR	Pig Manure	thermophilic	batch	solids	hrt_g4	7	small
Ref_47	Wen et al. (2021)	qPCR	Pig Manure	thermophilic	batch	solids	hrt_g4	8	small
Ref_48	Wu et al. (2020)	qPCR	Pig Manure	thermophilic	batch	metal	hrt_g2	7	small
Ref_49	Wu et al. (2020)	qPCR	Pig Manure	thermophilic	batch	NT	hrt_g2	7	small
Ref_50	Zhang et al. (2017)	qPCR	Pig Manure	mesophilic	batch	NT	hrt_g1	nd	small
Ref_51	Zhang et al. (2017)	qPCR	Pig Manure	mesophilic	batch	NT	hrt_g2	nd	small
Ref_52	Zhang et al. (2017)	qPCR	Pig Manure	mesophilic	batch	other	hrt_g1	nd	small
Ref_53	Zhang et al. (2017)	qPCR	Pig Manure	mesophilic	batch	other	hrt_g2	nd	small
Ref_54	Zhang et al. (2018)	qPCR	Pig Manure	mesophilic	batch	metal	hrt_g4	8	small
Ref_55	Zhang et al. (2018)	qPCR	Pig Manure	mesophilic	batch	NT	hrt_g4	7	small
Ref_56	Zhang et al. (2018)	qPCR	Pig Manure	mesophilic	batch	NT	hrt_g4	8	small
Ref_57	Zhang et al. (2018)	qPCR	Pig Manure	mesophilic	batch	other	hrt_g4	7	small
Ref_58	Zhang et al. (2018)	qPCR	Pig Manure	mesophilic	batch	other	hrt_g4	8	small
Ref_59	Zhang et al. (2020)	qPCR	Pig Manure	mesophilic	batch	metal	hrt_g1	6	small
Ref_60	Zhang et al. (2020)	qPCR	Pig Manure	mesophilic	batch	metal	hrt_g2	5	small
Ref_61	Zhang et al. (2020)	qPCR	Pig Manure	mesophilic	batch	metal	hrt_g2	7	small
Ref_62	Zhang et al. (2020)	qPCR	Pig Manure	mesophilic	batch	metal	hrt_g3	7	small
Ref_63	Zhang et al. (2020)	qPCR	Pig Manure	mesophilic	batch	metal	hrt_g3	8	small
Ref_64	Zhang et al. (2020)	qPCR	Pig Manure	mesophilic	batch	NT	hrt_g1	6	small
Ref_65	Zhang et al. (2020)	qPCR	Pig Manure	mesophilic	batch	NT	hrt_g2	6	small
Ref_66	Zhang et al. (2020)	qPCR	Pig Manure	mesophilic	batch	NT	hrt_g2	7	small
Ref_67	Zhang et al. (2020)	qPCR	Pig Manure	mesophilic	batch	NT	hrt_g3	8	small
Ref_68	Zhang R.M. et al. (2021)	metagenomics	Pig Manure	mesophilic	continuous	NT	hrt_g2	nd	full_scale

Table B4. 2 ARG included in the meta-analyses and the method used to quantify.

ARG	Quant.Method	ARG	Quant.Method	ARG	Quant.Method
AAC(2')-Ia	metagenomics	floR	metagenomics	qacEdelta1	metagenomics
AAC(3)-Ic	metagenomics	fosA	metagenomics	qepA	metagenomics
AAC(6')-Ib-cr	qPCR	FosB	metagenomics	QepA2	metagenomics
AAC(6')-Ib7	metagenomics	FosX	metagenomics	QnrA1	metagenomics, qPCR
AAC(6')-Ie-APH(2")-Ia	metagenomics	GES-1	metagenomics	QnrB1	metagenomics
aad(6)	metagenomics	gimA	metagenomics	QnrS1	metagenomics, qPCR
aadA	metagenomics	GOB-1	metagenomics	RanA	metagenomics
aadA10	metagenomics	gyr	qPCR	RanB	metagenomics
aadA11	metagenomics	gyrA	qPCR	RbpA	metagenomics
aadA14	metagenomics	ileS	metagenomics	rmtB	metagenomics
aadA16	metagenomics	IMP-37	metagenomics	rmtC	metagenomics
aadA17	metagenomics	IND-1	metagenomics	rmtF	metagenomics
aadA23	metagenomics	iri	metagenomics	ROB-1	metagenomics
aadA27	metagenomics	KLUY-4	metagenomics	rosA	metagenomics
aadA6/aadA10	metagenomics	KpnG	metagenomics	rosB	metagenomics
aadA7	metagenomics	LCR-1	metagenomics	rphA	metagenomics
aadK	metagenomics	linG	metagenomics	rphB	metagenomics
aadS	metagenomics	LlmA	metagenomics	rpoB	metagenomics
abeM	metagenomics	lmrB	metagenomics	rpoB2	metagenomics
acrA	metagenomics	lmrD	metagenomics	rsmA	metagenomics
acrB	metagenomics	lnuA	metagenomics	RTG	metagenomics
acrD	metagenomics	lnuB	metagenomics	salA	metagenomics
acrF	metagenomics	lnuC	metagenomics	SAT-1	metagenomics
adeA	metagenomics	lnuD	metagenomics	SAT-4	metagenomics
adeB	metagenomics	lnuE	metagenomics	SHV-1	metagenomics
adeC	metagenomics	lnuF	metagenomics	smeB	metagenomics
adeF	metagenomics	lnuG	metagenomics	smeC	metagenomics
adeI	metagenomics	LnuP	metagenomics	smeD	metagenomics
adeJ	metagenomics	LpsB	metagenomics	smeE	metagenomics
adeK	metagenomics	LptD	metagenomics	smeF	metagenomics
adeN	metagenomics	lrfA	metagenomics	smeR	metagenomics
AER-1	metagenomics	lsa(D)	metagenomics	spd	metagenomics
AIM-1	metagenomics	lsaA	metagenomics	sul1	metagenomics, qPCR
AmpC	metagenomics	lsaB	metagenomics	sul2	metagenomics, qPCR
ampC1	metagenomics	lsaC	metagenomics	sul3	metagenomics
ampH	metagenomics	lsaE	metagenomics	sul4	metagenomics
amrB	metagenomics	macA	metagenomics	TaeA	metagenomics
ANT(2")-Ia	metagenomics	macB	metagenomics	TEM-1	metagenomics
ANT(6)-Ia	metagenomics	marR	metagenomics	tet(31)	metagenomics
ANT(6)-Ib	metagenomics	mdfA	metagenomics	tet(33)	metagenomics
ANT(9)-Ia	metagenomics	mdsB	metagenomics	tet(34)	metagenomics

ARG	Quant.Method	ARG	Quant.Method	ARG	Quant.Method
APH(2")-IIa	metagenomics	mdtA	metagenomics	tet(35)	metagenomics
APH(3")-Ib	metagenomics	mdtB	metagenomics	tet(39)	metagenomics
APH(3')-IIa	metagenomics	mdtC	metagenomics	tet(40)	metagenomics
APH(3')-IIIa	metagenomics	mdtD	metagenomics	tet(41)	metagenomics
APH(6)-Ib	metagenomics	mdtE	metagenomics	tet(43)	metagenomics
APH(6)-Id	metagenomics	mdtF	metagenomics	tet(A)	metagenomics
arlR	metagenomics	mdtG	metagenomics	tet(B)	metagenomics
arlS	metagenomics	mdtH	metagenomics	tet(C)	metagenomics, qPCR
arnA	metagenomics	mdtK	metagenomics	tet(D)	metagenomics
arr-1	metagenomics	mdtL	metagenomics	tet(E)	metagenomics
AxyY	metagenomics	mdtM	metagenomics	tet(G)	metagenomics, qPCR
bacA	metagenomics	mdtN	metagenomics	tet(H)	metagenomics
BahA	metagenomics	mdtO	metagenomics	tet(J)	metagenomics
bcr-1	metagenomics	mdtP	metagenomics	tet(K)	metagenomics
bcrA	metagenomics	mecA	metagenomics	tet(L)	metagenomics
BlaB	metagenomics	MecI	metagenomics	tet(P)	metagenomics
blaCTX	qPCR	mecR1	metagenomics	tet(R)	metagenomics
blaR1	metagenomics	mef(D)	metagenomics	tet(V)	metagenomics
blaVIA	qPCR	Mef(En2)	metagenomics	tet(W/N/W)	metagenomics
blaVIM	qPCR	mefA	metagenomics	Tet(X3)	metagenomics
bleomycin_resistance	metagenomics	mefB	metagenomics	Tet(X4)	metagenomics
blt	metagenomics	mefC	metagenomics	Tet(X5)	metagenomics
bmr	metagenomics	mefE	metagenomics	Tet(X6)	metagenomics
bpeF	metagenomics	mel	metagenomics	tet(Y)	metagenomics
CARB-1	metagenomics	mepA	metagenomics	tet(Z)	metagenomics
CARB-5	metagenomics	MexA	metagenomics	tet32	metagenomics
CAT	metagenomics	MexB	metagenomics	tet36	metagenomics
catA4	metagenomics	MexC	metagenomics	tet37	metagenomics
catB	metagenomics	MexD	metagenomics	tet44	metagenomics
catB10	metagenomics	MexE	metagenomics	tetA(48)	metagenomics
catB3	metagenomics	MexF	metagenomics	tetA(60)	metagenomics
catD	metagenomics	mexI	metagenomics	tetA(P)	metagenomics
catQ	metagenomics	mexK	metagenomics	tetB(46)	metagenomics
catS	metagenomics	mexQ	metagenomics	tetB(60)	metagenomics
ceoB	metagenomics	mexT	metagenomics	tetB(P)	metagenomics
cfr(D)	metagenomics	mexW	metagenomics	tetM	metagenomics, qPCR
cfrA	metagenomics	mexX	metagenomics	tetO	metagenomics, qPCR
cfrC	metagenomics	mexY	metagenomics	tetQ	metagenomics, qPCR
CfxA	metagenomics	mphA	metagenomics	tetS	metagenomics
CfxA2	metagenomics	mphB	metagenomics	tetT	metagenomics
CfxA6	metagenomics	mphC	metagenomics	tetW	metagenomics, qPCR
cmeB	metagenomics	mphE	metagenomics	tetX	metagenomics, qPCR
cmlA	metagenomics	mphG	metagenomics	tolC	metagenomics
cmlA9	metagenomics	mphH	metagenomics	tsnR	metagenomics

ARG	Quant.Method	ARG	Quant.Method	ARG	Quant.Method
cmx	metagenomics	mphM	metagenomics	TUS-1	metagenomics
CMY-1	metagenomics	mphO	metagenomics	ugd	metagenomics
CMY-2	qPCR	mprF	metagenomics	vanD	metagenomics
CpxR	metagenomics	msbA	metagenomics	vanE	metagenomics
CRP	metagenomics	MSI-OXA	metagenomics	vanG	metagenomics
CTX-M-1	metagenomics	msrA	metagenomics	vanHM	metagenomics
dfrA1	metagenomics, qPCR	msrC	metagenomics	vanM	metagenomics
dfrA7	qPCR	msrE	metagenomics	vanO	metagenomics
dfrB1	metagenomics	mtrA	metagenomics	vanRA	metagenomics
dfrC	metagenomics	mtrD	metagenomics	vanRB	metagenomics
DHA-1	metagenomics	mtrR	metagenomics	vanRC	metagenomics
DHA-2	metagenomics	mupA	metagenomics	vanRD	metagenomics
EBR-1	metagenomics	mupB	metagenomics	vanRE	metagenomics
efmA	metagenomics	MUS-1	metagenomics	vanRG	metagenomics
efrA	metagenomics	MuxB	metagenomics	vanRI	metagenomics
efrB	metagenomics	nd	qPCR	vanRL	metagenomics
emeA	metagenomics	NDM-1	metagenomics	vanRN	metagenomics
emrA	metagenomics	norA	metagenomics	vanRO	metagenomics
emrB	metagenomics	norB	metagenomics	vanSA	metagenomics
emrD	metagenomics	novA	metagenomics	vanSF	metagenomics
emrE	metagenomics	NPS-1	metagenomics	vanSG	metagenomics
emrK	metagenomics	OCH-1	metagenomics	vanSO	metagenomics
EreA	metagenomics	omp36	metagenomics	vanTC	metagenomics
EreB	metagenomics	ompF	metagenomics	vanTE	metagenomics
EreD	metagenomics	ompR	metagenomics	vanUG	metagenomics
Erm(31)	metagenomics	oprA	metagenomics	vanWB	metagenomics
Erm(33)	metagenomics	oprC	metagenomics	vanXA	metagenomics
Erm(35)	metagenomics	OprJ	metagenomics	vanXM	metagenomics
Erm(36)	metagenomics	OprM	metagenomics	vanYA	metagenomics
Erm(38)	metagenomics	OprN	metagenomics	vanYF	metagenomics
Erm(39)	metagenomics	optrA	metagenomics	vanYG1	metagenomics
Erm(42)	metagenomics	oqxB	metagenomics	vanZA	metagenomics
erm(46)	metagenomics	OXA-278	metagenomics	vatA	metagenomics
Erm(47)	metagenomics	OXA-347	metagenomics	vatB	metagenomics
Erm(A)	metagenomics	OXY-1-1	metagenomics	vatE	metagenomics
erm(TR)	metagenomics	OXY-5-1	metagenomics	vatF	metagenomics
ErmA	metagenomics	patA	metagenomics	vatG	metagenomics
ErmB	metagenomics, qPCR	patB	metagenomics	VEB-1	metagenomics
ErmC	metagenomics	PBP	metagenomics	vgaA	metagenomics
ErmF	metagenomics, qPCR	penA	metagenomics	vgaB	metagenomics
ErmG	metagenomics	PER-1	metagenomics	vgaD	metagenomics
ErmQ	metagenomics, qPCR	pmrA	metagenomics	vgaE	metagenomics
ErmT	metagenomics	pmrF	metagenomics	VgbA	metagenomics
ErmX	metagenomics, qPCR	poxtA	metagenomics	VgbB	metagenomics

ARG	Quant.Method	ARG	Quant.Method	ARG	Quant.Method
evgS	metagenomics	pp-flo	metagenomics	ykkC	metagenomics
fexA	metagenomics	PSE	metagenomics		

Appendix C: Chapter 5 supplementary materials

Supplementary Figures

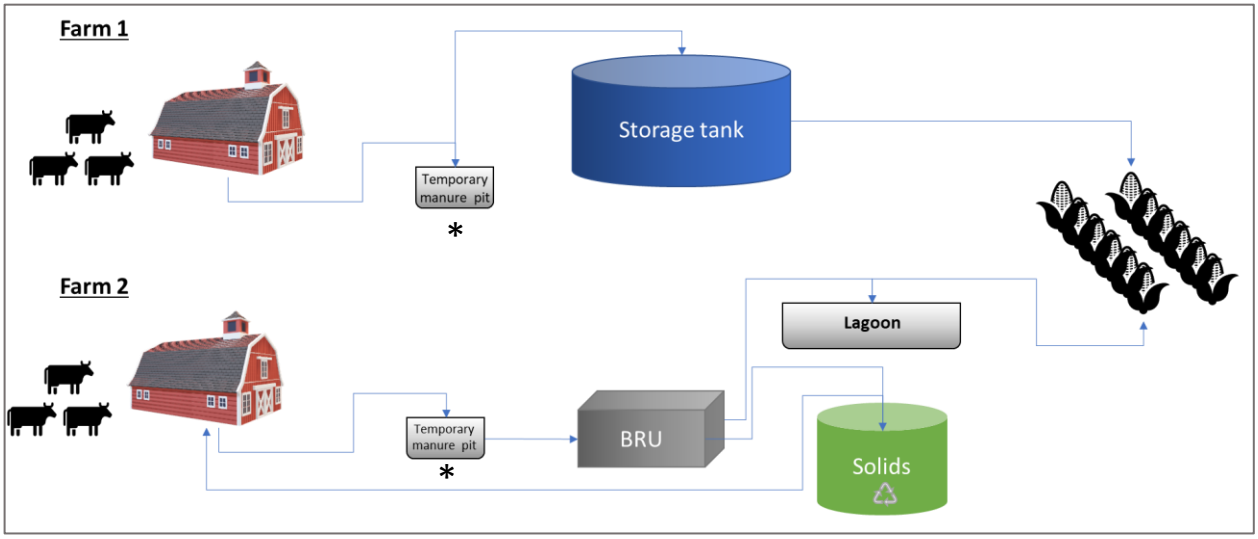

Figure C4.1 Layout of the manure management strategies of the two farms from where the dairy manure was collected.

Supplementary Tables

Table C5.1 Mode of action of the different antibiotics for which ARGs were found in this study.

Antibiotic Class	Mode of Action
acridine dye	Intercalates DNA
aminocoumarin	Binds DNA gyrase subunit B to inhibit ATP-dependent DNA supercoiling
aminoglycoside	Inhibits protein synthesis binding to ribosomal 30S subunit
beta-lactams	Inhibits cell-wall synthesis by binding to the penicillin-binding proteins
diaminopyrimidine	Blocks DNA synthesis inhibiting the enzyme dihydrofolate reductase
fluoroquinolone	Blocks DNA synthesis inhibiting topoisomerases II and IV
glycopeptide	Inhibits cell-wall synthesis by binding to peptidoglycan precursors.
MLS	Inhibits protein synthesis binding ribosomal 50S subunit
multidrug	Mainly efflux pumps
nitroimidazole	Prevent protein synthesis and affects DNA
nucleoside	Inhibits protein synthesis
peptide	Disrupts the cell membrane in several ways
phenicol	Prevents protein synthesis by binding to the 70S ribosome
pleuromutilin	Inhibits protein translation by binding the 23S rRNA
rifamycin	Inhibits bacterial RNA polymerase
sulfonamide	Inhibits DNA synthesis blocking folic acid production
Supplenntetracycline	Inhibits protein synthesis binding to ribosomal 30S subunit

Table C5.2 Changes on ARGs levels by antibiotic class in dairy manure after mesophilic AD

Antibiotic class ARG	DMF1 Δ Change ARG copies/16s rRNA	Relative change %	P value	DMF2 Δ Change ARG copies/16s rRNA	Relative change %	P value
acridine dye	-0.0128	-100	0.001	-0.0266	-100	0.0001
aminocoumarin	-0.0007	-100	0.50	-0.0017	-43.04	0.32
aminoglycoside	0.0510	34.88	0.13	-0.1256	-49.92	0.02
beta-lactams	-0.0426	-100	0.0001	-0.0543	-91.41	0.27
diaminopyrimidine				-0.0049	-100	0.50
fluoroquinolone	0.0060	148.8	0.50	-0.0039	-100	0.0001
glycopeptide	0.0158	39.62	0.43	0.0225	107.7	0.16
MLS	-0.1008	-20.15	0.43	-0.2047	-31.83	0.26
multidrug	-0.1784	-44.36	0.01	-0.3469	-61.2	0.31
nitroimidazole	0.0030	122.9	0.50	-0.0013	-14.84	0.41
nucleoside	0.0219	540.7	0.50	0.0036	87.8	0.5000
peptide	0.0374	17.74	0.18	-0.0359	-15.15	0.05
phenicol	-0.0106	-100	0.50	-0.0234	-71.89	0.13
pleuromutilin	-0.0023	-40.18	0.09	0.0134	Inf	0.18
rifamycin	0.0020	23.35	0.47	-0.0127	-71.35	0.36
sulfonamide	0.0003	3.871	0.77	-0.0067	-31.11	0.70
tetracycline	0.0146	6.369	0.68	-0.0855	-30.89	0.21

Appendix D: Chapter 6 supplementary materials

Supplementary Figures

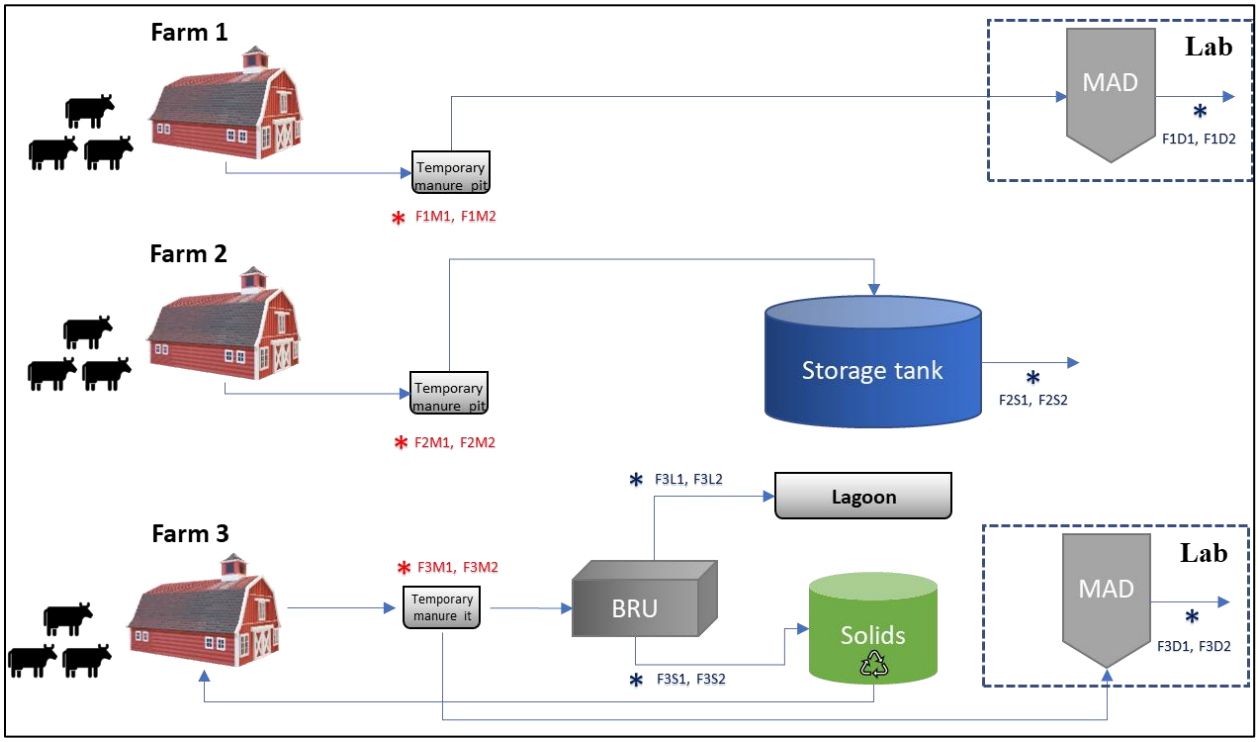

Figure D6.1 Manure management strategies and sampling points. Red stars (*) represent untreated manures; Blue stars (*) represent treated manures. Farm 2 operated under an antibiotic-free regime. BRU: bedding recovery unit. MAD: mesophilic anaerobic digester.

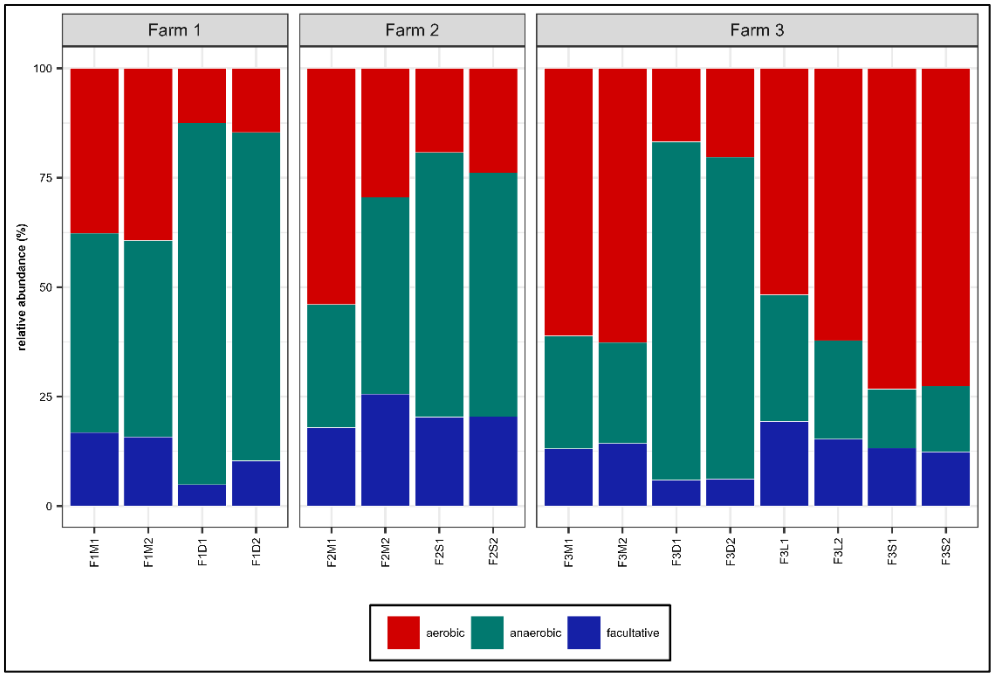

Figure D6.2 Microbial communities by respiration type.

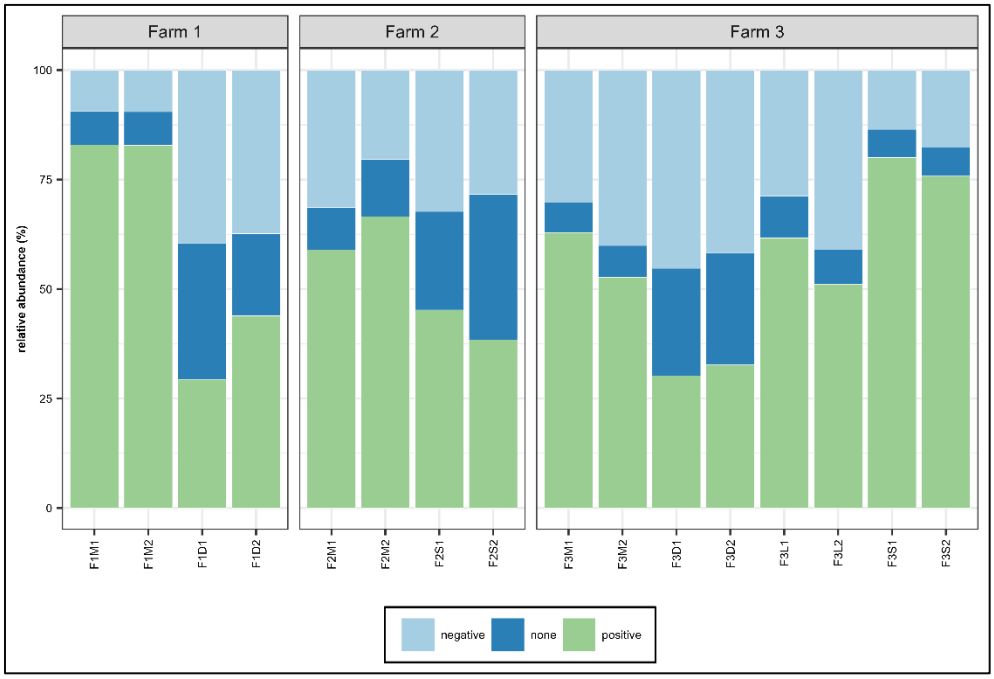

Figure D6.3 Microbial communities by Gram stain. Archaea and bacteria with non-defined stain were grouped as none.

Supplementary Tables

Table D6.1 Physicochemical properties of untreated and treated manures.

Farm	Sample	COD *g/L*	dCOD *g/L*	TS *g/L*	VS *g/L*	Alkalinity g/L
Farm 1	F1M1	73.6 ± 6.1	17.8 ± 1.2	76.9 ± 0.20	65.1 ± 0.1	6.20 ± 0.1
	F1M2	44.5 ± 5.1	14.6 ± 0.2	39.0 ± 0.3	29.2 ± 0.4	8.5 ± 0.1
	F1D1	40.1 ± 2.8	7.2 ± 0.5	46.5 ± 0.1	36.1 ± 0.1	11.3 ± 0.1
	F1D2	25.3 ± 3.6	6.2 ± 0.3	30.0 ± 0.2	20.0 ± 0.2	20.5 ± 0.1
Farm 2	F2M1			53.8 ± 0.7	42.5 ± 0.6	
	F2M2	54.5 ± 3.7	16.9 ± 0.10	49.8 ± 0.8	41.2 ± 1.5	9.1 ± 0.10
	F2S1	55.0 ± 1.0	24.0 ± 0.3	44.7 ± 0.8	34.1 ± 1.8	
	F2S2	65.6 ± 3	22.9 ± 0.1	55.9 ± 0.4	40.2 ± 0.3	10.6 ± 0.10
Farm 3	F3M1	63.7 ± 1.1	18.6 + 0.2	57.0 ± 0.5	46.5 ± 0.5	9.7 ± 0.1
	F3M2	53.6 ± 3.7	14.6 ± 0.3	46.8 ± 1.1	37.0 ± 1.0	7.5 ± 0.1
	F3D1	41.8 ± 2.0	8.2 ± 0.1	40.9 ± 0.2	30.3 ± 0.6	14.2 ± 0.1
	F3D2	33.7 ± 4.0	6.7 ± 0.5	34.2 ± 0.5	24.3 ± 0.6	10.7 ± 0.2
	F3L1					
	F3L2					
	F3S1					
	F3S2					

Table D6.2 ARGs in untreated and treated manures.

Farm	Treatment	No. ARGs	ARG
Farm 1	Fresh	52	*aad(6), aadA11, aadA17, aadA24, aadA6, adeJ, ANT(6)-Ia, ANT(9)-Ia, APH(3')-IIIa, APH(6)-Id, CfxA, CfxA2, CfxA4, cmx, efrB, Erm(35), ErmQ, ErmX, evgS, ileS, lnuA, lnuB, lnuC, lnuG, LnuP, lsaE, mel, mexK, mphO, mtrA, rpoB, rpoB2, spd, sul1, sul2, tet(40), tet(W/N/W), Tet(X4), tet(Z), tet32, tet36, tet44, tetA(P), tetB(P), tetM, tetO, tetQ, tetS, tetT, tetW, tetX, ugd*
	MAD	45	*aad(6), aadA11, aadA16, aadA23, aadA24, aadA6/aadA10, aadS, ANT(6)-Ia, ANT(9)-Ia, APH(3'')-Ib, APH(3')-IIIa, APH(6)-Id, Erm(33), Erm(47), ErmA, ErmB, ErmF, ErmG, linG, lnuA, lnuB, lnuC, lnuD, lnuF, lnuG, LnuP, lsaE, mefB, mel, mphB, rphB, rpoB, rpoB2, SAT-4, sul2, tet(W/N/W), Tet(X4), tetA(P), tetB(P), tetM, tetO, tetQ, tetT, tetW, tetX*
Farm 2	Fresh	77	*aad(6), aadA13, aadA17, aadA2, aadA23, aadA24, aadA25, aadS, acrS, adeJ, ANT(6)-Ia, ANT(6)-Ib, ANT(9)-Ia, APH(2'')-If, APH(3'')-Ib, APH(6)-Id, baeS, CARB-1, CARB-6, CfxA, CfxA2, CfxA3, CfxA4, CfxA5, CfxA6, cmx, dfrD, Erm(33), Erm(35), ErmA, ErmB, floR, ileS, LlmA, lnuA, lnuB, lnuC, lnuG, LnuP, lsaE, macB, mdfA, Mef(En2), mel, mexW, mphB, msbA, pp-flo, rphB, rpoB, rpoB2, smeE, sul1, sul2, tet(31), tet(40), tet(H), tet(J), tet(W/N/W), Tet(X3), Tet(X4), tet32, tet36, tet44, tetA(P), tetB(P), tetM, tetO, tetQ, tetS, tetT, tetW, tetX, VEB-3, VEB-5, vga(E), vgaE*
	Storage	64	*aad(6), aadA, aadA15, aadA23, aadA24, adeJ, ANT(3'')-IIa, ANT(6)-Ia, ANT(6)-Ib, ANT(9)-Ia, APH(3'')-Ib, APH(6)-Id, catQ, CfxA2, CfxA4, CfxA6, EreB, Erm(33), Erm(A), ErmA, ErmF, lnuA, lnuB, lnuC, lnuG, LnuP, lsaE, Mef(En2), mefB, mel, mexK, mphM, optrA, OXA-209, OXA-226, OXA-296, OXA-34, OXA-347, OXA-36, rphB, rpoB, rpoB2, smeE, sul1, tet(31), tet(40), tet(H), tet(J), tet(W/N/W), Tet(X3), Tet(X4), Tet(X6), tet(Y), tet32, tet36, tet44, tetA(P), tetM, tetO, tetQ, tetS, tetT, tetW, tetX*
Farm 3	Fresh	86	*aad(6), aadA23, aadA24, aadS, acrD, adeF, adeJ, ANT(6)-Ia, ANT(9)-Ia, APH(3'')-Ib, APH(3')-IIIa, APH(6)-Id, CARB-14, CARB-16, CARB-5, catQ, cfr(D), cfrA, cfrC, CfxA2, CfxA4, cmlA9, cmx, efrB, EreD, Erm(33), Erm(42), Erm(47), ErmA, ErmB, ErmF, ErmQ, evgS, fexA, floR, ileS, lnuA, lnuB, lnuC, lnuD, lnuG, LnuP, lsaE, mdtM, Mef(En2), mefB, mel, mexK, mphB, mphG, msrE, mtrA, optrA, oqxB, poxtA, pp-flo, qacE, qacEdelta1, rpoB, rpoB2, SAT-1, smeE, sul2, tet(33), tet(A), tet(G), tet(K), tet(W/N/W), Tet(X3), Tet(X4), Tet(X6), tet(Y), tet32, tet36, tet44, tetA(P), tetB(P), tetM, tetO, tetQ, tetS, tetT, tetW, tetX, ugd, vanRO*
	MAD	45	*aad(6), aadA, aadA15, aadA17, aadA23, aadA24, aadS, ANT(3'')-IIa, ANT(6)-Ia, ANT(6)-Ib, APH(3'')-Ib, APH(3')-IIIa, APH(6)-Id, cfr(D), Erm(47), ErmB, ErmF, ErmG, ErmQ, lnuB, lnuC, lnuG, LnuP, lsaE, mefB, mel, rpoB, rpoB2, SAT-4, sul1, sul2, tet(W/N/W), Tet(X3), Tet(X4), tet36, tet44, tetA(48), tetA(P), tetB(P), tetM, tetO, tetQ, tetT, tetW, tetX*
	BRU-liquids	102	*aad(6), aadA, aadA15, aadA17, aadA23, aadA24, aadA8, aadA8b, aadS, acrB, adeF, adeJ, ANT(3'')-IIa, ANT(6)-Ia, ANT(6)-Ib, ANT(9)-Ia, APH(3'')-Ib, APH(3')-Ia, APH(3')-IIIa, APH(6)-Id, BahA, CARB-14, CARB-5, catQ, ceoB, cfr(B), cfr(D), cfrA, CfxA, CfxA2, CfxA4, CfxA6, cmlA9, cmx, CRP, efrB, emeA, Erm(33), Erm(35), ErmA, ErmB, ErmF, ErmT, fexA, floR, ileS, lmrD, lnuA, lnuB, lnuC, lnuG, LnuP, lsaE, mdtC, mdtF, mdtG, mdtM, Mef(En2), mefE, mel, MexB, mexW, mphC, msrE, MuxB, optrA, OXA-209, OXA-347, poxtA, pp-flo, qacE, qacEdelta1, rpoB, rpoB2, smeE, sul1, sul2, tet(A), tet(G), tet(H), tet(J), tet(W/N/W), Tet(X3), Tet(X4), Tet(X5), Tet(X6), tet36, tet44, tetA(P), tetB(P), tetM, tetO, tetQ, tetS, tetT, tetW, tetX, ugd, vanE, vanRD, vga(E), vgaE*
	BRU-solids	93	*aad(6), aadA, aadA15, aadA2, aadA23, aadA24, aadA6, aadA6/aadA10, aadS, abeM, ACI-1, adeJ, adeK, ANT(3'')-IIa, ANT(6)-Ia, ANT(9)-Ia, APH(3'')-Ib, APH(3')-Ia, APH(3')-IIIa, APH(6)-Id, CARB-10, CARB-14, CARB-16, CARB-5, cfr(D), cfrA, cmx, dfrD, efrA, efrB, emeA, Erm(33), ErmA, ErmB, ErmC, ErmT, ErmX, ErmY, fexA, floR, ileS, IMP-11, IMP-27, lmrD, lnuA, lnuB, lnuC, lnuE, lnuG, LnuP, lsaE, mdtB, Mef(En2), mefC, mefE, mel, MexB, mexK, msrE, mupA, optrA, oqxB, OXA-347, poxtA, pp-flo, rpoB, rpoB2, SAT-1, smeE, sul1, sul2, TEM-117, TEM-118, TEM-192, tet(31), tet(39), tet(40), tet(L), tet(W/N/W), Tet(X3), Tet(X4), Tet(X6), tet32, tet36, tet44, tetA(P), tetM, tetQ, tetS, tetT, tetW, tetX, ugd*

Table D6.3 BacMet resistance genes in untreated and treated manures.

Farm	Treatment	No. genes	BacMet genes
Farm 1	Fresh	18	*acn, cadD, mco, silP, tcrB, arsB, merA, tcrY, tcrA, tcrZ, adeJ, evgS, fabK, mexK, smrA, copA, pcoA, copG*
	MAD	3	*tcrB, tcrA, copB*
Farm 2	Fresh	31	*acn, adeJ, czcA, czrA, fabI, gadC/xasA, merR, mexW, nreB, ruvB, rpoS, smeE, srpB, tbtB, tcrB, ttgH, yodD, bcrC, copA, tcrY, tcrA, baeS, gadA, gadB, mdfA/cmr, ompD/nmpC, ziaA, kdeA, nfsA, marR, sodB*
	Storage	10	*tcrB, adeJ, cusA/ybdE, mexK, silA, ruvB, recG, smeE, copA, tcrA*
Farm 3	Fresh	37	*acn, acrD/yffA, bepE, cadC, emrD, golT, mdtM/yjiO, mexK, nczA, qacE, qacEdelta1, silP, smrA, tcrB, acrD, arsB, copA, pcoA, tcrY, tcrA, copG, adeG, adeJ, cusA/ybdE, evgS, fabK, oqxB, pstA, rpoS, sdeB, silA, smeE, smeT, G2alt, copF, copD, copC*
	MAD	8	*tcrB, arsB, copB, bcrC, tcrA, acn, ziaA, copA*
	BRU-liquids	39	*adeJ, cadC, cusA/ybdE, gadC/xasA, mexW, ruvB, rpoS, sdeY, silA, recG, smeE, srpB, tcrB, terD, ttgH, vmeB, arsB, merA, tcrY, tcrA, tcrZ, acn, actP, adeG, bexA, dpr/dps, emeA, fabI, mdtC/yegO, mdtG/yceE, mdtM/yjiO, mexB, mexF, qacE, qacEdelta1, copA, mdtC, pcoA, copG*
	BRU-solids	40	*acn, adeJ, adeK, arsH, cadC, golT, merA, mexB, mexK, ruvB, pstB, rpoS, recG, tcrB, terC, ALU1-P, G2alt, actS, arsB, merB3, merP, merR1, merT, tcrY, tcrA, tcrZ, copG, copD, abeM, emeA, emhB, mdtB/yegN, oqxB, sdeB, smeE, srpB, tbtB, mdtB, bcrC, chtR*

Table D6.4 MGE-related genes in untreated and treated manures.

Farm	Treatment	No. MGEs	MGEs
Farm 1	Fresh	167	*uvrB, recA, Q5HMP5, ftsK1, trbE, tnsD, oppC, Q54944, repD, Q06238, tnpC1, hsdM, nisX1, tnpA_IS6100, tnp, repC, groL, mobE, rep, EF_0125, repE, ISS1N, WP_000351512.1, zeta, tnpA, mod, tnpA_1, dnaK, tnpB, hflB, traF, WP_002321882.1, traA, tnpA1, ftsK, hsdR_2, dcm, clpX, polC, dnaB, dnaX, clpB, topA, mutS2, smc, noc, uvrA, umuC, hsdM_1, gyrB, gyrA, pcrA, ltrA_2, parA, topB, alkA, ltrA_1, ssb_2, groEL, mutS, uvrC, dnaG, topB_1, clpC, mutL, higA, dnaE, hsdR, mobC, dpnA, helD, polA, traG, ltrA, clpP_2, cas2, clpP, virE, recR, hin, uvrA_2, tnpR, dnaA, ruvB, istB, uvrA_1, recJ, hin_1, F7LRR2, ung, radA, prrC, gp56, orf17, ardA, int, IS1216, repA, tnpA6100, mob, traC_2, traI, mobN1, A5UJT3, tnpAISAba125cp2, WP_001284311.1, parB, repB, int1, WP_001186919.1, Int-Tn, tra8, WP_002293753.1, uvrB_2, tnp1, xerD, recF, tnpB1, mobA, pre, IS1086, Q06237, bin3, WP_010890867.1, mutS_2, recT, ruvC, xerC, clpP1, rarA, rnr, rnhA, traK, rad50, hhaIM_3, umuD, nucS, recN, mcrB, nusA, hhaIM_2, ssb, holA, rdgB, recQ, bamA, hpaIIM, pinR, priA, ORF20, ORF21, ORF32, ISPpu12, virB4, lys, ORF, trbL, traC_1, tnpX, traN_1, tnpC, pilT_3, tsrF, mobB, dnaC, P03862, gp6*
	MAD	89	*clpP, tnpA_IS6100, tnp, mobE, dnaK, recA, hflB, tnpA, polC, uvrB, mutS_2, clpB, uvrA, polA, mutS2, umuC, dnaB, clpX, groL, gyrA, ltrA_2, dnaX, rarA, smc, clpC, mutS, dpnA, hin, ltrA, gyrB, dcm, hsdM, recQ, tnpR, dnaA, ltrA_1, traG, istB, uvrA_1, pinR, mcrB, ORF1, ORF2, ORF20, ORF21, ORF32, topB, eexR, eexS, hsdR, traE, rteB, int, IS1216, tnpZ, nikA, tnpA6100, traC_1, traC_2, repA, tnpB, Int-Tn, ftsK, xhlA, tnsD, Q57231, trbJ, parA, traA, noc, ssb_2, groEL, uvrC, dut, dnaE, ltrA_5, recR, hin_1, xerD_4, dinB, traK, prrC, A0A0M9FEW5, orf17, mob, topB_1, uvrD, A5UJT3, tnpB1*
	Fresh	169	*clpP, clpX, uvrB, recA, tnpA, tnsB, tnsA, intN1, Q57231, Q54944, tnpC1, gyrA, repF, WP_012816704.1, tnp, insI, parA, mobE, repE, EF_0125, tnpB, repA, mrr_2, ssb, rep, dnaK, hflB, WP_000798699.1, hsdR, uvrC, recO, hsdM, recJ, dnaB, groL, pcrA, uvrA, mutS2, smc, traG, lexA, comM, ltrA, hsdM_1, gyrB, dnaA, ltrA_2, clpB, xerD, dnaX, topB, groEL, mutS, parC, rex, dnaG, clpC, cinA, xerD_3, ssb_2, traK, rad50, ruvC, dnaE, dpnA, recQ, terL, hhaIM_2, polA, ydiP, recN, ltrA_5, ftsK, holA, ruvB, ung2, xerD_1, rarA, recR, hin, tnpR, mutY, uvrA_2, bamA, dcm, mazG, priA, istB, uvrA_1, hin_1, ligA, traM, hhaIM_3, topB_1, ung, dnaN, s035, ORF2, ORF21, ORF32, ISPpu12, traD, fic, prrC, traE, gp56, pglX, orf17, orf23, int, IS1216, tnpZ, mobA, mob, traC_1, traI, mobN1, traC_4, traC_2, Int-Tn, tnpX, exc, traN_1, istA, tnpC, WP_001284311.1, pilT_3, recG, tsrF, int1, repB, radA, dnaC, parE, tnpB1, Q99338, tnpA1, 23, gp23, B, insE3, P16943, pre, ISS1N, mutL, polC, pilT_1, topA, recT, sbcD, mcrB, vsr, mug, oppF, rnhA, F7LRR2, clpP1, hipA, hpaIIM_1, hsdR_2, A0A2X2IGH7, WP_087879933.1, traI_1, repR, tra8, mukF, uvrB_2, insE4, repN*
	Storage	156	*uvrB, dpnA, clpP, 20, nisX1, repF, tnp, tnpR, tnpA, insF, dnaK, recA, tnpB, hflB, dinB, recJ, dnaB, groL, mutS2, uvrA, traG, lexA, gyrA, clpX, dcm, hsdM_1, gyrB, hsdM, ltrA_2, clpP1, clpB, dnaX, rarA, topB, groEL, mutS, rnr, topB_1, xerD_3, mutL, traK, clpC, hhaIM_1, ltrA, umuD, umuC, dnaE, ung, ssb_2, ruvC, rep, polA, xerD, P, dut, hhaIM_3, ftsK, ung2, xerD_1, recQ, xerS, pcrA, mazG, ltrA_1, priA, uvrA_1, hin_1, ruvB, F7LRR2, hhaIM_2, hsdR, ydiP, prrC, traE, orf17, orf23, lys, traQ, traH, rteB, hpaIIM_1, int, Int-Tn, IS1216, mobA, traC_1, traC_2, mobN1, traC_4, tnpX, mobC, traN_1, pilT_3, topA, recR, dnaN, tnpB1, dam, ftsK1, trbE, tnsE, tnsA, oppA, tnpC1, hsdS, insB, tnpA_1, insI, pre, ISS1N, zeta, trbEB, insA, brxL, repC, polC, cas1, repA, hin, smc, ssb, hsdR_2, dpnM_2, Q79DZ0, yafQ_1, yafQ, clpP_2, ligA, virE, holA, dnaA, haeIIIM_1, pemK, higA, intS_4, ISPpu12, mobI, hipA, gp56, traP, nikA, mob, virB4_3, ardA, istA, kfrA, traA, repB, traN, repR, traM, ecoRIR, tra8, radA, parC, tnpA1*

Farm	Treatment	No. MGEs	MGEs
Farm 3	Fresh	231	*mutS, tnp, motB, 28, rIIB, NGR_a00240, NGR_a03160, xis, pre, trbF, tnsE, tnsA, oppD, repS, repR, P0A4M1, Q06238, Q06237, truncated-tnp, tnpC1, P0A4M2, traL, recN, hsdM, nisX1, EF_0125, transposase, tnpA, dinB, tnpA_1, groL, tnpR, rep, traA, tnpB, ISS1N, WP_000351512.1, zeta, mobA, hsdR, ruvB, dnaK, traG, recA, hflB, WP_002321882.1, brxL, parA, higB, ftsK, repB, uvrC, polC, dnaB, cas2, cas1, clpB, mutS2, smc, noc, dnaG, uvrB, uvrA, pcrA, comM, clpX, ltrA, hhaIM, gyrB, gyrA, radC, dnaA, ltrA_2, dnaX, dut, topB, ltrA_1, hup, ssb_2, groEL, rex, recR, xerD_3, addA, ruvC, mutL, clpC, nucS, intS, dnaE, dpnA, dcm, recQ, xerD, traK, clpP_2, hsdM_1, xerD_1, hhaIM_2, rarA, mutY, uvrA_2, hupB, repA, mazG, priA, istB, uvrA_1, recJ, F7LRR2, terL, ung, dnaN, radA, ORF2, ORF20, soj, prrC, hsdS1, soj_2, traM, orf23, traQ, rteB, traD, int, Xis-Tn, IS1216, topB_1, traC_1, traI, mobN1, traC_4, traC_2, traN_1, A5UJT3, WP_141194616.1, Q7BQ53, WP_011727856.1, A0A0P0CPN4, A0A3Q9IGW5, tnpAISAba125cp2, tnpC, tsrF, hsdS, trbL, mobL, mobB, tniR_3, hfq, traO, WP_001186919.1, Int-Tn, WP_002293753.1, ligA, uvrB_2, virB11, tnp1, tnpB1, tnpA1, A0A514DJL2, 7, gp16, gp18, gp42, gp13, 6, 18, g159, clpP, F, ftsK1, oppC, intN1, traJ, mobE, traR, mod, WP_010890867.1, traX_2, traF, traI_2, WP_000798699.1, traX, traI_1, insA, clpA, nth, cas9, umuC, xerC, hhaIM_3, rnr, ycbY, rad50, ssb, pilT, polA, insC1, pcrA_2, holA, ung2, hin, recT, gp26, ssb_1, virB4, ISPpu12, ORF, traE, gp56, orf17, traH, tnpX, parA1, A0A2Z3N9D2, ORF1, pilT_3, mob, mobC, dnaJ, int1, tra8, dnaC, parC, Q99338, ompA, rph, P03862, gp37, holB*
	MAD	92	*clpX, clpP, A, Q57231, gyrA, tnp, traA, dnaK, tnpB, hflB, ltrA, hsdR, hsdR_2, dnaX, ftsK, groL, uvrA, dnaB, traG, hhaIM_1, ltrA_2, clpB, tnpA, uvrB, tnpR, recA, groEL, mutS, clpC, dcm, dnaE, dpnA, hhaIM_2, gyrB, clpP_2, hsdM, virE, recQ, hin, uvrA_2, dnaA, uvrA_1, hin_1, ruvB, ORF1, ORF2, ORF20, ORF32, topB, prrC, traE, orf17, orf23, rteB, int, mob, traC_1, uvrD, repA, A5UJT3, WP_127822567.1, A0A1W7AEW0, tnsE, tnpB1, mobA, tnpA1, 41, ftsK1, parB, Q06237, tnpA_IS6100, ligD, insI, brxL, rarA, alkA, ltrA_1, smc, hsdS, dut, polA, xerD_4, traK, topB_1, traC_2, istB, WP_011727856.1, ligB, traM, WP_001186919.1, Int-Tn, hfq*
Farm 3	BRU-liquids	218	*uvrB, dpnA, recA, groL, tnpB, ftsK1, yubI, tnsE, tnsD, tnsC, repD, tnpC1, ligA, EF_0125, tnp, tnpA, insI, mobE, rumB, parA, repE, dnaK, dnaG, hflB, ftsK, rep, brxL, tnpR, hsdR_2, uvrC, clpA, clpX, hsdM, polC, dnaB, dnaX, mutS_2, cas2, cas1, clpB, polA, mutS2, smc, ruvC, uvrA, traG, pcrA, gyrB, gyrA, umuC, hsdM_1, hhaIM_1, dnaA, ltrA_2, dut, dcm, topB, ssb, dinD, groEL, rex, rdgB, topB_1, recR, addA, mutL, traK, rad50, clpC, mutS, ltrA, umuD, A0A0R5RPQ5, Q79DZ0, hsdR, rarA, recQ, dnaE, ung, mobC, hin, hhaIM_2, pilT_2, ruvA, hhaIM_3, ltrA_5, recJ, clpP, virE, holA, ung2, mutY, mrr, priA, ruvB, istB, uvrA_1, dnaN, mazG, xerC, hin_1, xerD, dinB, mecB, F7LRR2, ydiP, ORF21, ISPpu12, traH, fic, trhF, prrC, hipA, soj_2, traO, gp56, pglX, int, mobA, mob, mobN1, traC_4, traC_2, tnpX, traN_1, A5UJT3, tnpAISAba125cp2, pilT_3, sit, cpl, int1, repR, traM, radA, hda, pilB, parE, parC, tnpB1, tnpA1, repN, S', tnsA, oppA, oppF, intN1, repS, traA, Q06238, Q06237, truncated-tnp, hsdS, nisX1, insI3, insB, insI1, repA1, ISS1N, pifA, traI, insA, insL3, repB, repC, cas9, comM, radC, lexA, ssbB, ltrA_1, rnr, xerD_3, recN, hhaIM, lexA_1, tnsB, recT, xerD_1, uvrA_2, ssb3, gp26, ssb_1, ssb_2, dinG, recE_1, ORF2, ORF20, ORF32, parB, traR, traV, traE, orf17, orf23, lys, rteB, ardA, IS1216, traQ, yhhI, tra905, istA, tnpC, WP_127822567.1, rep3, tnpA_IS6100, A0A1W7AEW0, mobL, topA, mobB, hfq, dpnB, WP_001186919.1, Int-Tn, tra8, WP_002293753.1, tnp1, S*
	BRU-solids	222	*uvrB, hupB, ssb2, groL, clpP, tnp, Q5HMP5, dnaB, NGR_a00240, trbE, insA8, tnsE, tnsC, tnsA, repS, Q57231, Q54944, rlx, parB, parA, repR, orf19, Q06238, Q06237, truncated-tnp, cas3, tnpC1, traL, repA, mutS, hsdM, nisX1, gyrA, tnpR, EF_0125, repF, EDI97729.1, repB, tnpA, insB, insI, pre, repA1, insF, bin3, mobE, insA_1, tnpB, ISS1N, WP_000351512.1, ssb, zeta, insB6, hsdR, mod, tnpA_1, recD2, dnaK, recA, hflB, trbEB, traI, traF, traE, traD, WP_002321882.1, rep, brxL, traA, IS26, WP_000798699.1, insA_3, ftsK, hsdR_2, clpX, mutS2, traG, pcrA, dnaA, ltrA_2, clpB, ruvC, dnaX, topB, alkA, hup, groEL, rex, parC, recR, clpC, uvrA, gyrB, Q79DZ0, ung, dnaE, clpP_2, ltrA, sbcC, hsdM_1, hflD, rarA, recT, sbcB, mazG, priA, istB, uvrA_1, traK, dcm, smc, ruvB, F7LRR2, radA, ORF21, prrC, sth368IM, A0A3L8G246, soj_2, gp56, pglX, orf17, orf23, s035, int, IS1216, mob, traC_4, mobC, traN_1, A0A2Z3N9D2, A0A178TR40, Q7BQ53, tnpAISAba125cp2, tnpC, WP_001284311.1, WP_127822567.1, rep3, pilT_3, tsrF, dnaJ, trhW, mobL, mobB, pilR, int1, traM, dpnB, WP_001186919.1, Int-Tn, tra8, WP_002293753.1, addA, polB, seqA, ligA, uvrB_2, tnp1, P14506, cas1-1, dnaC, comEB, tnpB1, Q99338, tnpA1, ompA, mobA, polC, gp42, 10, orf14, ftsK1, tnsD, tnsB, insH_1, oppC, repE, traO, rumB, insH6, insA, traC_5, uvrC, clpA, ltrA_1, clpP1, recJ, lexA, comM, dnaG, topB_1, xerD_3, dinG, pilT, recQ, pilT_2, hin, xerD_1, uvrD, polA, hin_1, hhaIM, recN, xerD, dnaN, ORF32, intS_4, traN, traU, hipA, trbL, ardA, soj_7, traC_1, mobN1, recG, A0A1W7AEW0, pilB, parE, rph, ORF06, ORF16*

Table D6.5 Microbial genera associated with ARGs and MGEs

Genus	Phylum	Genes
Glutamicibacter	Actinomycetota	*adeJ, floR, pp-flo, smeE, optrA, CARB-14, CARB-5, fexA, EF_0125, Q06238, radA, tnpC1, traI, tnpC, tsrF, ligA, parC, pglX, tnsA, traD, repR, mobL, repS, soj_2, truncated-tnp, tnsC, BAC0018, BAC0293, BAC0335, BAC0359, BAC0373, BAC0056*
Comamonas	Pseudomonadota	*Tet(X3), floR, pp-flo, smeE, CARB-14, CARB-5, fexA, tnpC1, traI, ung, xerD, priA, recN, ruvC, tnpC, comM, ligA, mazG, mutY, rex, tnsA, xerD_3, addA, repS, clpA, BAC0293, BAC0335, BAC0359, BAC0373*
Staphylococcus	Bacillota	*efrB, optrA, fexA, EF_0125, IS1216, ISS1N, Q06238, WP_001186919.1, WP_002293753.1, WP_002321882.1, mod, tnp1, tnpC1, uvrB_2, Q06237, mobB, recT, tnpC, tsrF, mobL, repS, truncated-tnp, BAC0003, BAC0740*
Psychrobacter	Pseudomonadota	*efrB, floR, pp-flo, optrA, poxtA, CARB-14, CARB-5, fexA, Q06238, WP_000351512.1, WP_001186919.1, WP_002293753.1, traI, Q06237, tnpC, comM, traD, repR, addA, mobL, repS, truncated-tnp, BAC0056*
Amylolactobacillus	Bacillota	*efrB, EF_0125, IS1216, ISS1N, Q06238, WP_001186919.1, WP_002293753.1, WP_002321882.1, mod, tnp1, tnpC1, Q06237, mobB, recT, tnpC, tsrF, repS, BAC0003, BAC0740*
Carnobacterium	Bacillota	*efrB, tetS, adeJ, EF_0125, IS1216, Q06238, WP_001186919.1, WP_002293753.1, WP_002321882.1, int1, parA, radA, rep, tnp1, tnpC1, tnpC, tsrF, BAC0740, BAC0018*
Empedobacter	Bacteroidota	*APH(6)-Id, adeJ, Tet(X3), optrA, radA, tnpC, ligA, parC, traD, tnsE, BAC0018, BAC0335, BAC0355, BAC0056*
Advenella	Pseudomonadota	*floR, pp-flo, poxtA, CARB-14, CARB-5, fexA, WP_000351512.1, traI, comM, repR, addA, mobL, repS*
Macrococcus	Bacillota	*floR, pp-flo, poxtA, CARB-14, CARB-5, fexA, traI, comM, addA, mobL, repS*
Myroides	Bacteroidota	*Tet(X3), floR, pp-flo, traI, recN, comM, mazG, rex, tnsA, xerD_3, addA*
Petrocella	Bacillota	*floR, optrA, CARB-14, CARB-5, fexA, Q06238, WP_002293753.1, Q06237, tnpC, mobL, repS*
Thermus	Deinococcota	*pp-flo, optrA, Q06238, WP_000351512.1, WP_002293753.1, traD, repR, truncated-tnp, BAC0056*
Erysipelothrix	Bacillota	*efrB, IS1216, WP_002293753.1, int1, radA, rep, pilT_3, BAC0740*
Moraxella	Pseudomonadota	*floR, optrA, CARB-14, CARB-5, fexA, tnpC, addA, repS*
Brevibacterium	Actinomycetota	*floR, pp-flo, WP_000351512.1, nisX1, repB, mobB, BAC0003*
Caldimonas	Pseudomonadota	*floR, pp-flo, recN, comM, xerD_3, addA*
Parabacteroides	Bacteroidota	*Mef(En2), ung, hhaIM_2, rad50, ung2, xerD_1*
Paracoccus	Pseudomonadota	*floR, pp-flo, cfr(D), poxtA, mobB, trbL*

Genus	Phylum	Genes
Brucella	Pseudomonadota	*floR, pp-flo, cfr(D), poxtA, addA*
Oligella	Pseudomonadota	*ugd, cas2, nisX1, tnpC1, uvrC*
Phocaeicola	Bacteroidota	*CfxA2, CfxA4, Mef(En2), ISPpu12, ung2*
Dietzia	Actinomycetota	*ugd, poxtA, mobB, BAC0003*
Enterococcus	Bacillota	*tetS, hsdM_1, mobN1, traC_4*
Halopseudomonas	Pseudomonadota	*pglX, BAC0293, BAC0355, BAC0373*
Jeotgalicoccus	Bacillota	*tetS, ssb, ligA, parC*
Paracholeplasma	Mycoplasmatota	*Mef(En2), OXA-347, Tet(X6), xerD_1*
Pseudoxanthomonas	Pseudomonadota	*floR, pp-flo, cfr(D), addA*
Acholeplasma	Mycoplasmatota	*Mef(En2), Tet(X3), mobA*
Amphibacillus	Bacillota	*fexA, traI, recT*
Latilactobacillus	Bacillota	*ileS, tet(40), tnp1*
Mycolicibacterium	Actinomycetota	*floR, pp-flo, poxtA*
Pseudomonas	Pseudomonadota	*ligA, traC_4, BAC0355*
Rhodococcus	Actinomycetota	*cfr(D), poxtA, addA*
Acetivibrio	Bacillota	*ErmF, ORF1*
Acinetobacter	Pseudomonadota	*Tet(X3), tnpC1*
Aerococcus	Bacillota	*lnuG, tetS*
Aliarcobacter	Pseudomonadota	*traH, insA*
Aminipila	Bacillota	*rteB, traQ*
Flaviflexus	Actinomycetota	*cas2, mutL*
Gudongella	Bacillota	*ErmF, ORF1*
Haploplasma	Mycoplasmatota	*Mef(En2), traC_4*
Lactobacillus	Bacillota	*rad50, parE*
Lactococcus	Bacillota	*tet44, nisX1*
Limosilactobacillus	Bacillota	*BAC0574, BAC0575*
Mammaliicoccus	Bacillota	*nisX1, BAC0003*
Micromonospora	Actinomycetota	*cfr(D), poxtA*
Paucilactobacillus	Bacillota	*insB, truncated-tnp*

Genus	Phylum	Genes
Pediococcus	Bacillota	*ileS, tnp1*
Porphyromonas	Bacteroidota	*traH, traQ*
Pseudoclostridium	Bacillota	*ErmF, ORF1*
Ruminiclostridium	Bacillota	*ErmF, ORF1*
Streptococcus	Bacillota	*nisX1, uvrC*
Syntrophomonas	Bacillota	*ErmF, ORF1*
Thermoclostridium	Bacillota	*ErmF, ORF1*
Ureibacillus	Bacillota	*floR, pp-flo*
Aminobacterium	Synergistota	*ErmF*
Bacteroides	Bacteroidota	*traK*
Blautia	Bacillota	*topB_1*
Dehalobacterium	Bacillota	*mefB*
Dehalococcoides	Chloroflexota	*mefB*
Herbinix	Bacillota	*ORF1*
Kocuria	Actinomycetota	*noc*
Ligilactobacillus	Bacillota	*repE*
Luteimonas	Pseudomonadota	*cas2*
Methanosarcina	Euryarchaeota	*mefB*
Paeniclostridium	Bacillota	*uvrA_2*
Proteiniphilum	Bacteroidota	*mefB*
Pseudoprevotella	Bacteroidota	*ANT(6)-Ib*
Thermobacillus	Bacillota	*sul2*
Thermobispora	Actinomycetota	*poxtA*
Weissella	Bacillota	*cas2*
Xanthomonas	Pseudomonadota	*ANT(6)-Ib*

Appendix E: Chapter 7 supplementary materials

Supplementary Figures

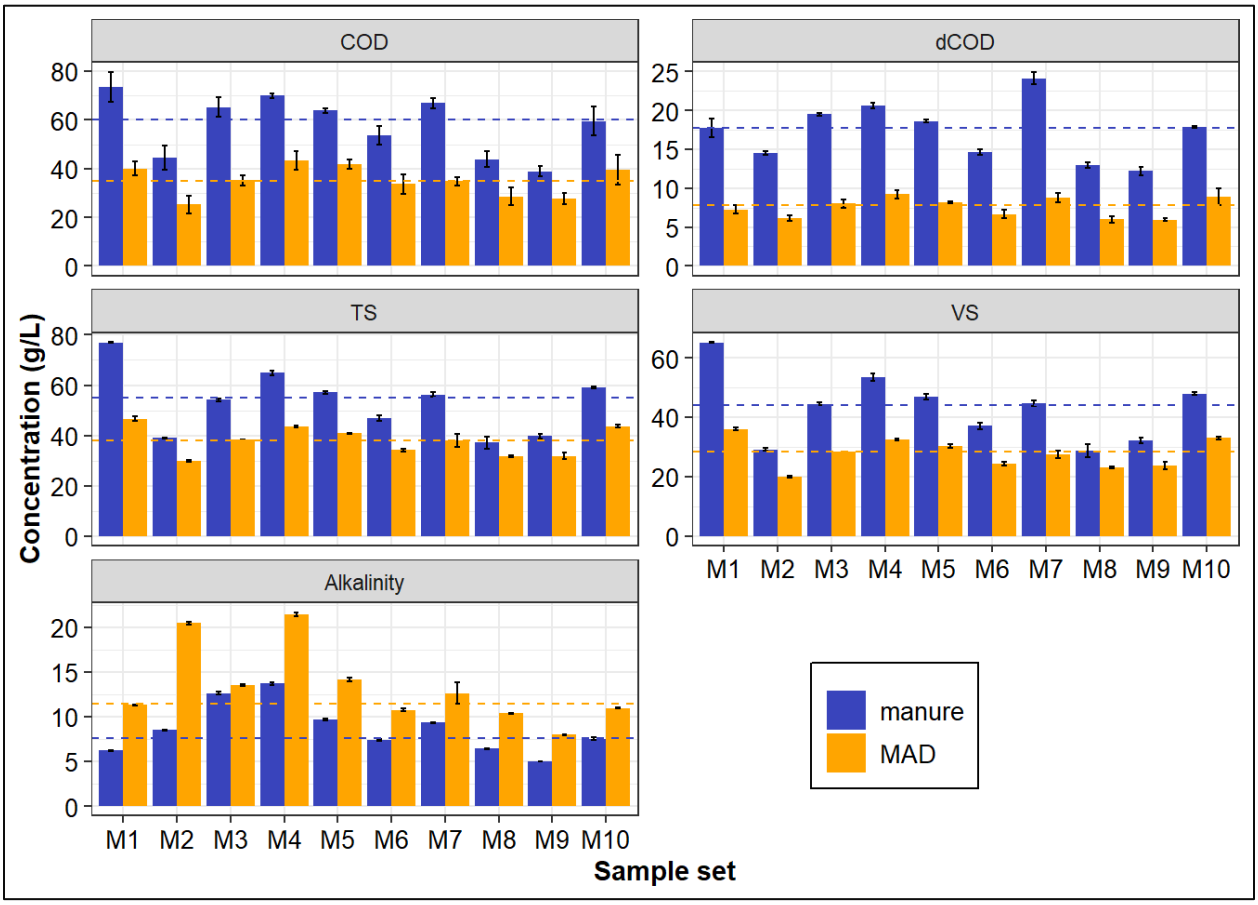

Figure E7. 1 Physicochemical properties of manures and digestates. Note that digestate samples MAD7.1, MAD7.2, MAD7.3, and MAD7 were averaged and included in sample set number 7.

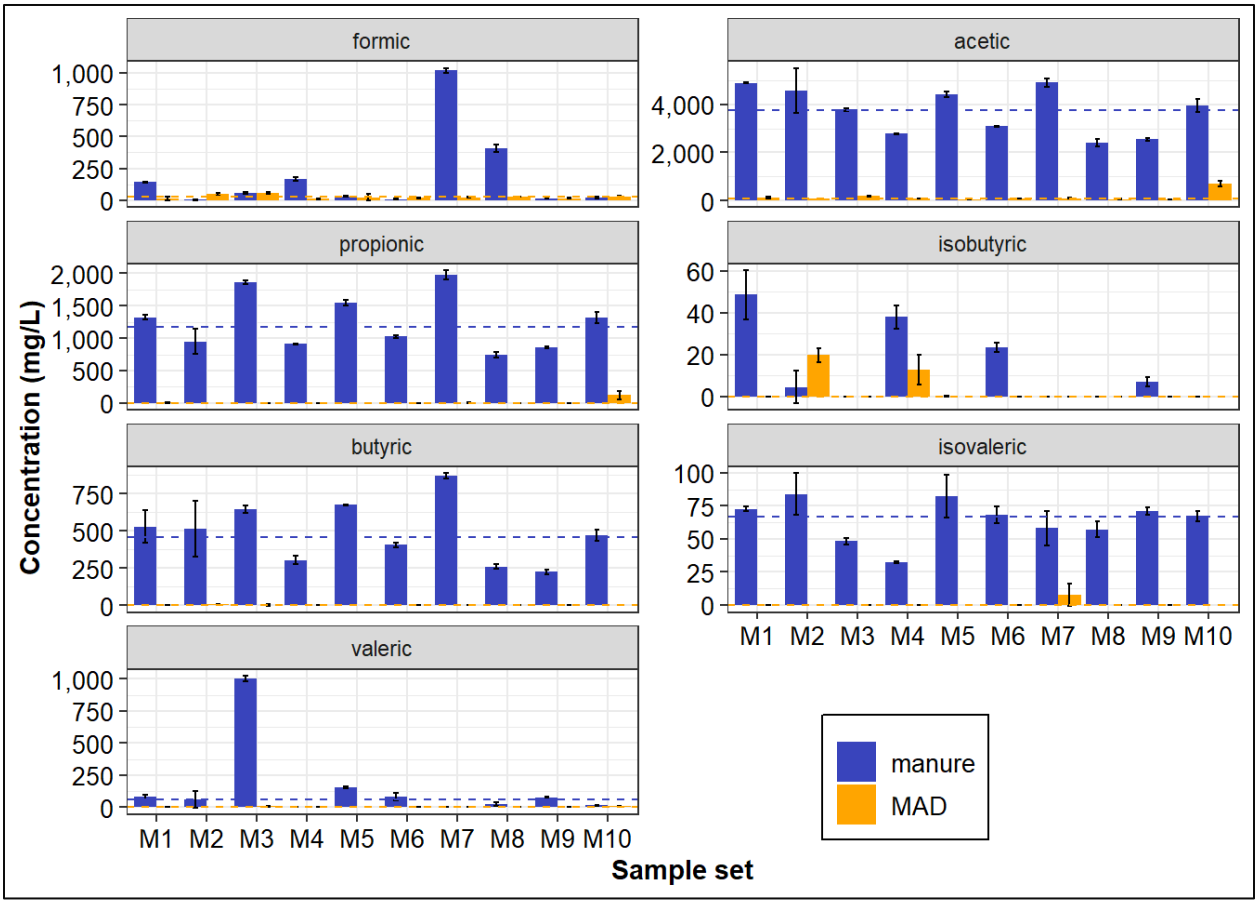

Figure E7.2 VFAs abundance in manures and digestates. Note that digestate samples MAD7.1, MAD7.2, MAD7.3, and MAD7 were averaged and included in sample set number 7.

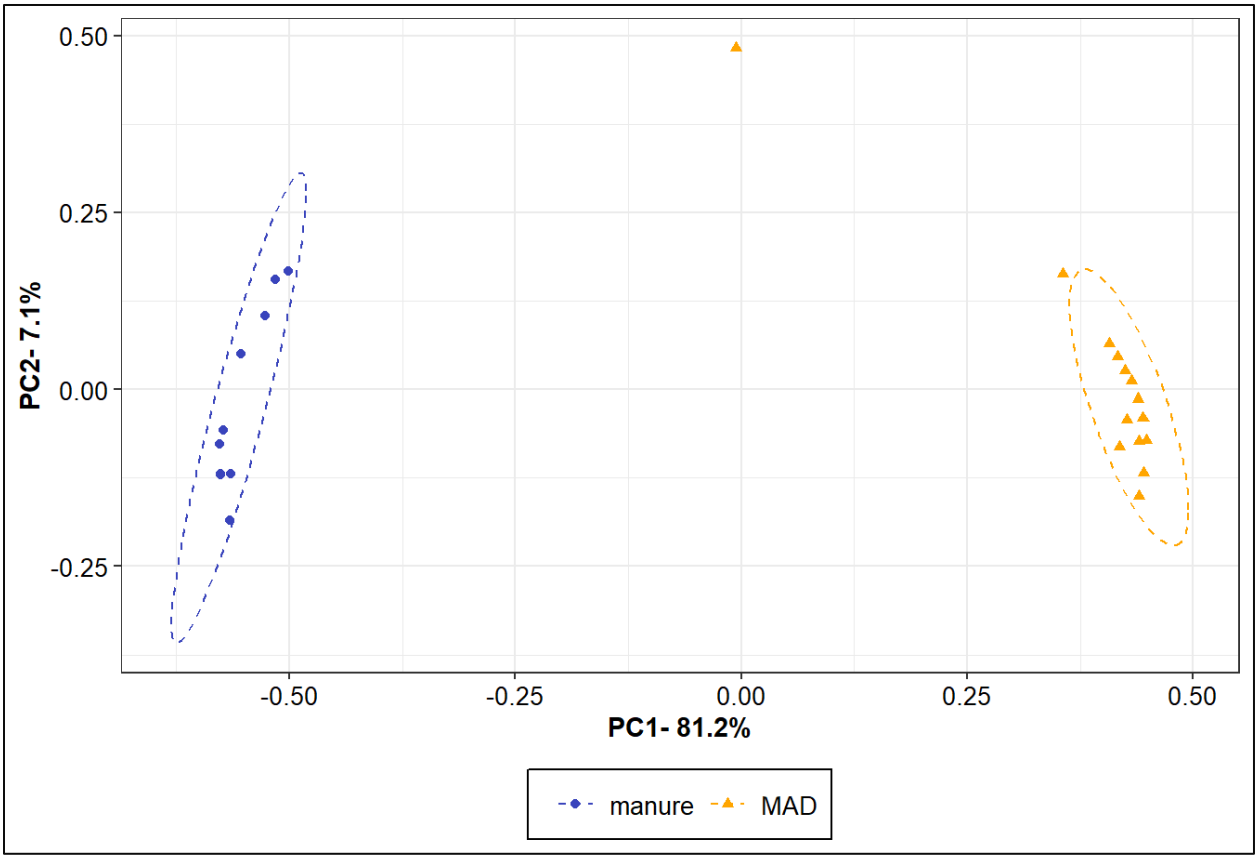

Figure E7.3 Principal coordinates analyses of physicochemical and VFAs profiles.

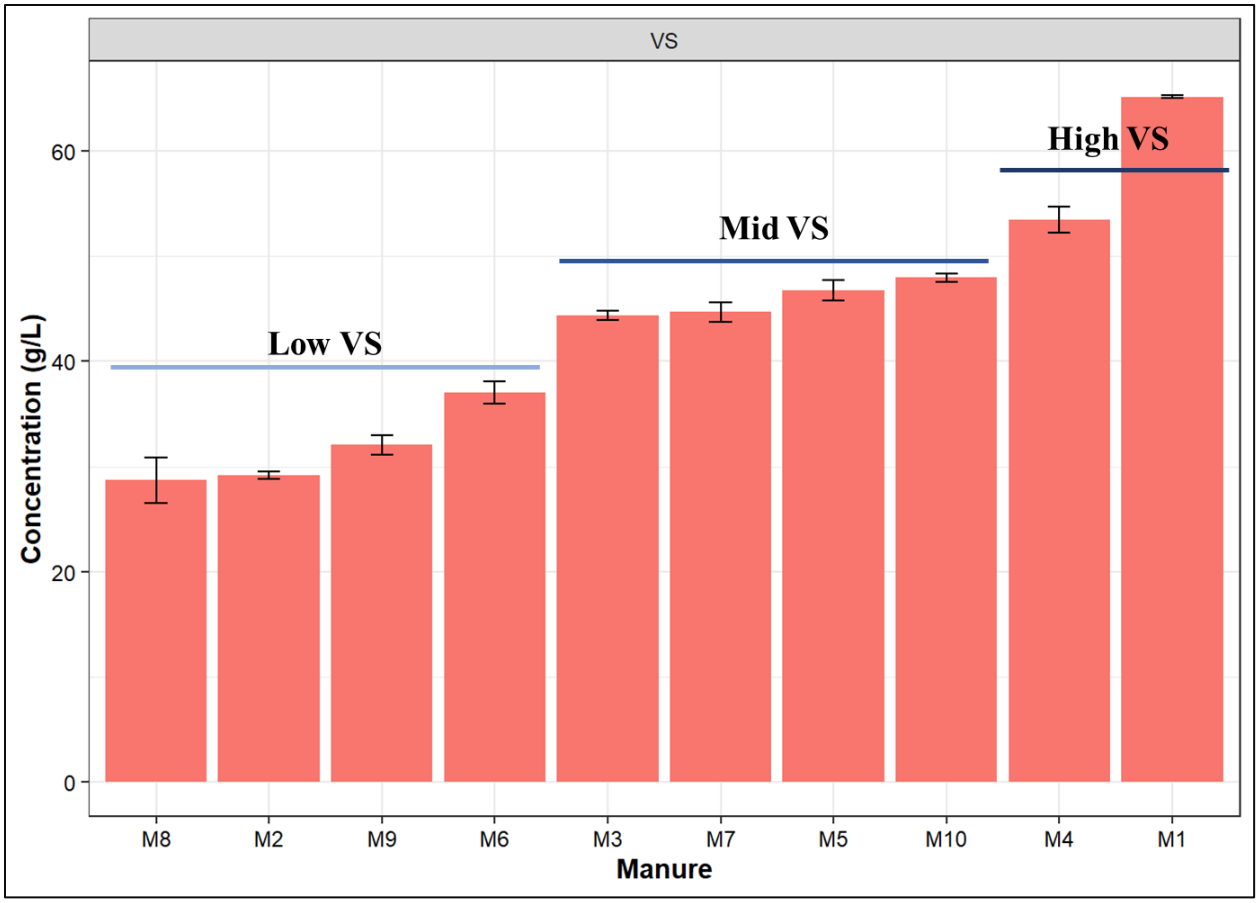

Figure E7.4 Levels of manure VS. Error bars represent STD.

Supplementary Tables

Table E7.1 ARGs in individual manure (M) and digestate (MAD) samples.

Sample	N. ARGs	ARGs
M1	32	*aad(6), ANT(6)-Ia, ANT(9)-Ia, efrB, ErmQ, ErmX, ileS, lnuA, lnuC, lnuG, LnuP, mel, mtrA, rpoB, rpoB2, spd, sul1, tet(40), tet(W/N/W), tet(Z), tet32, tet36, tet44, tetA(P), tetB(P), tetM, tetO, tetQ, tetS, tetT, tetW, ugd*
M2	46	*aad(6), aadA11, aadA17, aadA24, aadA6, adeJ, ANT(6)-Ia, ANT(9)-Ia, APH(3')-IIIa, APH(6)-Id, CfxA, CfxA2, CfxA4, cmx, efrB, Erm(35), evgS, ileS, lnuA, lnuB, lnuC, lnuG, LnuP, lsaE, mel, mexK, mphO, rpoB, rpoB2, sul1, sul2, tet(40), tet(W/N/W), Tet(X4), tet36, tet44, tetA(P), tetB(P), tetM, tetO, tetQ, tetS, tetT, tetW, tetX, ugd*
M3	68	*aad(6), aadA14, aadA23, aadA24, aadS, acrB, acrD, adeJ, adeK, ANT(6)-Ia, ANT(9)-Ia, APH(3'')-Ib, APH(6)-Id, CARB-14, CARB-5, catB3, cfrA, CfxA2, CfxA4, cmlA9, efrB, Erm(33), ErmA, ErmB, ErmG, ErmT, ErmX, floR, IMP-13, IMP-33, lnuA, lnuB, lnuC, lnuG, LnuP, lsaE, mdtE, mefC, mel, mphE, mphG, msrE, optrA, OXA-209, OXA-347, pp-flo, rpoB, rpoB2, sul1, sul2, tet(31), tet(39), tet(G), tet(W/N/W), Tet(X3), Tet(X4), Tet(X5), Tet(X6), tet44, tetA(P), tetB(P), tetM, tetQ, tetS, tetT, tetW, tetX, ugd*
M4	58	*aad(6), aadA, aadA10, aadA16, aadA23, aadA24, aadS, abeM, adeF, adeJ, ANT(3'')-IIa, ANT(6)-Ia, ANT(9)-Ia, APH(3'')-Ib, APH(6)-Id, cmlA9, efrB, Erm(33), ErmA, ErmB, ErmF, evgA, floR, ileS, lnuA, lnuB, lnuC, lnuG, LnuP, lsaE, mdtB, mel, MexB, mexK, mtrA, optrA, oqxB, pp-flo, qacE, qacEdelta1, rpoB, rpoB2, smeE, sul1, sul2, tet(39), tet(W/N/W), Tet(X3), Tet(X4), tet44, tetA(P), tetB(P), tetM, tetQ, tetS, tetT, tetW, tetX*
M5	58	*aad(6), acrD, ANT(6)-Ia, APH(3'')-Ib, APH(6)-Id, catQ, cfr(D), cfrA, cfrC, cmx, efrB, Erm(42), ErmB, ErmF, ErmQ, floR, ileS, lnuA, lnuB, lnuC, lnuD, lnuG, LnuP, lsaE, mdtM, Mef(En2), mel, mexK, mphB, msrE, mtrA, optrA, poxtA, pp-flo, qacE, qacEdelta1, rpoB, rpoB2, sul2, tet(G), tet(K), tet(W/N/W), Tet(X3), Tet(X4), tet(Y), tet36, tet44, tetA(P), tetB(P), tetM, tetO, tetQ, tetS, tetT, tetW, tetX, ugd, vanRO*
M6	67	*aad(6), aadA23, aadA24, aadS, adeF, adeJ, ANT(6)-Ia, ANT(9)-Ia, APH(3'')-Ib, APH(3')-IIIa, APH(6)-Id, CARB-14, CARB-16, CARB-5, cfr(D), CfxA2, CfxA4, cmlA9, efrB, EreD, Erm(33), Erm(47), ErmA, ErmQ, evgS, fexA, floR, lnuA, lnuB, lnuC, lnuG, LnuP, lsaE, Mef(En2), mefB, mel, mphG, optrA, oqxB, poxtA, pp-flo, qacE, qacEdelta1, rpoB, rpoB2, SAT-1, smeE, sul2, tet(33), tet(A), tet(W/N/W), Tet(X3), Tet(X4), Tet(X6), tet32, tet36, tet44, tetA(P), tetB(P), tetM, tetO, tetQ, tetS, tetT, tetW, tetX, ugd*
M7	48	*AAC(6')-Ie-APH(2'')-Ia, aad(6), aadA4, aadA5, ANT(6)-Ia, ANT(9)-Ia, APH(6)-Id, cfrC, CfxA2, CfxA4, cmx, dfrG, dfrK, efrB, Erm(33), Erm(A), ErmA, ErmB, floR, ileS, lnuA, lnuB, lnuC, lnuG, LnuP, lsaE, mel, mphC, mphE, msrA, pp-flo, rpoB, rpoB2, sul1, tet(K), tet(W/N/W), tet32, tet36, tet44, tetA(P), tetB(P), tetM, tetO, tetQ, tetS, tetT, tetW, vanYG1*
M8	47	*aad(6), aadA, aadA15, aadA27, ACI-1, ANT(3'')-IIc, ANT(6)-Ia, ANT(6)-Ib, ANT(9)-Ia, APH(3')-IIIa, APH(6)-Id, cfr(D), CfxA2, CfxA4, cmx, efrB, Erm(33), ErmA, ErmB, ErmT, ErmX, floR, ileS, lnuA, lnuB, lnuC, lnuE, lnuG, LnuP, lsaE, mel, optrA, pp-flo, rpoB, rpoB2, smeE, sul1, sul2, tet(K), tet(W/N/W), tet36, tetM, tetO, tetQ, tetS, tetT, tetW*
M9	53	*aad(6), aadS, ANT(6)-Ia, ANT(6)-Ib, ANT(9)-Ia, APH(3'')-Ib, APH(3')-IIIa, CARB-14, CARB-5, cfr(D), CfxA2, CfxA4, CfxA6, cmx, dfrA1, dfrA15, efrA, efrB, ErmB, ErmC, floR, ileS, lmrD, lnuA, lnuB, lnuC, lnuG, LnuP, lsaE, Mef(En2), mefB, mel, mphB, optrA, poxtA, pp-flo, rpoB, rpoB2, sul1, sul2, tet(A), tet(K), tet(W/N/W), Tet(X4), tet36, tetM, tetO, tetQ, tetS, tetT, tetW, tetX, ugd*
M10	58	*aad(6), aadA17, aadA2, aadA23, aadA24, aadA3, aadA9, ANT(6)-Ia, ANT(9)-Ia, APH(3'')-Ib, APH(6)-Id, blaR1, catQ, cfr(D), cfrA, CfxA, CfxA2, CfxA6, cmlA9, cmx, efrA, efrB, Erm(33), ErmA, ErmB, floR, lnuA, lnuB, lnuC, lnuG, LnuP, lsaE, Mef(En2), mefB, mel, mphB, optrA, OXA-347, poxtA, rpoB, rpoB2, tet(33), tet(W/N/W), Tet(X4), tet(Z), tet32, tet36, tet44, tetA(P), tetB(P), tetM, tetO, tetQ, tetS, tetT, tetW, tetX, ugd*

Sample	N. ARGs	ARGs
MAD1	34	*aad(6), aadA11, aadA23, aadA24, aadA6/aadA10, ANT(6)-Ia, ANT(9)-Ia, APH(3'')-Ib, APH(3')-IIIa, APH(6)-Id, Erm(33), ErmA, ErmB, ErmF, ErmG, linG, lnuA, lnuB, lnuC, lnuF, LnuP, lsaE, mefB, mel, rpoB2, tet(W/N/W), Tet(X4), tetA(P), tetB(P), tetM, tetQ, tetT, tetW, tetX*
MAD2	35	*aad(6), aadA16, aadA23, aadA24, aadS, ANT(6)-Ia, ANT(9)-Ia, APH(3')-IIIa, Erm(47), ErmB, ErmF, linG, lnuA, lnuB, lnuC, lnuD, lnuF, lnuG, LnuP, lsaE, mefB, mel, mphB, rphB, rpoB, rpoB2, SAT-4, sul2, tet(W/N/W), tetA(P), tetM, tetO, tetQ, tetT, tetW*
MAD3	37	*aad(6), aadA11, aadA23, aadA24, aadA6/aadA10, aadS, ANT(6)-Ia, cfr(D), Erm(33), Erm(35), ErmA, ErmB, ErmF, ErmG, ErmQ, linG, lnuB, lnuF, LnuP, lsaE, mefB, mel, rpoB, rpoB2, sul1, sul2, tet(B), tet(W/N/W), Tet(X3), Tet(X4), tetA(P), tetM, tetO, tetQ, tetT, tetW, tetX*
MAD4	25	*aad(6), aadS, ANT(6)-Ia, APH(3')-IIIa, ErmB, ErmF, lnuB, lnuC, lnuG, LnuP, lsaC, lsaE, mefB, mel, rphB, rpoB, rpoB2, SAT-4, tet(G), tet(W/N/W), tet36, tetA(P), tetM, tetQ, tetW*
MAD5	35	*aad(6), aadA, aadA23, aadA24, aadS, ANT(3'')-IIa, ANT(6)-Ia, ANT(6)-Ib, APH(3'')-Ib, APH(3')-IIIa, APH(6)-Id, cfr(D), Erm(47), ErmB, ErmF, ErmQ, lnuB, lnuC, LnuP, lsaE, mefB, mel, rpoB, rpoB2, SAT-4, sul1, tet(W/N/W), tet36, tet44, tetA(48), tetA(P), tetB(P), tetM, tetQ, tetW*
MAD6	36	*aad(6), aadA, aadA15, aadA17, aadA23, aadA24, aadS, ANT(6)-Ia, ANT(6)-Ib, APH(3'')-Ib, cfr(D), ErmB, ErmF, ErmG, ErmQ, lnuB, lnuC, lnuG, LnuP, lsaE, mefB, mel, rpoB, rpoB2, sul2, tet(W/N/W), Tet(X3), Tet(X4), tet36, tetA(P), tetM, tetO, tetQ, tetT, tetW, tetX*
MAD7	35	*aad(6), ANT(6)-Ia, ANT(6)-Ib, ANT(9)-Ia, APH(3')-IIIa, cfrC, Erm(47), Erm(A), ErmB, ErmC, ErmF, ErmT, lnuB, lnuC, lnuD, lnuE, lnuG, LnuP, lsaE, mel, OXA-347, rpoB, rpoB2, tet(W/N/W), tet36, tet44, tetA(P), tetB(P), tetM, tetQ, tetS, tetT, tetW, vanRI, vanRO*
MAD7.1	36	*aad(6), ANT(6)-Ia, ANT(9)-Ia, APH(3'')-Ib, APH(3')-IIIa, cfr(D), Erm(47), ErmB, ErmF, linG, lnuA, lnuB, lnuC, lnuF, lnuG, LnuP, lsaE, mefB, mel, mphB, optrA, OXA-347, rpoB, rpoB2, SAT-4, tet(L), tet(W/N/W), tet(Z), tet36, tet44, tetM, tetQ, tetS, tetT, tetW, vanRI*
MAD7.2	31	*aad(6), aadA23, aadA24, ANT(6)-Ia, ANT(9)-Ia, APH(3'')-Ib, APH(3')-IIIa, APH(6)-Id, Erm(47), Erm(A), ErmB, ErmF, lnuA, lnuB, lnuC, lnuG, lsaE, mefB, mel, OXA-209, OXA-347, rpoB, rpoB2, smeE, tet(W/N/W), tet32, tet44, tetM, tetQ, tetT, tetW*
MAD7.3	23	*ANT(6)-Ia, ANT(9)-Ia, APH(3')-IIIa, APH(6)-Id, EreA, EreA2, Erm(33), Erm(47), ErmA, ErmB, ErmC, ErmF, ErmG, lnuB, lnuC, lsaE, mel, rpoB, SAT-4, tet(W/N/W), tet36, tetM, tetW*
MAD7.4	36	*aad(6), aadA23, aadA24, ANT(6)-Ia, ANT(6)-Ib, ANT(9)-Ia, APH(3'')-Ib, APH(3')-IIIa, CARB-14, CARB-5, CfxA2, CfxA4, Erm(47), ErmB, ErmF, ErmT, ErmY, linG, lnuB, lnuC, lnuF, LnuP, lsaE, mel, rpoB, rpoB2, SAT-4, sul2, tet(G), tet(W/N/W), tet44, tetA(P), tetM, tetQ, tetS, tetW*
MAD8	33	*AAC(6')-Ie-APH(2'')-Ia, aadA10, aadA16, aadA23, aadA24, ANT(6)-Ia, ANT(9)-Ia, APH(3')-IIIa, APH(6)-Id, Erm(47), ErmB, ErmF, ErmG, lnuA, lnuB, lnuC, lnuG, LnuP, lsaE, mefB, mel, OXA-209, OXA-347, rpoB2, tet(31), tet(W/N/W), tet36, tetA(P), tetM, tetQ, tetS, tetT, tetW*
MAD9	37	*aad(6), aadA11, aadA23, aadA24, aadA6/aadA10, aadS, ANT(6)-Ia, ANT(9)-Ia, APH(3'')-Ib, APH(6)-Id, Erm(47), ErmB, ErmF, lnuA, lnuB, lnuC, lnuG, LnuP, lsaE, mefB, mel, optrA, rpoB, rpoB2, tet(C), tet(W/N/W), tet(Z), tet36, tet44, tetB(48), tetB(P), tetM, tetQ, tetS, tetT, tetW, vanRA*
MAD10	31	*aad(6), aadA10, aadA23, aadA24, aadA6/aadA10, ANT(6)-Ia, ANT(9)-Ia, APH(6)-Id, Erm(33), Erm(47), ErmA, ErmB, ErmF, lnuB, lnuC, lnuG, LnuP, lsaE, mel, OXA-347, rpoB, rpoB2, salA, tet(W/N/W), tetB(P), tetM, tetO, tetQ, tetT, tetW, vanRI*

Table E7.2 MGEs in individual manure (M) and digestate (MAD) samples.

Sample	no. MGEs	MGEs
M1	119	*uvrB, recA, Q5HMP5, ftsK1, trbE, tnsD, oppC, Q54944, repD, Q06238, tnpC1, hsdM, nisX1, tnpA_IS6100, tnp, repC, groL, mobE, rep, EF_0125;, repE, ISS1N, WP_000351512.1, zeta, tnpA, mod, tnpA_1, dnaK, tnpB, hflB, traF, WP_002321882.1, traA, tnpA1, ftsK, hsdR_2, dcm, clpX, polC, dnaB, dnaX, clpB, topA, mutS2, smc, noc, uvrA, umuC, hsdM_1, gyrB, gyrA, pcrA, ltrA_2, parA, topB, alkA, ltrA_1, ssb_2, groEL, mutS, uvrC, dnaG, topB_1, clpC, mutL, higA, dnaE, hsdR, mobC, dpnA, helD, polA, traG, ltrA, clpP_2, cas2, clpP, virE, recR, hin, uvrA_2, tnpR, dnaA, ruvB, istB, uvrA_1, recJ, hin_1, F7LRR2, ung, radA, prrC, gp56, orf17, ardA, int, IS1216, repA, tnpA6100, mob, traC_2, traI, mobN1, A5UJT3, tnpAISAba125cp2, WP_001284311.1, parB, repB, int1, WP_001186919.1, Int-Tn, tra8, WP_002293753.1, uvrB_2, tnp1, xerD, recF, tnpB1, mobA*
M2	125	*uvrB, recA, Q5HMP5, pre, IS1086, Q06237, tnpC1, hsdM, nisX1, tnpA_IS6100, int, tnp, tnpA, groL, bin3, repE, rep, EF_0125;, tnpB, ISS1N, hsdR, mod, dnaK, hflB, WP_010890867.1, WP_002321882.1, parA, dnaB, pcrA, mutS_2, dcm, ftsK, clpB, mutS2, recT, smc, noc, ruvC, uvrA, gyrA, clpX, umuC, gyrB, dnaA, polA, xerC, ltrA_2, clpP1, dnaX, rarA, topB, dnaG, alkA, uvrC, rnr, rnhA, traK, clpC, hhaIM_3, umuD, nucS, recN, mutS, mcrB, dnaE, nusA, dpnA, hhaIM_2, ssb, traG, clpP_2, ltrA, clpP, mutL, holA, rdgB, recQ, recR, tnpR, uvrA_2, bamA, ltrA_1, istB, hpaIIM, uvrA_1, groEL, pinR, recJ, priA, ORF21, ORF32, ISPpu12, virB4, orf17, lys, ORF, IS1216, trbL, tnpA6100, topB_1, traC_1, mobN1, repA, tnpX, mobC, traN_1, A5UJT3, tnpC, pilT_3, tsrF, mob, repB, mobB, int1, WP_001186919.1, Int-Tn, WP_002293753.1, uvrB_2, tnp1, dnaC, ruvB, tnpB1, tnpA1, P03862, gp6*
M3	162	*clpP, clpX, uvrB, recA, Q5HMP5, dnaB, NGR_a03160, Q93NB3, tnsD, tnsC, tnsB, tnsA, intN1, Q54944, repR, traA, Q06238, Q06237, traI, truncated-tnp, tnpC1, mutS, pcrA, nisX1, tnpA, IS26, EF_0125;, R00164, repC, xerC, tnp, traW, tnpR, sspA, insB, groL, insF, mobE, traO, int, repE, ISS1N, mod, rep, dnaK, tnpB, hflB, istB, traF, traE, WP_002321882.1, uvrA_2, ftsK, uvrA, hsdR, polC, recJ, dinB, clpB, mutS2, smc, recT, traG, gyrA, comM, thyA, recQ, gyrB, dnaA, ltrA_2, dnaX, rarA, topB, alkA, hup, ssb_2, groEL, uvrC, rex, dnaG, xerD_3, addA, mutL, clpC, dnaE, ltrA, dcm, dpnA, xerD, traK, hsdM, holA, ruvB, xerD_1, recR, mutY, clpA, mazG, ltrA_1, priA, uvrA_1, ruvC, recN, dnaN, repA, ydiP, ung, radA, ISPpu12, ORF, prrC, orf17, orf23, lys, traH, virD2, trbF, Int-Tn, IS1216, mobA, mob, tnpA6100, topB_1, hsdR_2, traQ, mobC, traN_1, A5UJT3, WP_141194616.1, tnpAISAba125cp2, tnpC, WP_001284311.1, WP_127822567.1, mobL, rnhA, pilT_3, recG, tsrF, A0A1W7AEW0, repB, dnaJ, hfq, cpl, dnaE2, repS, traM, WP_001186919.1, WP_002293753.1, atl, oppD, ung2, uvrB_2, tnp1, pilB, dnaC, tnpB1, tnpA1, rph, gp42, 61, 8, 22*
M4	149	*clpX, recA, c3172, dnaB, ftsK1, NGR_a03160, traG, tnsD, tnsA, Q54944, P0A4M1, repD, Q06238, Q06237, truncated-tnp, tnpC1, P0A4M2, pcrA, int, gyrA, tnp, tnpA_IS6100, EF_0125;, repC, insB, WP_048337391.1, istB, groL, traA, bin3, traO, traL, tnpB, rep, repE, ISS1N, WP_000351512.1, virB9, tnpC, hsdR, dnaK, hflB, ftsK, insA, WP_002321882.1, SE_p102, WP_000798699.1, higB, polC, cas1, clpB, mutS2, smc, uvrA, comM, hsdM_1, thyA, tnpA, gyrB, hsdM, dnaA, ltrA_2, dnaX, topB, uvrB, ltrA_1, ssb_2, groEL, mutS, uvrC, rex, recR, hsdR_2, ruvC, ltrA, dcm, 5, nucS, clpC, holA, dnaE, mobC, dpnA, recJ, recQ, recN, ltrA_5, ruvB, rarA, tnpR, uvrA_2, gp26, uvrA_1, mazG, dnaN, radA, s035, ORF21, ORF32, trbC, trbJ, prrC, pglX, orf23, traH, IS1216, mob, tnpA6100, traK, topB_1, traC_4, traI, mobN1, traC_2, traQ, tnpX, traN_1, nisX1, BQ2027_MB1076;, A5UJT3, CBU_0006;, WP_001284311.1, pilT_3, recG, tsrF, repB, mobL, pilX9, gin, ung, dnaE2, traM, WP_001186919.1, dinG, repA, Int-Tn, pre, cpl, WP_002293753.1, trbL, mukF, ligA, uvrB_2, nmoT, tnpB1, Q99338, tnpA1, ompA, mobA*
M5	168	*mutS, tnp, motB, 28, rIIB, NGR_a00240, NGR_a03160, xis, pre, trbF, tnsE, tnsA, oppD, repS, repR, P0A4M1, Q06238, Q06237, truncated-tnp, tnpC1, P0A4M2, traL, recN, hsdM, nisX1, EF_0125;, transposase, tnpA, dinB, tnpA_1, groL, tnpR, rep, traA, tnpB, ISS1N, WP_000351512.1, zeta, mobA, hsdR, ruvB, dnaK, traG, recA, hflB, WP_002321882.1, brxL, parA, higB, ftsK, repB, uvrC, polC, dnaB, cas2, cas1, clpB, mutS2, smc, noc, dnaG, uvrB, uvrA, pcrA, comM, clpX, ltrA, gyrB, gyrA, radC, dnaA, ltrA_2, dnaX, dut, topB, ltrA_1, hup, ssb_2, groEL, rex, recR, xerD_3, addA, ruvC, mutL, clpC, nucS, intS, dnaE, dpnA, dcm, recQ, xerD, traK, clpP_2, hsdM_1, xerD_1, hhaIM_2, rarA, mutY, uvrA_2, hupB, repA, mazG, priA, istB, uvrA_1, recJ, F7LRR2, terL, ung, dnaN, radA, ORF2, ORF20, soj, prrC, hsdS1, soj_2, traM, orf23, traQ, rteB, traD, int, Xis-Tn, IS1216, topB_1, traC_1, traI, mobN1, traC_4, traC_2, traN_1, A5UJT3, WP_141194616.1, Q7BQ53, WP_011727856.1, A0A0P0CPN4, A0A3Q9IGW5, tnpAISAba125cp2, tnpC, tsrF, hsdS, trbL, mobL, mobB, tniR_3, hfq, traO, WP_001186919.1, Int-Tn, WP_002293753.1, ligA, uvrB_2, virB11, tnp1, tnpB1, tnpA1, A0A514DJL2, 7, gp16, gp18, gp42, gp13, 6, 18, g159*

Sample	no. MGEs	MGEs
M6	173	*clpP, clpX, uvrB, dpnA, groL, F, ftsK1, tnsE, tnsA, oppC, intN1, repS, repR, P0A4M1, traA, mobA, Q06238, Q06237, tnpC1, P0A4M2, ligA, hsdM, int, nisX1, gyrA, traJ, EF_0125;, repB, tnp, traG, tnpA, mobE, traK, traR, rep, tnpB, ISS1N, WP_000351512.1, hsdR, mod, dnaK, recA, hflB, ftsK, WP_010890867.1, traX_2, repA, traF, WP_002321882.1, traI_2, brxL, traI, tnpR, WP_000798699.1, traX, traI_1, insA, uvrC, clpA, dut, nth, polC, dnaB, cas2, cas9, dinB, clpB, mutS2, smc, mutS, uvrA, pcrA, comM, umuC, gyrB, dnaA, xerC, ltrA_2, ltrA, dnaX, hhaIM_3, rarA, topB, ltrA_1, groEL, rex, rnr, recR, xerD_3, addA, ruvC, dnaE, ycbY, mutL, rad50, clpC, ssb, dcm, pilT, hhaIM_2, polA, xerD, recN, insC1, pcrA_2, holA, ung2, xerD_1, recQ, hin, mutY, recT, mazG, priA, gp26, ssb_1, ssb_2, uvrA_1, recJ, ruvB, F7LRR2, topB_1, ung, dnaN, radA, virB4, ORF2, ORF20, ISPpu12, ORF, prrC, traE, gp56, orf17, traH, rteB, traD, Int-Tn, IS1216, trbL, tnpX, traC_2, traQ, parA1, traN_1, istB, A5UJT3, A0A2Z3N9D2, ORF1, tnpC, pilT_3, tsrF, mob, mobC, dnaJ, mobL, mobB, int1, traM, WP_001186919.1, tra8, WP_002293753.1, dnaC, parC, tnpB1, Q99338, tnpA1, ompA, rph, P03862, gp37, 7, holB*
M7	139	*tnp, 19, dnaB, parA, pre, trbE, tnsA, oppD, repS, repR, orf19, rlx, hsdM, nisX1, bin3, tnpA_IS6100, tnpA, istA, mobA, int2, mob, mobE, EF_0125;, repE, ISS1N, rep, dnaK, recA, tnpB, trbEB, WP_010890867.1, WP_002321882.1, dnaG, hhaIM_2, mutS2, uvrB, groL, pcrA, mutS_2, ftsK, hflB, clpB, rnj, topA, polA, smc, uvrA, gyrA, clpX, gyrB, ltrA_2, uvrC, topB, ssb, dcm, ltrA_1, ssb_2, groEL, mutS, xerD, topB_1, dpnA, clpC, mcrB, hsdR, rarA, ung, dnaE, pilT, hin, dut, recT, traG, ltrA, ltrA_5, cas2, clpP, hhaIM_3, dnaA, ydiP, uvrA_2, recN, tnpR, erF, priA, gp26, istB, uvrA_1, clpP1, mazG, mecB, recJ, dnaN, vsr, ung2, radA, recR, ORF1, ORF32, prrC, soj_2, orf17, orf23, ardA, int, IS1216, tnpA6100, traI, mobN1, tnpX, traK, ORFAB, tpn, tnpC, repB, dnaJ, traA, repA, recG, holA, int1, traM, preA, Int-Tn, tra8, WP_002293753.1, sin, ruvA, uvrB_2, tnp1, parC, nmoT, P18416, tnpB1, tnpA1, dnaX, polC, mazF, P03862*
M8	115	*tnp, dnaB, tnsC, Q57231, Q54944, traA, Q06237, Rep, ltrA, int, tnpR, hsdS, EDI97729.1, tnpA, pre, repE, EF_0125;, tnpB, ISS1N, zeta, rep, ruvB, dnaK, recA, hflB, WP_010890867.1, traI, traE, dnaX, WP_002321882.1, SE_p102, repB, mutS2, clpX, hsdM, groL, nusG, clpB, topA, repA, uvrB, uvrA, gyrA, gyrB, dnaA, ltrA_2, uvrC, traG, dcm, topB, ltrA_1, groEL, dnaG, topB_1, smc, mutL, recN, nucS, mutS, dnaE, pcrA, dpnA, polA, traK, ftsK, lexA, hin, uvrA_2, mrr, priA, istB, recJ, hup, dnaN, umuC, hin_1, uvrA_1, clpC, dinB, cas7c, rarA, rnhA, prrC, hsdR, soj_2, trbC, res, Int-Tn, IS1216, mobA, traC_1, mobN1, traC_4, hsdR_2, tnpX, mobC, A5UJT3, tsrF, mobL, addA, holA, mobB, dnaE2, repR, parA, WP_001186919.1, WP_002293753.1, tnp1, dnaC, xerD, tnpB1, tnpA1, polC, mazF, P03862*
M9	133	*dpnA, recA, Q5HMP5, dnaB, pre, tnsB, intN1, P16942, repD, tnpC1, hsdS, hsdM, nisX1, tnpA_IS6100, EF_0125;, repC, tnp, tnpA, int2, rep, repE, ISS1N, mobA, hsdR, mod, ruvB, dnaK, traD, tnpB, hflB, traK, WP_002321882.1, traN, traA, traI, WP_115203650.1, uvrC, dcm, clpX, uvrB, pcrA, dinB, ftsK, clpB, groL, mutS2, uvrA, traG, gyrA, comM, gyrB, dnaA, ltrA_2, ruvC, ssb, dnaX, rarA, dnaE, topB, alkA, hup, mutS, rex, dnaG, smc, recR, hsdR_2, xerD_3, addA, mutL, clpC, ltrA, ssb_2, mutY, polA, xerD, recN, hsdM_1, clpP, xerD_1, recQ, hhaIM, hin, uvrA_2, tnpR, ltrA_1, priA, istB, uvrA_1, recJ, groEL, mazG, hin_1, F7LRR2, ung, dnaN, ORF2, ORF20, prrC, orf17, orf23, lys, rteB, int, IS1216, mob, tnpA6100, topB_1, virB4_3, traC_1, mobN1, traC_4, traQ, traC_2, traN_1, A5UJT3, tpn, tnpC, repA, repB, mobC, trbL, topA, mobB, int1, Int-Tn, WP_002293753.1, uvrB_2, traB, tnp1, tnpB1, tnpA1, gp42*
M10	155	*clpP, C, A0A5Q3BC69, intN1, Q54944, repR, rlx, Q06238, Q06237, truncated-tnp, sohB_1, hsdM, resR, tnp, insB, repA1, EF_0125;, traA, tnpB, ISS1N, WP_000351512.1, hin_1, dnaK, recA, hflB, WP_010890867.1, traI, traE, WP_002321882.1, ftsK, hsdR_2, uvrC, polC, dnaB, groL, pcrA, cas9, dinB, clpB, topA, polA, mutS2, smc, hhaIM, uvrA, traG, gyrA, comM, clpX, hsdM_1, gyrB, radC, dnaA, ssb, ltrA_2, uvrB, ltrA, thyA, dnaX, rarA, ydiP, topB, tnpA, dcm, hup, groEL, rex, dnaG, topB_1, recR, clpC, xerD_3, hhaIM_1, ssb_2, addA, ruvC, mutL, 5, lexA, nucS, hsdR, dnaE, dpnA, mutS, traK, hhaIM_2, xerD, recN, clpP_2, ltrA_5, holA, ung2, xerD_1, recQ, hin, mutY, uvrA_2, terL, tnpR, rep, mazG, ltrA_1, priA, ruvB, istB, ssb_1, uvrA_1, recJ, F7LRR2, ung, dnaN, radA, virB4, prrC, repA, soj_2, orf17, traQ, traH, rteB, virD2, res, int, IS1216, mobA, mob, tnpA6100, traC_2, mobC, parA1, traN_1, tpn, A0A2Z3N9D2, A0A3G6JR17, WP_001284311.1, trbI, hsdS, dnaJ, mobL, int1, repS, parA, WP_001186919.1, preA, Int-Tn, WP_002293753.1, hflK, trbL, uvrB_2, tnpB1, tnpA1, P03862, 15, 23, gp23*
MAD1	62	*clpP, tnpA_IS6100, tnp, mobE, dnaK, recA, hflB, tnpA, polC, uvrB, clpB, uvrA, polA, mutS2, umuC, dnaB, clpX, groL, gyrA, ltrA_2, dnaX, rarA, smc, clpC, mutS, dpnA, hin, ltrA, gyrB, dcm, hsdM, recQ, tnpR, dnaA, ltrA_1, traG, istB, uvrA_1, pinR, mcrB, ORF1, ORF2, ORF20, ORF21, ORF32, topB, eexR, eexS, hsdR, traE, rteB, int, IS1216, tnpZ, nikA, tnpA6100, traC_1, traC_2, repA, tnpB, Int-Tn, ftsK*

Sample	no. MGEs	MGEs
MAD2	71	*dpnA, xhlA, clpP, tnsD, Q57231, trbJ, tnp, parA, traA, dnaK, recA, tnpB, hflB, hsdM, dnaX, dcm, smc, uvrB, noc, uvrA, tnpA, clpX, gyrB, ltrA_2, clpB, groL, rarA, topB, ltrA_1, ssb_2, groEL, uvrC, gyrA, clpC, ltrA, dut, mcrB, mutS, dnaE, hin, polA, ltrA_5, int, recQ, recR, dnaA, uvrA_1, hin_1, xerD_4, dinB, tnpR, traK, ORF1, ORF2, ORF20, ORF32, prrC, hsdR, A0A0M9FEW5, orf17, rteB, nikA, mob, topB_1, uvrD, traC_2, repA, traG, A5UJT3, Int-Tn, tnpB1*
MAD3	70	*uvrB, clpP, trbJ, tnpA_IS6100, traA, tnpB, hflB, tnpA, clpB, groL, uvrA, dnaB, traG, clpX, gyrB, ltrA_2, dnaX, rarA, topB, alkA, ltrA_1, ssb_2, smc, recA, hsdR_2, mutS, gyrA, traK, clpC, umuC, hsdR, ltrA, hin, clpP_2, hsdM, virE, recQ, recR, tnpR, dnaA, uvrA_1, clpP1, hin_1, dinB, clpA, ORF1, ORF2, ORF20, ORF21, ORF32, dcm, prrC, gp56, int, tnp, mob, traC_2, repA, mobC, istB, dnaK, tsrF, groEL, tnsB, Int-Tn, ftsK, dnaC, nmoT, tnpB1, repB*
MAD4	56	*clpP, tnpC1, tnpA_IS6100, tnp, traA, dnaK, xerD, hflB, cas9, clpB, groL, polA, dnaB, traG, dcm, ltrA_2, dnaX, rarA, tnpA, tnpR, groEL, mutS, dnaG, smc, recA, uvrB, clpC, uvrA, repA, dpnA, gyrA, ltrA, traK, hsdM, recQ, recR, gyrB, clpX, dnaA, ltrA_1, uvrA_1, hsdR, ORF1, prrC, topB, rteB, int, mob, traC_2, Int-Tn, WP_127822567.1, A0A1W7AEW0, ftsK, tnpB, tnpB1, dam*
MAD5	67	*clpX, clpP, A, Q57231, gyrA, tnp, traA, dnaK, tnpB, hflB, ltrA, hsdR, hsdR_2, dnaX, ftsK, groL, uvrA, dnaB, traG, hhaIM_1, ltrA_2, clpB, tnpA, uvrB, tnpR, recA, groEL, mutS, clpC, dcm, dnaE, dpnA, hhaIM_2, gyrB, clpP_2, virE, recQ, hin, uvrA_2, dnaA, uvrA_1, hin_1, ruvB, ORF1, ORF2, ORF20, ORF32, topB, prrC, traE, orf17, orf23, hsdM, rteB, int, mob, traC_1, uvrD, repA, A5UJT3, WP_127822567.1, A0A1W7AEW0, tnsE, tnpB1, mobA, tnpA1, 41*
MAD6	74	*uvrB, clpP, ftsK1, Q57231, parB, Q06237, tnp, hsdM, tnpA_IS6100, ligD, dnaB, insI, dnaK, recA, tnpB, hflB, ftsK, brxL, clpX, dcm, clpB, groL, uvrA, traG, gyrA, ltrA_2, dnaX, rarA, topB, tnpA, alkA, ltrA_1, smc, clpC, hsdS, mutS, dut, dpnA, gyrB, polA, ltrA, int, recQ, hin, tnpR, dnaA, uvrA_1, hin_1, xerD_4, hsdR, traK, ORF1, ORF2, ORF20, ORF32, prrC, traE, mob, topB_1, traC_1, uvrD, traC_2, repA, istB, A5UJT3, WP_011727856.1, ligB, groEL, traM, WP_001186919.1, Int-Tn, tnpB1, tnpA1, hfq*
MAD7	70	*uvrB, clpP, Q06237, tnp, rep, zeta, dnaK, mecB, recA, tnpB, hflB, EF_0125;, polC, ftsK, clpB, groL, uvrA, dnaB, gyrA, clpX, hsdM, ltrA_2, dnaX, rarA, topB, alkA, ssb_2, groEL, smc, traK, clpC, mcrB, mutS, dnaE, dpnA, gyrB, cas7c, tnpR, uvrA_2, dnaA, ltrA_1, uvrA_1, ruvB, ORF2, ORF20, ORF32, soj_2, orf17, rteB, int, IS1216, mob, traG, traC_2, traI, hsdR, repA, tnpX, hin, A0A2Z3N9D2, tnpA, mobC, repB, parA, WP_001186919.1, Int-Tn, tnpB1, tnpA1, 8, gp8*
MAD7.1	64	*uvrB, hupB, clpP, Q57231, tnp, tnpB, ISS1N, dnaK, hflB, WP_002321882.1, clpX, hsdM, groL, ftsK, clpB, uvrA, dnaB, hsdR, pcrA, gyrB, gyrA, ltrA_2, clpP1, tnpA, traJ, dnaX, rarA, topB, hup, groEL, dnaG, clpC, dcm, mutS, dpnA, hin, polA, ltrA_5, ltrA, int, uvrA_2, tnpR, dnaA, uvrA_1, smc, hin_1, xerD_4, traK, ORF1, ORF2, ORF20, ORF32, A0A3L8G246, hsdS1, orf17, orf23, traG, repA, WP_127822567.1, recA, Int-Tn, WP_002293753.1, tnpB1, tnpA1*
MAD7.2	61	*clpP, repL, tnpR, tnp, ruvB, dnaK, recA, hflB, clpX, uvrB, dnaB, dnaX, clpB, groL, ltrA, hsdM_1, gyrA, hsdM, ltrA_2, rarA, topB, dcm, dnaG, topB_1, sbcC, clpC, tnpA, uvrA, banIM, mutS, dpnA, hin, gyrB, traG, int, recQ, ydiP, uvrA_2, dnaA, ltrA_1, hhaIM_3, uvrA_1, smc, hin_1, xerD_4, hsdR, ORF20, prrC, orf17, res, IS1216, trbF, mob, uvrD, traC_2, repA, mobC, Int-Tn, xerD, parE, polC*
MAD7.3	50	*xhlA, tnp, tnpR, tnpA, hflB, repA, ftsK, clpB, groL, uvrA, mutS2, traG, clpX, pglX, gyrA, ltrA_2, topB, hsdM, recA, clpC, uvrB, mutS, dpnA, hin, fokIM, dcm, ltrA, int, recQ, uvrA_2, ltrA_1, uvrA_1, gyrB, smc, hin_1, pinR, xerD_4, traK, hsdR, ORF2, ORF20, ORF32, prrC, orf17, mob, traC_2, mobC, dnaK, tnpB, tnpB1*
MAD7.4	57	*clpP, Q57231, repA, tnp, dnaK, tnpB, hflB, hsdM, polC, clpB, smc, dnaB, gyrB, gyrA, clpX, groL, tnpA, ltrA_2, recA, uvrB, clpC, uvrA, dinD, dnaE, mutS, dut, clpP_2, ltrA, int, recR, uvrA_2, recT, tnpR, dnaA, hsdR, uvrA_1, traG, rarA, ORF20, ORF21, dcm, topB, prrC, orf17, rteB, IS1216, mob, uvrD, traC_2, traC_4, hin, xerD_4, mobL, Int-Tn, uvrB_2, tnpB1, tnpA1*

Sample	no. MGEs	MGEs
MAD8	51	*clpP, tnp, ltrA, tnpA_1, tnpA, dnaK, tnpB, hflB, dnaB, clpX, groL, hsdM_1, gyrA, ltrA_2, clpB, traG, dnaX, rarA, topB, groEL, rnr, gyrB, uvrB, clpC, uvrA, hin, clpP_2, int, ruvC, dcm, ltrA_1, hsdR, uvrA_1, hin_1, xerD_4, ORF1, ORF2, ORF20, ORF21, ORF32, prrC, A0A3L8G246, hsdM, mob, uvrD, traC_2, repA, WP_127822567.1, recA, trbG, tnpB1*
MAD9	76	*clpP, Q57231, repA, tnp, groL, ISS1N, tnpA, dnaK, xerD, recA, WP_002321882.1, WP_000798699.1, clpX, polC, cas9, hflB, clpB, dnaB, gyrB, uvrA, ltrA_2, rarA, topB, alkA, ssb_2, groEL, umuC, smc, clpC, uvrB, gyrA, ltrA, dnaE, mcrB, mutS, hhaIM_3, traK, traG, hsdM_1, hsdM, int, recQ, uvrA_2, kilA, tnpR, dnaA, dpnA, ltrA_1, uvrA_1, dcm, ruvB, xerD_4, hsdR, ORF1, ORF2, ORF20, ORF21, ORF32, prrC, rteB, IS1216, mobA, mob, topB_1, virB4_3, traC_2, traC_4, traN_1, nisX1, tnpC, rep3, rep, mobL, WP_002293753.1, parC, Q99338*
MAD10	66	*clpP, tnp, tniQ, parA, ruvB, recA, hflB, traE, tnpR, clpX, hsdM, dnaB, nusG, dcm, groL, clpB, repA, dut_2, traG, ltrA_2, uvrB, dnaX, pcrA, topB, tnpA, groEL, rex, smc, hsdR_2, clpC, uvrA, hsdR, dpnA, mutS, gyrA, gyrB, clpP_2, int, comM, recR, uvrA_2, dnaA, traK, uvrA_1, xerD_4, mcrB, ORF20, ORF32, prrC, orf17, lys, traH, rteB, mobA, mob, topB_1, mobN1, traC_2, mobC, hin, traN_1, Q7BQ53, dnaK, traA, Int-Tn, tnpA1*

Table E7.3. Microbial genera associated with MGEs. Significative association defined as significant co-occurrence with positive Spearman correlation coefficients. Alpha = 0.05, r > 0.50

Genus	Phylum	MGEs
Jeotgalicoccus	Bacillota	*dnaE, dnaG, EF_0125;, F7LRR2, ftsK, int1, IS1216, ISS1N, istB, mobA, mobN1, mutL, mutS2, nisX1, pcrA, Q06238, Q54944, radA, recJ, recR, rep, repB, repE, ruvB, ssb_2, tnp1, tnpA1, topA, topB_1, traA, traI, ung, uvrB_2, uvrC, WP_000351512.1, WP_001186919.1, WP_002293753.1, WP_002321882.1, xerD, holA, P03862, pre, priA, recN, ruvC, ssb, tnpC, traN_1, trbL, WP_010890867.1, addA, comM, dinB, dnaJ, dnaN, hup, intN1, mazG, mobL, mutY, repR, repS, rex, tnsA, traQ, truncated-tnp, ung2, xerD_1, xerD_3, hsdS, soj_2, tpn*
Lentilactobacillus	Bacillota	*dnaE, EF_0125;, F7LRR2, IS1216, ISS1N, istB, mobA, mutL, mutS2, pcrA, radA, recJ, rep, repB, ssb_2, tnp1, tnpA1, topA, topB_1, traA, traI, ung, uvrB_2, uvrC, WP_001186919.1, WP_002293753.1, WP_002321882.1, xerD, holA, mobB, nucS, P03862, pre, priA, Q06237, recN, ruvC, ssb, tnpC, traN_1, trbL, WP_010890867.1, addA, comM, dinB, dnaJ, dnaN, hup, intN1, mazG, mobL, mutY, oppD, orf23, repR, repS, rex, tnsA, traM, traQ, truncated-tnp, ung2, xerD_1, xerD_3, hsdS, soj_2, tpn*
Amylolactobacillus	Bacillota	*A5UJT3, dnaE, EF_0125;, F7LRR2, int1, IS1216, ISS1N, istB, mobA, mobC, mod, mutL, mutS2, nisX1, pcrA, Q06238, Q5HMP5, radA, recJ, recR, rep, repC, repE, ruvB, ssb_2, tnpA1, tnpA6100, tnpC1, topB_1, traF, traI, ung, uvrB_2, uvrC, WP_000351512.1, WP_001186919.1, WP_001284311.1, WP_002293753.1, WP_002321882.1, holA, ISPpu12, ORF, pilT_3, priA, Q06237, recN, ruvC, ssb, tnpC, traN_1, trbL, virB4, xerC, addA, comM, dinB, dnaN, intN1, mazG, mutY, rex, traQ, truncated-tnp, xerD_1, xerD_3*
Mammaliicoccus	Bacillota	*A5UJT3, dnaE, dnaG, EF_0125;, F7LRR2, int1, IS1216, ISS1N, istB, mobA, mobN1, mod, mutL, mutS2, nisX1, noc, parA, pcrA, polA, Q06238, Q54944, Q5HMP5, radA, recJ, recR, rep, repB, repE, ruvB, ssb_2, tnp1, tnpA1, tnpA6100, tnpC1, topA, topB_1, traA, traI, ung, uvrB_2, uvrC, WP_000351512.1, WP_001186919.1, WP_002293753.1, WP_002321882.1, xerD, holA, mobB, nucS, P03862, pre, priA, recN, ssb, trbL, WP_010890867.1, addA, dinB, dnaN, mazG, repR*
Aerococcus	Bacillota	*dnaE, dnaG, EF_0125;, F7LRR2, ftsK, int1, IS1216, ISS1N, istB, mobA, mod, mutL, mutS2, nisX1, pcrA, polA, radA, recJ, recR, rep, repB, repE, tnp1, tnpA1, tnpA6100, topA, topB_1, traA, traI, ung, uvrB_2, uvrC, WP_002293753.1, WP_002321882.1, xerD, hhaIM_2, holA, mobB, P03862, pre, priA, recN, ruvC, ssb, trbL, WP_010890867.1, addA, dnaJ, dnaN, intN1, mazG, mutY, repR, repS, traQ, ung2, xerD_1, xerD_3*
Brevibacterium	Actinomycetota	*dnaE, dnaG, EF_0125;, ftsK, IS1216, ISS1N, istB, mobA, mobN1, mutL, mutS2, nisX1, pcrA, Q06238, Q54944, radA, recJ, recR, rep, repB, repE, ssb_2, tnp1, tnpA1, topA, topB_1, traA, traI, ung, uvrB_2, uvrC, WP_000351512.1, WP_001186919.1, WP_002293753.1, WP_002321882.1, holA, mobB, nucS, P03862, pre, priA, Q06237, recN, ruvC, trbL, tsrF, WP_010890867.1, addA, dinB, dnaN, hup, mazG, mobL, repR, traQ, truncated-tnp*
Streptococcus	Bacillota	*A5UJT3, dnaE, dnaG, EF_0125;, F7LRR2, ftsK, int1, IS1216, ISS1N, istB, mobA, mobN1, mod, mutL, mutS2, nisX1, pcrA, Q06238, Q54944, Q5HMP5, radA, recJ, recR, rep, repB, repE, tnp1, tnpA1, tnpA6100, topA, topB_1, traA, traI, ung, uvrB_2, uvrC, WP_000351512.1, WP_001186919.1, WP_002293753.1, WP_002321882.1, holA, mobB, nucS, P03862, pre, priA, recN, ruvC, ssb, trbL, WP_010890867.1, addA, dinB, dnaN, mazG, repR*
Lactococcus	Bacillota	*dnaE, dnaG, EF_0125;, F7LRR2, int1, IS1216, ISS1N, istB, mobA, mod, mutL, mutS2, nisX1, pcrA, Q5HMP5, radA, recJ, recR, rep, repB, repE, ssb_2, tnp1, tnpA1, tnpA6100, topA, topB_1, traI, ung, uvrB_2, uvrC, WP_002293753.1, WP_002321882.1, xerD, holA, pre, priA, recN, ruvC, ssb, tnpC, traN_1, trbL, addA, dnaN, mazG, mutY, repR, traQ, xerD_1, xerD_3*

Genus	Phylum	MGEs
Weissella	Bacillota	*dnaE, EF_0125;, ISS1N, istB, mutL, mutS2, pcrA, recJ, recR, rep, repB, topB_1, traA, traI, ung, uvrB_2, uvrC, WP_002293753.1, WP_002321882.1, xerD, holA, mobB, nucS, P03862, pre, priA, recN, ruvC, ssb, tnpC, trbL, tsrF, WP_010890867.1, addA, dinB, dnaJ, dnaN, hup, intN1, mazG, mobL, mutY, repR, repS, traQ, ung2, xerD_1, xerD_3, hsdS, tpn*
Blautia	Bacillota	*cas2, dnaE, EF_0125;, F7LRR2, ftsK, int1, IS1216, ISS1N, istB, mobA, mod, mutL, mutS2, nisX1, pcrA, Q06238, radA, recJ, recR, rep, repC, ssb_2, tnpA1, tnpA6100, traI, ung, uvrB_2, uvrC, WP_000351512.1, WP_001284311.1, WP_002293753.1, WP_002321882.1, priA, recN, ruvC, ssb, trbL, addA, dnaJ, dnaN, intN1, mazG, mutY, repS, traQ, ung2, xerD_1, xerD_3, tpn*
Flaviflexus	Actinomycetota	*dnaE, dnaG, EF_0125;, F7LRR2, ftsK, int1, ISS1N, istB, mod, mutL, mutS2, nisX1, pcrA, Q5HMP5, recJ, recR, rep, repB, tnp1, tnpA1, topA, topB_1, traI, ung, uvrC, WP_002293753.1, WP_002321882.1, xerD, dnaC, ISPpu12, mobB, ORF, priA, recN, ssb, xerC, addA, dinB, dnaN, hup, intN1, mazG, mutY, repR, xerD_1, xerD_3*
Enterococcus	Bacillota	*dnaE, dnaG, EF_0125;, ftsK, int1, IS1216, ISS1N, istB, mutL, mutS2, pcrA, Q54944, radA, recJ, recR, rep, repB, repE, ssb_2, tnp1, tnpA1, topA, traI, ung, uvrB_2, uvrC, WP_001186919.1, WP_002293753.1, WP_002321882.1, holA, P03862, pre, priA, recN, ssb, tnpX, WP_010890867.1, addA, dnaN, hup, mazG, repR, soj_2*
Bacteroides	Bacteroidota	*dnaE, F7LRR2, int1, ISS1N, mobA, mutL, mutS2, nisX1, pcrA, radA, recJ, recR, rep, tnpC1, topB_1, ung, WP_002293753.1, WP_002321882.1, xerD, priA, recN, ruvC, ssb, tnpC, traK, traN_1, trbL, comM, dnaN, mazG, mutY, repS, rex, traH, traQ, xerD_1, xerD_3*
Ligilactobacillus	Bacillota	*dnaG, EF_0125;, ftsK, ISS1N, istB, mobN1, mutS2, Q06238, Q54944, radA, recJ, recR, rep, repB, repC, repE, ssb_2, tnp1, tnpA1, tnpA6100, tnpAISAba125cp2, traA, ung, uvrB_2, uvrC, WP_001284311.1, WP_002293753.1, WP_002321882.1, nucS, pre, recN, NGR_a03160, oppD, orf23, recG, traO, truncated-tnp*
Pediococcus	Bacillota	*dnaE, dnaG, EF_0125;, int1, IS1216, ISS1N, mobN1, mutL, mutS2, parA, recJ, rep, repB, tnp1, tnpA1, topA, traI, uvrC, WP_002293753.1, WP_002321882.1, zeta, mobB, P03862, pre, priA, recN, ssb, WP_010890867.1, hsdS, soj_2, tpn*
Acinetobacter	Pseudomonadota	*A5UJT3, dnaE, EF_0125;, groEL, ISS1N, istB, mobA, mutL, nisX1, radA, recJ, recR, rep, tnpC1, topB_1, traA, ung, uvrC, WP_002293753.1, WP_002321882.1, xerD, holA, priA, recN, tnpC, tsrF, dnaN, mazG*
Rhodococcus	Actinomycetota	*Q06238, radA, WP_000351512.1, WP_001186919.1, Q06237, ruvC, tsrF, comM, dinB, dnaN, hfq, mazG, mutY, NGR_a03160, repS, tnsA, traM, traO, traQ, truncated-tnp, xerD_1, xerD_3, ligA, P0A4M1, P0A4M2, brxL, tnsE*
Ruminococcus	Bacillota	*dnaG, EF_0125;, int1, ISS1N, istB, mutL, mutS2, pcrA, polA, recJ, rep, repE, tnp1, tnpA6100, topA, traI, ung, uvrC, WP_002293753.1, WP_002321882.1, P03862, pre, priA, recN, ssb, WP_010890867.1*
Empedobacter	Bacteroidota	*EF_0125;, mobA, nisX1, Q06238, radA, recJ, tnpC1, traI, ung, WP_001186919.1, Q06237, recN, ruvC, tnpC, traN_1, tsrF, addA, comM, dnaN, mazG, mobL, rex, traM, traQ*
Heyndrickxia	Bacillota	*F7LRR2, mutL, ung, priA, recN, ruvC, traN_1, trbL, addA, comM, dinB, dnaN, mazG, mutY, rex, traQ, xerD_1, xerD_3, hsdS*
Methanobrevibacter	Euryarchaeota	*dnaG, dpnA, EF_0125;, ftsK, IS1216, ISS1N, istB, mutS2, polA, recJ, rep, tnpA6100, traI, uvrC, WP_002293753.1, WP_002321882.1, recN*
Staphylococcus	Bacillota	*dnaG, int1, ISS1N, istB, mobN1, repE, tnp1, tnpA6100, topA, uvrB_2, uvrC, WP_002293753.1, WP_002321882.1, nucS, pre, tpn*
Carnobacterium	Bacillota	*ISS1N, mutS2, recJ, uvrC, WP_002321882.1, holA, P03862, priA, recN, ssb, WP_010890867.1, dnaJ, dnaN, repR, ung2*
Paracholeplasma	Mycoplasmatota	*mutL, priA, recN, ruvC, trbL, addA, comM, dinB, mazG, mutY, traQ, xerD_1, xerD_3*

Genus	Phylum	MGEs
Thermobacillus	Bacillota	*Q06238, WP_001186919.1, Q06237, hfq, NGR_a03160, traM, traO, traQ, truncated-tnp, ligA, P0A4M1, P0A4M2, brxL*
Pseudoxanthomonas	Pseudomonadota	*mobA, Q06238, traA, dnaC, tsrF, dinB, dnaN, mobL, tnsA, traM, traQ*
Sphingobacterium	Bacteroidota	*Q06238, radA, tnpC1, traA, WP_000351512.1, WP_001186919.1, Q06237, tsrF, traQ, truncated-tnp*
Niallia	Bacillota	*ISS1N, topB_1, WP_001186919.1, nucS, pre, Q06237, trbL, traC_4, hsdS*
Oligella	Pseudomonadota	*F7LRR2, int1, mutL, trbL*
Syntrophomonas	Bacillota	*ORF2, ORF20, ORF1, Q57231*
Acetivibrio	Bacillota	*ORF20, uvrD, xerD_4*
Aminipila	Bacillota	*ruvC, trbL, dinB*
Aminobacterium	Synergistota	*ORF20, ORF1, xerD_4*
Denitrobacterium	Actinomycetota	*int1, Q5HMP5, tnpA6100*
Glutamicibacter	Actinomycetota	*dnaC, tsrF, mobL*
Herbinix	Bacillota	*ORF20, uvrD, xerD_4*
Butyrivibrio	Bacillota	*dpnA, pre*
Caldibacillus	Bacillota	*hsdM_1, topB_1*
Symbiobacterium	Bacillota	*WP_001186919.1, Q06237*
Syntrophotalea	Pseudomonadota	*uvrD, xerD_4*
Syntrophus	Pseudomonadota	*uvrD, xerD_4*
Thermobispora	Actinomycetota	*WP_001186919.1, Q06237*
Acidilutibacter	Bacillota	*ORF1*
Bacillus	Bacillota	*noc*
Bifidobacterium	Actinomycetota	*Int-Tn*
Brevefilum	Chloroflexota	*xerD_4*
Clostridium	Bacillota	*xerD_4*
Comamonas	Pseudomonadota	*tsrF*
Croceibacter	Bacteroidota	*xerD_4*
Erysipelothrix	Bacillota	*repE*
Lacrimispora	Bacillota	*xerD_4*

Genus	Phylum	MGEs
Lactobacillus	Bacillota	*holA*
Mesotoga	Thermotogota	*xerD_4*
Methanosarcina	Euryarchaeota	*ORF20*
Micromonospora	Actinomycetota	*traM*
Paracoccus	Pseudomonadota	*traM*
Petrimonas	Bacteroidota	*ORF20*
Proteiniphilum	Bacteroidota	*xerD_4*
Ruminiclostridium	Bacillota	*ORF20*
Trueperella	Actinomycetota	*traC_4*
Ureibacillus	Bacillota	*traM*
Weizmannia	Bacillota	*traN_1*

Appendix F: Chapter 8 supplementary materials

Supplementary Figures

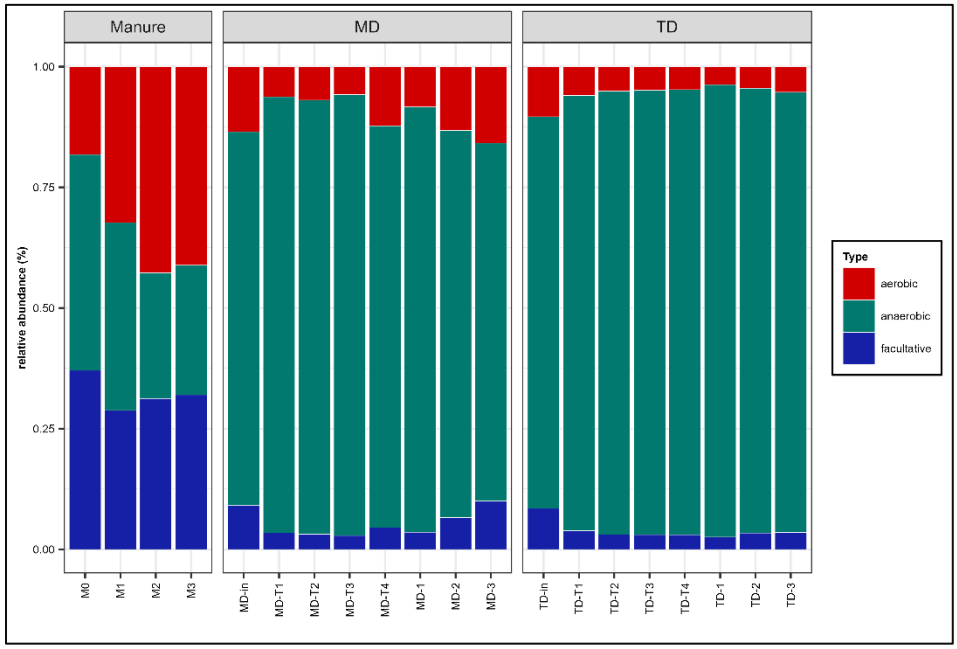

Figure F8.1 Microbiome structure by respiration phenotype.

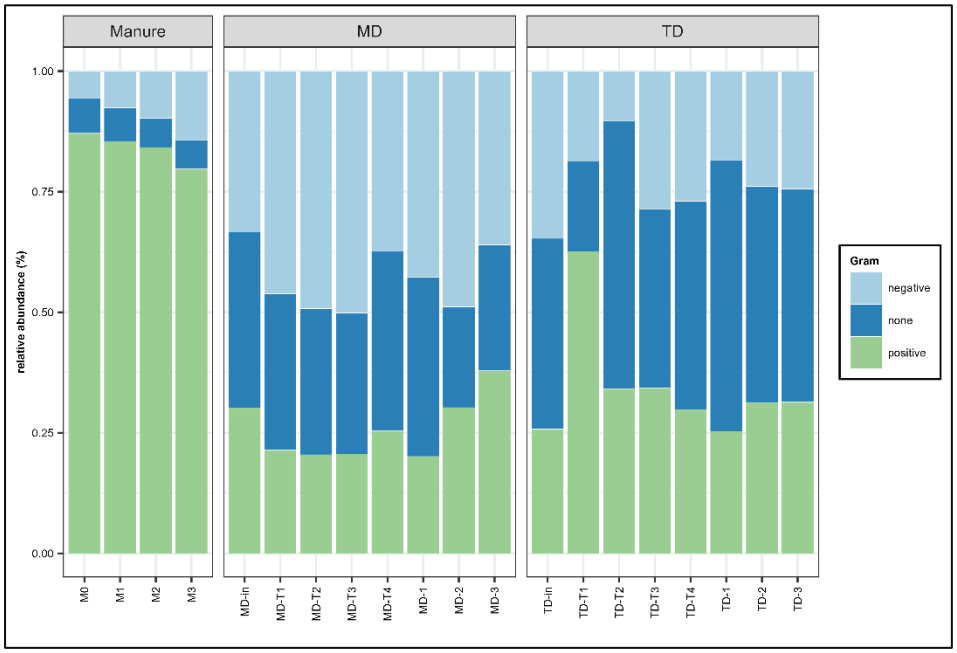

Figure F8.2 Microbiomes structures by Gram stain phenotypes.

Supplementary Tables

Table F8.1 ARG-like sequences detected in individual samples. M: manure; MD: mesophilic digester; TD: thermophilic digester.

Sample	no. ARGs	ARGs
M0	48	*AAC(6')-Ie-APH(2'')-Ia, aad(6), aadA4, aadA5, ANT(6)-Ia, ANT(9)-Ia, APH(6)-Id, cfrC, CfxA2, CfxA4, cmx, dfrG, dfrK, efrB, Erm(33), Erm(A), ErmA, ErmB, floR, ileS, lnuA, lnuB, lnuC, lnuG, LnuP, lsaE, mel, mphC, mphE, msrA, pp-flo, rpoB, rpoB2, sul1, tet(K), tet(W/N/W), tet32, tet36, tet44, tetA(P), tetB(P), tetM, tetO, tetQ, tetS, tetT, tetW, vanYG1*
M1	47	*aad(6), aadA, aadA15, aadA27, ACI-1, ANT(3'')-IIc, ANT(6)-Ia, ANT(6)-Ib, ANT(9)-Ia, APH(3')-IIIa, APH(6)-Id, cfr(D), CfxA2, CfxA4, cmx, efrB, Erm(33), ErmA, ErmB, ErmT, ErmX, floR, ileS, lnuA, lnuB, lnuC, lnuE, lnuG, LnuP, lsaE, mel, optrA, pp-flo, rpoB, rpoB2, smeE, sul1, sul2, tet(K), tet(W/N/W), tet36, tetM, tetO, tetQ, tetS, tetT, tetW*
M2	53	*aad(6), aadS, ANT(6)-Ia, ANT(6)-Ib, ANT(9)-Ia, APH(3'')-Ib, APH(3')-IIIa, CARB-14, CARB-5, cfr(D), CfxA2, CfxA4, CfxA6, cmx, dfrA1, dfrA15, efrA, efrB, ErmB, ErmC, floR, ileS, lmrD, lnuA, lnuB, lnuC, lnuG, LnuP, lsaE, Mef(En2), mefB, mel, mphB, optrA, poxtA, pp-flo, rpoB, rpoB2, sul1, sul2, tet(A), tet(K), tet(W/N/W), Tet(X4), tet36, tetM, tetO, tetQ, tetS, tetT, tetW, tetX, ugd*
M3	58	*aad(6), aadA17, aadA2, aadA23, aadA24, aadA3, aadA9, ANT(6)-Ia, ANT(9)-Ia, APH(3'')-Ib, APH(6)-Id, blaR1, catQ, cfr(D), cfrA, CfxA, CfxA2, CfxA6, cmlA9, cmx, efrA, efrB, Erm(33), ErmA, ErmB, floR, lnuA, lnuB, lnuC, lnuG, LnuP, lsaE, Mef(En2), mefB, mel, mphB, optrA, OXA-347, poxtA, rpoB, rpoB2, tet(33), tet(W/N/W), Tet(X4), tet(Z), tet32, tet36, tet44, tetA(P), tetB(P), tetM, tetO, tetQ, tetS, tetT, tetW, tetX, ugd*
MD-in	35	*aad(6), ANT(6)-Ia, ANT(6)-Ib, ANT(9)-Ia, APH(3')-IIIa, cfrC, Erm(47), Erm(A), ErmB, ErmC, ErmF, ErmT, lnuB, lnuC, lnuD, lnuE, lnuG, LnuP, lsaE, mel, OXA-347, rpoB, rpoB2, tet(W/N/W), tet36, tet44, tetA(P), tetB(P), tetM, tetQ, tetS, tetT, tetW, vanRI, vanRO*
MD-T1	31	*aad(6), aadA23, aadA24, ANT(6)-Ia, ANT(9)-Ia, APH(3'')-Ib, APH(3')-IIIa, APH(6)-Id, Erm(47), Erm(A), ErmB, ErmF, lnuA, lnuB, lnuC, lnuG, lsaE, mefB, mel, OXA-209, OXA-347, rpoB, rpoB2, smeE, tet(W/N/W), tet32, tet44, tetM, tetQ, tetT, tetW*
MD-T2	23	*ANT(6)-Ia, ANT(9)-Ia, APH(3')-IIIa, APH(6)-Id, EreA, EreA2, Erm(33), Erm(47), ErmA, ErmB, ErmC, ErmF, ErmG, lnuB, lnuC, lsaE, mel, rpoB, SAT-4, tet(W/N/W), tet36, tetM, tetW*
MD-T3	36	*aad(6), aadA23, aadA24, ANT(6)-Ia, ANT(6)-Ib, ANT(9)-Ia, APH(3'')-Ib, APH(3')-IIIa, CARB-14, CARB-5, CfxA2, CfxA4, Erm(47), ErmB, ErmF, ErmT, ErmY, linG, lnuB, lnuC, lnuF, LnuP, lsaE, mel, rpoB, rpoB2, SAT-4, sul2, tet(G), tet(W/N/W), tet44, tetA(P), tetM, tetQ, tetS, tetW*
MD-T4	36	*aad(6), ANT(6)-Ia, ANT(9)-Ia, APH(3'')-Ib, APH(3')-IIIa, cfr(D), Erm(47), ErmB, ErmF, linG, lnuA, lnuB, lnuC, lnuF, lnuG, LnuP, lsaE, mefB, mel, mphB, optrA, OXA-347, rpoB, rpoB2, SAT-4, tet(L), tet(W/N/W), tet(Z), tet36, tet44, tetM, tetQ, tetS, tetT, tetW, vanRI*
MD-1	34	*AAC(6')-Ie-APH(2'')-Ia, aadA10, aadA16, aadA23, aadA24, aadS, ANT(6)-Ia, ANT(9)-Ia, APH(3')-IIIa, APH(6)-Id, Erm(47), ErmB, ErmF, ErmG, lnuA, lnuB, lnuC, lnuG, LnuP, lsaE, mefB, mel, OXA-209, OXA-347, rpoB2, tet(31), tet(W/N/W), tet36, tetA(P), tetM, tetQ, tetS, tetT, tetW*
MD-2	37	*aad(6), aadA11, aadA23, aadA24, aadA6/aadA10, aadS, ANT(6)-Ia, ANT(9)-Ia, APH(3'')-Ib, APH(6)-Id, Erm(47), ErmB, ErmF, lnuA, lnuB, lnuC, lnuG, LnuP, lsaE, mefB, mel, optrA, rpoB, rpoB2, tet(C), tet(W/N/W), tet(Z), tet36, tet44, tetB(48), tetB(P), tetM, tetQ, tetS, tetT, tetW, vanRA*
MD-3	31	*aad(6), aadA10, aadA23, aadA24, aadA6/aadA10, ANT(6)-Ia, ANT(9)-Ia, APH(6)-Id, Erm(33), Erm(47), ErmA, ErmB, ErmF, lnuB, lnuC, lnuG, LnuP, lsaE, mel, OXA-347, rpoB, rpoB2, salA, tet(W/N/W), tetB(P), tetM, tetO, tetQ, tetT, tetW, vanRI*
TD-in	39	*aad(6), acrD, ANT(6)-Ia, ANT(6)-Ib, ANT(9)-Ia, APH(3'')-Ib, APH(3')-IIIa, cfrC, Erm(33), ErmA, ErmB, ErmF, ErmY, ileS, linG, lnuA, lnuB, lnuC, lnuF, lnuG, LnuP, lsaE, mefB, mel, optrA, OXA-347, rpoB, rpoB2, SAT-4, tet(W/N/W), Tet(X4), tet44, tetB(P), tetM, tetQ, tetT, tetW, tetX, vanRI*

Sample	no. ARGs	ARGs
TD-T1	22	*aad(6), aadS, ANT(6)-Ia, ANT(9)-Ia, APH(3')-IIIa, ErmB, ErmF, lnuC, LnuP, mel, poxtA, rpoB, rpoB2, SAT-4, tet(W/N/W), Tet(X5), Tet(X6), tet32, tet44, tetM, tetQ, tetW*
TD-T2	28	*aad(6), ANT(6)-Ia, ANT(9)-Ia, APH(6)-Id, cfrA, efrB, Erm(33), ErmA, lnuA, lnuB, lnuC, lnuE, lnuG, LnuP, lsaE, mefB, mel, optrA, poxtA, rpoB, rpoB2, tet(W/N/W), tet44, tetM, tetS, tetT, tetW, ugd*
TD-T3	30	*AAC(6')-Ie-APH(2'')-Ia, aad(6), ANT(6)-Ia, ANT(9)-Ia, cfrC, efrB, ErmB, ErmQ, ileS, lnuA, lnuB, lnuC, lnuE, lnuG, LnuP, lsaE, mel, rpoB, rpoB2, tet(33), tet(K), tet(W/N/W), tet44, tetM, tetO, tetS, tetT, tetW, ugd, vanRI*
TD-T4	28	*aad(6), ANT(6)-Ia, ANT(9)-Ia, cfrA, ErmG, ileS, LlmA, lnuA, lnuB, lnuC, lnuE, lnuG, LnuP, lsaE, mel, optrA, qacE, qacEdelta1, rpoB, rpoB2, sul1, tet(W/N/W), tet44, tetB(P), tetM, tetS, tetT, tetW*
TD-1	23	*aad(6), ANT(6)-Ia, APH(3')-IIIa, APH(6)-Id, bmr, cfr(B), CfxA, CfxA2, clcD, ErmB, ErmX, lnuA, lnuG, LnuP, mel, rpoB, rpoB2, tet(W/N/W), tet(Z), tetB(P), tetM, tetS, tetW*
TD-2	25	*aad(6), ANT(6)-Ia, ANT(9)-Ia, cmx, efrA, ileS, lnuA, lnuB, lnuC, lnuE, lnuG, LnuP, lsaE, mel, mtrA, rpoB, rpoB2, tet(G), tet(W/N/W), tet44, tetM, tetO, tetS, tetT, tetW*
TD-3	24	*aad(6), ANT(6)-Ia, dfrD, dfrE, ErmB, ileS, lnuA, lnuB, lnuC, LnuP, lsaE, mefB, mel, rpoB, rpoB2, tet(W/N/W), tet44, tetB(P), tetM, tetO, tetQ, tetT, tetW, ugd*

Table F8.2 BacMet genes detected in individual samples. M: manure; MD: mesophilic digester; TD: thermophilic digester.

Sample	No. genes	BacMet genes
M0	9	*cadC;copA;fieF/yiip;merA;tcrB;actP/yjcG;tcrY;tcrA;copF*
M1	8	*acn;cadC;smeE;tcrB;arsB;bcrC;tcrY;tcrA*
M2	12	*cadC;cadX;cusB;golT;mexB;smrA;soxS;srpB;tcrB;ttgH;tcrY;tcrA*
M3	5	*cadC;cusC/ylcB;tcrB;tcrY;tcrA*
MD-in	4	*acn;cadC;tcrB;tcrA*
MD-T1	5	*acn;ruvB;smeE;tcrB;tcrA*
MD-T2	2	*copB;tcrA*
MD-T3	1	*copB*
MD-T4	5	*cadC;tcrB;arsB;copB;tcrA*
MD-1	4	*merA;silP;tcrB;tcrA*
MD-2	6	*merA;srpB;tcrB;ttgH;copB;tcrA*
MD-3	10	*bmr;copA;emrD;pcoA;smrA;tcrB;arsB;copB;copR;tcrA*
TD-in	6	*acrD/yffA;tcrB;acrD;arsB;copB;tcrA*
TD-T1	5	*ruvB;tcrB;ttgE;arsB;tcrA*
TD-T2	5	*cadC;tcrB;arsB;copB;tcrA*
TD-T3	4	*cadC;tcrB;copB;tcrA*
TD-T4	5	*cadC;qacE;qacEdelta1;tcrB;tcrA*
TD-1	6	*acn;bmr;cadC;fabL/ygaA;tcrB;tcrA*
TD-2	5	*acn;cadC;tcrB;copA;tcrA*
TD-3	4	*acn;cadX;tcrB;tcrA*

Table F8.3 MGE-like and related gene sequences detected in individual samples. M: manure; MD: mesophilic digester; TD: thermophilic digester.

Sample	No. MGEs	MGEs
M0	139	*tnp, 19, dnaB, parA, pre, trbE, tnsA, oppD, repS, repR, orf19, rlx, hsdM, nisX1, bin3, tnpA_IS6100, tnpA, istA, mobA, int2, mob, mobE, EF_0125, repE, ISS1N, rep, dnaK, recA, tnpB, trbEB, WP_010890867.1, WP_002321882.1, dnaG, hhaIM_2, mutS2, uvrB, groL, pcrA, mutS_2, ftsK, hflB, clpB, rnj, topA, polA, smc, uvrA, gyrA, clpX, gyrB, ltrA_2, uvrC, topB, ssb, dcm, ltrA_1, ssb_2, groEL, mutS, xerD, topB_1, dpnA, clpC, mcrB, hsdR, rarA, ung, dnaE, pilT, hin, dut, recT, traG, ltrA, ltrA_5, cas2, clpP, hhaIM_3, dnaA, ydiP, uvrA_2, recN, tnpR, erF, priA, gp26, istB, uvrA_1, clpP1, mazG, mecB, recJ, dnaN, vsr, ung2, radA, recR, ORF1, ORF32, prrC, soj_2, orf17, orf23, ardA, int, IS1216, tnpA6100, traI, mobN1, tnpX, traK, ORFAB, tpn, tnpC, repB, dnaJ, traA, repA, recG, holA, int1, traM, preA, Int-Tn, tra8, WP_002293753.1, sin, ruvA, uvrB_2, tnp1, parC, nmoT, P18416, tnpB1, tnpA1, dnaX, polC, mazF, P03862*
M1	115	*tnp, dnaB, tnsC, Q57231, Q54944, traA, Q06237, Rep, ltrA, int, tnpR, hsdS, EDI97729.1, tnpA, pre, repE, EF_0125, tnpB, ISS1N, zeta, rep, ruvB, dnaK, recA, hflB, WP_010890867.1, traI, traE, dnaX, WP_002321882.1, SE_p102, repB, mutS2, clpX, hsdM, groL, nusG, clpB, topA, repA, uvrB, uvrA, gyrA, gyrB, dnaA, ltrA_2, uvrC, traG, dcm, topB, ltrA_1, groEL, dnaG, topB_1, smc, mutL, recN, nucS, mutS, dnaE, pcrA, dpnA, polA, traK, ftsK, lexA, hin, uvrA_2, mrr, priA, istB, recJ, hup, dnaN, umuC, hin_1, uvrA_1, clpC, dinB, cas7c, rarA, rnhA, prrC, hsdR, soj_2, trbC, res, Int-Tn, IS1216, mobA, traC_1, mobN1, traC_4, hsdR_2, tnpX, mobC, A5UJT3, tsrF, mobL, addA, holA, mobB, dnaE2, repR, parA, WP_001186919.1, WP_002293753.1, tnp1, dnaC, xerD, tnpB1, tnpA1, polC, mazF, P03862*
M2	133	*dpnA, recA, Q5HMP5, dnaB, pre, tnsB, intN1, P16942, repD, tnpC1, hsdS, hsdM, nisX1, tnpA_IS6100, EF_0125, repC, tnp, tnpA, int2, rep, repE, ISS1N, mobA, hsdR, mod, ruvB, dnaK, traD, tnpB, hflB, traK, WP_002321882.1, traN, traA, traI, WP_115203650.1, uvrC, dcm, clpX, uvrB, pcrA, dinB, ftsK, clpB, groL, mutS2, uvrA, traG, gyrA, comM, gyrB, dnaA, ltrA_2, ruvC, ssb, dnaX, rarA, dnaE, topB, alkA, hup, mutS, rex, dnaG, smc, recR, hsdR_2, xerD_3, addA, mutL, clpC, ltrA, ssb_2, mutY, polA, xerD, recN, hsdM_1, clpP, xerD_1, recQ, hhaIM, hin, uvrA_2, tnpR, ltrA_1, priA, istB, uvrA_1, recJ, groEL, mazG, hin_1, F7LRR2, ung, dnaN, ORF2, ORF20, prrC, orf17, orf23, lys, rteB, int, IS1216, mob, tnpA6100, topB_1, virB4_3, traC_1, mobN1, traC_4, traQ, traC_2, traN_1, A5UJT3, tpn, tnpC, repA, repB, mobC, trbL, topA, mobB, int1, Int-Tn, WP_002293753.1, uvrB_2, traB, tnp1, tnpB1, tnpA1, gp42*
M3	155	*clpP, C, A0A5Q3BC69, intN1, Q54944, repR, rlx, Q06238, Q06237, truncated-tnp, sohB_1, hsdM, resR, tnp, insB, repA1, EF_0125, traA, tnpB, ISS1N, WP_000351512.1, hin_1, dnaK, recA, hflB, WP_010890867.1, traI, traE, WP_002321882.1, ftsK, hsdR_2, uvrC, polC, dnaB, groL, pcrA, cas9, dinB, clpB, topA, polA, mutS2, smc, hhaIM, uvrA, traG, gyrA, comM, clpX, hsdM_1, gyrB, radC, dnaA, ssb, ltrA_2, uvrB, ltrA, thyA, dnaX, rarA, ydiP, topB, tnpA, dcm, hup, groEL, rex, dnaG, topB_1, recR, clpC, xerD_3, hhaIM_1, ssb_2, addA, ruvC, mutL, 5, lexA, nucS, hsdR, dnaE, dpnA, mutS, traK, hhaIM_2, xerD, recN, clpP_2, ltrA_5, holA, ung2, xerD_1, recQ, hin, mutY, uvrA_2, terL, tnpR, rep, mazG, ltrA_1, priA, ruvB, istB, ssb_1, uvrA_1, recJ, F7LRR2, ung, dnaN, radA, virB4, prrC, repA, soj_2, orf17, traQ, traH, rteB, virD2, res, int, IS1216, mobA, mob, tnpA6100, traC_2, mobC, parA1, traN_1, tpn, A0A2Z3N9D2, A0A3G6JR17, WP_001284311.1, trbI, hsdS, dnaJ, mobL, int1, repS, parA, WP_001186919.1, preA, Int-Tn, WP_002293753.1, hflK, trbL, uvrB_2, tnpB1, tnpA1, P03862, 15, 23, gp23*
MD-in	70	*uvrB, clpP, Q06237, tnp, rep, zeta, dnaK, mecB, recA, tnpB, hflB, EF_0125, polC, ftsK, clpB, groL, uvrA, dnaB, gyrA, clpX, hsdM, ltrA_2, dnaX, rarA, topB, alkA, ssb_2, groEL, smc, traK, clpC, mcrB, mutS, dnaE, dpnA, gyrB, cas7c, tnpR, uvrA_2, dnaA, ltrA_1, uvrA_1, ruvB, ORF2, ORF20, ORF32, soj_2, orf17, rteB, int, IS1216, mob, traG, traC_2, traI, hsdR, repA, tnpX, hin, A0A2Z3N9D2, tnpA, mobC, repB, parA, WP_001186919.1, Int-Tn, tnpB1, tnpA1, 8, gp8*
MD-T1	61	*clpP, repL, tnpR, tnp, ruvB, dnaK, recA, hflB, clpX, uvrB, dnaB, dnaX, clpB, groL, ltrA, hsdM_1, gyrA, hsdM, ltrA_2, rarA, topB, dcm, dnaG, topB_1, sbcC, uvrA, clpC, tnpA, banIM, mutS, dpnA, hin, gyrB, traG, int, recQ, ydiP, uvrA_2, dnaA, ltrA_1, hhaIM_3, uvrA_1, smc, hin_1, xerD_4, hsdR, ORF20, prrC, orf17, res, IS1216, trbF, mob, uvrD, traC_2, repA, mobC, Int-Tn, xerD, parE, polC*

Sample	No. MGEs	MGEs
MD-T2	50	*xhlA, tnp, tnpR, tnpA, hflB, repA, ftsK, clpB, groL, uvrA, mutS2, traG, clpX, pglX, gyrA, ltrA_2, topB, hsdM, recA, clpC, uvrB, mutS, dpnA, hin, fokIM, dcm, ltrA, int, recQ, uvrA_2, ltrA_1, uvrA_1, gyrB, smc, hin_1, pinR, xerD_4, traK, hsdR, ORF2, ORF20, ORF32, prrC, orf17, mob, traC_2, mobC, dnaK, tnpB, tnpB1*
MD-T3	57	*clpP, Q57231, repA, tnp, dnaK, tnpB, hflB, hsdM, polC, clpB, smc, dnaB, gyrB, gyrA, clpX, groL, tnpA, ltrA_2, recA, uvrB, clpC, uvrA, dinD, dnaE, mutS, dut, clpP_2, ltrA, int, recR, uvrA_2, recT, tnpR, dnaA, hsdR, uvrA_1, traG, rarA, ORF20, ORF21, dcm, topB, prrC, orf17, rteB, IS1216, mob, uvrD, traC_2, traC_4, hin, xerD_4, mobL, Int-Tn, uvrB_2, tnpB1, tnpA1*
MD-T4	64	*uvrB, hupB, clpP, Q57231, tnp, tnpB, ISS1N, dnaK, hflB, WP_002321882.1, clpX, hsdM, groL, ftsK, clpB, uvrA, dnaB, hsdR, pcrA, gyrB, gyrA, ltrA_2, clpP1, tnpA, traJ, dnaX, rarA, topB, hup, groEL, dnaG, clpC, dcm, mutS, dpnA, hin, polA, ltrA_5, ltrA, int, uvrA_2, tnpR, dnaA, uvrA_1, smc, hin_1, xerD_4, traK, ORF1, ORF2, ORF20, ORF32, A0A3L8G246, hsdS1, orf17, orf23, traG, repA, WP_127822567.1, recA, Int-Tn, WP_002293753.1, tnpB1, tnpA1*
MD-1	51	*clpP, tnp, ltrA, tnpA_1, tnpA, dnaK, tnpB, hflB, dnaB, clpX, groL, hsdM_1, gyrA, ltrA_2, clpB, traG, dnaX, rarA, topB, groEL, rnr, gyrB, uvrB, clpC, uvrA, hin, clpP_2, int, ruvC, dcm, ltrA_1, hsdR, uvrA_1, hin_1, xerD_4, ORF1, ORF2, ORF20, ORF21, ORF32, prrC, A0A3L8G246, hsdM, mob, uvrD, traC_2, repA, WP_127822567.1, recA, trbG, tnpB1*
MD-2	77	*clpP, Q57231, repA, tnp, groL, ISS1N, tnpA, dnaK, xerD, recA, WP_002321882.1, WP_000798699.1, clpX, polC, cas9, hflB, clpB, dnaB, gyrB, uvrA, ltrA_2, dnaX, rarA, topB, alkA, ssb_2, groEL, umuC, smc, clpC, uvrB, gyrA, ltrA, dnaE, mcrB, mutS, hhaIM_3, traK, traG, hsdM_1, hsdM, int, recQ, uvrA_2, kilA, tnpR, dnaA, dpnA, ltrA_1, uvrA_1, dcm, ruvB, xerD_4, hsdR, ORF1, ORF2, ORF20, ORF21, ORF32, prrC, rteB, IS1216, mobA, mob, topB_1, virB4_3, traC_2, traC_4, traN_1, nisX1, tnpC, rep3, rep, mobL, WP_002293753.1, parC, Q99338*
MD-3	66	*clpP, gyrA, tnp, tniQ, parA, ruvB, recA, hflB, traE, tnpR, clpX, hsdM, dnaB, nusG, dcm, groL, clpB, repA, dut_2, traG, ltrA_2, uvrB, dnaX, pcrA, topB, tnpA, groEL, rex, smc, hsdR_2, clpC, uvrA, hsdR, mutS, dpnA, gyrB, clpP_2, int, comM, recR, uvrA_2, dnaA, traK, uvrA_1, xerD_4, mcrB, ORF20, ORF32, prrC, orf17, lys, traH, rteB, mobA, mob, topB_1, mobN1, traC_2, mobC, hin, traN_1, Q7BQ53, dnaK, traA, Int-Tn, tnpA1*
TD-in	65	*Q57231, Q06238, hsdS, EF_0125, tnp, ISS1N, dnaK, recA, hflB, WP_002321882.1, clpB, uvrB, dnaB, clpX, groL, gyrA, ltrA_2, dnaX, rarA, topB, tnpA, ltrA_1, hsdM, cas7c, clpC, ltrA, uvrA, dpnA, mutS, dcm, hin, hsdM_1, gyrB, recQ, recR, tnpR, uvrA_2, dnaA, recN, hsdR, traG, uvrA_1, banIM, smc, hhaIM_2, ORF2, ORF20, prrC, traE, orf17, int, IS1216, mobA, mob, repA, Q7BQ53, ORF19, dnaJ, Int-Tn, WP_002293753.1, trbL, ftsK, tnpB1, tnpB, tnpA1*
TD-T1	70	*clpP, Q93NB3, Q57231, tnp, Q06238, int, nisX1, R02224, mob, ISS1N, tnpA, ruvB, dnaK, recA, tnpB, hflB, traF, WP_002321882.1, polC, uvrB, mutS_2, clpB, groL, polA, smc, uvrA, gyrA, clpX, hsdM_1, gyrB, ltrA_2, traG, dnaX, rarA, topB, groEL, mutS, dnaG, clpC, hhaIM, dpnA, clpP_2, hsdM, ftsK, recQ, recR, dnaA, ltrA_1, uvrA_1, hin_1, ltrA, mcrB, dnaB, tnpR, dcm, hsdR, traK, ORF20, ORF32, prrC, orf23, IS1216, traC_2, repA, dnaJ, rep, tra8, tnpB1, tnpA1, pre*
TD-T2	80	*xis, repS, Q57231, repR, rlx, Q06238, tnpC1, nisX1, hsdM, tnp, istA, mobE, EF_0125, tnpB, ISS1N, ruvB, dnaK, recA, hflB, repE, WP_010890867.1, WP_002321882.1, traA, clpX, polC, uvrB, groL, clpB, gyrA, mutS2, tnpA, gyrB, ltrA_2, topB, uvrA, dnaG, alkA, hup, groEL, mutS, dnaB, uvrC, clpC, ltrA, dnaE, dpnA, ltrA_5, recQ, tnpR, dnaA, ftsK, ltrA_1, hsdR, uvrA_1, dnaX, radA, dcm, prrC, orf23, int, Xis-Tn, IS1216, mob, repA, tnpX, mobC, traG, tsrF, rep, repB, dnaJ, tra8, WP_002293753.1, recN, dnaC, tnpB1, tnpA1, mobA, P03862, repN*
TD-T3	79	*clpX, dnaB, NGR_a03160, Q57231, Q54944, traA, repD, Q06238, EF_0125, tnp, tnpB, repE, ISS1N, WP_000351512.1, zeta, mobA, rep, ruvB, dnaK, xerD, hflB, dnaX, WP_002321882.1, repR, polC, groL, smc, uvrB, uvrA, gyrA, polA, ltrA_2, clpB, tnpA, traG, topB, recA, ltrA_1, uvrC, dnaG, dcm, clpC, umuC, mutS, dnaE, gyrB, groEL, dpnA, hhaIM_2, ydiP, ltrA, hsdM, ftsK, mutS2, dnaA, hsdR, istB, uvrA_1, pinR, pcrA, ORF21, tnpR, IS1216, mob, WP_001284311.1, WP_127822567.1, pcrA_2, tsrF, mobC, A0A1W7AEW0, mobB, repS, WP_001186919.1, preA, WP_002293753.1, int, tnpB1, tnpA1, repN*

Sample	No. MGEs	MGEs
TD-T4	97	*clpP, ssb, dnaB, xis, cas3, repS, repR, Q9AL19, Q9AL01, repD, rlx, Q06238, tnpC1, hsdM, resR, EF_0125, hsdS, tnp, repA1, tnpB, ISS1N, hin_1, rep, ruvB, dnaK, recA, hflB, WP_002321882.1, bin3, traA, hsdR_2, repC, mutS_2, dcm, ftsK, clpB, groL, smc, uvrB, uvrA, hsdR, gyrA, clpX, umuC, hsdM_1, gyrB, ltrA_2, tnpA, traG, topB, hup, ssb_2, uvrC, ycbY, ltrA, higA, dnaE, mutS, dpnA, dnaG, polA, clpP_2, recR, uvrA_2, tnpR, dnaA, ltrA_1, groEL, uvrA_1, pcrA, rph, ORF20, prrC, sth368IM, soj_2, orf17, int, Xis-Tn, IS1216, tnpX, mobC, ORFAB, WP_127822567.1, pcrA_2, tsrF, A0A1W7AEW0, mutL, parA, dnaE2, Int-Tn, clpC, WP_002293753.1, uvrB_2, tnpB1, tnpA1, mobA, polC*
TD-1	59	*ssb2, clpP, repD, tnp, tnpB, repE, recA, tnpA, uvrA_2, EF_0125, hsdM, groL, clpX, polC, uvrB, mutS_2, ftsK, hflB, clpB, gyrA, hsdR, repA, gyrB, dnaJ, uvrA, ltrA_2, topB, dcm, groEL, uvrC, dnaG, addA, ltrA, umuC, dnaE, dpnA, mutS, hhaIM_4, terL, tnpR, dnaA, ltrA_1, recQ, hin_1, uvrA_1, clpC, rarA, ORF20, int, IS1216, tnpX, parA1, traG, A5UJT3, dnaK, Int-Tn, tnpB1, tnpA1, P41*
TD-2	66	*uvrB, clpP, ltrA, hsdS, nisX1, tnp, insI, mobE, EF_0125, tnpB, ISS1N, ruvB, dnaK, istB, clpX, mutS_2, ftsK, hflB, clpB, groL, ligA, uvrA, lexA, mutS2, tnpA, gyrA, ltrA_2, rarA, topB, recA, dnaG, alkA, uvrC, xerD, clpC, dnaE, umuC, repA, dpnA, mutS, hsdM, uvrA_2, tnpR, dnaA, ltrA_1, gyrB, uvrA_1, pinR, dnaN, sth368IM, orf17, orf23, int, IS1216, mobC, traG, rep, dnaJ, traA, hsdR, int1, traM, Int-Tn, tnpB1, mobA, tnpA1*
TD-3	70	*dpnA, traA, traL, hsdS, tnp, groL, insF, ISS1N, ruvB, recA, tnpB, hflB, EF_0125, hsdM, clpX, polC, uvrB, ligA, mutS_2, dcm, clpB, uvrA, lexA, gyrA, ltrA, gyrB, polA, ltrA_2, topB, smc, tnpA, alkA, groEL, mutS, rex, pcrA, 5, dnaE, recQ, ftsK, uvrA_2, dnaA, ltrA_1, uvrA_1, pinR, tnpR, F7LRR2, soj_2, orf17, orf23, int, IS1216, mob, mobC, traG, A5UJT3, WP_011727856.1, dnaK, rep, pre, repA, int1, parA, Int-Tn, clpC, hsdR, tnpB1, mobA, dnaX, tnpA1*

Table F8.4 Microbial Genera and ARGs significantly correlated (R > 0.50, p-value < 0.05).

Genus	Phylum	ARGs
Jeotgalicoccus	Bacillota	*cmx, efrB, ileS, lnuA, tetO, ugd, BAC0056*
Amylolactobacillus	Bacillota	*CfxA2, cmx, efrB, floR, sul1, BAC0740*
Flaviflexus	Actinomycetota	*CfxA2, cmx, efrB, floR, tetO, BAC0740*
Ligilactobacillus	Bacillota	*cmx, floR, ileS, sul1, tetO, BAC0740*
Staphylococcus	Bacillota	*efrB, floR, sul1, tet(K), BAC0056, BAC0740*
Brevibacterium	Actinomycetota	*CfxA2, cmx, efrB, floR, BAC0740*
Erysipelothrix	Bacillota	*cmx, efrB, floR, poxtA, BAC0740*
Paeniclostridium	Bacillota	*floR, sul1, cfr(D), BAC0056, BAC0740*
Acinetobacter	Pseudomonadota	*CfxA2, cmx, efrB, tetO*
Blautia	Bacillota	*cmx, floR, tetO, BAC0740*
Curtobacterium	Actinomycetota	*efrB, ileS, sul1, tet(K)*
Lentilactobacillus	Bacillota	*CfxA2, cmx, efrB, tetO*
Mammaliicoccus	Bacillota	*CfxA2, floR, sul1, BAC0740*
Pantoea	Pseudomonadota	*CfxA2, cmx, efrB, tetO*
Syntrophomonas	Bacillota	*Erm(47), ErmF, SAT-4, BAC0629*
Weissella	Bacillota	*cmx, ileS, tetO, BAC0056*
Aminobacterium	Synergistota	*Erm(47), ErmF, BAC0629*
Brevefilum	Chloroflexota	*Erm(47), ErmF*
Carnobacterium	Bacillota	*efrB, BAC0056*
Collinsella	Actinomycetota	*ileS, tetO*
Denitrobacterium	Actinomycetota	*tetO, ugd*
Enterococcus	Bacillota	*ileS, BAC0056*
Mesotoga	Thermotogota	*Erm(47), ErmF*
Petrimonas	Bacteroidota	*Erm(47), ErmF*
Proteiniphilum	Bacteroidota	*Erm(47), ErmF*
Ruminococcus	Bacillota	*tetS, BAC0056*
Streptococcus	Bacillota	*cmx, BAC0056*
Syntrophus	Pseudomonadota	*Erm(47), ErmF*
Aerococcus	Bacillota	*BAC0056*

Genus	Phylum	ARGs
Clostridium	Bacillota	*tet44*
Lactococcus	Bacillota	*efrB*
Latilactobacillus	Bacillota	*BAC0056*
Leuconostoc	Bacillota	*efrB*
Methanobrevibacter	Euryarchaeota	*BAC0056*
Methanothrix	Euryarchaeota	*ErmF*
Pediococcus	Bacillota	*efrB*
Ureibacillus	Bacillota	*tetB(P)*

Table F8.5 Microbial Genera and MGE significantly correlated (R > 0.50, p-value < 0.05).

Genus	Phylum	MGEs
Staphylococcus	Bacillota	*dnaE, dnaG, EF_0125, ISS1N, istB, mobA, mutS2, P03862, pcrA, polA, priA, recJ, recN, rep, repE, repR, repS, rlx, ssb, topA, traA, uvrC, WP_002293753.1, WP_002321882.1, WP_010890867.1, hup, mutL*
Amylolactobacillus	Bacillota	*dnaN, istB, pcrA, polA, priA, recJ, recN, repR, soj_2, ssb, ssb_2, topA, traA, traI, uvrB_2, uvrC, WP_002293753.1, hsdR_2, hup, mutL*
Ligilactobacillus	Bacillota	*dnaN, EF_0125, int1, mobA, parA, pcrA, polA, pre, priA, recJ, rep, soj_2, ssb, topA, traA, traI, hsdR_2, hsdS, mutL*
Mammaliicoccus	Bacillota	*dnaE, EF_0125, parA, pcrA, polA, priA, recJ, soj_2, ssb, topA, uvrC, A5UJT3, addA, hsdS, mutL*
Blautia	Bacillota	*dnaN, int1, istB, mobA, mobN1, priA, recJ, topA, topB_1, traA, xerD, lexA, rex, traN_1*
Curtobacterium	Actinomycetota	*dnaG, EF_0125, mobA, mutS2, rep, repB, repE, repR, repS, traA, uvrC, WP_002293753.1, WP_002321882.1, tsrF*
Jeotgalicoccus	Bacillota	*dnaE, dnaG, dnaN, EF_0125, ftsK, int1, istB, mobA, mutS2, rep, repE, repR, traA, uvrC*
Erysipelothrix	Bacillota	*dnaG, dnaN, mutS2, P03862, pre, priA, recJ, recN, rep, topA, traI, WP_002321882.1, WP_010890867.1*
Weissella	Bacillota	*dnaE, dnaG, dnaN, EF_0125, int1, istB, mobA, pcrA, polA, rep, traA, uvrC, hsdS*
Flaviflexus	Actinomycetota	*dnaN, int1, istB, mutS2, priA, recJ, recN, topA, traA, traI, uvrC, xerD*
Paeniclostridium	Bacillota	*Int-Tn, parA, pcrA, polA, priA, recJ, soj_2, ssb, ssb_2, topA, traI, mutL*
Lactococcus	Bacillota	*dnaE, dnaG, EF_0125, IS1216, ISS1N, istB, mobA, nisX1, rep, traA, uvrC*
Brevibacterium	Actinomycetota	*dnaN, istB, priA, recJ, recN, repE, topA, traI, uvrC, addA*
Collinsella	Actinomycetota	*EF_0125, mobA, parA, pcrA, polA, rep, repR, repS, soj_2, traA*
Denitrobacterium	Actinomycetota	*EF_0125, int1, mobA, pcrA, polA, rep, repS, ssb, traA, uvrB_2*
Streptococcus	Bacillota	*dnaE, dnaG, dnaN, EF_0125, int1, mobA, rep, traA, uvrC, hsdS*
Pediococcus	Bacillota	*EF_0125, IS1216, recN, rep, repE, repR, soj_2, tnpA1, uvrC*
Latilactobacillus	Bacillota	*dnaG, EF_0125, repE, repR, repS, tnpX, uvrC, tsrF*
Acinetobacter	Pseudomonadota	*dnaN, istB, mutS2, recN, traI, xerD*
Carnobacterium	Bacillota	*EF_0125, recN, repR, soj_2, tnpX, uvrC*
Lentilactobacillus	Bacillota	*dnaN, istB, mutS2, recN, traI, xerD*
Leuconostoc	Bacillota	*repR, repS, rlx, uvrC, WP_002293753.1, Q06238*
Pantoea	Pseudomonadota	*dnaN, istB, mutS2, recN, traI, xerD*
Aerococcus	Bacillota	*EF_0125, ISS1N, rep, WP_002293753.1, WP_002321882.1*
Bacillus	Bacillota	*parA, pcrA, soj_2, traI, hsdR_2*
Enterococcus	Bacillota	*EF_0125, ftsK, ISS1N, tnpA1, uvrC*

Genus	Phylum	MGEs
Niallia	Bacillota	*dnaE, A5UJT3, addA, hsdS, lexA*
Proteiniphilum	Bacteroidota	*ORF32, ORF20, traC_2, xerD_4*
Aminobacterium	Synergistota	*ORF32, ORF20, xerD_4*
Ruminococcus	Bacillota	*dnaE, EF_0125, uvrC*
Brevefilum	Chloroflexota	*ORF32, xerD_4*
Clostridioides	Bacillota	*mcrB, ORF32*
Heyndrickxia	Bacillota	*int1, alkA*
Methanobrevibacter	Euryarchaeota	*dnaG, ftsK*
Ureibacillus	Bacillota	*parA, soj_2*
Aminipila	Bacillota	*rteB*
Bacteroides	Bacteroidota	*traN_1*
Defluviitoga	Thermotogota	*mutS_2*
Dehalobacterium	Bacillota	*xerD_4*
Keratinibaculum	Bacillot	*mutS_2*
Mesotoga	Thermotogota	*xerD_4*
Methanobacterium	Euryarchaeota	*mutS_2*
Methanothermobacter	Euryarchaeota	*mutS_2*
Parabacteroides	Bacteroidota	*rteB*
Petrimonas	Bacteroidota	*traC_2*
Syntrophomonas	Bacillota	*xerD_4*
Syntrophotalea	Pseudomonadota	*xerD_4*
Syntrophus	Pseudomonadota	*traC_2*
Thermoanaerobacterium	Bacillota	*mutS_2*